Beyond chemically defined –

Characterization of chemically defined cell culture medium for the cultivation of CHO cells

By

Florian Krattenmacher

Thesis presented for the degree of

Doctor Rerum Naturalium

of the Bielefeld University

Faculty of Technology

Experiments conducted in the laboratories of

Boehringer Ingelheim Pharma GmbH & Co. KG

in Biberach an der Riß

Supervisors

Prof. Dr. Thomas Noll
Head of research group cell culture technology
Faculty of technology
Bielefeld University

Prof. Dr. Uwe Bücheler
Head of Corp. Div. Biopharmaceuticals
Boehringer Ingelheim Biopharmaceuticals GmbH

December 2019

Abstract

Chemically defined media (CDM) for cell culture are routinely used in industrial processes for recombinant protein production from mammalian expression systems as for example Chinese hamster ovary (CHO) cells. As CDM are nowadays considered as the industry standard the focus has shifted from implementation and improvement of performance to additionally their chemical behavior and the impact on process robustness. Since CDM are highly concentrated aqueous mixtures of versatile chemical compounds one particular problem in this context is the high risk for chemical reactions and instability.

Therefore, a major focus of this thesis is the generation of understanding for chemical interactions of CDM compounds and especially the establishment of analytical technologies for the purpose of media characterization. Thus, a mixed mode liquid chromatography tandem mass spectrometry (LC-QqQ-MS) method that is able to simultaneously quantify the majority of media compounds has been developed and validated. This powerful method has been applied to characterize the chemical behavior of feed media under process relevant conditions as preparation and storage. Further on-line and off-line analytics have been applied to gain insight into CDM chemistry.

The application of probes measuring standard parameters have shown the dynamic behavior of chemical key parameters during CDM powder hydration. A Particle probe, such as the focused beam reflectance measurement (FBRM), has been shown to be useful for dissolution behavior investigations of different media recipes or powder compositions. However, it is rather difficult to establish the technology for batch to batch comparison or the monitoring of deviations from the standard preparation conditions. Media preparations with simplified media powders revealed that the compounds ascorbic acid and phosphates cause an apparent drop in dissolved oxygen concentration upon iron compound addition. The combination of the experiments with the newly developed LC-QqQ-MS method confirmed the comparability of chemical behavior in different media matrixes of most of the CDM compounds but highlighted some differences. Furthermore, measurements with the LC-QqQ-MS showed that the effect of preparation temperature and relevant storage conditions on media stability were negligible. In contrast, measurement of samples over storage time identified unstable compounds. A closer look at the media after storage showed that some formulations formed precipitate during storage and the collection of the solid material on filter membranes revealed their different appearance. Investigations of the material with specialized analytics proved that their identity was heterogeneous. One precipitate that was drawing attention on itself was of silver color and could be shown to consist of Sulphur.

Publication

Parts of this thesis have been published in the Journal of Chemical Technology and Biotechnology published by John Wiley and Sons, Ltd with the title “Effect of manufacturing temperature and storage duration on stability of chemically defined media measured with LC-MS/MS”.[1]

Krattenmacher, F., T. Heermann, A. Calvet, B. Krawczyk, and T. Noll, (2019). ***Effect of manufacturing temperature and storage duration on stability of chemically defined media measured with LC-MS/MS***. Journal of Chemical Technology & Biotechnology, **94**(4): p. 1144-1155.

Table of Contents

1 Introduction

The very high importance of biotechnology for health and society underlines the importance to increase the understanding of the chemistry of chemically defined cell culture media (CDM) that are the fundamental raw material of biotherapeutics production. The high complexity of CDM is easily comprehensible when considering the versatility and the big number of blended compounds. Subsequently, the analytics of CDM to guarantee robust cell culture process development has high potential to be developed.

1.1 Biotechnology and recombinant DNA technology in health and society.

In order to correctly sort the importance of cultivation media a background of the principles of biotechnology, the products, their summarized chemical properties and the processes applied for biomanufacturing is necessary.

1.1.1 Historical benchmarks of biotechnology

Biotechnology, a term first mentioned in 1919, is the application of biological systems to manufacture products.[2] However, the principal has already been used in ancient times for baking of bread, making cheese or brewing beer. From early on biotechnological processes have been used to produce medicine. For example, penicillin has been isolated from fermentation processes with wildtype mold.[3] For decades the manufacturing of very important pharmaceutical compounds like vitamin C or insulin was dominated by either chemical synthesis or extraction from animal derived material.[4-6] The increasing demand for insulin in the 1970ties made pancreases of 56 million animals per year necessary to supply the patient's needs.[7] A benchmark in replacing insulin isolation of slaughtered animal glands was the development of recombinant protein production technology and the process yield optimization.[8] A technological breakthrough in 1982 was the FDA approval of the first genetically-engineered product humulin, human insulin expressed in an *Escherichia coli* K12 strain, for the treatment of diabetes.[9] Generally, recombinant DNA technology comprises genetic engineering of organisms by gene transfer and manipulation. It applies specific enzymes (restriction endonucleases) as tools to cut DNA into pieces.[10] The DNA pieces are eventually ligated *in vitro* to new combinations on suitable vector DNA molecules. Subsequently, the recombinant DNA on the vector is transfected into either bacterial, fungi, plant or animal host cells. The engineered expression systems use the recombinant DNA and translate it to protein created by engineers. This allows to produce protein foreign to the specific production host cells, which are usually well characterized and suitable for modern manufacturing processes. Furthermore, the large pool of enzymatic tools and DNA allows for entirely newly engineered protein. Since the early 1980ties the acceptance of pharmaceuticals produced from genetically modified organisms in the clinic and in the society has widely increased. Mainly due to their high safety, efficacy and the novel modes of action offered.

1.1.2 The significance of biotechnology for health and society

In 2017, more than 50% of the world wide best selling drugs were manufactured biotechnologically (Table 1). Furthermore, at the time the predominant (>60%) molecule format of biologics are monoclonal antibodies (mAb). Nowadays, the development goes beyond mAbs and peptides to a continuously growing number of new molecule formats like bispecific antibodies, Fab fragments or other engineered molecules.[11, 12] The success of recombinant technology in the production of pharmaceuticals is further emphasized by the development of engineered vesicular stomatitis virus with a high potential to achieve a next step in the treatment of cancer.[13-16] Furthermore, the volume of the biopharmaceuticals market was valued at USD >200000 million in 2017.[17] The predicted compound annual growth rate (CAGR) of 8.59% until 2023 underlines the continuously growing importance of the field for health and society. In 2018 the biotech industry represented already 20% of the entire global pharma market and the top ten best selling drugs are mainly mAbs.[18] The forecast for 2024 summarizing the top 20 selling pharmaceuticals shown in Table 1 contains 70% biologics (Appendix Table 14). All these examples emphasize the high importance of biopharmaceuticals for the treatment of patients and the not yet exhausted potential underlined by continuous innovation, development of new therapy approaches and growing markets.

Table 1. The pharmaceuticals product sales figures were adapted from EvaluatePharma®.[19] The table is sorted by the annual sales in the year 2017. Information about used cultivation media were collected from EMA assessment reports. CAGR=compound annual growth rate.

	Product	Generic name	Company	Pharmacological class	World Wide Product sales [$m] 2017	2024	CAGR	Production process	Production host	Cultivation medium
1	Humira	adalimumab	AbbVie+ Eisai	Anti-tumour necrosis factor alpha (TNFa) mAb	18,922	15,233	-3%	biotechnology	CHO	no human or animal derived ingredients, contains recombinant insulin
2	Enbrel	etanercept	Amgen + Pfizer + Takeda	Tumour necrosis factor alpha (TNFa) inhibitor	8,241	4,072	-10%	biotechnology	CHO	Serum was removed from cell culture, and highly defined medium was introduced
3	Revlimid	lenalidomide	Celgene + BeiGene	Immunomodulator	8,191	11,931	6%	chemcial synthesis	-	-
4	Avastin	bevacizumab	Roche	Anti-vascular endothelial growth factor receptor (VEGFr) mAb	6,795	2,767	-12%	biotechnology	CHO	enriched non-selective production medium (MTX-free) in production stage and MTX containing medium in seed train cultivation
5	Eylea	aflibercept	Regeneron Pharmaceuticals + Bayer + Santen Pharmaceutical	Vascular endothelial growth factor receptor (VEGFr) kinase inhibitor	6,282	6,827	1%	biotechnology	CHO	no material of biological origin other than medium for master cell bank contains foetal bovine serum
6	Opdivo	nivolumab	Bristol-Myers Squibb + Ono Pharmaceutical	Anti-programmed cell death-1 (PD-1) Mab	5,725	11,247	10%	biotechnology	CHO	no material of animal or human origin
7	Prevnar13	pneumococcal vaccine	Pfizer + Daewoong Pharmaceutical	Pneumococcal vaccine	5,693	5,756	0%	biotechnology	Streptococcus pneumoniae (wt)	soy media complemented with dextrose and magnesium sulfate
8	Xarelto	rivaroxaban	Johnson & Johnson + Bayer	Factor Xa inhibitor	5,640	5,915	1%	chemcial synthesis	-	-
9	Eliquis	apixaban	Bristol-Myers Squibb	Factor Xa inhibitor	4,872	10,535	12%	chemcial synthesis	-	-
10	Tecfidera	dimethyl fumarate	Biogen	Fumarate	4,214	3,020	-5%	chemcial synthesis	-	-
11	Stelara	ustekinumab	Johnson & Johnson	Anti-IL-12 & IL-23 mAb	4,011	6,466	7%	biotechnology	Sp2/0	CDM
12	Prolia/ Xgeva	denosumab	Amgen + Daiichi Sankyo	Anti-receptor activator of nuclear factor-kappaB ligand (RANKL) mAb	3,891	5,995	6%	biotechnology	CHO	no information found
13	Keytruda	pembrolizumab	Merck & Co + Otsuka Holdings	Anti-programmed cell death-1 (PD-1) mAb	3,823	12,686	19%	biotechnology	CHO	serum free culture medium without animal derived material added during fermentation
14	Genvoya	cobicistat; elvitegravir; emtricitabine; tenofovir alafenamide fumarate	Gilead Sciences + Torii Pharmaceutical	Nucleoside reverse transcriptase inhibitor (NRTI), cytochrome P450 (CYP) 3A & HIV integrase inhibitor	3,731	3,402	-1%	chemcial synthesis	-	-
15	Imbruvica	ibrutinib	AbbVie + Johnson & Johnson	Bruton's tyrosine kinase (BTK) inhibitor	3,196	9,557	17%	chemcial synthesis	-	-
16	Triumeq	abacavir sulfate; dolutegravir sodium; lamivudine	GlaxoSmithKline	Nucleoside reverse transcriptase inhibitor (NRTI) & HIV integrase inhibitor	3,172	4,731	6%	chemcial synthesis	-	-
17	Botox	onabotulinumtoxinA	Allergan	Neuromuscular blocker	3,169	4,573	5%	biotechnology	clostridium botulinum	e.g. a complex medium consisting of 2% casein hydrolysate and 1% yeast extract plus an appropriate concentration of glucose
18	Soliris	eculizumab	Alexion Pharmaceuticals	Anti-complement factor C5 mAb	3,144	5,208	7%	biotechnology	murine myeloma cell line (NS0)	bovine serum albumin (BSA) was included in media, cholesterol obtained from sheep wool grease included in cell culture media
19	Ibrance	palbociclib	Pfizer	Cyclin-dependent kinase (CDK) 4 & 6 inhibitor	3,126	8,284	15%	chemcial synthesis	-	-
20	Xtandi	enzalutamide	Astellas Pharma	Androgen receptor antagonist	2,656	4,500	8%	chemcial synthesis	-	-

1.1.3 Molecular properties of the main class of biologicals – recombinant monoclonal antibodies

The major class of biotherapeutics, recombinant monoclonal antibodies (mAbs), are large glycoproteins (~150 kDa) and are mainly of the immunoglobulin class G and subclass IgG1.[20] The IgG type molecules account for 10-20% of plasma protein in humans and are roughly described y-shaped molecules consisting of 4 polypeptide chains, two identical 50 kDa heavy chains and two identical 25 kDa light chains.[21, 22] The four antibody subunits are bound together by disulfide bridges, where the two heavy chains are directly connected and each light chain is connected to a heavy chain forming a symmetrical molecule. The therapeutic mAbs are named according to a common nomenclature. Until 2017 this was consisting of a random prefix, a substem A abbreviating the organism the amino acid sequence is derived from, a substem B describing the pharmacologic target and a stem "-mab" to categorize the molecule class.[23, 24] Since 2017 the names will again start with an individual prefix, followed by a single slightly modified target substem which is completed by the "-mab" stem. Just as for any other protein, mAb affinity to target molecules and functionality can be impacted by correct folding and post translational modifications (PTMs).[25] For example, Houde *et al.* showed that methionine oxidations and altered glycosylation patterns had impact on conformation whereas variation in glycan structures lead to dramatic effects in relative binding. The immunoregulatory role of antibody glycosylation is well accepted in medicine.[26] Zheng K. *et al.* confirmed that glycosylation pattern had an impact on mAb molecular properties but interestingly the storage stability (low and high molecular weight species in size exclusion chromatography) of investigated molecule was not impacted.[27] For glycosylation it is well known that either the glycan structure itself or the presence of glycans can change the protein conformation in such a way that it induces an immune response.[28] An interesting example reviewed by Kuriakose *et al.* is the formation of galactose-α1,3-galactose epitopes on the Fab region of a mAb by α1,3-galactosyltransferase expressed in murine SP2/0 cell line. The review article proposes to avoid immunogenic glycan formation by using an appropriate expression system as for example Chinese hamster ovary (CHO) cells. Even though most PTMs are recommended to be monitored during process development and commercial production their effect on immunogenicity is less understood than for glycosylation.[29]

1.1.4 Gold standard expression system for glycosylated recombinant protein production – The CHO cell

Since mAbs are large and complex molecules with several domains and molecule characteristics that depend on the correct PTM formation a well characterized expression host is fundamental. The usage of mammalian cell lines for the production of the approximately 40% approved glycosylated biopharmaceuticals is largely dictated by their therapeutically acceptable glycoprofiles.[30] The percentage of approved biotherapeutics produced in mammalian cell systems versus non-mammalian has tremendously increased over the time (almost 80% between 2015 and 2018).[31, 32] A comparison of glycosylation patterns on IgG molecules produced in murine and human cell line or derived from human plasma has shown that cell lines differ in glycosylation profiles.[33] CHO cell lines are known for their human-like PTMs including glycosylation.[34] Besides PTM profile, the advantages of CHO cells over other cell lines is versatile and only a few shall be named. For example, the robust growth in suspension cultures with chemically defined medium (CDM) and a reasonable safety profile for human pathogenic virus replication are important traits amongst others.[34] Due to this and other reasons the CHO cell lines are still the workhorse that accounts for 70% of industrially produced protein in 2007.[35, 36] Based on the score of publications of popular cell lines like HEK, NS0, BHK, PER.C6 and CHO in 2016 the CHO cell line remains dominant with a proportion of over 70%.[37] The nowadays very high presence in research and discovery shows that the CHO cell line will most likely also play an important role in the coming

decades. This is further emphasized by efforts of CHO cell engineering with for example approaches for glycoengineering.[34, 38] The good acceptance by authorities, good clinical safety and the routine application in industrial processes is further emphasized by instances of non-glycosylated protein as Fab fragments being produced in CHO.[39] Even though the multiple CHO cell lines share a common ancestor they exhibit a well characterized but broad genetic versatility that allows the researcher to pick the cell appropriate for the desired product quality spectrum and the desired productivity.[40]

1.1.5 Sophisticated manufacturing processes for biologics production

When biopharmaceuticals are compared to drugs and health products from non-biologic origin their cost effectiveness measured in quality adjusted life years is less favorable.[41] However, some authors compare the societal impact of biologics even with antibiotics.[42] In order to dare a glance in the future of cell culture development Wei-Shou Hu compares it to the fate of penicillin production from microbial bioprocesses. Over the time scientists and engineers succeeded with relentless effort in process development to improve titer exponentially and cut the costs of product.

For CHO cell culture biologics production facilities the investment costs are, with more than half a billion, still very high.[43] This is mainly due to the high requirements for sterility and the big variety of required high end equipment. Today, the most common upstream process format for recombinant mAb production with CHO cells in industry is fed-batch cultivation.[44] After batch cultivation, that is a closed system after inoculation with cells growing until limited by media consumption, the fed-batch format is the second easiest to operate.[45] Therefore, it finds widespread application in industry and most likely will, supplemented with single-use and perfusion technology, play an important role in the future.[46] A typical bioprocess for the manufacturing of recombinant protein with CHO cells is outlined in Figure 1. The first step of bioprocess development is the cell line development and engineering. Usually, it follows a well-established procedure that has been adapted to high-throughput with automated liquid handling systems and high-throughput analytics amongst others.[47] Briefly described, the typical cell line generation procedure includes recombinant gene transfection, medium and cultivation condition adaptation, gene amplification and single clone isolation. Technologies that have driven the CHO cell line productivity and longevity increase are for example selection and screening approaches, vector engineering, overexpression, RNA interference and gene editing with specific sequence recognition, nuclease activity and targeted gene integration. After successful cell line generation a cell bank is created that is the origin of each subsequent cultivation cycle. The fundamental ingredients of each bioprocess are the cell line and a cultivation medium. This is prepared separately for each scale in special tanks for medium preparation. After vial thaw the focus lies on cell mass generation in order to have sufficient cells to inoculate the production stage. Mainly due to low specific growth rate (doubling time of 14 – 23 h) of CHO cells the cell expansion phase takes a significant amount of time.[48] A commonly discussed approach to reduce seed train cultivation time and to increase plant throughput in the near future is the application of perfusion seed cultures to enable higher seeding cell densities of N-stage fed-batch reactor.[45, 49] For typical fed-batch cultivation the batch medium is equilibrated in the production scale fermenter, then the cells are inoculated and cultivated with the support of different feeding strategies until sufficient product concentration is reached. The way of feed addition varies from fixed volume bolus feed addition to continuous feeding coupled to feedback loops with online probes.[50-52] The fact that in the past the yield of fed-batch processes doubled every five years made it today the industry standard manufacturing process for stable protein production.[45] As on any product, the pressure to make more product out of less money is very high for biologicals both from market

and authorities. Pressure is not only coming from payers or capitals for new investments but also from changing markets that require flexibility, product success uncertainties, competition, clinical trial failures, growing clinical pipelines with versatile molecule formats or time to market presets.[45] Even though continuous manufacturing, as perfusion mammalian cell culture, is not a new development and known since the early 90ties in commercial protein production it is subject of ongoing discussion for the future plant design. Perfusion is not only for seed train cultivation time reduction or high density cell banking an interesting process setup but also for N-stage production. The process intensification in continuous perfusion processing by increased volumetric productivity has the potential to decrease plant footprint because the investment costs and the time from decision to inauguration of new plants is lower compared to fed-batch processes. A recent study has shown that the product heterogeneity in this specific example is lower in perfusion if directly compared to fed-batch.[53] Another long discussed topic is the media cost in perfusion process. But a recent study showed that if specific productivity in perfusion is high it can be even lower than in fed-batch processing.[54] However, the real potential of perfusion processes will only be fully appreciated if purification technologies keep pace with the continuously high amounts of harvested cell culture fluid produced in perfusion. In contrast to a typical fed-batch process where the cell culture broth is harvested at the end of cultivation and cells, DNA and viruses are removed by disk stack centrifugation and depth filtration (Figure 1) the cell free harvest from the cell retention device is continuously putting workload on the capturing and polishing steps. As shown in Figure 1 the downstream process is typically operated in the batch mode starting usually with a protein A column to capture mAb, followed by virus inactivation and polishing chromatography units. In order to cope with challenges of perfusion processes, approaches to develop continuous integrated processes including continuous downstream have been started to design the plant of the future.[55] The final step of each bioprocess is the fill and finish, where the bulk drug substance is finalized by the addition of excipients that shall keep the active pharmaceutical ingredient (API) in its functional conformation and guarantee for sufficient shelf life.

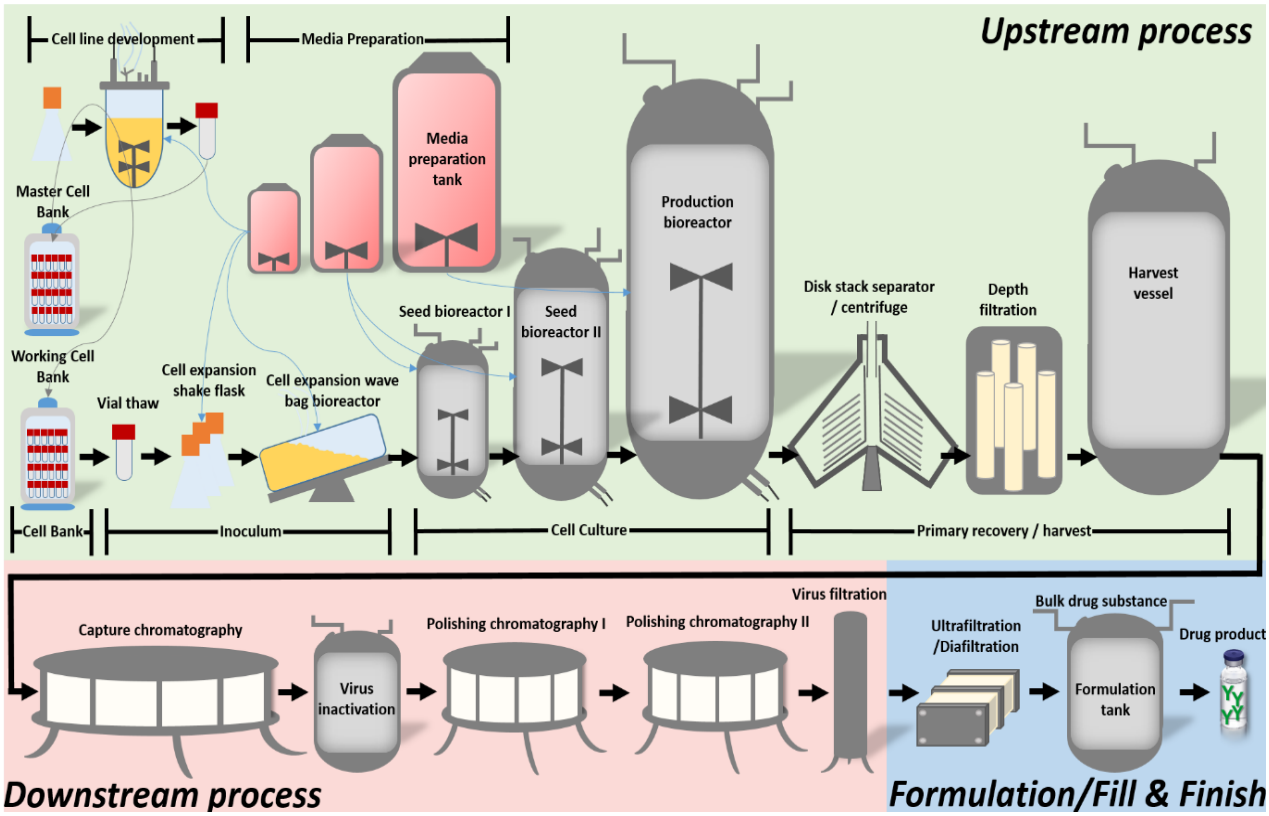

Figure 1: Example of typical biologics manufacturing process with CHO cell culture. The basis of each cell cultivation is medium prepared at different scales (Medium preparation unit). The first step in bioprocess development is the clone selection and cell line generation (Cell line development unit). Cells are frozen in cryovials and stored in a master cell bank (Cell banking). Cells from the master cell bank are used to generate a working cell bank. Vials from the working cell bank are used to start a manufacturing process. In the inoculum the cells are restored from the freezing medium, regenerated in shake flask cultivation vessels and cells are cultivated in wave bag bioreactors to generate cell mass. Cells from inoculum are used to start process up-scaling and pre-stage cultivation in stainless steel stirred bioreactors (Cell culture unit). Cells from pre-stage fermenters are used to seed the production stage bioreactor that can have as much as 15000 L working volume. After a typically 10 to 14 days lasting fed-batch cultivation the cell culture broth is centrifuged in a disk stack separator to separate and discard cells from supernatant (Harvest unit). The cell free broth is then filtered in depth filtration mode to remove cell debris as for example host cell DNA. The harvested cell culture fluid (HCCF) is filled into a storage vessel and the upstream process is complete. HCCF is then transferred to downstream processing. In a first capture chromatography step the product is separated from cell culture broth and concentrated in the same time. Afterwards, the eluent is acidified to inactivate potentially present endogenous or adventitious virus. Typically anion or cation-exchange chromatography steps are used afterwards to remove process related impurities or virus. A subsequent virus filtration step is applied to improve safety and remove remaining viruses. After this process step the material must be handled under even higher clean room grade than before (EU GMP classification grade C). Subsequently, the formulation process and the final fill and finish starts. First, the protein is concentrated and buffer exchanged in an ultrafiltration/diafiltration step and transferred to a tank where excipients for final formulation are added. As a sub-category of the entire biologics manufacturing process the inoculum, cell culture, harvest, downstream and formulation are summarized as the drug substance production and the final bulk drug substance is defined as the substance that is represented for the use in a drug. For example, in the case of mAb production it is the active pharmaceutical ingredient (API) itself in solvent with excipients added for the stabilization of the API. Finally, the formulated mAb is filled into vials and packed to become the final drug product (drug product is defined as the finished dosage form).

1.2 The cultivation medium for recombinant protein production

No matter which bioprocess format or which organism is used to produce biotechnological product, the fundamental prerequisite for biotechnology is a medium that can grow cells. It is the most important part for cell culture development in biomanufacturing because of its high relevance for process performance and safety.[45] In the following sections an overview of the main functionalities a medium has to provide to keep cells alive and to proliferate cells, a flashback of historic events that lead to CDM that are typically used for CHO cells and an overview of typically used components with their main functionalities in CDM is given. Furthermore, typical CDM preparation practices and critical factors impacting CDM matrix and stability are introduced.

1.2.1 The main functions of medium for production organism cultivation and the consequences of chemical alterations

The main environmental requirements cells need for survival and proliferation are temperature appropriate for the biologic system, correct pH, appropriate osmolality, essential chemicals for nutrition, removal or dilution of toxic waste products and substrate for cell attachment.[56] In the following paragraphs media related issues in cell culture are discussed that should be avoided or buffered by a successful CDM design with the focus on robust cell culture processes delivering good quality recombinant protein.

Fundamental role of media in cell culture –problems with CDM in preparation and storage can cause cell death In order to better understand the important functions of medium for cell culture and the impact of chemical imbalance and alteration it is worth considering factors that can cause stress in cell culture. The ultimate consequence of stress in cell culture is cell death. Three major morphological features of cell death are distinguished: necrotic cells in passive cell death and either apoptotic or autophagic cell morphology in programmed cell death.[57] Krampe *et al.* name nutrient and oxygen transport limitation, metabolic by products and high levels of osmolarity as the main reasons for cell death. Furthermore, they found that the major cell death pathway in industrial important cell lines was apoptosis and thus cell line engineering approaches are followed to reduce cell death susceptibility. Interestingly, there are methods described to induce necrosis in CHO cells by aeration shear and increased impeller speed.[58] Additionally, protocols to induce apoptosis, autophagy and necrosis in CHO cells have been recently applied to investigate cell death with proteomics in order to improve bioprocess control.[58, 59] With the evolution of cell culture technology also the analytics to measure cell death have developed and can provide an understanding of issues in cell culture.[60, 61]

Extracellular matrix provision Typically, eukaryotic cells isolated from tissue need an extracellular matrix as a cell survival factor.[62] The extracellular matrix is a complex three dimensional non-cellular macromolecular network in which all cells of tissues and organs reside. If the contact is suddenly interrupted the cells enter into programmed cell death.[63] A major advantage of CHO cells for biomanufacturing is their capability to adapt to suspension culture conditions. Several protocols have been described and normally these are accompanied by the adaptation of cell lines to serum free medium as most anchorage dependent cell lines detach due to serum removal.[64, 65] It has been shown that adaptation to chemically defined conditions makes the cells very sensitive to standard cell culture procedures as centrifugation or the usage of enzymes. The composition of CDM has been chosen with care to not killing the cells during the adaptation process.[66] This process of course induces drastic changes in the cell phenotype and the underlying gene transcription.[67-69] When the cells are successfully adapted to suspension and serum free cultivation conditions a CDM has to be able to maintain these cell properties.

pH In biomanufacturing, it has been shown that the specific antibody productivity of CHO cells is not only dependent on the clone but also on the cultivation pH.[70, 71] Generally, it can be said that in a range from pH 6.8 to 7.8 the glucose and glutamine consumption and the lactate and ammonium production rate were increased with increasing pH. Yoon *et al.* also observed an effect of culture pH on the amino acid consumption and production rates emphasizing the importance of this parameter for cellular metabolism. CHO cells seem to be able to adapt to chronically low pH conditions (pH 6.6) by a subsequent phenotype that has slower doubling rates, a 0.12 units higher intracellular pH and an altered heat tolerance.[72] The bioreactor is an environment where pH is well controlled in a defined pH range by base addition if the pH drops below the lower control limit. However, Matthias Brunner *et al.* investigated pH gradients that can occur in large-scale cultivation and showed that even short term exposure of a small compartment of bioreactor to basic pH can affect cell physiology and overall process performance.[73] This study supports the hypothesis that extracellular pH affects intracellular pH and thus impacts process performance. If the pH is too acidic or if the change is too sudden the cells react with apoptosis by increased caspase activity.[74-76] Therefore, a fundamental function of CDM is to provide sufficient buffer capacity at the targeted pH. Due to observations like these, cell culture engineers started early to investigate buffer systems suitable for CDM in order to keep pH stress in cell culture as minimal as possible.[77, 78] Typically, CDM for CHO cell cultivation are optimized to buffer pH values between 6.6 and 7.4.[79, 80] The major factors that impact pH of medium handled in the bioprocess are gas diffusion during preparation and storage and base addition.

Osmotic stress The regulation of the right cell volume is fundamental for cellular survival and function.[81] Osmotic stress gets induced when a change in osmotic pressure causes water to passage over a membrane driven by osmosis. Hypo-osmotic stress causes the cells to swell and induces a multitude of cellular responses, amongst them actin cytoskeleton disassembly.[81-83] In contrast, hyper-osmotic stress makes cells shrink and leads to intracellular molecular crowding. Both hypo- and hyper-osmotic stress can cause programmed cell death with apoptosis traits or, for instance in the case of CHO cells, it can also induce autophagy.[84-86] The numerous publications investigating osmotic stress in CHO cell culture show the high relevance for the field.[87-107] The CDM for successful cell culture must guarantee an osmolality high enough to promote cell proliferation in the growth phase but also low enough to save capacities for increasing osmolality during for example fed-batch processing. CDM for CHO cell cultivation is typically adjusted to a osmolality range between 260 to 320 mOsm/kg.[42, 91]

Shear stress/Hydrodynamic stress As mentioned, increased gas flow rates through the sparger and increased stirring induce shear stress in cell culture that leads to a necrosis phenotype cell death.[58] CHO cells exposed to energy dissipation rates caused by bubble bursting higher than 10^6 to 10^8 W/m^3 become necrotic with lactate dehydrogenase release.[108] Additionally, it could be shown that shear stress reduced productivity in CHO cells.[95, 109] Another work group showed that their CHO cells growth and productivity was resistant to hydrodynamic stress up to 6.4×10^6 W/m^3 but cell physiology was changed as could be concluded from changed glycosylation pattern.[110] A related issue is foam generation in bioreactors leading to cell entrapment causing disadvantageous nutrient supply and an interruption of gas transfer of cultivation broth to the air in the reactor headspace.[111] Even though gassing rates and impeller speed are cell culture process parameters that are not medium related it still can play and important role to hamper shear stress and foam formation by the addition of the right medium supplements like Pluronic F-68.

Oxidative stress Oxidative stress on cells has been examined in multiple systems.[112] Investigations of CHO cell metabolism have shown that they metabolize extraordinary high amounts of glucose in the pentose phosphate pathway and increase oxaloacetate production.[113] This altered cell metabolism is considered as an adaptation to oxidative stress in cell culture.[114] Experiments with gassing rates in stirred bioreactor CHO cell culture have shown that increased dissolved oxygen (DO) set points induce further oxidative stress.[115] Intracellularly, the antioxidant machinery impacted mitochondrial function, metabolism and finally decreased recombinant protein expression. Reactive oxygen or reactive nitrogen species (ROS/RNS) are the main compounds causing oxidative stress.[116] These reactive species are either derived from endogenous sources (e.g. mitochondria, peroxisomes, endoplasmatic reticulum) or from exogenous sources (e.g. transition metals, heavy metals or radiation). It is important to mention that free radicals are a product of normal cell metabolism and at low levels ROS/RNS have beneficial effects. But at higher concentration and when there is an excess of reactive species compared to non-enzymatic and enzymatic antioxidants the cells experience stress.[116] The ROS/RNS are oxygen and nitrogen species that consist of radicals and non-radicals that can readily form radicals. Radicals have at least one unpaired electron and can exist independently so they can attack various biomolecules and thereby alter the normal oxidative state that is necessary for biological function. If oxidative stress gets beyond levels tolerable by cells it induces apoptosis. Usually by receptor and caspase activation or by mitochondrial dysfunction, DNA damage or structural and functional dysfunction of certain proteins.[117-120] Furthermore, oxidative stress and apoptosis are considered as closely related physiological states, because ROS and the cellular redox alterations can be part of signaling pathways during apoptosis.[121] Positive effects of antioxidants in cell culture have to be interpreted carefully if a comparison to physiological systems is of interest. Very often their positive effect on cell culture is not representative for *in vivo* conditions since media are typically deficient in antioxidants. Interestingly, in some media anti-oxidant addition can act contrary to expectation because H_2O_2 formation is promoted in pro-oxidant media upon addition of for example ascorbate.[114, 122] In biomanufacturing, the comparability to *in vivo* conditions is not priority as long as cells grow and produce with desired product quality. Because of the high importance of oxidative stress for production cell culture, studies have been conducted to improve extracellular redox measurement during hybridoma cell culture.[123] Furthermore, reports of antioxidants as for example nitroxide or plant root extracts that are reducing stress in cell culture are highly interesting for media development.[124-127] Even more interesting are reports about baicalein, N-acetylcysteine, L-ascorbic acid 2-phosphate, reduced glutathione and rosmarinic acid tests in CHO cell culture.[128-131] Sources of oxidative stress in cell culture can be versatile. Barry Halliwell *et al.* explains that cells in culture are exposed to higher O_2 concentrations than under physiological conditions.[132] But more culture specific reasons oxidative stress are hyperglycemia and too few antioxidants in media as for example tocopherol, ascorbate and vitamin E. Furthermore, delivery of sufficient selenium to the cells can be challenging and if selenium supply is not sufficient cells may suffer from oxidative stress due to malfunction of selenium dependent antioxidant systems. A main reason for pro-oxidant properties of media is the high concentrations of transition metals. Especially iron and copper are absolutely essential for cellular function but can catalyze multiple reactions leading to ROS if not as well complexed as in the physiologically iron transporter transferrin. All the presented examples of the role of oxidative stress emphasize how important it is to develop media with a balanced redox state that can prevent cells from damage by for example high DO or excess ROS/RNS formation in metabolism.

Nutrient depletion and waste product accumulation The most obvious function of a medium is the delivery of nutrients to the cells. Basically, all chemical compounds the cell in culture can not synthesize itself from a precursor and that are absolutely indispensable for metabolism to grow and survive has to be delivered by the medium in a bioavailable form with the right feeding strategy.[50, 51, 133-146] The impact of media composition on cell metabolism and the underlying gene expression is high.[134] An often discussed topic in cell culture is the accumulation of lactate and ammonia over process duration and the subsequent performance limitation. Even though not directly cytotoxic, they can inhibit cell growth with increasing concentrations by decreasing intracellular pH and impacting cell metabolism.[147, 148] Therefore, strategies have been developed in modern cell culture to avoid the accumulation of especially these two waste products. Examples exist that use lactate feeding to support the lactate metabolic shift and others describe copper as essential to shift metabolism in that direction.[140, 149-154]
The right CDM composition with balanced medium formulation is fundamental for production cell cultivation and process robustness. Any deviation caused by degradation, error in recipe or problems during preparation and storage is critical. The metabolic response of GS-CHO cells on the lack of the key amino acids asparagine and glycine has been investigated.[155] Whereas the absence of asparagine as the main source of intracellular nitrogen led to growth arrest and dramatic pyruvate uptake increase, the absence of serine was also negative for cell growth and could trigger its *de novo* synthesis. In the case of glucose or glutamine starvation, for example if levels of the same are kept low to reduce lactate or ammonia accumulation, hybridoma cells have been shown to induce apoptosis by both mitochondria and death receptor pathway.[156] Similar responses are observed when CHO cells starve during prolonged cultivation when nutrient gets depleted and waste products accumulate.[157] A newer study describes feeding strategies to reduce apoptosis and autophagy towards the end of cell culture and discusses further nutrient deprivations that can cause cell death.[85] Not only the lack of organic nutrients but also Ca^{2+} and Mg^{2+} deficiency induces apoptosis by scavenger receptor in CHO cells.[158]

Media impacting recombinant protein quality The discussed examples highlight the fundamental importance of the medium for cell culture performance including cell growth, cell longevity and cell productivity. But not less important is the impact of CDM on the recombinant protein, the final product itself. mAbs HC and LC expression cassettes are typically cloned with an N-terminal signal sequence that directs the nascent protein to the co-translational translocation pathway via the endoplasmatic reticulum.[159] Once the only transmembrane transport step across the ER membrane is finalized the protein can enter in the secretory pathway by vesicular transport and is excreted from the cell into the extracellular matrix.[160] Therefore, the cell culture broth or in other words the CDM that is consumed over time with accumulated waste products is the first extracellular environment the recombinant protein faces. However, not only the chemistry of the extracellular matrix determines product quality because it is predominantly the intracellular protein expression itself that is highly dependent on culture and media conditions. It is important to mention that media compound concentration alterations with impact on product quality can not only occur due to addition or removal in media development. More critical and not predictive, they can also happen due to impurity concentration fluctuation, compound adsorption to for example filter materials, precipitation or further chemical reactions that make the compound or element non-bioavailable. The main quality attributes monitored in recombinant protein analytics are for example glycosylation, deamination, oxidation, C- and N-terminal modification, aggregates, fragments or amino acid misincorporation.[161-163] Since quality attributes are very important for molecule safety and efficacy strategies have been developed to tailor product quality by the cell culture process. One example of a quality attribute

typically affected by medium carbohydrate content is glycation and feed strategies with lowered glucose content have been shown effective to control levels.[164, 165] Another example for a control strategy for product quality is lowering the content of iron and B vitamins in CDM to reduce color.[166] In contrast, antifoam compounds have been found in a screening study to not impact the monomer content (≥95% monomer for all tested products).[167] However, high initial copper concentrations have been correlated with increased basic charge variants.[168, 169] Taurine has been shown to reduce basic charge variants, mainly caused by more efficient C-terminal lysine clipping and decreased oxidant variant levels.[170, 171] A reduction of iron in CDM, that could be for example also caused by precipitation, and a subsequent long term passage adaptation has been shown to increase basic charge variants while improving product color.[172] The removal of β-glycerol phosphate of CDM has decreased basic variants to acceptable levels. Chung *et al.* investigated the impact of the four factors culture temperature, iron concentration, feed media age and antioxidant concentration (rosmarinic acid) on acidic charge variants.[131] They found that processes forming high amounts of acidic peak species and highly glycated protein showed elevated levels of supernatant peroxide or intracellular ROS or both. An increase of tryptophan, copper and manganese concentration in CDM and a decreasing cysteine concentration have been shown to decrease tryptophan oxidation and acidic charge variants.[173] A subsequent study revealed that lowered tryptophan oxidation was mainly correlating with higher expression of genes that are involved in copper transport, glutathione regulation, iron storage, heme reduction, oxidative phosphorylation and Nrf2-mediated antioxidant response and therefore an improved ROS control.[174] Just as charge variants, glycosylation profile has a high impact on drug safety and efficacy including pharmacokinetics and pharmakodynamics.[29, 175-178] As for any post translational modification, if a structure-function relationship is present can be highly molecule specific. As shown by Higel *et al.* the understanding of the effect of N-glycosylation heterogeneities on pharmacokinetics and -dynamics can be challenging.[177, 178] However, evidence that glycosylation profiles have impact on clinical parameters is steadily increasing and a control of glycan species is anyway very important for glycosylated recombinant protein production because of its well-known high potential for immunogenicity.[29] Glycan composition can not only be controlled by expression host selection, glycoengineering or physical process parameter optimization but also by biochemical parameter control during cell culture.[139, 179] It has for example been shown that high mannose species increase with high medium osmolality and that $MnCl_2$ addition can reduce levels of mannose-5.[180] Similarly, Lee *et al.* found that hyperosmolality affected glycosylation by decreasing sialylation.[181] Brühlmann *et al.* have shown that they can promote high mannose glycan species with the target to increase antibody-dependent cell-mediated cytotoxicity (ADCC) by adding raffinose to CDM.[182] Comparably, Hossler *et al.* describe sucrose and tagatose as medium supplements to increase high mannose N-glycan species.[183] Furthermore, multivariate data analysis has found a correlation between glycosylation profile and methionine, threonine, tryptophan, and tyrosine media supplementation.[184, 185] Copper and Iron concentration in media has been shown to impact glycosylation pattern as well.[186] Ehret *et al.* screened a big variety of compounds on glycosylation profile.[187] They found that kifunensine enhanced high-mannose species, 2-F-peracetyl fucose decreased fucosylation and dexamethasone in combination with galactose, manganese and uridine showed an effect on galactosylation.[187, 188] Finally, Purdie *et al.* showed that cysteine and ferric ammonium citrate impacted not only soluble aggregates after harvest but optimized media decreased aggregate formation in drug product in an accelerated stability study.[189]

1.2.2 The history of CDM development for the cultivation of eukaryotic cells

Whereas prokaryotic cells can be cultivated in comparably simple media, as for example Davies minimal broth that consists of only 6 chemical compounds, the media for eukaryotic cells are way more complex.[190-192] The history of animal cell culture media and of media for recombinant protein expression in CHO cells has recently been thoroughly reviewed by Tatsuma Yao *et al.* and by Frank V. Ritacco *et al.*, respectively.[79, 193] Briefly summarized, the story of mammalian cell cultivation began with Sydney Ringers balanced salt solution in 1882 that was able to maintain frogs hearts beating after they have been dissected from the body. After that, further salt solutions, which all have in common that they were of simple composition including only organic salts and sometimes glucose as a nutrient, have been developed. The first experiment that is considered as the beginning of animal cell culture has been conducted in 1907 by Ross G. Harrison. He used lymph, drawn from an adult frog's lymph sacs, and observed a frog nerve fiber outgrowth for several weeks. After that a lot of work has been invested in research on media solutions. An important milestone in media development has been achieved in 1955 by Harry Eagle, who spent a lot of his career on media and cell cultivation.[194, 195] His experiments showed that a minimum of 13 amino acids (cyst(e)ine, tyrosine, arginine, valine, tryptophan, threonine, phenylalanine, methionine, lysine, glutamine, leucine, isoleucine and histidine), 7 vitamins (choline, folic acid, nicotinamide, pantothenate, pyridoxal, riboflavin and thiamine) and salts (Na^+, K^+, Ca^{++}, Mg^{++}, Cl^- and $H_2PO_4^-$) are required by mouse fibroblasts and HeLa cell strains.[194-199] Besides this fundamental discovery for cell culture medium development, Eagle worked on extremely important topics for mammalian cell culture like environment pH, metabolic control or buffer combinations amongst others.[200-222] In the time from 1955 until 1965 several media formulations were developed[79, 193] but they all had in common that a supplementation with serum to support cell growth was necessary. Serum is not only costly and ethically questionable but it is also of undefined origin and bears the risk to increase process variability and the transmission of infectious diseases.[223] From the end of the 1950ties first reports exist of serum free medium with for example Difco Bacto-peptone as a replacement of serum.[224] This is still problematic as these peptones are usually products of non-defined origin like for example enzymatic digests of animal protein. In 1965 Richard G. Ham described a fully synthetic medium (F12) for the cultivation of clonal Chinese hamster cells which worked but growth was still limited.[225] In 1976 three key discoveries for serum free animal cell culture have been published in short sequence. McKeehan, working in Ham´s group, found that selenium is an essential trace nutrient,[226] Guilbert and Iscove partially replaced serum by selenite, transferrin, albumin and lecithin[227] and Hayashi and Sato found that several combined hormones could replace serum.[228] After that, several cell specific serum free media have been developed. For example a medium supplemented with insulin, transferrin and a mixture of nonessential amino acids was sufficient to support serum free antibody production with hybridoma cells.[229] As many cells require insulin, transferrin and selenium for serum free growth a first commercial medium supplement (ITS) for serum free cell cultivation has been developed in 1980.[230-232] Two years later, Murakami *et al.* found that hybridomas essentially required ethanolamine and a follow up supplement (ITES) was developed by his group and found widespread application.[233]

Since the achievement of these major milestones in medium development many media recipes have been developed and optimized for their respective purposes. In appendix Table 15 commercially available CDM for CHO cell cultivation with published media recipes are summarized. The example media shown are Dulbecco's Modified Eagle's Medium with high glucose (DMEM),[66] E-RDF,[234, 235] Iscove's Modified Dulbecco's Medium (IMDM),[236] Nutrient Mixture F-12 Ham[236] and Hybri-Care Medium (ATCC ® 46-X)[237] with their compounds

grouped in salts, amino acids, vitamins and other compounds to improve comparability. Further important media recipes for CHO cell cultivation are summarized and discussed by Ritacco *et al.*.[79] Nowadays, several CDM for recombinant protein production are commercially available but the formulation is usually manufacturer proprietary information and thus not accessible. A comparability study of 8 commercially available products of 6 suppliers has shown that they varied significantly in amino acid composition and the media lead to very different process performances with titers ranging from 1 to 6 g/L after 14 d cultivation.[238] Since media still play a very big role for process performance and robustness and because the cost pressure on biotechnological companies rises the design of new media and improvement of existing formulations is a topic of current and future research.[54] Current approaches include stepwise improvement of existing publicly available recipes,[239] adaptation of existing feed media formulations,[240] application of statistical means as design of experiment,[79] high throughput approaches in cell culture to screen media blends in statistical design space,[241] and for perfusion processes a systematic blending of fed-batch basal and feed media followed by a removal of redundant components and concentration.[141] Beyond new media design approaches the factors that determine CDM stability are drawing more attention nowadays.[242]

1.2.3 Chemical compounds typically contained in CHO cell production media

As an outcome of historical development the media nowadays used for CHO cell cultivation are complex mixtures of 50 to 70 compounds.[79] In the following section the chemical properties and potential reactions of CDM compounds are reviewed.

Water – matrix of life

Aspects for cell culture media: Water is not only a passive solvent but it is an important participant in the "life of the cell" because of its structural and dynamic characteristics.[243] Since mammalian cells can be highly sensitive to water impurities typically high purity grades as water for injection are used for CDM preparation.[79]

Chemical properties: Water is a complex and structured liquid.[243] Furthermore, it is a polar, protic and amphoteric reagent.

Energy and carbon source (carbohydrates, glutamine and glutamic acid)

Main compound(s), and aspects for cell culture media: Heterotrophs as mammals need energy rich chemical structures to derive energy of coupled redox reactions. Glucose is, especially in CDM, the main carbon source used.[79] It is imported over the cell membrane by glucose transporter GLUT1 and is either entering the tricarboxylic acid (TCA) cycle via pyruvate or is converted to lactate in aerobic glycolysis.[79, 244] Other saccharides can be used to replace or supplement glucose in media.

Additionally to carbohydrates, CHO cells require glutamine as energy source. It is metabolized by glutaminolysis and enters the TCA cycle as α-ketoglutarate.[79] This reaction is the main source of ammonia. Alternatively, glutamate can be used. This is of special interest for CHO cells transfected with glutamine-synthetase selection system.[245]

Another energy source that prevents ammonia production from glutaminolysis is sodium pyruvate.[79] It can enter the TCA cycle and is an intermediate in lactate formation.

Chemical properties and potential reaction(s): Glucose bears an aldehyde group (CH=O) and five hydroxyl (-OH) functional groups. A typical bioprocess related reaction of glucose and carbohydrates is glycation.[164, 165, 246, 247] It is a reaction between a primary amine and an aldehyde

group (e.g. in open ring form of glucose) leading to for example non-enzymatic glycosylation of protein or saccharide-amino acid condensation products.[248-250] It is a reaction mechanism known for a long time and was first described by Maillard and Amadori.[251, 252] The type of functional groups is the same for all saccharides and therefore the expected reaction mechanisms are similar but not identical, as for example reaction rates may be significantly different.[253] Furthermore, carbohydrates are known to be able to form complexes with metal cations.[254, 255]

The chemical properties of glutamine and glutamic acid are discussed in the amino acid section.

Pyruvate is a simple α-keto acid with a carboxylic acid (C(=O)OH) and a ketone functional group (R(C=O)R). As other α-keto acids, pyruvate is known as a scavenger of hydrogen peroxide.[256-259] Furthermore, it has been observed that it can complex Fe^{2+} and Fe^{3+} ions and hints on alterations of redox behavior are discussed.[260] Pyruvate can be decarboxylized under metal catalysis and a conversion to 3-Deoxy-2-C-methylpentaric acid in aqueous storage can be observed.[261] In addition, it can impact transition metal redox behavior and protect from toxic effects of vanadium.[260, 262]

Alternative compounds: Some examples of alternative compounds for energy supply tested in cell culture are the monosaccharides galactose,[79] tagatose,[183] psicose,[263] disaccharides as fructose,[79] mannose, maltose,[264] sucrose, lactose, trehalose,[265] turanose, palatinose, lactulose,[263] and trisaccharides as raffinose,[182] and melezitose.[263]

Amino acids – starting material for protein synthesis

Main compound(s), and aspects for cell culture media: Amino acid (AA) composition of CDM is very important for cell growth and final product concentration.[79, 137, 155, 266] Not glucose but other amino acids than glutamine are the source of mammalian cell mass.[267] All the proteinaceous AAs and hydroxyproline are typically used in CDM in different ratios and concentrations.[268]

L-cysteine is especially in focus in media development because it belongs to the essential amino acids for cells in culture (amongst them CHO cells) and has high reactivity due to thiol group. It is one of the least abundant amino acids but in the same time one of the most conserved in protein because of its unique functional group.[42, 269] Due to the special chemical properties of the thiol group it imparts in functional sites. For example in a classical IgG1 mAb each of the 11 L-cysteines on the heavy chain and 5 L-cysteines on the light chain are involved in disulphide bond formation which are essential for tertiary and quaternary protein structure.

Chemical properties and potential reaction(s): The functional groups each amino acid has are an amine (NH_2) and a carboxyl group (C(=O)OH). Side chain functional groups of the 20 proteinogenic AAs include nonpolar AAs with hydrophobic side chains including alkyl groups, aromatic groups (phenyl, hydroxyphenyl and indole) and thioether group (C-S-C), hydrophilic AAs with neutral but polar groups as hydroxyl (OH) and sulfhydryl groups (SH), hydrophilic AAs with acidic and negatively charged carboxyl side group (C(=O)OH), and hydrophilic AAs with basic and positively charged amine (NH_2) groups. AA chemistry is a topic with a long history in science.[270] AA solubility,[271-273] complex formation with metal ions, mixed crystal formation and stability[274, 275] has been reviewed in 2016 by Andrew Salazar *et al.*[268] The effect of ROS mediated oxidation of free amino acids leading to aromatic group hydroxylation or nitration, nitrosylation of sulfhydryl groups, sulfoxidation of methionine, chlorination of aromatic groups and primary amino groups and conversion of some amino acids to carbonyl derivates was reviewed by Stadtman and Levine.[276] Metal catalyzed oxidation of AA and tautomerization were also a subject of relevant

studies.[276, 277] Specific amino acids have been investigated on their individual reactivity in model systems.[278-294]

Alternative compounds: Dipeptides,[197, 295] polypeptides,[294, 296-298] s-sulfocysteine[299] and the modified tyrosine derivate phosphotyrosine with improved solubility[300, 301] have been tested in cell culture.

Vitamins – Enzyme cofactors and antioxidants

Main compound(s), and aspects for cell culture media: Vitamins can typically not be synthesized by cells and essential ones for cell culture have been described by Eagle. In the cells vitamins fulfill functions as coenzymes, prosthetic groups or cofactors in enzymes and in the medium they can protect cells from oxidative radicals due to high reductive capacity.[79, 302] Even though their concentration is typically low in CDM they are important for cell culture.[303] Typical vitamins used in CHO cell culture are biotin, folic acid, inositol, niacinamide, choline,[138, 304, 305] 4-aminobenzoic acid, pantothenic acid, pyridoxine, riboflavin, thiamine, cobalamin[79] and vitamin C.[306]

Chemical properties and potential reaction(s): The vitamins used in cell culture are structurally very heterogeneous. Some examples for potential reactions vitamins could undergo in CDM shall be discussed. Very well known to cell culture engineers is the photosensitivity of riboflavin that can act as a sensitizer in the formation of ROS.[274, 307-309] Furthermore, most of the vitamins are described as antioxidants and therefore for most of them redox reactions are described.[127, 310-323] Thiamine has been described to complex metal ions.[324-329] Cobalamins are photosensitive as well, can degrade in aqueous solution and can react with protein.[330-333] Pyridoxal, pyridoxine and pyridoxamine are involved in transamination reactions that can be photoinduced, can act as glycosylation inhibitors or complex metals.[326, 334-345]

Salts – osmolality, cellular membrane potential and buffering

Main compound(s), and aspects for cell culture media: Bulk salts (e.g. Na^+, Cl^-, HCO_3^-) contribute the most to the osmotic balance of unspent medium.[42, 79] Na^+ and K^+ are important for the maintenance of the transmembrane potential, Mg^{2+} conjugates with DNA and has effects in cell adhesion, PO_4^{3-} is important for nucleotide formation, Ca^{2+} is involved in signaling and cell adhesion. Furthermore, ions as HCO_3^- and HPO_3^{4-} are important for medium buffer capacity. Studies on CHO cells have shown that the sodium to potassium ratio can impact productivity and cell growth.[346, 347] Strategies to adapt CHO cells to phosphate limitations have been developed and subsequently improved growth characteristics in repleted media.[348] At low Ca^{2+} and Mg^{2+} concentrations the cell growth slows down.[349]

Chemical properties and potential reaction(s): Water readily dissolves salts because of its polar nature and anions and cations are formed. Because of the water polarity a hydration shell is formed for each ion. The coordination numbers can be individual to each ion and can also be dependent on the properties of the solution (osmolality etc.).[350-353] When ions form in aqueous solution from dissolving salts, for example the sodium atom (Na: $1s^2 2s^2 2p^6 3s^1$) of NaCl achieves an octet in its outermost shell by losing one valence electron. The sodium ion (Na^+: $1s^2 2s^2 2p^6$) loses its electron to the chlorine (Cl: $1s^2 2s^2 2p^6 3s^2 3p^5$) of the salt lattice and this forms a chloride ion in aqueous solution that has one negative charge (Cl^-: $1s^2 2s^2 2p^6 3s^2 3p^6$). Because the vast majority of bulk salts fulfill the noble gas electron configuration upon dissolution they are rather stable.

The numerous solubility charts or solubility tables published show various combinations of ions formed by bulk salts in CDM that can form poorly soluble or insoluble ion combinations. The most

relevant solubility rules for CDM are that compounds that contain the ions Na^+, K^+, NH_4^+, Cl^- and SO_4^{2-} are soluble and that compounds that contain sulfides (S^{2-}, except of Na^+, K^+, NH_4^+, Mg^{2+}, Ca^{2+} and Ba^{2+}), carbonates (CO_3^{2-}, except of Na^+, K^+ and NH_4^+), phosphate (PO_4^{3-}, except of Na^+, K^+ and NH_4^+) or hydroxides (OH^-, except of Na^+, K^+ and NH_4^+) are insoluble. These rules of thumb are published in several textbooks and give a good estimate for the susceptibility of a compound mixture to precipitate. But the details may have to be checked individually for each combination.[354] The versatile combinations that can form preciptate shows how important a well-balanced salt composition is for stable medium formulations.

Transition metals – important cofactors for enzymes

Main compound(s), and aspects for cell culture media: The trace metal content of cell culture media has drawn a lot of attention in the recent past.[186] The major trace elements used in CHO cell culture media are Cu, Fe, Zn, Mn, Mo, Se, V and Co.[79] A very good introduction to trace element functionality in CDM and typical concentration ranges are listed by Ritacco *et al.*, but since it is a topic of high interest for cell culture engineers a couple of more studies have been published. The importance of trace elements in cell culture media has been emphasized by studies that describe approaches to specifically remove the metals.[355, 356] The effect of copper on cell culture, gene transcription, cell energy metabolism with a focus on lactate, product quality (e.g. glycosylation, charge variants and open thiols) and molecular uptake mechanisms into the cell have been studied.[152, 154, 168, 169, 357-365] The provision of cells with iron in a soluble and bioavailable form is a big challenge in CDM development. Since the bioactive form Fe^{3+} readily forms insoluble ferric oxyhydroxide ($Fe(OH)_{3(s)} \leftrightharpoons Fe^{3+} + 3\ OH^-$ reaction equilibrium is far on the left side)[366] it is typically added with chelator, as Fe^{2+} or in the early days of CDM development with the iron-transport protein transferrin.[367-376] Multiple enzymes in the cell are dependent on iron[377] and amongst the effects of iron in cell culture are an inhibition of polyethylenimine-mediated transient transfection,[378] the modulation of uptake by polyamine,[379] dose dependent differentiation,[369, 380] or effects on product quality as glycosylation and color.[166, 172, 381] Likewise, the effect of Zink on metabolism, glycosylation and as a replacement of insulin has been investigated.[382-386] Manganese has drawn a lot of attention in protein glycosylation studies.[188, 387, 388] On the contrary, the number of reports available on the effect of molybdenum in cell culture is small, even though it is essential in almost all biological systems because of its involvement in carbon, nitrogen and sulfur metabolism.[389] The fact that selenium is essential for many cultivated cells is known for a long time and therefore the roles of selenium in cell cycle, apoptosis and the usage of selenite as an iron carrier have been discussed.[226, 390, 391] Vanadium itself is known for its cytotoxicity on CHO cells that is increased by inorganic selenium or mitigated by pyruvate.[262, 392] Even though no essential function[392] of the element is known for higher animals it can be used in cell culture to mimic the metabolic function of insulin and enhance cell growth.[79] Similar to other trace elements cobalt is actively taken up by CHO cells and has been reported to have effects on glycosylation profile (in one study along with nickel, effect reverted by uridine and galactose), transcriptomics and proteomics in cell culture.[393-396]

Chemical properties and potential reaction(s): With the exception of Se, a nonmetal belonging to the chalcogens that can be compared to sulfur,[397] all the discussed trace metals belong to the d block metals. According to the IUPAC definition elements of the periodic table d block, which form one or more stable ions with incompletely filled d orbitals, are called transition metals. Because of their incompletely filled d orbitals upon dissolution the elements Cu, Fe, Mn, Mo, V and Co function as good catalysts and can readily change oxidation states. Therefore, the elements are involved in a wide range of chemical reactions and many of them are relevant for CDM matrix. Amongst the many chemical reactions transition metals are involved are redox

reactions with organic molecules,[260, 313, 398-407] reactions like Fenton reaction that form radicals,[404, 408-418] photochemical reactions[419, 420] and, due to their charge, complex or precipitate formation.[366, 403, 421-430] Especially radicals formed in a reaction can induce further downstream chemical modification of other compounds, start a chain reaction and become toxic.[276, 410, 411, 431, 432]

Lipids - major building block of cell membranes

Main compound(s), and aspects for cell culture media: The most commonly used lipid precursors in cell culture are choline and ethanolamine.[79, 433] Even though CHO cells can synthesize lipids, these compounds can show positive effects in cell culture. On a cellular level lipids have important functions as the main constituent of membranes of the cell membrane, endoplasmatic reticulum and Golgi apparatus. Several compounds like cholesterol, triglycerides and phospholipids have been applied in media and effects on glycosylation could be observed.[434-436]

Chemical properties and potential reaction(s): Lipids are defined as compounds that are soluble in nonpolar solvents and not or very poorly soluble in water. It is a chemically quite versatile group that includes fatty acids, glycerolipids, glycerophospholipids, sphingolipids, sterol lipids, prenol lipids, saccharolipids and polyketides. As the bad water solubility of lipids can cause precipitate formation in CDM they have to be used with care. Therefore, most media use either choline or ethanolamine which have better solubility. Ethanolamine has a low stability in media because it can degrade in the presence of amino acids and methods to stabilize it have been developed.[437] In solid state, choline has been reported to be radiosensitive and degrade into trimethylamine and acetaldehyde and if not adequately stored this may happen in aqueous solution, too.[304, 438]

Polyamines

Main compound(s), and aspects for cell culture media: Polyamines are important for e.g. DNA synthesis and transcription, cell signaling, ribosome function and ion channel regulation.[79] In mammalian cells most polyamines are synthesized from ornithine in the urea cycle. Most commonly used exogenous polyamines to supplement CDM are putrescine, spermidine and spermine. They have been shown to impact cell growth and viability positively but at too high concentration they can readily reach a level of cytotoxicity. An inhibition of ornithine decarboxylase by retinoids in CHO cells increased transglutaminase activity and impacted cell proliferation and differentiation.[439]

Chemical properties and potential reaction(s): L-ornithine is a non-proteinogenic amino acid that is very similar to lysine. The chemical properties are therefore as described in the amino acid section and due to its two primary amine groups it can be expected to be prone to undergo Schiff base formation. Putrescine has been shown to have capabilities to protect protein from glycation and prevent the formation of fluorescent advanced glycation end products (AGE´s).[440] This anti-glycation property could be confirmed in media with high glucose.[441] Pyrrolin and Piperidein have been described as enzymatic oxidation products of putrescine and cadaverin.[442]

Growth factors

Main compound(s), and aspects for cell culture media: Compounds with growth promoting effects used in cell culture media are usually peptides, small proteins and hormones.[79] Most of these growth factors were very important for the adaptation of mammalian cells to serum free growth media. Today, the most commonly used growth factor in industrial cell culture is recombinant insulin.[443] The effects of insulin on CHO cells are well studied. It promotes cell survival, receptor activation and second messenger pathways.[444, 445] The absence of insulin was described to induce alteration in cellular morphology.[446] Approaches to mimic insulin functionality with metal complexes and metals have been described.[447-449]

Chemical properties and potential reaction(s): The chemical properties of insulin are mainly determined by its amino acid functional groups and the protein conformation. It has been shown to have an affinity to metal ions, especially zinc and copper.[450]

Dissolved gases

Main compound(s), and aspects for cell culture media: Oxygen as the final electron acceptor in the respiratory chains of aerobic cells is absolutely indispensable for normal cell function. In CHO cell culture a correlation between nutrient concentration in CDM and oxygen uptake could be detected in batch and perfusion process. However, effects of reduced dissolved oxygen became only evident if below 5% of air saturation.[451] Interestingly, approaches to improve oxygen supply to cells in cultures include the supplementation of media with fluorinert, a perfluorochemical that functions as a gas carrier.[452-458] Studies with TES and HEPES buffer systems showed that CO_2 is essential for cell growth.[78] In high density large scale cultivation pCO_2 in a range between 30-76 mm Hg seems to be ideal for CHO cells.[459] Furthermore, pCO_2 had an apparent impact on lactate metabolism shift.[150]

Chemical properties and potential reaction(s): Especially dissolved oxygen can readily form reactive species in aqueous solution. Hydrogen peroxide formation has been demonstrated in natural waters upon irradiation with sunlight.[460] Furthermore, ROS can be readily formed as products of metal catalyzed oxidation reactions.[411, 461, 462] Besides their function as messenger in cellular signal transduction ROS can have highly cytotoxic effects and show high reactivity towards organic molecules.[276, 431, 432, 463]

Compounds without nutritional functions and compounds not suitable to other groups

The main functions of compounds that are considered to have no nutritional effect are buffering of pH, mechanical stress protection and antifoaming.[79] Typically used buffering compounds for cell culture media are bicarbonate (CO_2/$NaHCO_3$), phosphate, TES and HEPES.[77, 78, 464, 465] Agents with surfactant properties commonly used in cell culture are poloxamers as Pluronic F-68. They are supposed to protect cells from effects of bubble aeration and reduce cell adhesion.[466, 467] It has been shown that Pluronic F-68 gets internalized by CHO cells and thus shear protection effects can alter over culture time.[468] The importance of poloxamers for cell culture gets emphasized by screening systems that have been applied to investigate lot-to-lot variation in the raw material used to control cell damage.[469] Another compound used to prevent cell aggregation is dextran sulfate.[470] Foam formation during biotechnological processes remains a major challenge and several antifoam formulations have been developed.[471] However, the silicone polymer-based antifoaming agents have been reported to impact cell viability, productivity and downstream processing.[167]

Other compounds that have been applied in cell culture are alkanoic acids, as sodium propionamide, to decrease growth and improve titer.[472] Other strategies include the feeding of

organic acid lactate.[473] Furthermore, growth promoting effects of lysolecithin have been shown on CHO cells.[474]

Reaction products and impurities – unforeseen effects on cell culture

The chapter gives an overview of the versatility of chemical compounds used in CDM. The large number of compounds in media recipes and the wide ranges of concentrations makes CDM highly complex chemical mixtures (Examples for media recipes used to cultivate CHO cells are given in appendix Table 15). The diversity of chemical structures and structural relationships of CDM compounds is illustrated in Figure 2. The three major branches separate organic compounds without ring structures, inorganic salts and organic aromatic compounds. The eight colors in the dendogram symbolize structurally related compounds clustering. Especially in the case of feed- and perfusion media the concentrations of compounds can be very high and close to solubility maxima. Simply because of the increased likelihood of molecules to collide high concentrations even increase the potential for chemical reactions in solution. This chemical complexity is even increased if impurities of the individual compounds are present and therefore the manufacturer of CDM powders put a lot of focus on the characterization of raw materials.[475] Not only cellular metabolism during culture can generate growth inhibitory compounds or compounds that become reactive and negatively impact product quality[314, 476] but also within the chemical matrix reaction products can be formed. A well-known example for chemical degradation in CDM that will be discussed in more detail in a following section is the photosensitized degradation of amino acids in the presence of riboflavin.[274, 309] Furthermore, compounds as pyruvate, bicarbonate and glutamate have been described as factors that determine the stability of highly concentrated media.[242] Kuschelewski *et al.* reviewed several reports that indicate that CDM itself is a source of reactive species.[477] Main factors impacting the formation of reactive species were medium age, storage conditions and light exposure.

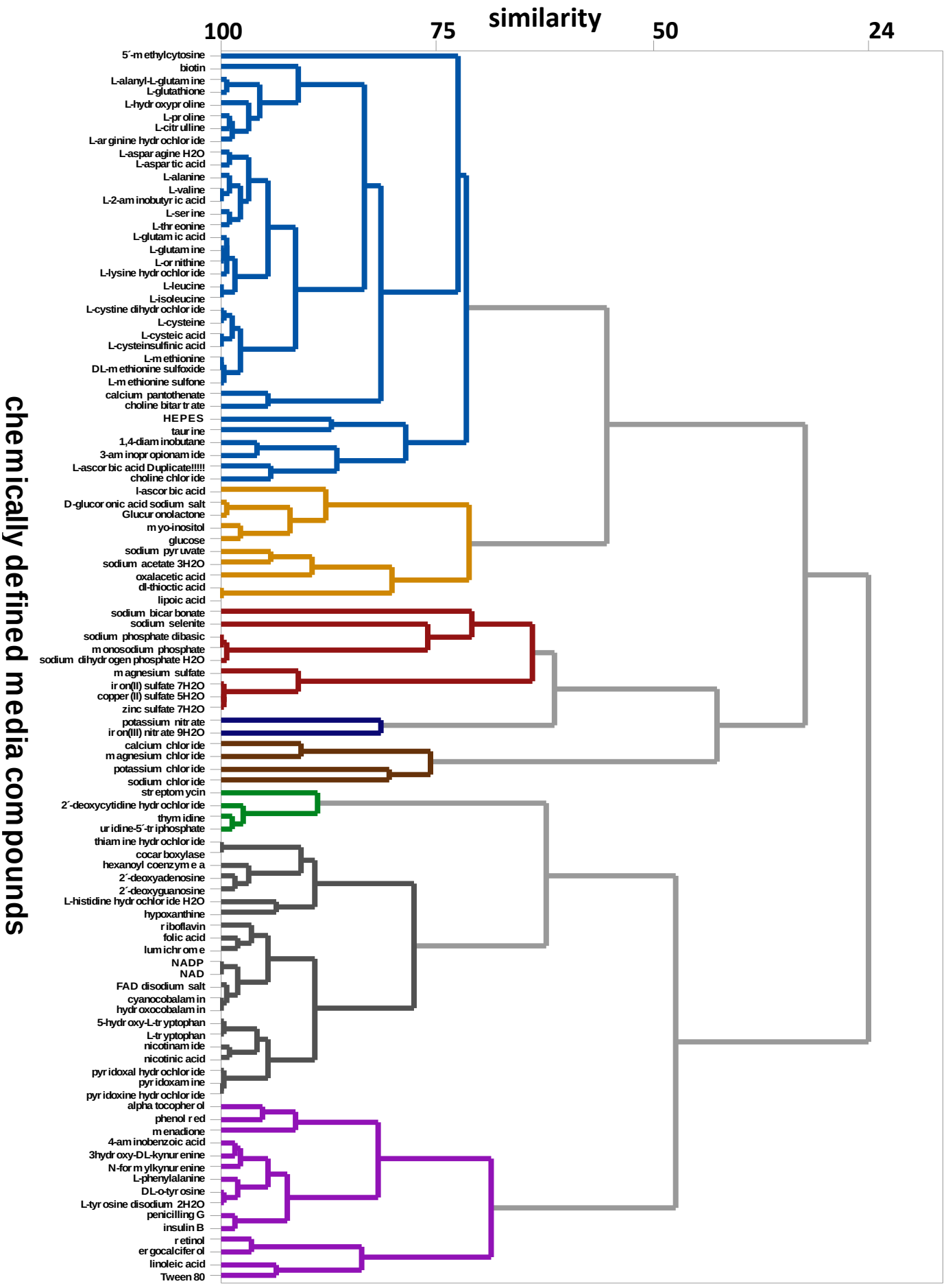

Figure 2: Typical compounds used for CHO CDM plotted by similarity index showing the diversity and high complexity of chemical compound structures mixed together in one solution. The clustering of compounds symbolized by the eight different colors shows structural relationships.

1.2.4 Challenges with CDM in the bioprocess

Media are the basis of each bioprocess. Therefore, reproducible media is fundamental for robust process performance. However, the chemical versatility of CDM and thereof resulting effects bear challenges for robust bioprocess development.

CDM preparation for bioprocess development and at-scale manufacturing from dry basal powders

Considering the complexity of CDM recipes it is easy to imagine that adding each medium compound separately is extremely time consuming and error prone work. In order to facilitate medium preparation, the majority of the recipe is manufactured dry. Each individual compound is scaled according to the recipe and milled to a powder.[478] The resulting product is the medium basal powder. The CDM dry powders offer big advantages in storage and handling. Briefly described, storage gets simplified by less need for individual vessels for media compounds. This saves storage space and facilitates warehousing. But more importantly, the usage of CDM dry powder reduces the amount of weighing positions in medium makeup. The addition and dissolution of one powder is much simpler and more robust than the scaling and addition of 50 to 70 individual compounds. Therefore, this approach saves not only time in medium preparation but also mitigates the risk of false powder weighing. One approach to make medium preparation reproducible is to define criteria for the addition time point of compound addition. An example of such a rule is that a subsequent recipe position is only to be added when the previous one is visually entirely dissolved. Even though preparation from one basal powder is technically feasible, especially in process development not all required CDM compounds are milled. This is mainly due to stability issues of individual compounds in the powder, negative effects on powder properties or to increase flexibility during process development. Thus, the next compound or powder is added if the previous is visually completely dissolved and a homogenous solution/suspension is formed. Even though the medium preparation from dry basal powders has many apparent advantages over single compound addition the milling and powder compaction is challenging and needs to be as robust as possible. Hence, the process variance at the basal powder supplier can be a source of lack of bioprocess robustness. It also has to be mentioned that the storage and handling of CDM in the dry powder form bears the risk of segregation leading to inhomogeneity.[478, 479] But since the advantages of CDM dry powder surpass the risks in manufacturing it is a widely and routinely used practice in biomanufacturing.

Critical factors during powder dissolution and prepared media storage with potential impact on CDM matrix and stability

For decades, the focus in medium development has been on cell proliferation, cell viability and titer improvement. This led to highly complex media formulations and especially high concentrated feed or perfusion media. Even though the total composition of media has become simpler through the exclusion of undefined raw materials as serum or hydrolysates, their missing function as supporting agent, buffer of chemical reactions or carrier of compounds has raised further challenges in media preparation. In this thesis, two distinct CDM feed formulations with different basal powders have been investigated on their phenomena during medium preparation and storage in detail. As the CDM´s chemical composition in its entirety is ultimately defined by all the physico-chemical influences during preparation and storage it is critical to evaluate process related factors on their criticality. With the nowadays routinely used equipment for CDM preparation there are several parameters that can be controlled well and others that generate trouble either at small scale, large scale or both.

A major factor that can impact CDM matrix and stability are impurities. A prerequisite for preparation of medium with the desired properties is the avoidance of process related or non-process related impurities because any unexpected change in chemical composition can alter the CDM properties and subsequently can have an impact on cell culture. Impurities, or more specifically any compound that is not part of the recipe and of external source, can have several origins (Table 2). But also compounds that are expected to be in the CDM can originate from undefined sources and lead to unexpected concentration levels. A very critical source for impurities is the raw materials.[480, 481] CDM basal powder manufacturers started programs to characterize impurities in high risk raw materials.[475] Especially salts that are manufactured from ores can be a source for unexpected compounds. Similar, water can be contaminated with unwanted chemical compounds and therefore highest standards are applied to get the solvent as pure as possible.[79] But also process related impurities on equipment and extractables and leachables (E&Ls) mainly from single use plastic material can be sources of unwanted impurities. Strategies to mitigate these risk factors continuously evolve whereby most activities for that kind of improvements are not in the hands of the biomanufacturer. In contrast, the preparation of CDM is something that can be well controlled with dual control, process control systems and the definition of powder amounts that are reasonably to handle over different scales. The preparation equipment is in theory easily exchangeable but especially in existing large-scale GMP facilities this can be quite complicated and expensive. Therefore, biomanufacturers sometimes use mathematical models to simulate and optimize mixing properties in order to improve CDM homogenization. A highly critical factor for CDM and cell culture is pH. The pH of the CDM is not only determined by the compounds added to the medium but also by dissolved gas concentration because of the CO_2/HCO_3^- equilibrium. During preparation most media have an acidic pH. Therefore, the equilibrium of the chemical reaction $CO_2 + H_2O \leftrightharpoons H_2CO_3 \leftrightharpoons H^+ + HCO_3^-$ is on the left side since the pka of carbonic acid is 6.1. Mixing can lead to either gas saturation or gas stripping effects. If extensive stripping occurs by high vortex formation through stirring the pH and buffer capacity of the medium can be impacted. pH is not only highly relevant for cell physiology but also for each chemical reaction with involvement of hydrogen or hydroxide ions as reactants or catalysts. In chemical reactions with electron-transfer steps that are accompanied by proton transfer the pH can determine the reaction rate.[482] As dissolved molecular oxygen is a precursor of ROS that can be formed by photolysis, electron or energy transfer reactions mixing also influences the concentration of a precursor for reactive species.[483] During the course of CDM shelf life dissolved gases play not only a role during preparation but also during storage. This of course depends on the type of storage vessel. But for example, in the case vessels are equipped with sterile filters to allow for pressure balance during feeding continuous gas diffusion into the CDM is possible. Another critical factor that can impact concentration of compounds in CDM is the sterilization. Two commonly applied techniques are sterile filtration or high temperature short time (HTST) pasteurization but also alternatives like UV irradiation have been tested.[484-487] However, both main techniques can cause issues during media preparation. Filter materials are known to adsorb metals, release contaminants or clog from contaminating materials.[488, 489] Similarly, HTST is known to increase Maillard product concentration and lead to precipitate formation.[490, 491]

As a typical CDM formulation contains 50 to 70 compounds that can be of distinct chemical characteristics the potential for chemical reactivity in solution is high. This is even true if no unexpected changes occur due to impurities or process related factors. CDM matrix and the concentration of components or CDM stability is inherently combined with chemical reactions. Thus, an evaluation of critical factors for CDM quality during preparation and over storage time

until usage has to be based on chemical aspects. The main physical parameters that determine if a chemical reaction is happening at which rate are pressure, temperature, activation energy and concentration of reactants or catalysts. Pressure increases the rate of chemical reactions if gases are involved but changing pressure has negligible effect on reactions that involve only solids or liquids. The environmental temperature of a reaction mixture determines how much energy is needed to overcome the energy barrier to start a reaction and how likely a collision of molecules is. Typically, the activation energy for a reaction system is heat but other mechanisms of providing energy to reaction systems are known. In the case of photochemistry for example this can be radiation. The reactant concentration directly impacts the collision frequency. Catalysts increase the proportion of collisions that result in reaction by providing a reaction mechanism with decreased activation energy. If the concentration is in the right balance to the reactants this will further increase the reaction rate. In summary, rates of simple A + B elementary reactions are determined by collision frequency, steric orientation of reactants and the fraction of collisions with an energy above activation energy level. Therefore, concentration of compounds is not only critical for CDM stability and matrix because they can have effects on cell culture themselves but also because the concentration of compounds (reactants or catalysts) is a critical factor that impacts reaction rates. This means that any unexpected concentration change of expected or unexpected compounds can shift reaction equilibria, impact chemical matrix and can thus have negative effects on batch to batch comparability. The rate of chemical reactions can also be determined by temperature. A widely used rule of thumb derived from the Arrhenius equation says that an increase of temperature by 10 °K approximately doubles the reaction rate. The temperature during CDM preparation is extremely complicated to control because preparation vessels both in small- and large-scale are typically not equipped with heating devices. Especially feed media are highly concentrated and in order to dissolve the powders faster cell culture engineers tend to use pre-heated solvent. But as mentioned the unavailability of temperature control causes the liquid to cool down during preparation. This effect is emphasized since most raw materials are stored in the cold room until used. In large-scale preparation the filling of the tank with WFI can take several hours. Thus, it is hard to estimate at what temperature the WFI has to be tapped to reach the right temperature when the CDM preparation begins. Therefore, CDM preparation temperature can be highly variable and especially in GMP large-scale facilities it is extremely difficult to control. Due to the high potential impact on chemical reactivity this factor is highly critical for cell culture engineers and requires deeper understanding. Temperature does not only impact chemical reactions by increasing the likelihood that molecules interact by molecular motion but it is also important as activation energy. Effects of elevated temperature becomes for example obvious when media is heated.[490, 491] Another highly critical factor that impacts CDM is light as activation energy. The fact that light induces degradation of media is known at least since the early 1990ies.[492, 493] Compounds as riboflavin, tryptophan, histidine, HEPES and folic acid are known to induce negative light induced effects in cell culture media[274, 307, 308, 477, 494, 495] and ROS formation is known to be impacted by light.[496] However, this highly critical factor for CDM matrix with known detrimental effects on cell culture can be well controlled by protecting the media solutions from light by non-transparent vessels or light protecting covers.

Table 2: Critical factors impacting CDM matrix and stability in liquid medium formulations.

	Critical factors	Control strategy	Impact on bioprocess robustness / Controllability / Responsible organization
Concentration (reactants and catalysts)	Amount of impurities in raw materials (e.g. metals)	Auditing of raw material suppliers / raw material suppliers develop strategies / analytics to control impurity levels[475]	High / Medium / Supplier
	Purity of water	Application of high-standard WFI production methods and equipment	High / Good / Biomanufacturer
	Process related impurities on media preparation equipment and in storage vessels	Well-defined cleaning procedures and thorough application thereof or usage of single-use equipment	High / Good / Supplier
	Extractable and leachable (E&Ls) compounds of equipment get released into CDM (mainly plastic based single use equipment)[497-500]	E.g. usage of plastic films to prevent the release of E&Ls[501]	High / Good / Supplier
	Identity and amount of powders / compounds added to solutions	Process control systems that ask the operator to confirm powder identity by scanning a barcode, qualified scales and process control system asks for scaling result	High / Good / Biomanufacturer
	Preparation tank geometry can impact mixing properties (concentration gradient)	Qualified equipment in manufacturing facilities often not easily exchangeable, CFD simulations and adjusted stirring	Medium / Difficult / Biomanufacturer
	Mixing rate: - concentration gradient - impact on dissolved gas concentration → impact on pH (CO_2) and redox potential (O_2)	- Simulation of mixing properties in tanks and definition of stirrer rate (power input per volume) - Avoidance of vortex formation during media preparation → buffer capacity in CDM formulation	- Medium / Good / Biomanufacturer - High / Good / Biomanufacturer
	Removal of compounds by adsorption to filter membranes[488] or removal of compounds that form precipitates during preparation and clog filters	Evaluation of filter material and development of CDM without precipitate formation	High / Difficult / Filter supplier and Biomanufacturer
	Exposure of CDM to air during storage	Control of storage vessel headspace and careful usage of vent filters	Medium / Good / Biomanufacturer
Temperature	Over the time of preparation: media preparation equipment does not have temperature control but compounds dissolve better at elevated temperatures	Tapping at defined temperature and timing of media preparation duration on experience	Unknown / Difficult / Biomanufacturer
	Over the time of storage	Controlled storage temperature at 2-8°C for longer term storage and at room temperature in the case of feed media during cell cultivation	High / Good / Biomanufacturer
Activation	- Temperature (preparation and storage) - Energetic radiation (e.g. ultraviolet radiation, visible light or infrared radiation)	- Compare to temperature - Reduction to minimum (stainless steel vessel at scale, light protection small scale model, light protection during storage)	- Compare to temperature - High / Good / Biomanufacturer

1.3 Analytical methods for the characterization of CDM

The multitude of critical factors show the versatile opportunities to induce chemical variability in CDM. In order to control effects on process performance, process robustness and product quality the application of analytical methods is fundamental. Up to today, the only routinely measured and monitored quality parameters of CDM are osmolality and pH. The increasing evidence for product changes caused by chemical modification or conjugation with CDM reaction product underlines the need for appropriate analytics to monitor CDM matrix.[1] Spectroscopic approaches have been widely used to characterize media raw materials.[481] Trunfio *et al.* used the four spectroscopic technologies near infrared (IR) spectroscopy, middle IR spectroscopy, Raman spectroscopy and fluorescence spectroscopy in combination with chemometrics (principal component analysis) to characterize the variability of wheat hydrolysates.[480] Similarly, Boyan Li *et al.* developed a CDM characterization and control strategy using Raman spectroscopy and chemometrics.[502] They mentioned the chemometric processing of spectral data as the key element to use it as robust method in routine applications to eliminate baseline drift, background fluctuations and other instrumentation artifacts. Even though extremely useful for batch to batch comparability and fingerprinting in routine applications the vibrational spectrometry approaches can be non-specific for some chemical compounds and are generally more used for characterization than for quantification.

Mass spectrometry (MS) based methods have been developed to specifically quantify the ratio of cysteine and cystine in complex defined media feedstock.[503] This approach emphasizes the big interest of the cell culture engineer for quantitative compound concentrations in the media matrix. But also other MS based methods have been shown to be capable to quantify compounds as amino acids or glycated amino acids with high sensitivity in complex matrixes.[504, 505] In the case of ICP-MS, a special MS technology explained later in the text, the MS detector is applied to quantify metal content in CDM.[186] But MS technology can not only be used for quantification but is also a great tool for unknown compound identification in media matrix with a non-targeted approach.[309, 490] Floris *et al.* demonstrated that untargeted approaches in combination with chemometrics can be useful to identify differences upon exposure to HTST.[490] A LC-MS method that comes close to cover the purposes of CDM compound concentration monitoring and quality determination is the one described by Jinshu Qiu *et al.* from Amgen Inc. in 2016.[506] However, it uses ion-pairing to chromatographically retain small polar compounds. This can cause severe problems as will be discussed later. Thus, an important goal of this thesis was to fill the analytical gap for simultaneous compound quantification to characterize the cell culture media in its most critical process states. In order to characterize CDM further analytical approaches are needed which will be introduced in the following paragraphs. These analytics can be used to characterize media during preparation (probe technologies) or during and after shelf life (at line analytics to track compounds or off-line analytics to identify solid materials).

1.3.1 On-line probes for medium preparation characterization

The opportunity to measure process variables continuous and in real time is highly desired for bioprocess monitoring.[507, 508] Two commonly used sensors in cultivation technology used are pH and DO probes. Since these parameters are of fundamental importance for cell cultivation it immediately suggests itself to use these sensors for the characterization of CDM during preparation. The typically used glass pH sensors are made of glass that contains alkali ions (Na^+ or Li^+). The alkali ions form a thin gel layer on the inner and outer side of the glass (Figure 3 A). This layer acts as an ion exchanger between alkali ions from the glass and the protons from solution. As the inner side of the probe is filled with a buffer the inner gel layer has a constant binding of protons, but the outside proton binding varies with the sample solutions pH. Thus, the

difference in pH between the inner reference solution and the outer sample solution generates a voltage that is read by the pH meter. The oxidative reductive potential (ORP) or Redox potential measurement is a potentiometrical measurement of the oxidizing or reducing power of a solution. The construction of ORP sensors is highly similar to pH sensors (Figure 3 B). The major difference is that the redox sensing electrode is typically made of inert noble metal (e.g. platinum). ORP can be measured relative to any practical or theoretical reference electrode as Ag/AgCl or the standard hydrogen electrode. The probes used in this thesis work with a phermlyte reference electrolyte system. Other probes commonly used to characterize chemical solutions are dissolved oxygen (DO) and conductivity sensors. Modern DO probes work with optical technology. The probe emits a blue light that excites the sensing element (lumiphore) to luminesce and return a red light (Figure 3 C). If no oxygen is present the luminescence signal is at maximum. But as soon as oxygen is part of the system the luminescence gets quenched and signal decreases. Most sensors contain also a red LED for sensor diagnostics. Similarly to ORP probes, the conductivity sensors also often use platinum as electrode material. In contrast, the conductivity is not measured to a reference electrode. In conductivity measurement ions are drawn to the opposite charged electrode (Figure 3 D). This small current in the solution is measured by the meter and since the distance between the electrodes is known the conductivity can be calculated in Siemens per centimeter. Since all measurement parameters discussed so far are temperature dependent these four types of probes contain temperature sensors for temperature effect compensation. A fifth sensor type that has been used to characterize particle size distribution during CDM preparation. The focused beam reflectance measurement (FBRM) has found widespread application in the process analytical technologies for granule formation but also for monitoring of dissolution processes.[509-513] The fundamental measurement principle of FBRM is rotating laser optics that detects the chord length of particles by the reflected light from the particle.[510] The rotating laser optics make the laser light scan a defined circle with a highly specific scan speed (Figure 3 E). The particle reflects light as long as the path of the laser crosses a section of the particle and the reflected light is propagated back into the probe through the sapphire window. The particle size is measured as chord length in µm which is the scanned particle cross section. Chord length is calculated from the time the probe measures reflected laser light and the scan velocity in µm (Formula in Figure 3 E). As described by Kumar *et al.* the measurement signal is impacted by particle shape, particle refractive index, dispersion media refractive index, focal length, suspension concentration, amount of fines and particle size.[510] Furthermore, it has been shown that FBRM technology is sensitive to the presence of air bubbles which can impact the particle size distribution.[514] Salazar *et al.* have shown that FBRM technology was a suitable tool to determine CDM powder dissolution and defined the complete dissolution when the standard deviation of FBRM counts smaller than 10 µm remained below twice the standard deviation at a defined time.[478] The aim of testing FBRM technology in the medium characterization was to determine if the technology was useful to draw conclusions on medium preparation robustness and to visualize effects of compounds on dissolution behavior.

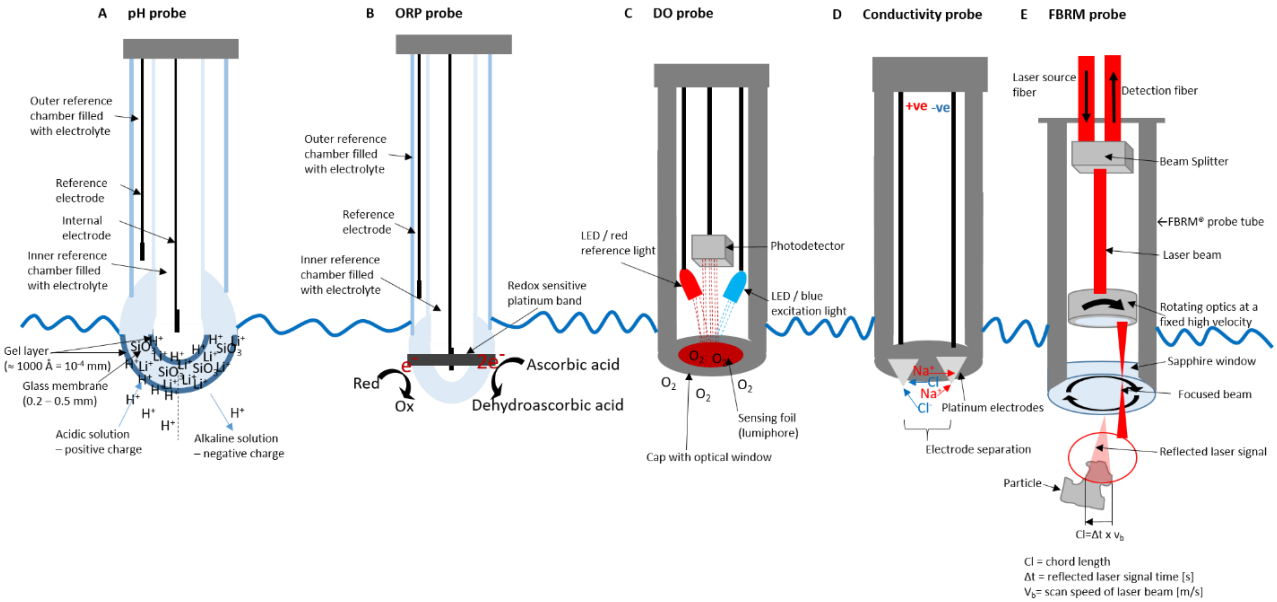

Figure 3: Online probe technologies used for CDM preparation characterization. A) pH probe with pH sensitive glass sensor. Magnification of glass bulb shows how the Li^+ in glass forms the gel layer (dark blue) on the sensor surface. An acidic solution is symbolized by multiple protons whereas the symbolic alkali solution with little or no protons is separated by a dashed line. B) The setup of ORP sensors is highly comparable to pH probes with the major difference that the sensor electrode is a platinum band sensitive for Redox. C) Optical DO sensor that uses a lumiphore to quantitate dissolved oxygen quenching D) Conductivity sensor measures the current between two electrodes in µS/cm. E) shows focused beam reflectance measurement (FBRM) principle and was derived from Kumar *et al.*.[510]

1.3.2 Liquid chromatography triple quadrupole mass spectrometry (LC-QqQ-MS)

Liquid chromatography mass spectrometry (LC-MS) is a widespread analytical technique for the identification of compounds from complex mixtures. The liquid chromatography is a first dimension that allows to separate compounds of a mixture on their distribution coefficient between the stationary and mobile phase. There are several combinations of chemical solid state materials and the selection of mobile phases that determine the chemical separation principle of LC. However, there is no chromatographic method that is ideal for all compound classes.[515] A powerful and widespread (estimated 80% of all HPLC applications[516]) high resolution chromatographic mode is reversed phase (RP) LC. The stationary phase in RP chromatography is typically hydrocarbonaceous with a variety of functional groups with strongly hydrophobic surfaces.[516] Two retention mechanisms are discussed for RP. One states that the solute adsorbs to the liquid-solid interface due to hydrophobic interactions between the nonpolar analyte and the hydrophobic ligates on the surface of the stationary phase. Another claims the partitioning of solute into the bonded stationary phase chains and the transfer of analyte from the bulk solution into a immiscible solvent.[516, 517] Therefore, the mobile phases used for RP chromatography are rarely pure water but rather hydroorganic mixtures or polar organic solvents that cause the "solvophobic" effect. The high volatility of solvents typically used in RP chromatography and their ability to donate protons make it well compatible to atmospheric pressure ionization with electrospray ionization technology. A multitude of methods have been developed and several approaches for method development exist.[518] However, a major drawback of classic RP chromatography is that polar, weakly acidic or basic samples are typically not sufficiently retained or separated.[519, 520] An approach to improve retention of compounds with too polar properties on RP stationary phase is the addition of an ion-pair reagent to the mobile phase.[521, 522] This reagent is typically a lipohilic ion.[523] When the ion-pair reagent is allowed to equilibrate with the column the non-polar end of the compound is strongly interacting with the stationary phase leading to a strong retention while the typically charged end of the molecule is sticking into the mobile phase thus attracting and retaining inversely polar or charged analytes.[524, 525] Since it has been shown

that the simple formation of ion-pairs in the eluent decreases analyte retention the mode should be named ion interaction chromatography. However, the term ion-pairing chromatography meaning the combination of ion-paring reagent with RP chromatography (IP RP HPLC) is most commonly used. A typical indicator for the utility of ion-paring reagents can be if some compounds start to be retained at low pH on RP while others elute at the column dead time. Those non-retained compounds are most likely ionized bases.[525] A major drawback of IP RP HPLC is that it is problematic for robust handling. Two of the multiple examples for problems in handling shall be mentioned. One is that ion-pair concentration in the stationary phase is difficult to control (content in mobile phase, mobile phase organic content, column temperature) and that gradient elution is nearly impossible.[525] Furthermore, ion-pairing reagents are known to be non-removable from the analytical column and the same is true for the LC-MS system. Thus, alternatives to IP RP mode should be considered first and most laboratories would decide for it only if inevitable. An attractive alternative is the combination of several separation modes in one stationary phase. This provides multimodal interactions of the analyte with the solid phase and therefore improves separation of complex analyte mixtures. The last decade has shown that the mixed-mode chromatographic stationary phases have become very popular.[526-528] The column material developed by Imtakt Corp. combines an octadecylsilica (ODS) stationary phase with anion and cation exchange properties. Figure 4 A and B depicts the schematic composition of column material with weak ionic ligands that are adequately bonded to the C18 material. The cartoon symbolizes the ODS ligands in a collapsed state near to the silica gel surface that is caused by strong hydrophobic repulsion by nearly pure water mobile phase.[529] Because of the special composition of the stationary phase polar and non-polar retention can be achieved under RP conditions. However, due to the multimodal properties of the material these mixed-mode columns can be operated not only in RP mode but also in anion and cation exchange and normal phase mode all on the same column. Furthermore, chromatographic methods developed with this stationary phase material can be simultaneously optimized on organic, buffer and pH gradients. The combination of these properties makes the mixed-mode chromatography ideal for a simultaneous analysis of non-polar and polar compounds. For the sake of completeness it shall be mentioned that normal phase chromatography, also known as HILIC (hydrophilic interaction chromatography), offers high potential to separate mixtures of small and polar compounds in combination with MS detector.[519, 520]

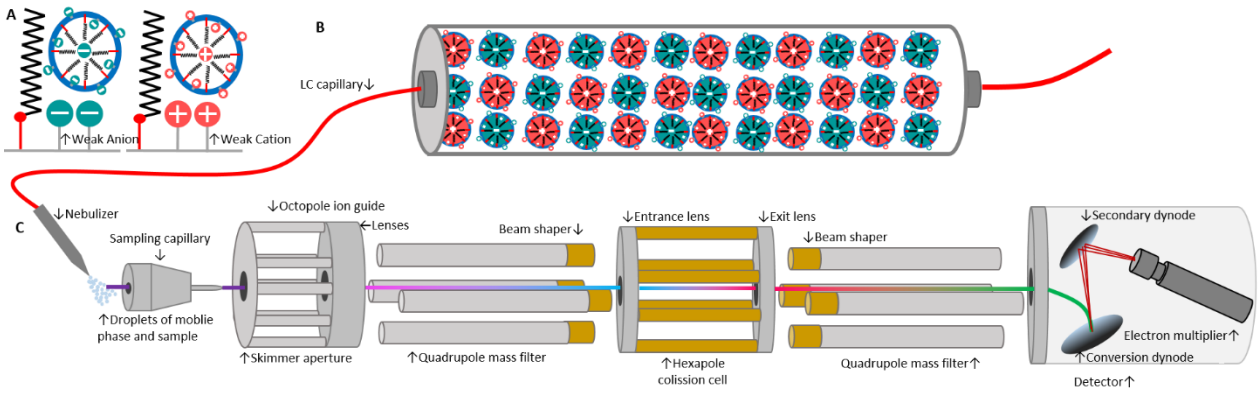

Figure 4: Mixed mode liquid chromatography coupled to an Agilent 6410 triple quadrupole mass spectrometer with an electrospray ionization source.

A) Shows the magnification of the solid-state material of Imtakt Corp. Scherzo SM-C18 mixed mode column. The left side represents the stationary phase of the weak cation exchanger beads with octadecyl residues (black zigzag line) and weak cation residues (green circles) bound on the silica particles. Similarly, the right side shows the surface of the weak anion exchanger beads with octadecyl residues and weak cation (red circles) residues bound on the silica particles (Adapted from a product publication of Imtact Corp.).

B) Illustrated assembly of the bead material in the column forming the stationary phase of the analytical mixed mode column.

C) Schematic illustration of an Agilent 6400 triple quadrupole mass spectrometer with an ESI ionization source. The most important elements along the ion path are shown.

A schematic illustration of a typical QqQ-MS detector for the identification of molecules is given in Figure 4 C. It combines high sensitivity and high specificity with mass resolution and mass accuracy. One of the key elements of MS is the production of gas phase ions. An extensively used soft ionization principle is the electrospray ionization (ESI).[530] Soft in this context means an ionization process that does not break down analyte molecules into fragments because little residual energy is retained by it. Introduced by Fenn *et al.* in 1989, ESI was the first technology to overcome the in-source fragmentation problem. A detailed presentation of the ESI is given in Figure 5 A. Briefly described, the LC eluent gets sprayed into the source by a nebulizer and is accompanied by heated drying gas. The electric potential applied to the capillary tip will cause the eluent to form a Taylor cone that emits a fine mist of droplets.[531, 532] The initial ESI droplets have diameters of several micrometers. Evaporation causes the droplets to shrink and therefore the charge density increases until the surface tension is balanced by Coulomb repulsion. If the Rayleigh limit is reached a fission causes the formation of highly charged daughter droplets.[531] The shrinking of the droplets due to evaporation and fission proceeds until droplet diameters in the range of several nanometers are reached. These ultimately formed tiny and highly charged droplets release molecule ions into the gas phase. As the majority of analytes present in CDM are low molecular weight species they will probably be released by the ion evaporation model.[531] However, ESI is strongly matrix dependent as has been confirmed by many examples described in literature.[533] This is not only caused by co-eluting molecules as described in Figure 5 A but also by for example mobile phase pH.[534] However, matrix effect in MS is not a hindrance for quantitative methods and can be addressed with matrix evaluation experiments.[533]

The history of mass spectrometry can be traced back to the beginning of the 20iest century.[535] The valuable contributions to triple quadrupole development by Enke and Yost in the late 1970ties have helped to turn mass spectrometry to the high sensitivity and selectivity tool with a wide dynamic range in analytical chemistry.[536] The high sensitivity and selectivity, achieved by its ability to select ions from a sample and select fragments of those in a second stage, made it to the workhorse in quantitative mass spectrometry.[537, 538] Before the invention of triple quadrupole MS

the mass spectrometry technology has been mainly used by physical and organic chemists for molecule identification only. An overview of a triple quadrupole MS and the main processes happening in the ion beam are depicted in Figure 5 B and C. Briefly described, the triple quadrupole consists of three quadrupoles with each having a distinct function in multiple reaction monitoring (MRM) mode. The first quadrupole is set to filter for targeted precursor ions. After that, the precursor ions are fragmented by collision induced dissociation in the second quadrupole into product ions. More strictly spoken the second quadrupole is a hexapole in the shown Agilent 6400 triple quadrupole but generally scientists speak of quadrupoles in these instruments. Subsequently, the third quadrupole filters the formed fragment ions of interest with distinct mass to charge ratios and guides them to the detector. The fragmentation of a precursor to a product ion is referred to as an ion transition and is highly specific for each analyte. The advantage of MRM scan mode is its capability to apply selected reaction monitoring to multiple product ions from one or more analyte/s eluting from the first dimension (LC). Thus, a high number of compounds can be monitored in a single run. Though the MS is a powerful detector it is not universal and can, just as others, not cover the entire chemical complexity of CDM. The applicability of the MS detector has a high dependence on the successful formation of gas phase ions. Metal ions are analytes that have principally be shown to be detectably by ESI-MS but only with special means, as charge reduction on solvation sphere or ion pairing.[539] More recent work has shown that ESI-MS is capable to reveal information about analyte elemental composition by measurement of metal ligand complexes.[540, 541] But these approaches are highly specialized and complex and thus the key strength of ESI triple quadrupole MS should be used to first develop quantitative methods for as many organic CDM compounds as possible.

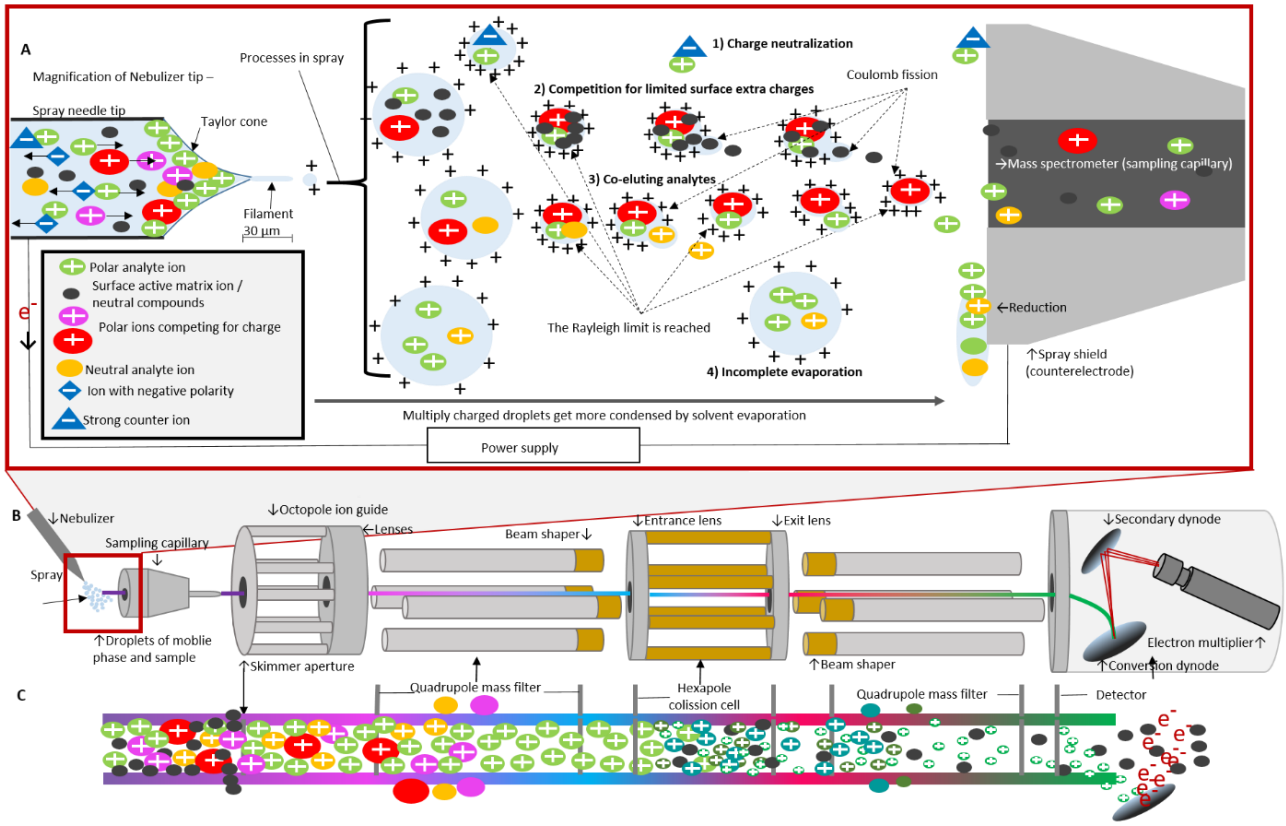

Figure 5: Mechanistic description of Agilent 6410 triple quadrupole mass spectrometer with an electrospray ionization source.

A) Detailed schematic depiction of an ESI ionization source operated in the positive ion mode. The analyte flow is coming from the left. For the purpose of simplification, the heated nitrogen drying gas is not shown. The capillary in the nebulizer is held at an electric potential of several kV with positive potential versus ground. The form of the liquid at the surface of the nozzle is determined by two main forces. A surface tension derived force that pulls the liquid back and an electrostatic Coulomb attraction that pulls the liquid to the counter electrode.[532] From the very tip of the formed Taylor cone a spray is emitted. The magnification after the bracket shows four exemplary depictions of type of droplets that can be formed. Example 1: Ion and counter-ion equal charge and thus the strong ion pairs are kept in the interior neutral phase of the droplet and prevent the analyte from capturing charge in the surface phase of the charged droplet. Example 2: Shows a droplet very crowded with analyte ions that compete for the limited excess surface charge thus decreasing the likelihood for each individual one to get ionized. Furthermore, the black dots symbolize that gas phase reactions (charge neutralization, charge stripping and charge transfer) can happen impacting the ESI response. Example 3: Three different co-eluting analytes in one droplet get all transferred from liquid to gas phase by Coulomb explosions when the Rayleigh limit is reached in the evaporating droplet. Example 4: Incomplete evaporation, caused by for example polar matrices or the presence of nonvolatile salts, can cause ion-suppression as well. Parts of the figure were derived from Mei Hong *et al.*.[533]

B) Schematic illustration of an Agilent 6400 triple quadrupole mass spectrometer with an ESI ionization source.

C) Zoom into schematic mechanisms in the ion beam passing through the MS. The skimmer aperture removes neutral and lighter molecules (e.g. drying gas) that have not enough momentum to pass the aperture. Thus, they are deflected and removed from the ion beam. The octopole ion guide focuses the ions with radio-frequency voltage applied to the octopole rods. The ions focused by the octopole pass into the quadrupole. The opposing metal rods in the quadrupole are electrically connected. Alternating positive and negative radio frequency (RF) voltage with a direct current (DC) voltage offset is capable to selectively filter a distinct population of ions. The chance of ions hitting the rods, and therefore being filtered out, depends on the mass to charge ratio of the ions and the strength of the field and the oscillation frequency. The filtered ions that pass the first quadrupole filter are directed through a collision cell. This second element of the triple quadrupole mass spectrometer is typically called the second quadrupole. But in the case of the instrument used in this thesis the collision cell is hexapole filled with nitrogen (same as the drying gas). The collision of analyte ions with the nitrogen molecules causes them to fragment into product ions. These fragment ions are then sent to the third quadrupole which works with the same principle as in the first quadrupole. It is set to filter for distinct fragment ions that pass into the detector. The conversion dynode is a kind of deflector electrode that is put in front of the detector (electron multiplier). It is held at high voltage with reverse polarity to the analyte ions. The physical principle behind the conversion dynode is an effect called secondary electron emission. If charged particles like electrons or ions strike the surface of a dynode secondary electrons are released from the atoms in the surface. The number of emitted electrons and thus the signal intensity depends on the type of incident particles and their energy.

1.3.3 Inductively coupled plasma mass spectrometry (ICP-MS) and inductively coupled plasma optical emission spectrometry (ICP-OES)

Inductively coupled plasma is a dominant technology for spectroscopic multielement analysis.[542] This is mainly due to its attributes as short measurement time, low detection limit, wide linear dynamic range, high precision and minimum matrix effects. In comparison to ICP-OES the coupling of ICP to a MS detector is more sensitive (often up to three orders of magnitude) and offers isotope resolution of the same element whereas the OES is more tolerant to high concentration. Both analytical methods have in common the inductively coupled plasma. A plasma is an ionized gas and a fundamental state of matter. An ICP of mostly Argon is generated by an electromagnetic alternating field that forces the charged molecules to move and reaches temperatures up to 10000°K. The processes that lead to the plasma formation are shown in Figure 6 A. The samples are typically treated by acid digestion to dissolve all the analytes and to decompose solids before they are introduced into the plasma. In the case of solution ICP-MS and –OES the sample gets sprayed into the plasma (Figure 6 B). One of the two key differences between ICP-MS and ICP-OES is that in the case of MS the ions have to be physically transported from the plasma to the MS whereas the photon collection in the case of OES is non-intrusive.[542] The second difference is that the emission intensity is dependent on the excited atom whereas MS signal intensities are dependent on ionization efficiencies. Therefore, the experimental conditions determining the properties of the plasma are chosen different for both technologies (power, gas flow, position of signal acquisition within the plasma and sample matrix). An element that has special issues in ICP-MS detection is Sulphur. Especially in single quadrupole MS the ^{36}S is indistinguishable from the elemental isobar $^{36}Ar^+$. Furthermore, the S detection can be impacted by spectral interferences with oxygen dimers that form inside the plasma and are difficult to resolve from the analyte of interest.[543] Thus, quantitative results for Sulphur presented in this thesis were determined with ICP-OES.

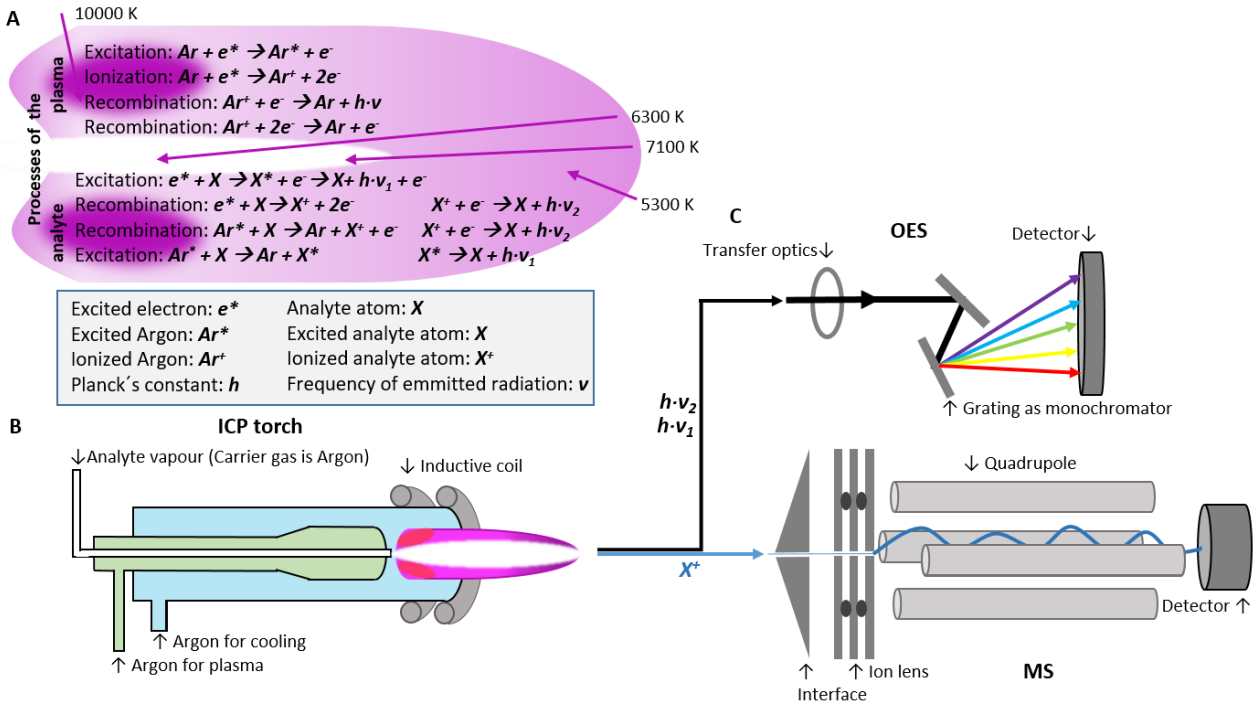

Figure 6: ICP-MS and ICP-OES for elemental analysis. A) Fundamental processes that happen during plasma formation and that form analyte ions when the sample is injected into the plasma. B) Exemplary setup of an ICP torch. C) Simplified schemes of optical emission spectrometry and mass spectrometry detectors used for ICP-MS and ICP-OES.

1.3.4 Raman microscopy and infrared microscopy

The Raman and infrared vibrational spectroscopy technologies have the capability to provide detailed chemical and structural information. The principle of vibrational spectroscopy is that the detected energy changes correspond to the energy that is needed to cause atomic motion in a molecule. Depending on the number of atoms a molecule can present a number of 'vibrational degrees of freedom'. A molecule of N atoms has 3N-6 degrees of freedom. An exception to the rule are linear molecules with 3N-5 degrees of freedom. However, the way of employing radiation is different in Raman and infrared spectroscopy.[544] In infrared (IR) spectroscopy a range of frequencies of IR energy are directed on a sample. It absorbs the energy of the incident radiation at the frequency that matches the intramolecular vibration. In other words, the energy of the incident photon needs to match the energy gap between ground state and excited state (Figure 7). If this is the case the sample molecule is promoted to a vibrational excited stage. This is detected by the loss of this frequency from the radiation of the incident beam that passes through the sample.

In contrast, in Raman spectroscopy a single radiation frequency (monochromatic light) is used to excite the sample. It does not necessarily need to match the energy gap between molecular energy states, but it interacts with the matter and gets scattered at an angle different from the incident beam. The output signal used to characterize chemical identity is the radiation scattered from the molecule that is one unit of vibrational energy different from the incident beam. A characteristic trait of a scattering process is that the light interacts with the molecule and distorts (polarizes) the electron cloud around the atomic nuclei to form a non-durable virtual energy state.[544] The dominant process is elastic scattering that is known as Rayleigh scattering for molecules. In this scattering event the electron cloud is distorted to the virtual short-lived state and it returns to the energetic starting level. Thus, the photons are scattered with the same frequency as the incident radiation (Figure 7). In contrast, the inelastic scattering is characterized by light induced nuclear motion that is induced during the scattering process. It is an inherently weak process, only every 10^6-10^8 photon is scattered that way, but modern technology as lasers and microscopes make measurement principle sensitive. In these scattering processes the energy of the scattered photon is different to the incident photon by one vibrational unit. It can be distinguished in two different types of inelastic scattering that are summarized as Raman scattering. As shown in Figure 7 in one type the energy is transferred from the incident photon to the molecule (Raman Stokes) and in the other type the energy gets transferred from the molecule to the scattered photon (Raman anti-Stokes).

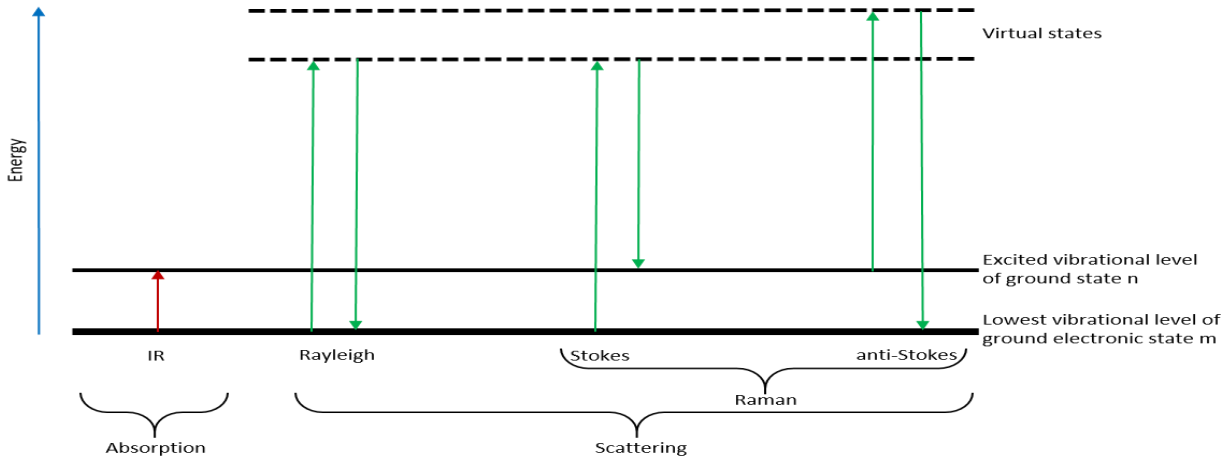

Figure 7: Energetic consideration of infrared absorption, Rayleigh and Raman (Stokes and anti-Stokes) scattering. Graph was adapted from Ewen Smith and Geoffrey Dent.[544]

1.3.5 Scanning electron microscopy with energy-dispersive x-ray spectroscopy (SEM/EDX)

Microscopes are used to magnify objects or surfaces that cannot be seen with the naked eye. In CDM preparation and development surfaces of high interest are clogged filter membranes or precipitate that forms thick filter cakes. The resolution of light microscopy is limited by the electromagnetic waves that can be used. The shortest visible wavelength around 400 nm is a limiting factor for special resolution. But even if detectors are used that make electromagnetic waves with shorter wavelength (UV light) visible their applicability is limited due to absorption in solid state optical elements. A typical threshold where absorption becomes too high is below 200 nm. Wavelength of electrons are very short and since electro-magnetic fields can be used as "optical"-elements the absorption problem of light microscopy is avoided. A simplified representative setup of a scanning electron microscope (SEM) is shown in Figure 8 A. With SEM technology structures in the atomic scale as small as 1 nm (10^{-9} m) can be resolved.[545] The back scattered electron (BSE) detector and the secondary electron (SE) detector are the two main detector types used in SEM. The BSE is the primary electron from the electron source that experiences elastic scattering from the nucleus and gives information about the material contrast. The signal increases with higher atomic number and thus heavier atoms (material) appear darker in the BSE image. In contrast to the BSE, the secondary electron signal is mainly detected from the sample surface and is thus ideal to generate high resolution images from the surface topology. Secondary electrons are formed when either an outer shell or inner shell electron gets removed by the energy of the primary electron.

If coupled to an energy dispersive X-ray (EDX) detector the electron microscopy can be applied to do elemental analysis of the surface of the sample (the upper 1 to 10 µm).[546] EDX is a commonly used method in the field of analytical electron microscopy that is used in parallel to SE detector.[547] Electrons that incide on the sample during electron microscopy bear energy. This energy causes the phenomenon of inner-shell excitation. The example in Figure 8 B shows the excitation of an electron in the K shell. Because all the energy levels in the atomic shells are occupied the excited electron can only transit to the unoccupied states beyond the Fermi level (E_F). The Fermi level chemical potential is the thermodynamic work that is needed to remove an electron of matter. If the electron is excited to an energetic level beyond the fermi level the hole in the inner shell is filled by an electron at a higher energy level (e.g. L_3 level). When the atom relaxes to the ground state by filling the electron holes it emits the surplus of energy as characteristic X-ray. As the energy of the X-ray is specific to each material (energy between electron at higher level and electron hole), the energy of the characteristic X-rays can be used to identify elements. The emission process drawn in Figure 8 B shows $K_{\alpha 1}$ characteristic X-ray formation. This results from hole formation in the 1s inner shell (K shell) that leads to the transition $L_3 \rightarrow K$. However, there is not only this one transition mechanism. Transitions that relax into the K-shell from other energy levels (L and M) are summarized in the K-series and transitions that fill up electron holes in the L-shell are summarized in the L-series. Subsequently, the emitted X-rays can be detected by e.g. a silicon drift detector. It is important to mention that the signal intensity correlates with element concentration, but the signal is not quantitative. Mainly, because uncontrolled geometric factors can modify the generation of X-ray and this can lead to a big systematic error (factor of ten or more).[548] If the surface however is smooth, the PB-ZAF (peak to background - atomic number, absorption factor, fluorescence factor) model is commonly used to generate quantitative results with a detection limit of 0.1 percent by mass. The discussed properties of SEM-EDX make it an ideal technique for the characterization of unknown solid materials observed over CDM shelf life.[491]

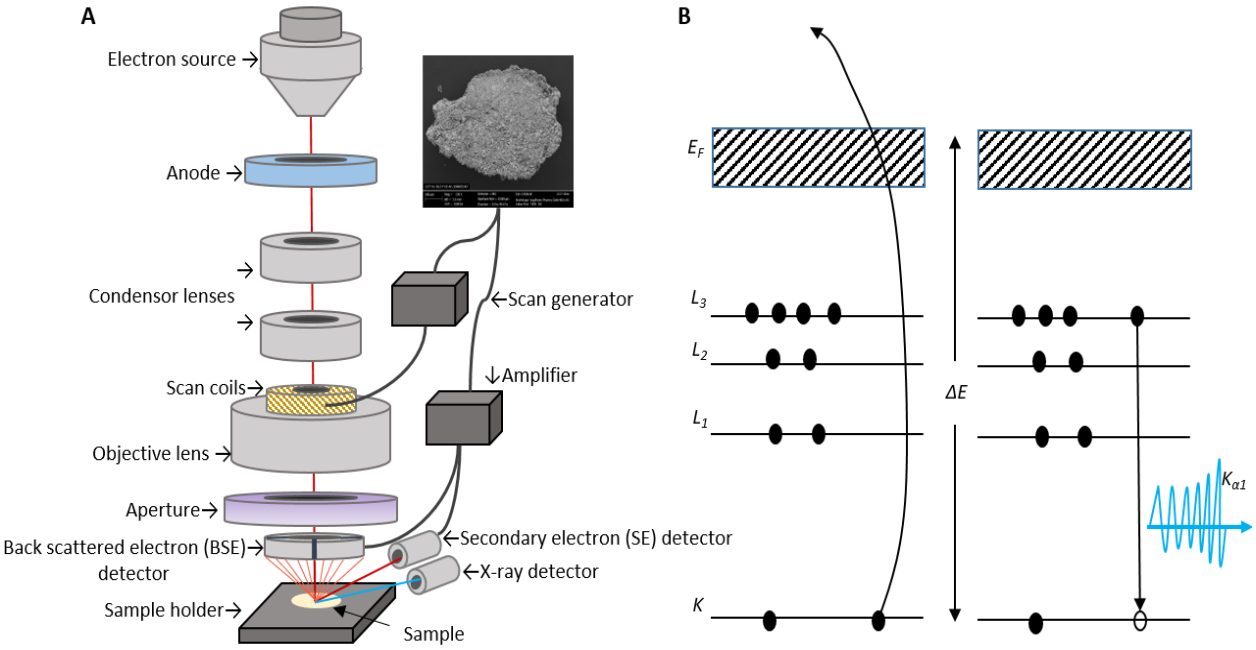

Figure 8: A) Simplified setup of electron microscope (electron beam in red) and B) the principle of X-ray formation in samples excited with electrons (adapted from Shindo D. *et al*.[547]).

1.3.6 Liquid scintillation counting (LSC)

Radioactive tracers are commonly used to follow the behavior of elements or chemical species in chemical processes.[549] Methods which use radioactivity to trace elements offer advantages as very high sensitivity, robustness to changing conditions and the possibility to quantify materials that stem from discrete classes of chemicals.[550] The radioactivity can be measured with different detectors as the liquid scintillation counter. The LSC is a universal method that can measure several types of nuclear radiation (e.g. α-, β^+-, β^--, γ- and ε-nuclides) simultaneously. The basic principle of LSC is the transformation of radioactive energy to light by a liquid scintillation cocktail (Figure 9 A). For example in the case of an α- or β-decay a solvent molecule absorbs a portion of the energy of the emitted particle and passes it over to other solvent molecules until it reaches e.g. a phosphor that absorbs the energy and re-emits it as light and relaxes to its ground state. For the sake of completeness, it shall be mentioned that most scintillation cocktails contain not only primary scintillation molecules that emit light but also secondary scintillators that function as a wave length shifter to improve signal. The light is then captured by an optical system and the signal gets amplified in a photomultiplier that converts light to an electric signal by a photosensitive surface. The light is emitted in pulses as for example β-decay events happen in pulses with a correspondingly short time and path within the scintillation cocktail, too. Therefore, the burst of photons resulting from one emission event is derived from a small local area and arrives at the photomultiplier with sufficient simultaneity to be considered as one pulse of light. The energy of the light pulses corresponds with the energy of the emission events and the number of pulses per time corresponds to the number of radioactive emissions. This is of course only true if quenching is not considered. In reality, concentration-, self-absorption-, optic-, chemical- and color-quench can have a strong impact on counting yields. A LSC classifies each pulse of photons according to the energy of the β-emission event (number of photons) and collates them into channels (Figure 9 B). A common approach is to divide the energy spectrum into three energy ranges, where the lowest corresponds to ^{3}H emission and the highest corresponds to ^{32}P emission. In case the element of interest is the Sulphur of L-cysteine a radioactively labelled derivative of the amino acid can be used to do radioactive tracing experiments. Since the energy of S-35 and C-14 is nearly the same it would be tracked in the C-14 range (Figure 9 C).[551]

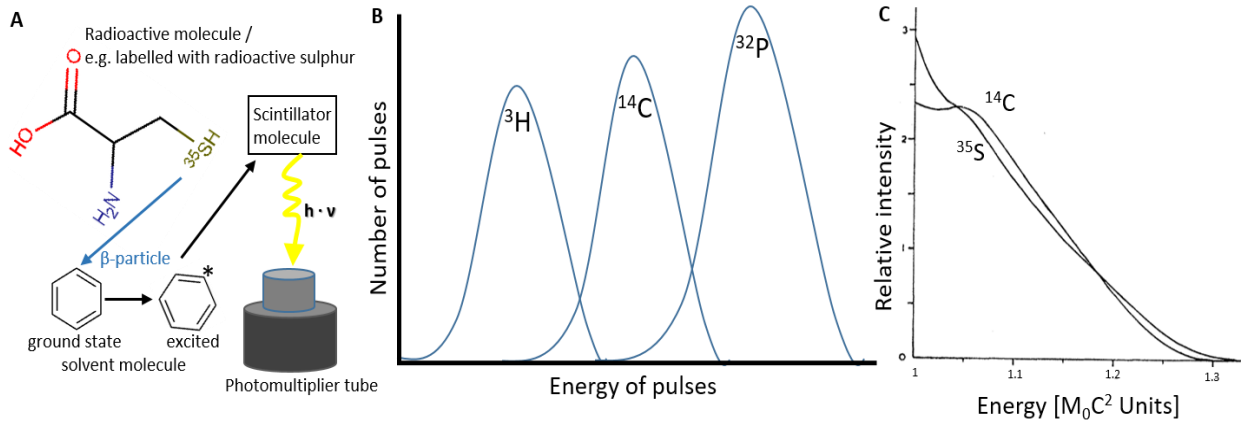

Figure 9: Liquid Scintillation Counting. A) Radioactivity detection principle. B) Pulse channels divide the spectrum into isotope specific windows that collate the pulses of specific energy. C) The similar energy of ^{14}C and ^{35}S decays (Graph was adapted from Moljk *et al.*[551]).

2 Objectives

For a long time, the two only CDM quality parameters assessed were osmolality and final pH after preparation. However, the importance of the medium as the nutrition source for cells and as source of chemical components for recombinant protein expression underlines the outstanding importance for robust bioprocess engineering. In the same time the CDM is an aqueous solution of high chemical complexity and the versatile factors it is exposed to during preparation and storage emphasize the need to shed light on the chemical behavior. For years, medium at Boehringer Ingelheim (BI) has been developed with a focus on chemically defined formulation, cell growth and productivity. This has led to the situation that the development of specific analytics for the quantification of media compounds has not kept pace and that the media formulations showed difficult to explain phenomena like drastic oxygen consumption during preparation and precipitate formation over the course of storage time.

As instable medium is a major concern for prolonged CHO cell fed-batch processes a major focus of this thesis was to evaluate and develop analytical technologies for the characterization of CDM. An ideal analytical technology for the highly specific and sensitive quantification of compounds added to the CDM solution is triple quadrupole MS. If evaluated for matrix effects, it is ideal to measure several compound classes in parallel and can be adapted to cover different compound concentration levels. Therefore, a part of this thesis aims at the development of a LC-QqQ-MS method especially adapted to the Boehringer Ingelheim media formulations and the specific laboratory situation.

Furthermore, this thesis aims at the application of the LC-QqQ-MS method to develop a chemical understanding of CDM liquid formulations. Additionally, multiple probe technologies have been evaluated on their applicability as online monitoring tools with the goal to estimate their usefulness as live media quality estimator during powder hydration. In parallel, the goal to assess the meaningfulness of the measured on-line profiles to compare the reproducibility of media batches was followed. Moreover, the application of online probes during raw material dissolution has the potential to describe the chemical behavior of liquid media. An example is the major oxygen consuming reaction happening in Boehringer Ingelheim feed medium after iron salt addition.

Another major concern that occurred over the time working with Boehringer Ingelheim proprietary media formulations was the formation of precipitate during storage. The criticality of liquid media forming precipitate is not only caused by the concern that cells may lack nutrients but also by process related problems like filter clogging and batch to batch variability. A first major step in understanding the impact of precipitation on cell culture robustness and more importantly to avoid the solid formation is to collect information about chemical identity.

Since the feed media have a tremendous impact on process performance in fed-batch cultivation and because of the high concentration they are expected to be especially prone for chemical instability. This, and their comparability to other CDM types, makes them an ideal subject for the characterization of media. Thus, in this thesis exclusively feed media were investigated.

3 Results and Discussion

This work has been structured into three main parts. The first and most important step of characterization studies is the development and implementation of suitable analytics. Therefore, the first chapter describes the LC-QqQ-MS method development and validation for CDM matrix. In the second part, the focus lies on the application of on-line and off-line analytics for the generation of insight to the chemical behavior of CDM during medium preparation. Consequently, the chemical characterization of CDM over the storage period with versatile analytical technologies is described in the third part.

3.1 Development of dynamic multiple reaction monitoring (dMRM) method on an triple quadrupole MS for CDM compound quantification

The number of compounds used for CDM preparation is large and the compound structures are very heterogeneous (Compare introduction Figure 2). Triple quadrupole mass spectrometry (QqQ-MS) has the necessary properties to simultaneously quantify a majority of CDM compounds in a targeted approach. Method development and method validation of a LC-QqQ-MS method to quantify small organic compounds in CDM is described in this chapter.

3.1.1 MS parameter determination

Similar to Gika *et al*. the first step in method development was to determine MS parameters giving highest sensitivity for a broad class of analytes.[552] For this purpose pure stock solutions of organic compounds shown in Figure 10 were prepared and MS parameters were optimized by direct infusion of those into the triple quadrupole instrument. Both negative and positive ionization mode were investigated. Since most of the compounds were giving best intensities in positive ionization mode for the sake of simplification the method was developed in this mode only. After optimization of fragmentor voltage (U_F), cell accelerator voltage (CAV) and collision energy (CE) a set of 48 compounds known from CDM recipes and 12 compounds known as potential reaction products from literature were chosen to be followed for method development (Figure 10 and Table 3). First, the optimum U_F and CAV were adjusted to achieve maximum signal intensity for parent ion. Product ion spectra were analyzed and the transition with a unique product ion and highest intensity was selected for each individual compound. In cases the highest intensity product ion was resulting of a neutral loss the second most intense product ion was chosen as quantifier ion. The ideal fragmentor voltage settings and collision energies used for fragmentation are summarized in Figure 10.

The analyte precursor *m/z* ratio observed is given next to the compound names. In order to understand molecular breakdown upon fragmentation in the collision cell a simulation with Mass Spec Calculator Pro™ (Scientific Instrument Services, Ringoes, New Jersey, USA) has been conducted. The result of that analysis is symbolized by the arrows on the chemical structures in Figure 10 which shows the chemical structures behind the *m/z* of qualifier (black arrows) and quantifier (blue arrows) ions. Furthermore, the experimentally determined transitions have been compared to values reported in literature. The results are well in accordance with scientific standards (Reported values shown in Figure 10 in the right column of each compound cell). Just as described for the compounds that are part of media recipes the MS parameters have been determined for potential medium degradation products identified in literature (Table 3). Since the presence of these compounds has not been known at time of method development these compounds were searched for in separate chromatographic runs. However, the work with these additional compounds showed the ease of expanding the developed method.

L-alanine *m/z* 90.2

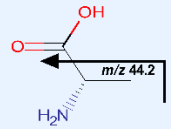

rt 5 min
Δ rt 2 min
U_F 10 V
CE 6 eV
IS L-asparagine $^{13}C_5$, ^{15}N

ESI +
Quantifier 90→44
Qualifier 90→72
Ref.: 1-3, 26, 27

L-arginine *m/z* 175.2

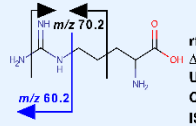

rt 7 min
Δ rt 6 min
U_F 10 V
CE 20 eV
IS L-arginine $^{13}C_5$, ^{15}N

ESI +
Quantifier 175→70
Qualifier 175→60
Ref.: 1-3, 26, 27, 31, 32

1.4-diaminobutane *m/z* 89

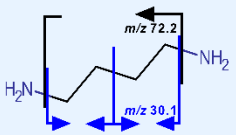

rt 17 min
Δ rt 16 min
U_F 40 V
CE 8 eV
IS calcium pantothenate $^{13}C_5$, ^{15}N

ESI +
Quantifier 89→72
Ref.:1-5

2`-deoxyadenosine *m/z* 252.1

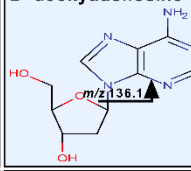

rt 19.3 min
Δ rt 2.5 min
U_F 130 V
CE 12 eV
IS L-tryptophan $^{13}C_5$, ^{15}N

ESI +
Quantifier 252→136
Qualifier 252→119
Ref.: 3, 6-9

L-asparagine *m/z* 133.1

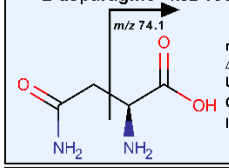

rt 4.8 min
Δ rt 3.9 min
U_F 60 V
CE 12 eV
IS L-asparagine $^{13}C_5$, ^{15}N

ESI +
Quantifier 133→74
Qualifier 133→87
Ref.: 1-3, 26, 27, 32

L-aspartic acid *m/z* 134.1

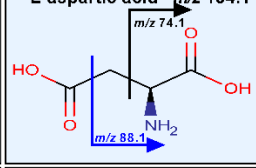

rt 9.8 min
Δ rt 12 min
U_F 70 V
CE 10 eV
IS glutamic acid $^{13}C_5$, ^{15}N

ESI +
Quantifier 133→74
Qualifier 133→88
Ref.: 1-3, 26, 27, 31-33

2`-deoxycytidine *m/z* 228.1

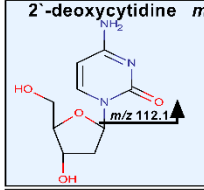

rt 17.7 min
Δ rt 2.3 min
U_F 120 V
CE 28 eV
IS L-tyrosine $^{13}C_5$, ^{15}N

ESI +
Quantifier 228→112
Qualifier 252→95
Ref.: 6, 7, 10

2`-deoxyguanosine *m/z* 268.1

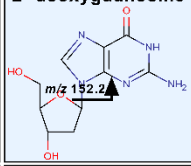

rt 15.8 min
Δ rt 2.5 min
U_F 70 V
CE 26 eV
IS L-phenylalanine $^{13}C_5$, ^{15}N

ESI +
Quantifier 268→152
Qualifier 268→135
Ref.: 3,6,8,11

L-cysteine *m/z* 122.2

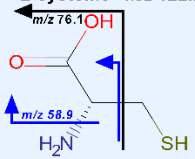

rt 5.3 min
Δ rt 2.65 min
U_F 70 V
CE 10 eV
IS L-threonine $^{13}C_5$, ^{15}N

ESI +
Quantifier 122→59
Qualifier 122→76
Ref.: 1-3, 26

L-cystine *m/z* 241.1

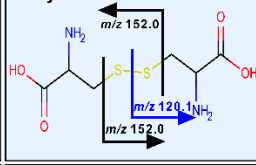

rt 4.9 min
Δ rt 2.4 min
U_F 60 V
CE 10 eV
IS L-glutamine $^{13}C_5$, ^{15}N

ESI +
Quantifier 241→74
Qualifier 241→152
Qualifier 241→120
Ref.: 26, 34-36

4-aminobenzoic acid *m/z* 138.1

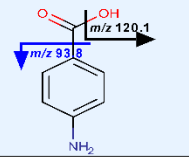

rt 24 min
Δ rt 12 min
U_F 70 V
CE 16 eV
IS calcium pantothenate $^{13}C_5$, ^{15}N

ESI +
Quantifier 138→77
Qualifier 138→120
Qualifier 2 138→94
Ref.: 3, 12-15

5-methylcytosine *m/z* 126.2

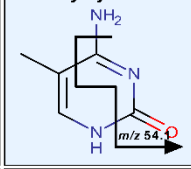

rt 12.2 min
Δ rt 2.5 min
U_F 60 V
CE 30 eV
IS L-tyrosine $^{13}C_5$, ^{15}N

ESI +
Quantifier 126→83
Qualifier 126→109
Ref.: 8,16

L-glutamine *m/z* 147.2

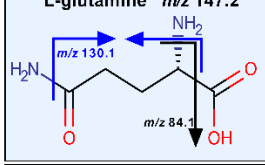

rt min
Δ rt 3.9 min
U_F 80 V
CE 10 eV
IS L-lysine $^{13}C_5$, ^{15}N

ESI +
Quantifier 147→84
Qualifier 147→130
Ref.: 1-3, 26, 32, 33

L-histidine *m/z* 156.2

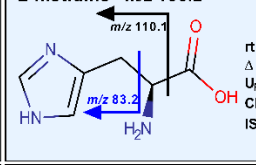

rt 6.7 min
Δ rt 5.0 min
U_F 150 V
CE 14 eV
IS L-glutamic acid $^{13}C_5$, ^{15}N

ESI +
Quantifier 156→110
Qualifier 156→83
Ref.: 1-3, 26, 27, 32

biotin *m/z* 245.1

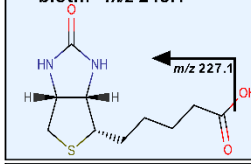

rt 31 min
Δ rt 16 min
U_F 50 V
CE 10 eV
IS calcium pantothenate $^{13}C_5$, ^{15}N

ESI +
Quantifier 245→227
Qualifier 245→97
Ref.: 1, 17-19

calcium pantothenate *m/z* 220.1

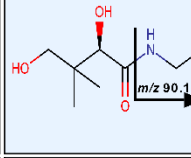

rt 24.5 min
Δ rt 5 min
U_F 50 V
CE 12 eV
IS calcium pantothenate $^{13}C_5$, ^{15}N

ESI +
Quantifier 220→90
Qualifier 220→124
Ref.: 1, 3, 18, 20

L-hydroxyproline *m/z* 132.2

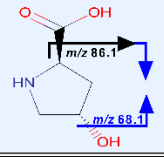

rt 5.0 min
Δ rt 3 min
U_F 60 V
CE 16 eV
IS L-glutamine $^{13}C_5$, ^{15}N

ESI +
Quantifier 132→86
Qualifier 132→68
Ref.: 26, 37-39,7

L-isoleucine *m/z* 132.2

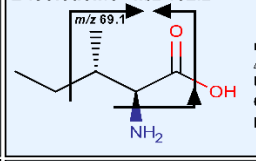

rt 9.1 min
Δ rt 4.5 min
U_F 10 V
CE 10 eV
IS L-tyrosine $^{13}C_5$, ^{15}N

ESI +
Quantifier 132→86
Qualifier 132→69
Ref.: 1-3, 26, 27, 32

cyanocobalamin *m/z* 678.4

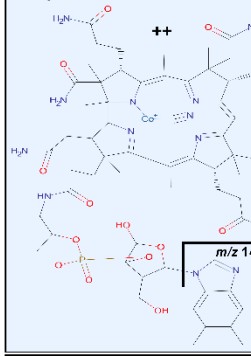

rt 22.7 min
Δ rt 3.7 min
U_F 130 V
CE 30 eV
IS calcium pantothenate $^{13}C_5$, ^{15}N

ESI +
Quantifier 678→147
Qualifier 678→359
Ref.: 19, 21-24

ethanolamine *m/z* 62.1

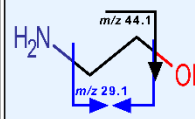

rt 5.9 min
Δ rt 3.8 min
U_F 50 V
CE 14 eV
IS L-lysine $^{13}C_5$, ^{15}N

ESI +
Quantifier 62→44
Qualifier 62→45
Ref.: 25-29

L-isoleucine + L-leucine *m/z* 132.2

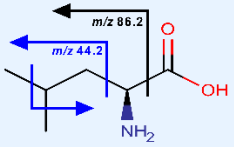

rt 9.8 min
Δ rt 5 min
U_F 10 V
CE 10 eV
IS L-tyrosine $^{13}C_5$, ^{15}N

ESI +
Quantifier 132→86
Qualifier 132→44
Ref.: 1-3, 26, 27, 32

L-lysine *m/z* 147.2

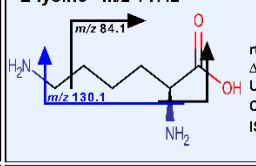

rt 5.5min
Δ rt 4 min
U_F 70 V
CE 20 eV
IS L-lysine $^{13}C_5$, ^{15}N

ESI +
Quantifier 147→84
Qualifier 147→130
Ref.: 1-3, 27, 34, 36

hypoxanthine *m/z* 137.1

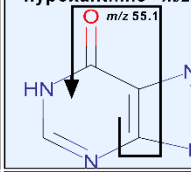

rt 12.3 min
Δ rt 2.2 min
U_F 70 V
CE 30 eV
IS L-tyrosine $^{13}C_5$, ^{15}N

ESI +
Quantifier ?→?
Qualifier ?→?

L-methionine *m/z* 150.1

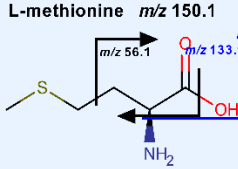

rt 7.5 min
Δ rt 4 min
U_F 110 V
CE 10 eV
IS L-arginine $^{13}C_5$, ^{15}N

ESI +
Quantifier 150→133
Qualifier 150→104
Ref.: 1-3, 26, 27, 31, 32

L-ornithine *m/z* 133.2

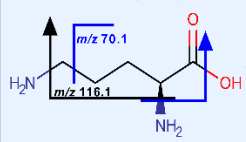

rt 4.8 min
Δ rt 2.8 min
U_F 110 V
CE 8 eV
IS L-asparagine $^{13}C_5$, ^{15}N

ESI +
Quantifier 133→70
Qualifier 133→116
Ref.: 1-3, 26, 34

L-glutathione *m/z* 308.2

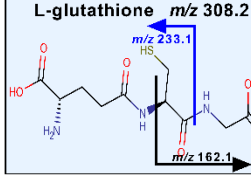

rt 13.8 min
Δ rt 10 min
U_F 70 V
CE 14 eV
IS L-phenylalanine $^{13}C_5$, ^{15}N

ESI +
Quantifier 308→162
Qualifier 308→179
Qualifier 308→76
Ref.: 1-3, 26, 30

L-2-aminobutyric acid *m/z* 104.1

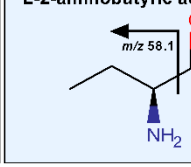

rt 5.2 min
Δ rt 1.5 min
U_F 100 V
CE 6 eV
IS L-threonine $^{13}C_5$, ^{15}N

ESI +
Quantifier ?→?
Qualifier ?→?

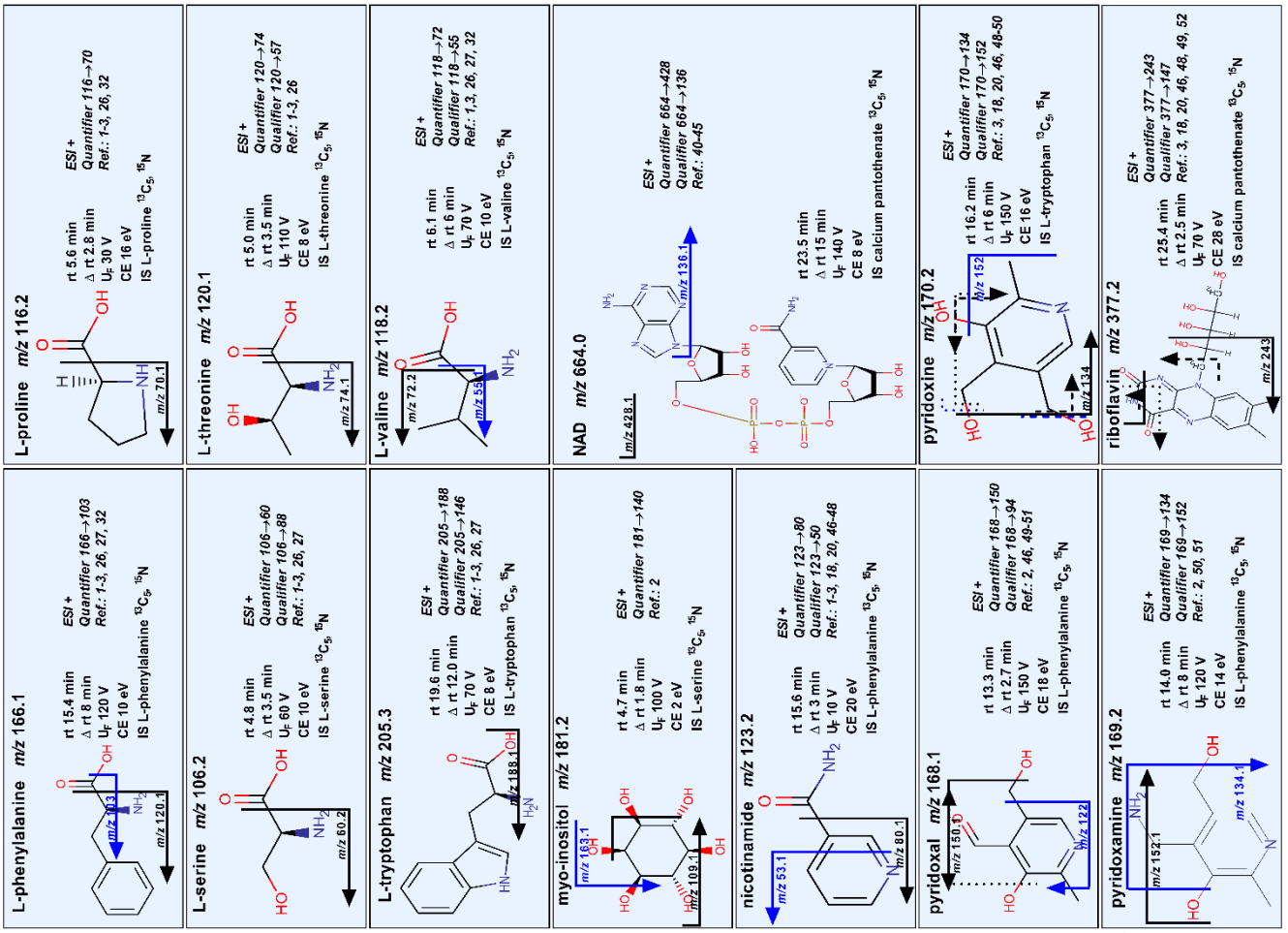

1. Bajad, S.U., et al., J Chromatogr A., 2006. 1125(1): p. 76-88. Epub 2006 Jun 6.
2. Gika, H.G., et al., J Chromatogr A., 2012. 1259:121-7.(doi): p. 10.1016/j.chroma.2012.02.010. Epub 2012 Feb 13.
3. Lu, W., E. Kimball, and J.D. Rabinowitz, J Am Soc Mass Spectrom., 2006. 17(1): p. 37-50. Epub 2005 Dec 15.
4. Yu, C., et al., Anal Bioanal Chem., 2015. 407(22): p. 6891-7. doi: 10.1007/s00216-015-8860-6. Epub 2015 Jul 3.
5. Daniel, D., et al., J Chromatogr A., 2015. 1416:121-8.(doi): p. 10.1016/j.chroma.2015.08.065. Epub 2015 Sep 3.
6. Thomas, D., et al., Anal Bioanal Chem., 2015. 407(13): p. 3693-704. doi: 10.1007/s00216-015-8588-3. Epub 2015 Mar 8.
7. Abdel Rahman, A.M., et al., ACS Chem Biol., 2013. 8(9): p. 2053-62. doi: 10.1021/cb4004173. Epub 2013 Jul 22.
8. Preinerstorfer, B., et al., J Chromatogr A., 2010. 1217(3): p. 312-28. doi: 10.1016/j.chroma.2009.11.051. Epub 2009 Nov 20.
9. Wei, R., G. Li, and A.B. Seymour, Anal Chem., 2010. 82(13): p. 5527-33. doi: 10.1021/ac100331b.
10. Abdel Rahman, A.M., et al., Anal Chim Acta., 2014. 845:53-61.(doi): p. 10.1016/j.aca.2014.06.012. Epub 2014 Jun 12.
11. Stentoft, C., et al., J Chromatogr A., 2014. 1356:197-210.(doi): p. 10.1016/j.chroma.2014.06.065. Epub 2014 Jun 27.
12. Zhang, G.F., et al., Rapid Commun Mass Spectrom, 2005. 19(6): p. 963-9.
13. Dhananjeyan, M.R., et al., J Chromatogr B Analyt Technol Biomed Life Sci., 2007. 847(2): p. 224-30. Epub 2006 Oct 27.
14. Nortje, C., et al., Bioanalysis, 2015. 7(10): p. 1211-24. doi: 10.4155/bio.15.54.
15. Brain, R.A., et al., Environ. Sci. Technol. 2, 2008.
16. Hu, C.W., et al., Chem Res Toxicol., 2012. 25(2): p. 462-70. doi: 10.1021/tx2004954. Epub 2012 Feb 8.
17. Holler, U., et al., (1570-0232 (Print)).
18. Tayade, A.B., et al., Anal Chim Acta., 2013. 789:65-73.(doi): p. 10.1016/j.aca.2013.05.062. Epub 2013 Jun 11.
19. Marakova, K., et al., Vol. 69. 2014. 663-8.
20. Bhandari, D. and G.J. Van Berkel, J Agric Food Chem., 2012. 60(34): p. 8356-62. doi: 10.1021/jf302653d. Epub 2012 Aug 16.
21. Schwertner, H.A and V.S. Bebarta, J Chromatogr B Analyt Technol Biomed Life Sci., 2012. 905:10-6.(doi): p. 10.1016/j.jchromb.2012.07.012. Epub2012 Aug 9.
22. Heal, K.R., et al, Rapid Commun Mass Spectrom., 2014. 28(22): p. 2398-404. doi: 10.1002/rcm.7040.
23. Zironi, E., et al., J Dairy Sci., 2013. 96(5): p. 2832-6. doi: 10.3168/jds.2012-6451. Epub 2013 Mar 15.
24. Owen, S.C., M. Lee, and C.B. Grissom, Journal of Chromatographic Science, 2011. 49(3): p. 228-233.
25. Shin, K.O. and Y.M. Lee, Arch Pharm Res., 2016. 39(1): p. 66-72. doi: 10.1007/s12272-015-0677-8. Epub 2015 Nov 14.
26. Piraud, M., et al., Rapid Commun Mass Spectrom, 2003. 17(12): p. 1297-311.
27. Zoppa, M., et al., J Chromatogr B Analyt Technol Biomed Life Sci., 2006. 831(1-2): p. 267-73. Epub 2006 Jan 4.
28. Waterval, W.A., et al., Clin Chim Acta., 2009. 407(1-2): p. 36-42. doi: 10.1016/j.cca.2009.06.023. Epub 2009 Jun 24.
29. da Silva, E.F., et al., 2012. 51(41): p. 13329-13338.
30. Valverdu-Queralt, A., et al., J Agric Food Chem., 2015. 63(1): p. 142-9.
31. Midttun, O., G. Kvalheim, and P.M. Ueland, Anal Bioanal Chem., 2013. 405(6): p. 2009-17. doi: 10.1007/s00216-012-6602-6. Epub 2012 Dec 13.
32. Shama, N., et al., J Chromatogr B Analyt Technol Biomed Life Sci., 2008. 865(1-2): p. 18-24. doi: 10.1016/j.jchromb.2008.01.027. Epub 2008 Jan 20.
33. Bathena, S.P., et al., J Chromatogr B Analyt Technol Biomed Life Sci., 2012. 893-894:15-20.(doi): p. 10.1016/j.jchromb.2012.01.035. Epub 2012 Feb 28.
34. Le, A., et al., J Chromatogr B Analyt Technol Biomed Life Sci., 2014. 944:166-74.(doi): p. 10.1016/j.jchromb.2013.11.017. Epub 2013 Nov 18.
35. Wear, J.E. and B.G. Keevil, Clinical Chemistry, 2005. 51(4): p. 787.
36. Guerrasio, R., et al., Anal Bioanal Chem., 2014. 406(3): p. 915-22. doi: 10.1007/s00216-013-7456-2. Epub 2013 Dec 12.
37. Conventz, A., et al., J Chromatogr B Analyt Technol Biomed Life Sci., 2007. 860(1): p. 78-85. Epub 2007 Nov 19.
38. Servillo, L., et al., J Agric Food Chem., 2011. 59(1): p. 274-81. doi: 10.1021/jf102833v. Epub 2010 Dec 3.
39. Chen, J., et al., Anal Bioanal Chem., 2016. 408(10): p. 2527-42. doi: 10.1007/s00216-016-9352-z. Epub 2016 Feb 12.
40. Seifar, R.M., et al., J Chromatogr A., 2013. 1311:115-20.(doi): p. 10.1016/j.chroma.2013.08.076. Epub 2013 Aug 28.
41. Trammell, S.A. and C. Brenner, Comput Struct Biotechnol J., 2013. 4:e201301012.(doi): p. 10.5936/csbj.201301012. eCollection 2013.
42. Liu, L., et al., J Chromatogr B Analyt Technol Biomed Life Sci., 2016. 1011:69-76.(doi): p. 10.1016/j.jchromb.2015.12.040. Epub 2015 Dec 24.
43. Magdenoska, O., et al., Anal Biochem., 2015. 487:17-26.(doi): p. 10.1016/j.ab.2015.06.033. Epub 2015 Jul 2.
44. Yamada, K., et al., Anal Biochem., 2006. 352(2): p. 282-5. Epub 2006 Mar 9.
45. Luo, B., et al., J Chromatogr A., 2007. 1147(2): p. 153-64. Epub 2007 Feb 16.
46. Hampel,D., E.R.York,andL.H. Allen, J Chromatogr B Analyt Technol Biomed Life Sci., 2012. 903:7-13.(doi): p.10.1016/j.jchromb.2012.06.024.Epub 2012 Jun27.
47. Liu, M., et al., J Chromatogr B Analyt Technol Biomed Life Sci., 2012. 904:107-14.(doi): p. 10.1016/j.jchromb.2012.07.030. Epub 2012 Aug 8.
48. Santos, J., et al., J Chromatogr A., 2012. 1261:179-88.(doi): p. 10.1016/j.chroma.2012.04.067. Epub 2012 May 3.
49. Midttun, Ø., et al., Clinical Chemistry, 2005. 51(7): p. 1206.
50. van der Ham, M., et al., Anal Chim Acta., 2012. 712:108-14.(doi): p. 10.1016/j.aca.2011.11.018. Epub 2011 Nov 18.
51. Footitt, E.J., et al., J Inherit Metab Dis., 2013. 36(1): p. 139-45. doi: 10.1007/s10545-012-9493-y. Epub 2012 May 11.
52. Bishop, A.M., et al., J Chromatogr B Analyt Technol Biomed Life Sci., 2011. 879(20): p. 1823-6. doi: 10.1016/j.jchromb.2011.04.032. Epub 2011 May 6.
53. Boudra, H., et al., J Chromatogr A, 2012. 1256: p. 169-76.
54. Hazleton, K.Z., et al., Chem Biol, 2012. 19(6): p. 721-30.
55. Chen, Y., et al., Yao Xue Xue Bao., 2014. 49(11): p. 1593-9.
56. Chen, F., et al., Journal of Chromatographic Science, 2014. 52(8): p. 852-861.

Figure 10: Compounds included in the dMRM for CDM. Included are compounds that are important constituents of CDM recipes.

Table 3: Compounds that were measured in MRM mode. The compounds listed here are no constituent of CDM recipes. Because presence of these compounds in CDM was not sure a broad time frame was chosen to not miss any interferences with other compounds.

Compound	Precursor ion [*m/z*]	Quantifier [*m/z*]	Qualifier [*m/z*]	Retention time	U_F [V]	CE [eV]
hydroxocobalamin	359	147.1	n.a.	22.7	200	10
7,8-dimethylalloxazine	243.1	198.1	170.1	32.1	30	26
N-formylkynurenin	237.1	136	174.2	17.1	40	12
3-hydroxy-DL-kynurenine	225.1	110	190.1	12.2	50	10
5-hydroxy-L-tryptophan	221.1	204.1	162	15.3	50	8
L-methionine sulfone	182.1	56.1	136	5.49	50	10
DL-o-tyrosine	182.1	136.1	119	14.9	100	12
L-citrulline	176.1	113	70	5.24	70	8
L-cysteic acid	170.1	124.1	n.a.	10	80	12
DL-methionine sulfoxide	166.1	74	56	5.3	50	10
L-cysteinesulfinic acid	154,1	44	74	10,1	80	8
3-aminopropanamide	89,2	30,2	72,2	6,54	40	16

3.1.2 Chromatographic conditions that enable simultaneous quantification of CDM compounds

The structural similarity analysis of compounds included in LC-QqQ-MS method development showed six main groups with similarity less than 70% (Figure 11). This result raised the expectation of big differences in chromatographic behavior of the analytes. Especially with regards to small polar compounds, which comprise a big percentage of CDM, problems in chromatographic retention would occur with standard reversed phase LC.[524] Therefore, a mixed mode column was used to retain and resolve small polar compounds. The developed mixed mode chromatography method is similar to reversed phase chromatography with regards to mobile phase and was therefore easiest to implement in a laboratory that routinely used that technology. Application of for example HILIC chromatography would have needed more specific adaptations but would have been principally feasible, too. Especially mobile phase composition would have varied largely from already implemented methods.[552]

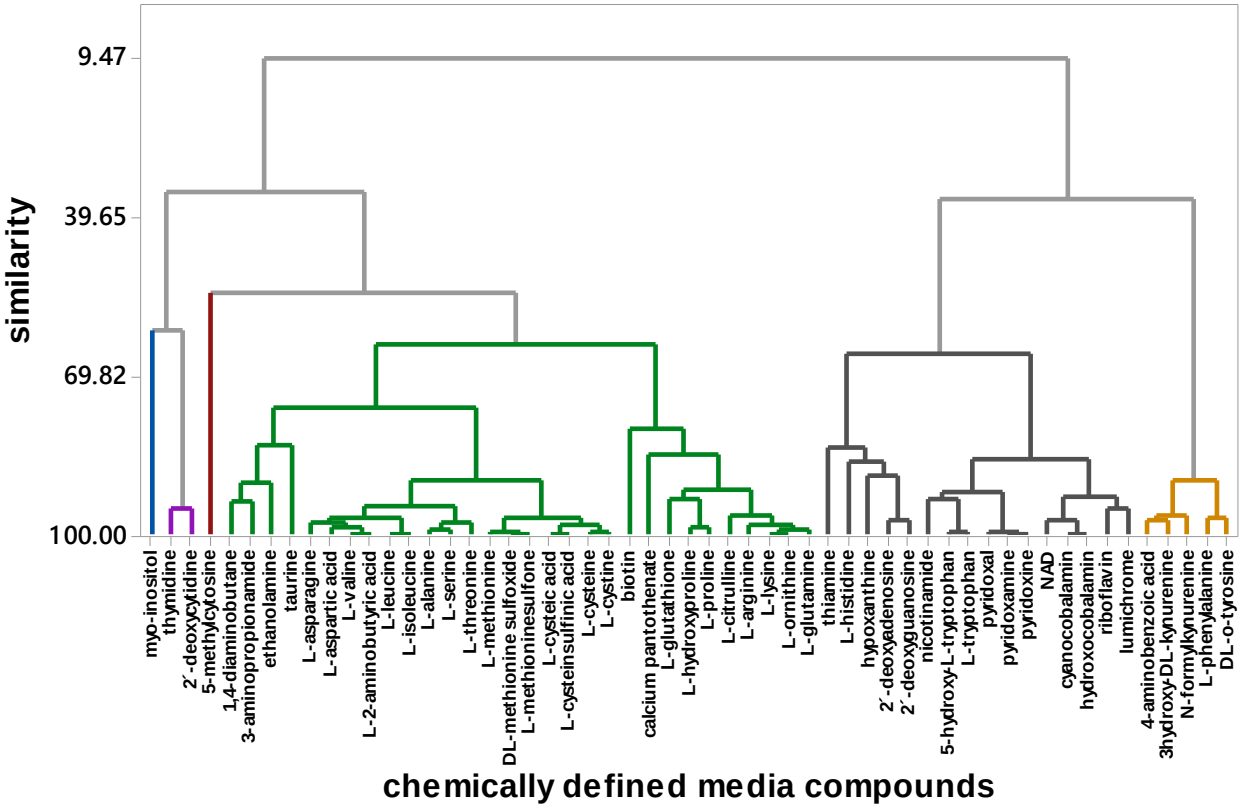

Figure 11: Compounds that were investigated in dMRM method development plotted after their structural similarity index in a dendogram. The colors blue, magenta, brown, green, grey and yellow mark the groups that have less than 70% structural similarity.

In order to obtain good chromatographic separation and maximize selectivity in dMRM, various conditions like mobile phase composition and chromatographic gradient were evaluated and optimized. The result of gradient optimization work is shown in Table 13 (Section Materials and Methods). The gradient was separated into different ramps with the goal to obtain ideal analyte separation. A shallow gradient was used to separate compounds that eluted at similar retention times (0 – 7 min) and a steeper elution profile was used to speed up chromatography at retention times where less compounds eluted (7 – 32 min). The rest of the time the column was flushed and equilibrated with a sped-up flow rate to increase the column volumes per time.

For final retention time determination solutions of 5 combined compounds were prepared. Grouping was done based on similarity index (Figure 11). Specific retention times for each single compound are shown in Figure 10 and Table 3.

The successful gradient optimization resulted in good chromatographic resolution (Figure 12). The small and polar compounds were eluting early but retention was still sufficient to analyze these compounds that are usually not retained by reversed phase chromatography with MS compatible solvents. Inherent selectivity of MRM mode makes co-elution unproblematic. The dynamic MRM mode only scans for analyte of interest in a defined time window around the expected retention time. This allows to increase the ion dwell time which increases sensitivity.

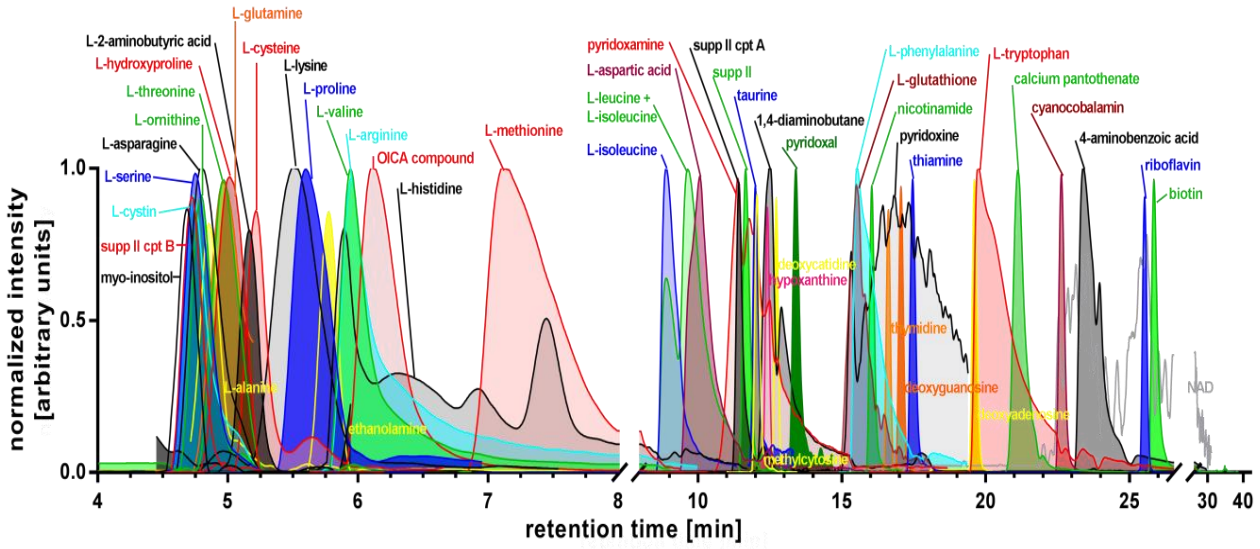

Figure 12: Extracted ion chromatogram (EIC) scan using mixed mode column with QC sample. Compounds that were not validated are shown in yellow, magenta and orange whereas the compounds that were validated for model medium 2 are shown in all the other colors.

Mass spectrometry with its chemical specificity bears challenges in quantitative method development.[553] Urban *et al.* list a table which describes most instrument or sample related factors that affect MS capability to quantify chemical compounds.

In the case of CDM method development with QqQ-MS many compounds are analyzed in parallel. Mass spectrometry is intrinsically not quantitative meaning that the MS detector does not have a universal response to each analyte. Therefore, calibration for each analyte and the application of internal standards is necessary to make analysis quantitative and comparable from batch to batch. The challenge with a multi-component method is to calibrate without an explosion of analysis time due to the number of calibration curve injections. Grouping of compounds depending on their concentration is an approach for compound quantification optimization.[552] In the case of dMRM method development for CDM a compound clustering based on similarity index was considered. However, validation experiments with the calibration standard mixture of all relevant compounds confirmed that it was sufficiently stable. Thus, one calibration stock solution was prepared at concentrations that could be diluted in a way to obtain at least three calibration points above and three below expected concentration level in CDM. Another major limiting factor of stock solution preparation was compound solubility. The stability of the calibration stock solution in comparison to CDM was expected to benefit largely from the absence of metal ions. Additionally, special care was taken to aliquot and freeze (-80°C) the solution right after preparation.

The usage of isotope-labelled internal standards is common practice to compensate for matrix effects and system or sample preparation variability. An ideal case for MRM methods is to have an isotopically labelled internal standard for each analyte. However, isotopically labelled

compounds are very costly and in parts not easily available on the market. Therefore, a retention time region specific approach, similar to examples from metabolomics, has been applied for this method.[554, 555] The commercially available mixture of isotopically labelled amino acids distributed well over the entire chromatogram. The internal standard that has been used for individual compounds is assigned in Figure 10. Because the late retention time area has not been sufficiently covered by amino acid mixture an additional isotopically labelled compound $^{13}C,^{15}N$-calcium pantothenate was purchased and included into dMRM method.

Calibration samples were prepared by diluting freshly thawed aliquots of the reference stock solution at 15 dilution levels with LC-MS grade water (1:1.5:1.33:1.25:1.4:1.28:1.38:1.48:1.35: 1.5:1.33:2:2.5:2:2). For the sake of batch to batch comparability and to minimize sample hold time in autosampler the number of samples analyzed per batch was limited to 30. The batch was started with 3 blank injections for equilibration and the first injections were calibration standards in randomized order. Afterwards QC and actual samples were injected in randomized order interrupted by a water sample every five injections. QC samples were originating of an independently prepared model medium 2 which was measured to demonstrate system suitability and batch to batch comparability at three concentration levels (1:10, 1:50 and 1:250).

3.1.3 Validation of dMRM method

Since the three media described in this thesis were very similar a validation for the most frequently used model medium 2 was considered representative. As pointed out by Kruve *et al.* there is a variety of guidelines for mass spectrometry method validation.[556, 557] In the case of CDM dMRM validation for model medium 2 the FDA guidelines for industry were followed if possible.[558]

Selectivity and Calibration

The dMRM mode in QqQ-MS with individual transitions for each compound is highly specific due to the combination of precursor ion *m/z* and the daughter ions *m/z* (Quantifier and Qualifier). The fast scan rates of modern mass spectrometers allow to measure several compounds in parallel. This makes the detector not only specific for a single compound but also selective for several analytes. Chromatographic resolution adds another dimension of selectivity to the method (Figure 12).

The compounds in CDM are used at a wide range of concentrations. The calibration stock solution has been diluted at 15 concentration levels and injected in randomized order. In a first step, data was evaluated with Pearsons correlation coefficient calculation which indicates a positive linear correlation if values are close to 1 (Table 4 Pearson´s R). Second, all the calibration curves were fitted with linear regression model. If the R^2 values, Pearson´s R and visual observation of regression curves suggested a non-linear correlation (Low numbers for forced linear fit R^2 in Table 4) either quadratic or power regression models were used for calibration. For a multitude of analytes chi-squared Breush, Pagan and Koenker test showed heteroscedasticity impacting the calibration (Table 4, Null hypothesis of homoscedasticity was rejected if pValue ≤ 0.05). Heteroscedasticity means that the calibration data population is heterogeneous with for example higher residuals at higher x values. This can impact the accuracy of concentrations calculated in this calibration curve area and also increase variability.

Table 4: Regression model determination for calibration.

Compound	Regression model	R^2	Forced linear fit R^2	Pearson´s R	Average pVal
1.4-diaminobutane	power	0.982	0.891	0.953	0.077
4-aminobenzoic acid	power	0.980	0.947	0.959	0.127
biotin	linear	0.990	n.a.	0.991	*0.038*
calcium pantothenate	linear	0.996	n.a.	0.998	*0.022*
cyanocobalmin	linear	0.998	n.a.	0.995	0.197
glutathione	linear	0.987	n.a.	0.993	0.159
L-2-aminobutyric acid	linear	0.994	n.a.	0.997	*0.048*
L-arginine	linear	0.999	n.a.	1.000	0.093
L-asparagine	power	0.999	0.983	0.996	0.248
L-aspartic acid	linear	0.994	n.a.	0.997	0.100
L-cysteine	linear	0.985	n.a.	0.993	*0.008*
L-cystine	quadratic	0.999	0.963	0.983	*0.002*
L-histidine	power	0.938	0.728	0.830	0.774
L-hydroxyproline	linear	0.996	n.a.	0.998	0.162
L-isoleucine	linear	0.972	n.a.	0.986	0.112
L-isoleucine + L-leucine	linear	0.953	n.a.	0.976	0.111
L-lysine	power	0.998	0.957	0.979	0.060
L-methionine	quadratic	0.996	0.980	0.990	0.143

Compound	Regression model	R^2	Forced linear fit R^2	Pearson´s R	Average pVal
L-ornithine	linear	0.994	n.a.	0.997	*0.012*
L-phenylalanine	power	0.997	0.964	0.984	*0.020*
L-proline	power	0.998	0.978	0.987	0.300
L-serine	linear	0.996	n.a.	0.998	0.065
L-threonine	linear	0.999	n.a.	1.000	0.158
L-tryptophan	power	0.998	0.966	0.985	*0.027*
L-valine	power	0.998	0.969	0.985	0.479
myo-inositol	linear	0.975	n.a.	0.987	*0.023*
nicotinamide	linear	0.994	n.a.	0.997	0.125
pyridoxal	linear	0.977	n.a.	0.988	*0.032*
pyridoxine	linear	0.997	n.a.	0.998	0.085
pyridoxamine	quadratic	0.997	0.985	0.996	0.263
riboflavin	linear	0.986	n.a.	0.993	*0.032*
taurine	linear	0.958	n.a.	0.963	0.115
thiamine	linear	0.980	n.a.	0.990	0.058
OICA compound	power	0.981	0.927	0.970	*0.009*
supplement II	linear	0.967	n.a.	0.966	0.095
supplement II compound A	linear	0.998	n.a.	0.999	0.148
supplement II compound B	linear	0.991	n.a.	0.993	*0.021*

Sensitivity and carryover

Some compounds (e.g. vitamins) are used at very low concentrations in CDM (compare recipes in appendix Table 15). However, targeted approaches as dMRM mode in QQQ-MS generally have high sensitivity for low concentrated compounds. Lower limit of quantification (LLOQ) and limit of detection (LOD) values have been calculated to estimate method sensitivity. As shown in Table 5 the LLOQ and LOD were in the lower µM range for a majority of analytes. This makes the method well suitable to measure compounds at their expected concentrations in CDM and to detect potential instability. Nevertheless, a minority of compounds like 4-aminobenzoic acid, L-glutathione, biotin and taurine were only quantifiable above 100 µM due to instability (see Table 5). Results below LLOQ were excluded from further data analysis. Carryover from injection to injection was estimated from a blank injected after a series of samples. It was negligible for all compounds (see Table 5).[559]

Table 5: Sensitivity and precision determination of dMRM method. LLOQ/LOD for quadratic regression was determined based on S/N ratio.

Compound	LOD [µM]	LLOQ [µM]	Carryover [%]	Interday precision [%]	Intraday precision [%]
1.4-diaminobutane	9.1	27.7	0.1	6.0	2.6
4-aminobenzoic acid	166.0	503.2	0.0	2.5	1.3
biotin	0.1	0.3	0.0	3.7	1.6
calcium pantothenate	0.1	0.4	0.0	2.6	1.4
cyanocobalmin	0.3	0.8	0.3	4.4	2.2
glutathione	1.7	5.1	0.3	4.7	2.6
L-2-aminobutyric acid	0.3	1.0	-0.3	4.6	2.9
L-arginine	1.2	3.6	0.0	2.2	1.7
L-asparagine	3.2	9.6	0.0	5.9	2.8
L-aspartic acid	16.3	49.5	0.1	4.3	2.9
L-cysteine	17.3	52.3	0.0	5.5	3.1
L-cystine	0.06[1]	0.2[1]	0.0	13.4	3.4
L-histidine	4.5	13.7	0.0	4.0	2.9
L-hydroxyproline	0.9	2.6	0.2	3.8	2.2
L-isoleucine	247.8	751.0	0.0	4.5	3.2
L-isoleucine + L-leucine	1128.6	3420.0	0.1	3.6	2.8
L-lysine	5.3	15.9	0.0	7.2	2.3
L-methionine	3[1]	9[1]	0.0	4.3	3.1

Compound	LOD [µM]	LLOQ [µM]	Carryover [%]	Interday precision [%]	Intraday precision [%]
L-ornithine	0.1	0.3	0.0	4.2	2.9
L-phenylalanine	2.7	8.2	0.0	3.3	1.6
L-proline	2.5	7.6	0.0	7.1	4.5
L-serine	80.3	243.4	0.0	3.7	2.4
L-threonine	40.3	122.1	0.0	3.3	2.2
L-tryptophan	3.7	11.1	0.0	5.1	1.4
L-valine	3.2	9.7	0.3	5.9	5.5
myo-inositol	5.1	15.5	0.0	10.3	5.7
nicotinamide	0.2	0.5	0.0	3.2	1.5
pyridoxal	0.2	0.7	0.5	12.4	3.4
pyridoxine	0.1	0.4	0.2	6.6	2.6
pyridoxamine	0.7[1]	2.1[1]	0.1	5.0	2.0
riboflavin	0.1	0.3	0.4	3.8	3.1
taurine	1.7	5.0	1.6	15.9	4.1
thiamine	0.2	0.5	0.0	5.8	2.7
OICA compound	4.2	12.6	0.0	8.2	4.7
supplement II	247.8	750.8	0.0	14.1	2.4
supplement II compound A	3.1	9.3	0.0	12.4	2.4
supplement II compound B	6.4	19.5	0.1	3.5	2.7

Precision

The intraday precision was determined by triplicate measurements on the same day and the interday precision was determined on six subsequent measurement days. Good intraday and interday precision were demonstrated by low CV for all CDM compounds (see Table 5). Although analytes like L-cystine, myo-inositol, pyridoxal and taurine display percentual interday precision values above 10% the method generally had high precision because it has to be taken into account that these compounds are present in concentrations close to their LLOQs and thus lower precision can be expected.[560] Other than that only supplement II and supplement II compound A show interday precision higher than 10%. Since a new calibration curve has been injected each day and because these two compounds are used at rather high concentrations in model medium 2 it is very likely that this effect is caused by heteroscedasticity in the calibration.

Matrix effect

Cell culture media contain a multitude of chemical compounds. A stock solution with all compounds of interest was used for calibration. In order to reduce the risk of reactivity in this calibration standard solution no further matrix compounds as glucose and metal salts were included. A stock solution with all these compounds not included in the dMRM method was prepared at excess concentration that final concentration of dilution with matrix was comparable to CDM. Retention time stability of stock solution diluted with water and stock solution diluted with full matrix was compared. The relative standard deviation (RSD) of 53 injections of stock solution diluted in simplified matrix, full matrix and in WFI at 1:4, 1:50, 1:100 and 1:500 measured in triplicates is listed in Table 6. This experiment showed that the matrix compounds such as metal salts and glucose did not impact the chromatographic performance of dMRM method. The average retention time of compounds in stock in water, stock in simplified matrix and stock in full matrix does show minimal variation and the retention time observed matches with CDM.

[1] LLOQ/LOD for quadratic regression determined based on S/N ratio

Co-elution of analytes can cause matrix effect in mass spectrometry.[561] This is especially critical for quantitative method development as for the discussed CDM dMRM method. Most of the compounds included in this method did not only show no impact of matrix on retention time but also no effect on signal intensity (Table 6 columns 2 to 5). No major matrix effect was observed for full matrix compared to stock solution in water. Furthermore, no difference could be observed between full and simplified matrix without compounds in trace amounts. As reported in literature our results showed that L-histidine signal intensity is impacted by metallic CDM compounds.[562] Additionally to L-histidine, also L-methionine and L-lysine were shown to be sensitive to matrix composition. Amongst others, these three compounds are tridentate amino acids with side chain functional groups that have high ligand coordination potential.[563] They can for example form complexes with Cu(II) ions.[564] However, copper being the main complex forming agent responsible for matrix effect for these three compounds is unlikely because copper was no constituent of simplified matrix. If copper had been the compound responsible for matrix effect a difference is expected between full and simplified matrix. Most likely these compounds complex with more abundant metals in CDM as for example iron.

After full method validation the measurement of completely metal free CDM basal powders has confirmed that L-lysine signal response in dMRM method was highly matrix dependent. The measurement of completely metal free solution gave L-lysine concentrations that matched the expectation pretty much 100%. However, as soon as sodium hydroxide has been added the concentration increased by a factor of four. Therefore, it is very likely that sodium adduct formation increased the response. The sodium adducts with plus 23 Da were probably not stable enough to withstand the fragmentation in Q2. Thus, it can be assumed that these complexes increased ionization efficiency in the ESI source but broke down in the gas phase of the mass spectrometer.

Table 6: Matrix effect in dMRM method. The norm of a matrix is a scalar that gives a measure of the magnitude of elements of the matrix. 1 indicates the same slope. 0 indicates different slope. The stock solution was mixed with full artificial matrix at a ratio of 1:2. Calculation was done on peak area. Dilution levels with water included were 1:4; 1:10; 1:50; 1:100; 1:500; 1:1000. Values marked in green when x≥0.98. The percent difference of absolute values between different matrix cells marked in green when -30%≤x≥30%.

	Matrix effect; stock in full matrix vs. stock in water		Matrix effect; stock in full matrix vs. stock in simplified matrix		Matrix effect on retention time (rt)	
	Norm of matrix	Difference absolute values [%]	Norm of matrix	Difference absolute values [%]	Impact of full matrix on rt [%]	Average rt [min]
1.4-diaminobutane	0,998	10,2	1,000	10,0	3,4	12,8
4-aminobenzoic acid	1,000	-2,2	1,000	-2,3	1,8	23,4
biotin	0,998	-11,4	0,999	-14,8	1,2	25,8
calcium pantothenate	0,986	51,3	1,000	-6,3	1,2	23,1
cyanocobalmin	1,000	5,4	1,000	-3,6	1,6	22,4
L-glutathione	0,988	-100,5	0,966	51,2	4,6	15,7
L-2-aminobutyric acid	0,996	-6,2	0,998	2,5	0,9	5,2
L-arginine	0,984	-23,7	0,992	-14,1	1,3	6,1
L-asparagine	0,999	8,8	0,998	4,3	0,5	4,8
L-aspartic acid	1,000	-18,1	1,000	-6,7	2,3	10,3
L-cysteine	0,972	-50,8	0,964	37,3	2,8	5,2
L-cystine	0,958	32,0	0,956	-56,8	0,9	4,8
L-histidine	0,972	-36,7	0,987	-3,6	1,7	7,5
L-hydroxyproline	0,999	23,1	0,999	0,3	1,0	5,1
L-isoleucine	0,996	-8,1	0,997	1,7	1,0	9,0
L-isoleucine+ L-leucine	0,993	-4,5	0,997	2,2	1,0	9,7
L-lysine	0,996	-64,1	0,999	4,5	1,2	5,6
L-methionine	0,999	-38,0	0,999	-21,0	1,9	7,3

	Matrix effect; stock in full matrix vs. stock in water		Matrix effect; stock in full matrix vs. stock in simplified matrix		Matrix effect on retention time (rt)	
	Norm of matrix	Difference absolute values [%]	Norm of matrix	Difference absolute values [%]	Impact of full matrix on rt [%]	Average rt [min]
L-ornithine	0,999	6,1	0,997	5,2	0,5	4,8
L-phenylalanine	1,000	-5,4	0,999	-2,5	1,4	15,6
L-proline	0,997	-27,9	0,998	8,1	0,6	5,6
L-serine	0,998	3,7	0,999	5,7	0,5	4,8
L-threonine	1,000	0,3	1,000	0,7	0,6	5,0
L-tryptophan	0,987	13,3	0,994	7,5	1,6	19,6
L-valine	0,998	-15,6	0,999	3,4	0,8	6,0
myo-inositol	0,978	21,7	0,998	15,1	2,3	4,7
nicotinamide	0,991	7,7	0,996	11,6	1,3	15,9
pyridoxal	0,958	-73,5	0,994	-6,7	1,2	13,4
pyridoxine	0,999	-10,0	1,000	-5,0	4,1	15,9
pyridoxamine	1,000	-5,0	0,999	1,6	2,8	11,9
riboflavin	0,990	45,2	1,000	-20,0	1,3	25,4
taurine	0,961	6,1	0,995	-2,2	1,1	12,0
thiamine	0,999	-9,2	1,000	-9,4	1,6	17,5
OICA compound	0,976	67,4	0,976	67,8	1,4	
supplement II	1,000	-15,2	1,000	-3,5	0,9	
supplement II compound A	0,996	-4,8	0,999	-5,8	3,7	
supplement II compound B	0,997	0,5	0,998	8,0	0,6	

Accuracy

The accuracy is a key validation parameter for quantitative methods. It gives the scientist an idea if the analytical method can meet the expected concentrations. Good accuracy was demonstrated for most of the compounds included in CDM dMRM method (Table 7). An exception thereof are compounds that were shown to be impacted by stability or matrix effects, e.g. L-histidine, L-lysine, L-methionine and cyanocobalamin, L-glutathione, L-cysteine, L-histidine, pyridoxal, taurine, L-2-aminobutyric acid, supplement II compound B, biotin and L-hydroxyproline. Most of these compounds are impacted by reactivity (e.g. Lhydroxyproline increases by L-proline oxidation[565]).

The method reproducibility has also been calculated (Table 7). As expected, unstable compounds are characterized by decreased reproducibility. Additionally to these calculations, the concentrations measured in QC samples (model medium 2) were plotted in Xbar-R charts to

monitor reproducibility and instrument stability. That the presented data measured with dMRM were valid could be confirmed by comparing QC samples of each individual batch to expected values in model medium 2 and to historic data (See appendix Figure 63 to Figure 65). The fact that there were pretty much no violations of variation in R-charts shows that the measurement variation was in control. The process means shown in the Xbar charts showed if a batch was deviating from expected value. Because it was assumed that the off-trending of QC samples behaved the same as the samples these system suitability samples gave an opportunity to normalize the data to system variation.

Table 7: Method accuracy and reproducibility.

	Accuracy [%][2]	Reproducibility [%][3]
1.4-diaminobutane	-8,1	16,6
4-aminobenzoic acid	n.a.	n.a.
biotin	41,6	25,8
calcium pantothenate	-5,0	3,3
cyanocobalmin	-49,4	10,1
L-glutathione	-70,5	33,1
L-2-aminobutyric acid	-26,3	5,1
L-arginine	-2,8	1,4
L-asparagine	-10,4	2,1
L-aspartic acid	1,6	3,8
L-cysteine	-77,6	50,9
L-cystine	n.a.	17,2
L-histidine	-23,1	8,7

	Accuracy [%][2]	Reproducibility [%][3]
L-hydroxyproline	797,7	4,4
L-isoleucine	-14,5	25,0
L-isoleucine+L-leucine	-8,4	25,2
L-lysine	126,5	4,5
L-methionine	-15,4	5,8
L-ornithine	8,2	4,0
L-phenylalanine	0,7	2,4
L-proline	3,1	7,4
L-serine	-10,3	2,1
L-threonine	-9,5	2,4
L-tryptophan	3,0	2,1
L-valine	9,2	13,7

	Accuracy [%][2]	Reproducibility [%][3]
myo-inositol	-24,2	8,7
nicotinamide	-7,6	6,9
pyridoxal	-44,6	10,6
pyridoxine	-1,8	10,8
pyridoxamine	n.a.	6,1
riboflavin	-2,9	12,8
taurine	-96,1	107,1
thiamine	-10,9	7,0
OICA compound	-0,7	7,7
supplement II	-7,4	16,6
supplement II compound A	n.a.	23,9
supplement II compound B	-24,6	5,3

Autosampler stability of samples and calibration stock solution

The method was developed with the goal to investigate if CDM compounds are impacted by instability over preparation and storage. Thus, demonstration of sample stability during autosampler hold time is tremendously important to make sure that measurement results were not impacted by instabilities. The maximum batch size was limited to 30 samples resulting in a maximum run time of 2 days for a batch. The QC sample stability at 2-8°C was determined by measuring this sample over 5 subsequent days. Since the stock solution used for calibration curves did not contain catalysing metal salts it was analysed for a two-day period only but at three concentrations that cover the calibration range. Compounds impacted by reactivity or matrix effect were also showing reduced stability. For example cyanocobalamin, L-glutathione, L-cysteine, L-cystine, pyridoxal and taurine were shown to be unstable within a three-day batch. If accurate ratios between redox couples as L-cysteine and L-cystine are of interest, a derivatization might improve compound stability and could be easily adopted for this method.[503]

[2] $\frac{nominal\ concentration - measured\ conc\ CCFMSS.}{nominal\ concentration} * 100 = accuracy$; the average of all QC samples from cell culture feed medium stability study (CCFMSS) is given; accuracy assumed and values marked in green when x≤ +/- 15%

[3] $\frac{\sigma\ measured\ conc.CCFMSS}{\mu\ measured\ conc.CCFMSS} * 100 = reproducibility$; given as CV of QC samples; reproducibility assumed and values marked in green when x≤15%

Table 8: Autosampler stability of samples over 5 days and autosampler stability of stock solution for calibration over 2 days.

	Processed QC sample stability [%][4]					Processed stock solution/calibration curve stability [%][5]						
	1d	2d	3d	4d	5d	1to10 1d	1to10 2d	1to50 1d	1to50 2d	1to100 1d	1to100 2d	
1.4-diaminobutane	93,4	93,6	91,9	98,0	129,4	293,4	348,5	459,5	519,3	80,6	88,2	
4-aminobenzoic acid	~~152,5~~	~~156,4~~	~~263,4~~	~~272,9~~	~~319,8~~	96,8	96,0	93,8	93,9	93,0	93,9	
biotin	88,3	120,5	111,6	151,1	172,4	33,5	270,2	45,6	132,8	279,4	315,0	
calcium pantothenate	97,0	100,8	101,5	99,2	97,5	99,2	97,8	100,7	101,6	100,1	96,6	y
cyanocobalmin	92,1	80,8	84,9	81,2	130,2	88,9	86,1	77,5	74,3	79,8	66,3	
L-glutathione	84,1	89,1	82,2	55,8	55,0	94,1	88,3	104,5	79,5	102,3	71,1	reactivity
L-2-aminobutyric acid	94,0	103,9	99,0	100,8	102,8	117,6	105,7	115,3	107,2	111,7	93,4	
L-arginine	98,2	100,6	101,6	103,5	102,0	99,5	94,8	96,4	97,0	102,4	93,1	
L-asparagine	96,9	100,8	100,1	102,0	103,7	101,5	104,4	102,0	102,5	95,7	96,7	
L-aspartic acid	95,9	88,0	89,3	75,3	73,9	121,0	114,5	128,4	115,3	106,9	122,4	
L-cysteine	11,9	11,6	10,8	10,9	9,9	101,0	97,4	93,2	80,0	82,4	66,9	reactivity
L-cystine	136,7	141,3	136,7	134,6	142,5	104,1	120,2	128,1	164,1	131,5	188,0	reactivity
L-histidine	398,0	3737,2	3973,9	337,1	401,8	1480,3	99,5	1693,2	133,5	146,6	1222,0	y
L-hydroxyproline	103,3	105,7	95,9	97,2	102,5	98,5	106,2	94,6	88,2	120,7	84,5	
L-isoleucine	96,8	100,0	93,7	91,6	97,0	95,6	94,3	99,8	92,5	103,8	103,9	
L-isoleucine+L-leucine	96,8	99,6	92,7	92,3	97,2	97,2	95,2	100,5	94,7	102,2	105,9	
L-lysine	99,3	96,6	101,7	99,3	102,6	103,8	100,9	99,6	100,2	101,6	101,3	y
L-methionine	105,8	104,4	110,5	120,7	116,0	96,6	89,1	94,6	91,0	102,7	86,2	y
L-ornithine	99,4	110,4	113,8	117,2	124,1	105,1	105,1	115,2	112,2	94,4	96,3	
L-phenylalanine	102,2	108,5	111,6	109,4	114,5	100,1	99,2	98,6	102,1	99,3	102,5	
L-proline	97,1	94,4	100,6	96,5	96,8	102,6	102,0	98,5	98,6	102,8	102,5	
L-serine	102,2	105,3	107,2	103,3	104,0	104,3	97,8	100,1	101,3	102,8	104,0	
L-threonine	103,3	112,2	115,5	115,0	120,3	104,3	102,8	100,8	105,4	104,6	111,9	
L-tryptophan	100,5	100,6	101,1	101,1	106,7	101,0	100,4	101,5	100,4	100,8	101,0	
L-valine	107,4	117,8	111,8	115,8	121,1	99,3	101,0	98,5	100,3	105,9	107,5	
myo-inositol	90,6	118,6	95,8	77,7	88,4	109,0	85,6	187,1	131,6	4812,0	1886,3	y
nicotinamide	95,1	97,9	97,1	92,3	97,3	98,1	93,1	102,3	98,3	93,8	95,0	
pyridoxal	126,8	142,7	154,7	143,5	154,4	123,8	134,3	144,2	184,4	99,9	142,8	reactivity
pyridoxine	90,3	98,8	111,8	119,1	139,3	102,6	102,5	103,9	100,9	78,8	75,5	
pyridoxamine	102,6	109,2	114,8	109,2	117,8	104,5	105,2	98,4	100,6	97,3	96,3	
riboflavin	104,0	103,2	100,4	104,9	139,8	89,8	71,9	74,2	82,3	84,7	93,0	
taurine	23,2	33,8	33,0	29,8	55,9	153,7	154,3	134,1	139,3	116,0	108,9	reactivity
thiamine	97,4	114,3	125,8	127,1	153,1	101,2	103,6	99,6	106,2	89,4	98,6	
OICA compound	105,3	118,2	120,0	126,4	135,5	110,4	114,4	93,5	97,6	112,1	108,6	reactivity
supplement II	104,9	108,0	103,2	102,8	107,9	113,6	116,1	131,5	124,5	104,6	107,5	
supplement II compound A	114,3	104,8	115,1	94,2	110,6	101,0	101,0	104,5	102,0	105,9	103,9	
supplement II compound B	95,5	98,1	102,5	96,6	95,9	96,2	93,2	98,9	93,7	101,3	102,6	

[4] $\frac{relative\ response\ when\ either\ made\ 1d,2d,3d,4d\ or\ 5d\ pause}{initial\ relative\ response} * 100 = processed\ QC\ sample\ stability$; QC sample was prepared by 1:10 dilution with water and stored in autosampler and measured on 6 successive days; stability assumed when values marked in green 85%≤x≥115% recovery rate

[5] $\frac{relative\ response\ calibration\ curve\ at\ dilution\ levels\ 1{:}10{,}1{:}50\ and\ 1{:}100\ after\ 1\ and\ 2\ d}{initial\ relative\ response} = processed\ stock\ solution/calibration\ curve\ stability$; calibration curve was prepared three times and put in autosampler. Samples were measured on 3 successive days. stability assumed and values marked in green 85%≤x≥115%

Concluding remarks on CDM dMRM method validation

The method was valid to measure BI model medium 2. Considering the high similarity of recipes, it is also suitable to investigate the other media described in this thesis. The method development and validation work resulted in a method that covers more than 50% of BI media compounds. In summary, the novel dMRM method was shown to be highly sensitive, selective and enables straight forward data interpretation. It is thus suitable for the monitoring of CDM composition.

3.2 Feed Medium Preparation

High reproducibility is fundamental for commercial drug manufacturing and at scale media makeup. Especially parameters like stirring speed, addition time of specific recipe positions, tank geometries and material, the dissolution time at certain pH and the temperature of WFI at the beginning and during preparation are very important. Nowadays, the only routinely measured and documented medium parameters are pH right after adjustment and osmolality. This can make comparability between medium batches very vague and inaccurate. Especially in the case of possible trouble shooting activities the measurement and documentation of only two medium parameters leaves a lot of room for speculation and complicates root cause definition. Therefore, both technologies that enable online monitoring for the comparison of medium preparation profiles and off-line technologies that enable a deeper understanding of CDM quality are highly desirable.

3.2.1 Online sensors to monitor and compare cell culture medium preparation

The application of online probes is ideal for live observations and they provide high resolution. Furthermore, the monitoring of key chemical parameters increases knowledge about CDM properties.

Evaluation of univariate sensors to monitor dissolution of powders in medium preparation

Because the medium plays an essential role in biomanufacturing its make up should be controlled and monitored to understand the impact on process robustness. A very simple way to monitor the CDM makeup is the application of online univariate sensors. These technologies enable a live monitoring of parameters such as dissolved oxygen (DO), potential of hydrogen (pH), the conductivity and the oxidation reduction potential (ORP), which is the capacity of a liquid system to release or accept electrons. The following paragraphs discuss the usage of univariate sensors as monitoring tool during medium preparation with a focus on how to judge when the added compounds are fully dissolved and when the next addition can be done.

Dissolved oxygen

Even though oxygen mass transfer was determined by gassing for the chosen preparation vessel, the determination of oxygen diffusion rates over surfaces is usually more complex and not routinely determined for cultivation vessels.[566] With the chosen stirrer speed of 485 rpm it looks like a DO of 19 to 20% is the maximum that can be reached and the increase is not linear (Figure 13). It is noteworthy that all the univariate probes used are temperature corrected. A value of 90% saturation means an approximate oxygen concentration of 6 mg/ml in water due to the high temperature of 35°C (See appendix Figure 66 and compare to oxygen saturation monograms[567]). Figure 13 shows that the dissolution of cysteine does not impact DO values. Addition of basal powder however increased the slope of the DO curve in the first moment. By mass, the basal powder is the biggest portion of the medium after water. Because of the sheer amount of loose solid added to the preparation vessel some subsequent problems may arise. When getting moist, the medium powder can form a thick layer of wet powder on the liquid surface covering the entire diameter of the preparation vessel. To understand why lumping can happen, it is important to know what is happening when the powder is added to the solvent. The liquid starts to penetrate through the powders pores by capillary forces.[568] This increases the contact area between the liquid and the medium compounds in the powder. If wetting of powder is not fast enough lumps of dry powder with an outer gel layer can appear. This can be prevented by increasing temperature or shear forces. Since further heating was no option due to possible impact on chemical reaction rates a spoon was used to shatter lumps and increase shear forces on the surface of the medium under preparation in the small-scale medium preparation model. Additionally to luring, powder

can also trap air. Thus, when big amounts of powder are added at once it will entrain air that rises to the surface while solid material dissolves. If there are foam stabilizing ingredients (e.g. protein) in the powder this can even lead to foam formation. Both the additional mixing right after basal powder addition and the air trapping effects of some powders can explain why the slope of DO increases for some time after basal powder addition. The peak in Figure 13 marks the time point where powder dissolution is close to completion and before mentioned effects get overlaid by oxygen consumption. Due to the complexity of the basal powder composition this effect cannot be accounted on specific chemical reactions. Because the slope of DO curves flattens after a while it can be assumed that a solution containing only cysteine and basal powder would equilibrate at a DO level around 16% under the chosen conditions. The addition of basal powder is considered as critical in CDM preparation because of the versatile potential issues described for basal powder dissolution and the chemical complexity of the powder.

The addition of an insulin stock solution shows negligible effect on DO profile. In contrast, the addition of organic iron compound (OIC) causes a drastic decrease of DO. Within minutes the DO drops from 16% to around 2%. This effect was not known to the Boehringer Ingelheim media development group until the first time a DO probe was used during medium preparation. The drastic decrease of DO was hypothesized to be caused by a redox reaction. Due to the goal of having media as stable as possible during manufacturing and storage with as little chemical reactivity as possible this DO drop was considered very important to be understood. More detailed investigations of this specific phenomenon are discussed in more detail in chapter *3.2.3 Identification of oxygen consuming reaction after organic iron compound addition during medium* preparation. The subsequent compound addition in the recipe of model medium 1 is glucose. As this is the solid adding the second most mass to medium the slight increase of DO after addition can again be explained by air trapping in the powder. The dissolution of supplement II does not have an impact on DO concentration. The filling up step with WFI briefly increased DO. This can be expected because the water used to adjust to final volume should have the same level of DO as the starting condition. Before pH adjustment with NaOH was started the DO profile dropped back down to where it was before WFI addition (around 2%). The addition of base finally decreased DO to close to zero. Over several hours of observation the DO level remained low. This is remarkable because the medium was stirred during that time and this is normally expected to increase oxygen diffusion into the medium.

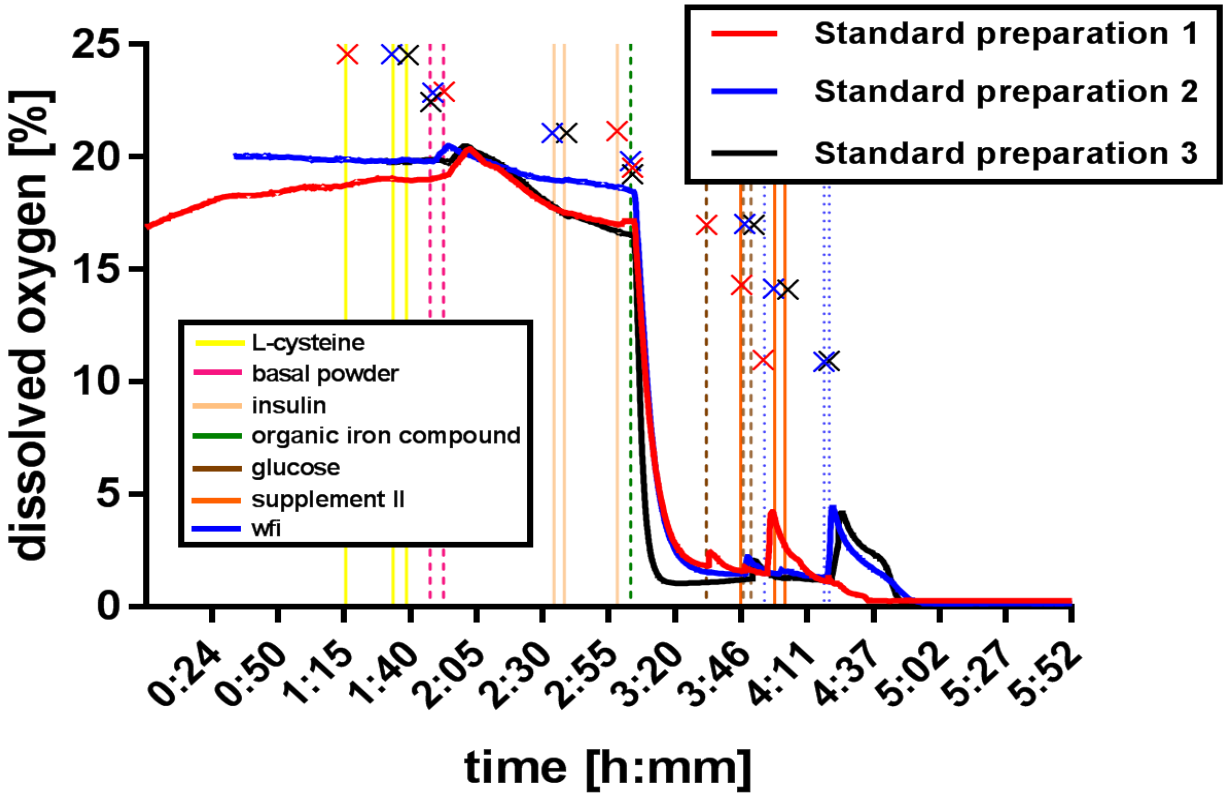

Figure 13: Dissolved oxygen over the time course of three independent model medium 1 preparations. The addition time points of media compounds are marked by vertical lines in the respective colors. Each compound addition line is marked with a cross in the color of the respective medium preparation. The data was aligned that the time point of organic iron compound addition is plotted in parallel. The time scale is starting with the preparation that had the most data points until organic iron compound was added.

pH – concentration of hydrogen ions

The pH probe profile (Figure 14) shows that a drastic drop of pH value occurs right after Cysteine addition. Due to the fact that the hydrochloride salt of cysteine was used for this medium preparation this is expected. More interesting is the fact that basal powder has some basic effect on the solution. Besides of a lot of amino acids it also contains buffer compounds to maintain stable pH during storage and cultivation. After basal powder addition it took about 15 minutes until pH reached a constant value. This may be an indication of the time needed for all the compounds of basal powder to dissolve. The time when pH is constant around 4.1 also correlated very well with the moment when it was noticed that all the powder was visually dissolved. The addition of all the following compounds had a negligible effect on the pH. When pH adjustment was started with NaOH the titration steps can be followed live with the online probe. The target pH for this specific medium was 7 and it was exactly reached after titration. A minimum of 5 minutes was given for the pH to stabilize. Waiting some time after reaching target pH is common practice in cell culture media make up. But this time is not further specified and can thus lead to a different amount of base added to the medium. An effect that can only be observed if an online probe is used is the pH starting to drift down after adjustment. This effect has not been further investigated up to date. It is possible that the mainly carbonate buffered system has its optimum under atmosphere at this pH. For a feed medium, as model medium 1, this slight difference to target pH is tolerable for cell culture. Both closed cultivation systems and open shaking flasks are operated with a pH control that can rapidly correct for discrepancies to the pH set point.

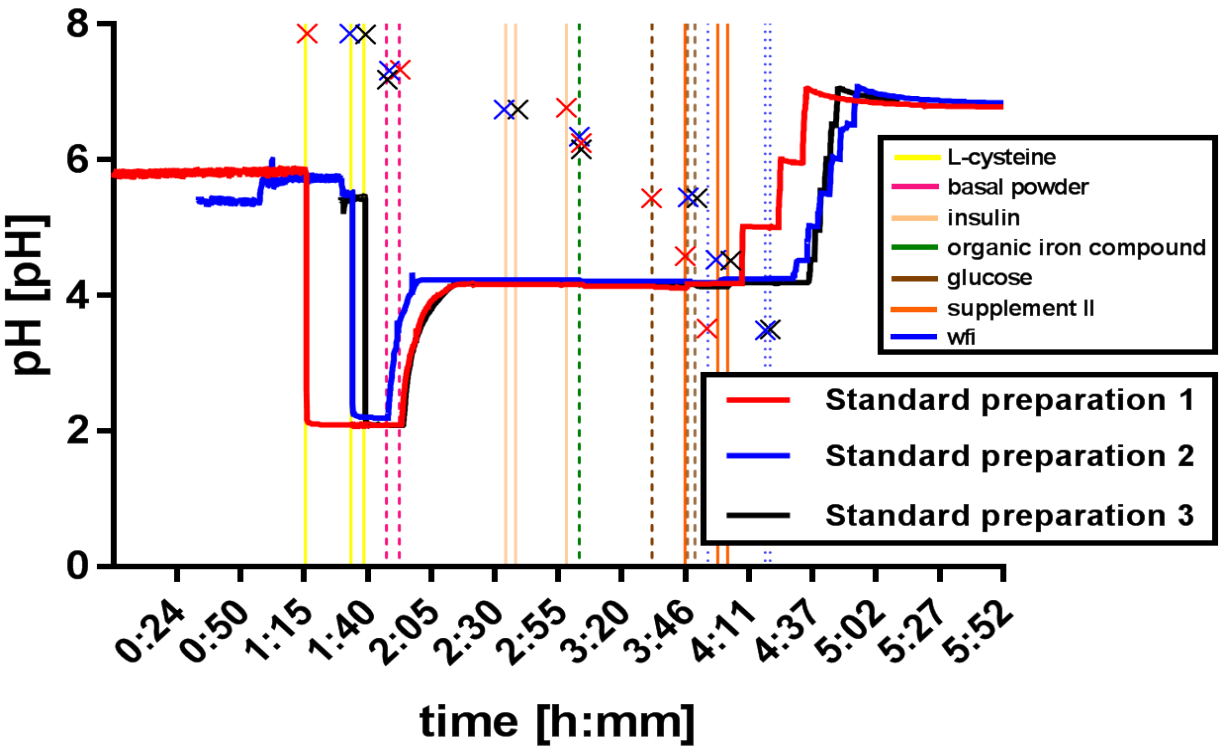

Figure 14: pH over the time course of three independent model medium 1 preparations. The addition time points of media compounds are marked by vertical lines in the respective colors. Each compound addition line is marked with a cross in the color of the respective medium preparation. The data was aligned that the time point of organic iron compound addition is plotted in parallel. The time scale is starting with the preparation that had the most data points until organic iron compound was added.

Oxidation reduction potential (ORP)

The ORP is an indicator of a solution system´s capability to donate or accept electrons and it gives a measure of the oxidizing or reducing power.[569] Because of the fact that a redox systems potential depends on the redox state of all present compounds it can take a long time until a stable reading is achieved. This mainly depends on reaction rates of involved chemical reactions but also on the compounds concentration. Variability and long time to constant reading can for example come from dissolved oxygen that makes up the biggest portion of oxidizing compounds in WFI. Oxygen reacts slowly with the platinum electrode and therefore it takes a long time until equilibrium has formed. Just as other ions like HCO_3^- the dissolved oxygen is not electroactive and does not readily take up or give off electrons at the platinum ring ORP element of the EasyFerm Plus ORP Arc sensor.[570] Additionally, in open atmosphere systems as the small scale medium preparation tank with constant stirring oxygen diffusion is always present. This leads to varying dissolved oxygen concentrations over time. Besides, ORP can be significantly impacted by pH.[571] Due to these two effects it is not surprising that ORP is not constant when only WFI was held in the preparation tank (Figure 15). The addition of the first compound L-cysteine showed a drastic drop from oxidizing (+ 250 mV) to almost neutral in comparison to the AgCl reference electrode. Even though the initial reaction of the probe to the compound addition is spontaneous, the still drifting values showed that equilibrium had not formed. The first approximately constant value was reached at 30 mV. The addition of basal powder pushed the ORP to negative values (-80 mV). Due to the complexity of basal powder composition this can hardly be accounted to a specific compound group. Without supporting experiments every statement remains highly speculative and addressing this topic is beyond the scope of this thesis. The insulin addition can barely be distinguished from permanently occurring signal drift due to equilibrium formation. In contrast, the addition of organic iron compound resulted in a steep increase of approximately 80 mV to

approximately +10 mV. However, the maximum after organic iron compound addition lasted only for several seconds before drifting to values close to 0 mV. All the following compounds added had a minimal effect on ORP signal. The only noteworthy step is the addition of water. This increased ORP by approximately 10 mV before the pH adjustment with NaOH. The addition of base could be followed in steps until an ORP of -200 mV was reached with the last NaOH addition to a final pH of seven. But as it can be seen from behavior of ORP after pH adjustment it takes a very long time until ORP has reached equilibrium (Figure 15 and Figure 24).

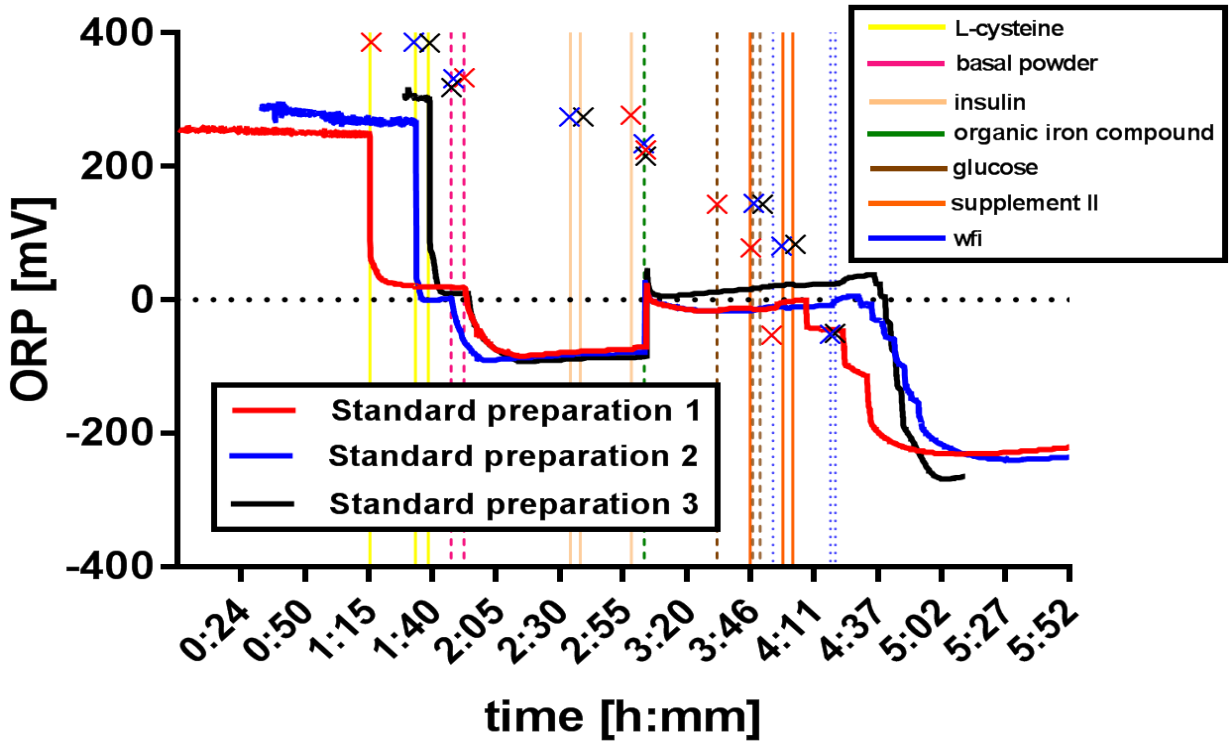

Figure 15: ORP over the time course of three independent model medium 1 preparations. The addition time points of media compounds are marked by vertical lines in the respective colors. Each compound addition line is marked with a cross in the color of the respective medium preparation. The data was aligned that the time point of organic iron compound addition is plotted in parallel. The time scale is starting with the preparation that had the most data points until organic iron compound was added.

Conductivity

As expected, the conductivity of WFI is with 3 µS/cm extremely low (Figure 16). Due to the highest purification standards it should be free of any ions that can conduct electricity. Even though the small scale preparation system was intensively cleaned and rinsed with WFI after each usage it is always possible that some minimal traces of contaminants remain on surfaces. The addition of the first compound to the water increased the conductivity to 6700 µS/cm. This is a magnitude over the value of WFI and can be explained by the now available ions that can carry the electric current. The conductivity reacts instantly to the addition of L-cysteine showing the good dissolution properties of this compound and the fast response of the probe. When the basal powder is added the conductivity first drops in comparison to previous values. As explained earlier, powder can trap air and pull it under the liquid surface. The two poles of the probe are sitting on the flat end of the probe shaft. The flat surface and the two outstanding poles showed to trap air bubbles preferably when those were present in the liquid. Because air is known as a bad conductor of electricity this drop at the beginning of basal powder addition is well explainable. When the addition of powder was finished the air bubble got off the probe by the turbulence generated by the stirrer. Then an increase of conductivity until it reached a maximum at 20000 µS/cm was observed. It then took a while until the signal becomes constant and less noisy.

For standard preparation 2 however, the signal remained very noisy until the next compound addition. This may be accounted to more air in the system as confirmed by the dissolved oxygen plot (Figure 13). The time point when signal got constant again correlates pretty well with the time when it has been noted that visually all the basal powder was dissolved. The next few compound additions did not change much in the overall conductivity signal but increased noise right after addition or for a longer time. Whether this comes from the powder dissolution or of air bubble formation is extremely hard to judge and makes the evaluation of complete dissolution time point ambiguous and error prone. One interesting observation that has been made during medium preparation is that after organic iron compound addition a lot of small gas bubbles have formed. In contrast to compounds where air trapping is likely the cause of bubble formation, the bubbles after organic iron compound addition only formed when the powder was dissolved, and the bubbles were distributed homogeneously over the entire liquid volume. The fact that glucose addition is not increasing conductivity is not a surprise. Due to the molecular structure with only covalent bonds glucose is not able to form ions. Why glucose addition indeed decreased conductivity will be discussed in the chapter about glucose addition. The next step in CDM preparation that decreased conductivity is the WFI fill up step. This is expected due to the minimal conductivity of WFI as could be seen from the starting conditions and the medium matrix dilution caused by the fill up step. The addition of sodium and hydroxide ions during pH adjustment then slightly increases conductivity to its final value of 14900 µS/cm.

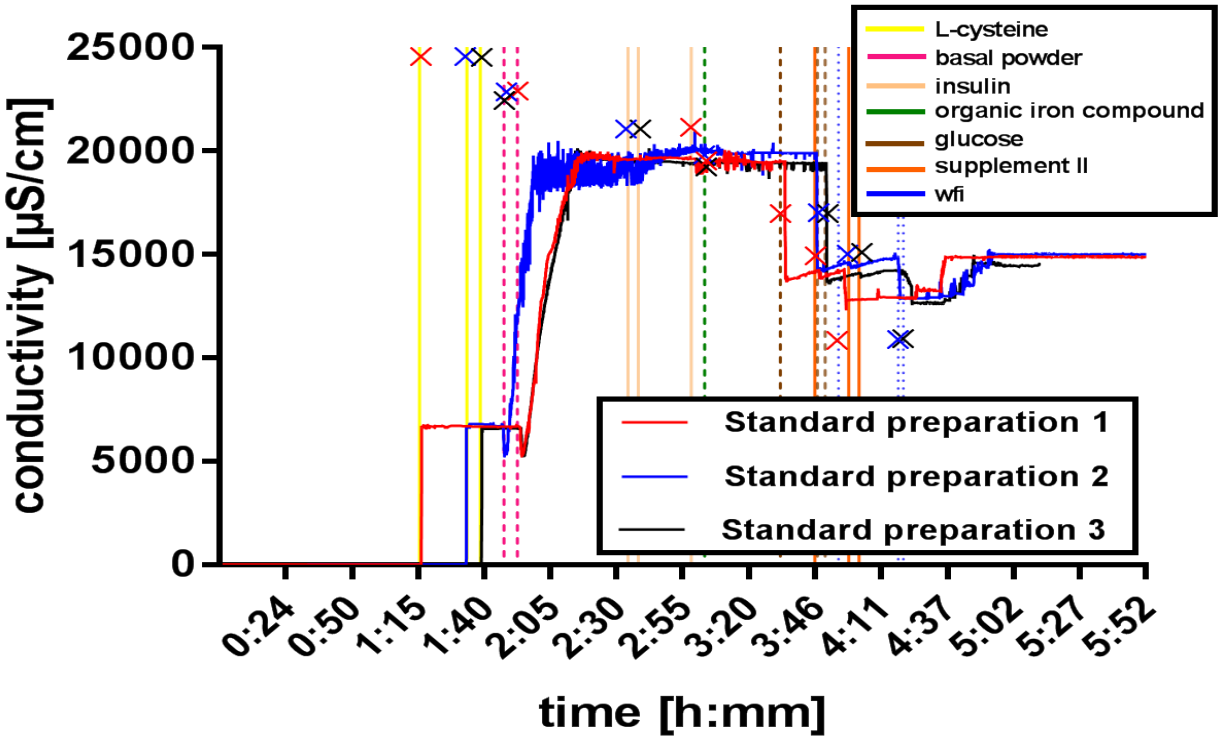

Figure 16: Conductivity over the time course of three independent model medium 1 preparations. The addition time points of media compounds are marked by vertical lines in the respective colors. Each compound addition line is marked with a cross in the color of the respective medium preparation. The data was aligned that the time point of organic iron compound addition is plotted in parallel. The time scale is starting with the preparation that had the most data points until organic iron compound was added.

Comparison of all used univariate sensors in parallel

For a final judgement of the value of univariate sensors for media preparation it is interesting to compare the responsiveness to compound additions and how the signals correlate (Figure 17). As already mentioned, before medium preparation was started the WFI was kept at constant temperature under stirring. Whereas the signal of conductivity remains stable, the signals of the three other used probes show a very slight drift that is most probably caused by gas diffusion at the surface enhanced by the stirring. ORP and pH are depending on each other as will be explained later. However, the saturation rates are different because the ORP is not only depending on the hydrogen ion concentration but also impacted by the presence of other chemical compounds. For example, Sessa *et al.* presented an example where a solution with a strong oxidant persulfate shows decreasing redox potential with increasing pH. Because of the logarithmic scale of pH, a slight change can already mean a dramatic concentration change in hydrogen ion concentration. Therefore, it is not surprising that the rates of equilibrium formation for the two probe types are not correlating. When the first compound is added pH, ORP and conductivity show a signal change at the same time. Whereas the pH and conductivity signals remain stable pretty fast after the addition the ORP needs some more equilibration time. When the basal powder is added these three probes again show a fast response. The behavior of dissolved oxygen has been described before and is strongly impacted by the effects of powder addition. It is interesting to note that the shallowing of the peak after basal powder addition in DO profile happens closely before the other probe signals become constant. As can be seen from the behavior of DO signal after L-cysteine addition with zero response and the delayed response to basal powder addition this still very important parameter is proven to be unsuitable as online monitoring tool of medium preparation. It does not reliably give information when a powder is completely dissolved and when the next one should be added to keep media preparations comparable. In contrast, the three other probes show direct responsiveness to when the powders are added. The ORP reaches the fastest a minimum value upon the addition of the first compound. But after that it takes time until an equilibrium is reached and this time can be long, depending on the compounds dissolved. The pH and conductivity reach a constant value pretty much with the time point of visual dissolution and the signals remained stable afterwards. For basal powder addition both the pH and conductivity signal are a good parameter to judge the powder dissolution. However, these two probe types show no response to the following supplement III addition. In contrast, the dissolved oxygen and ORP signal clearly show a chemical change in the solution. For the pH adjustment of course the pH probe is the most useful one. But also ORP and conductivity show some signal change upon base addition. The examples discussed show that all online probes for water parameters tested have their advantages and limitations. From the set of the four tested probe systems no clear recommendation can be given for an online monitoring tool of medium preparation. The most general probe that gives an estimation of powder dissolution time point might still be conductivity measurement.

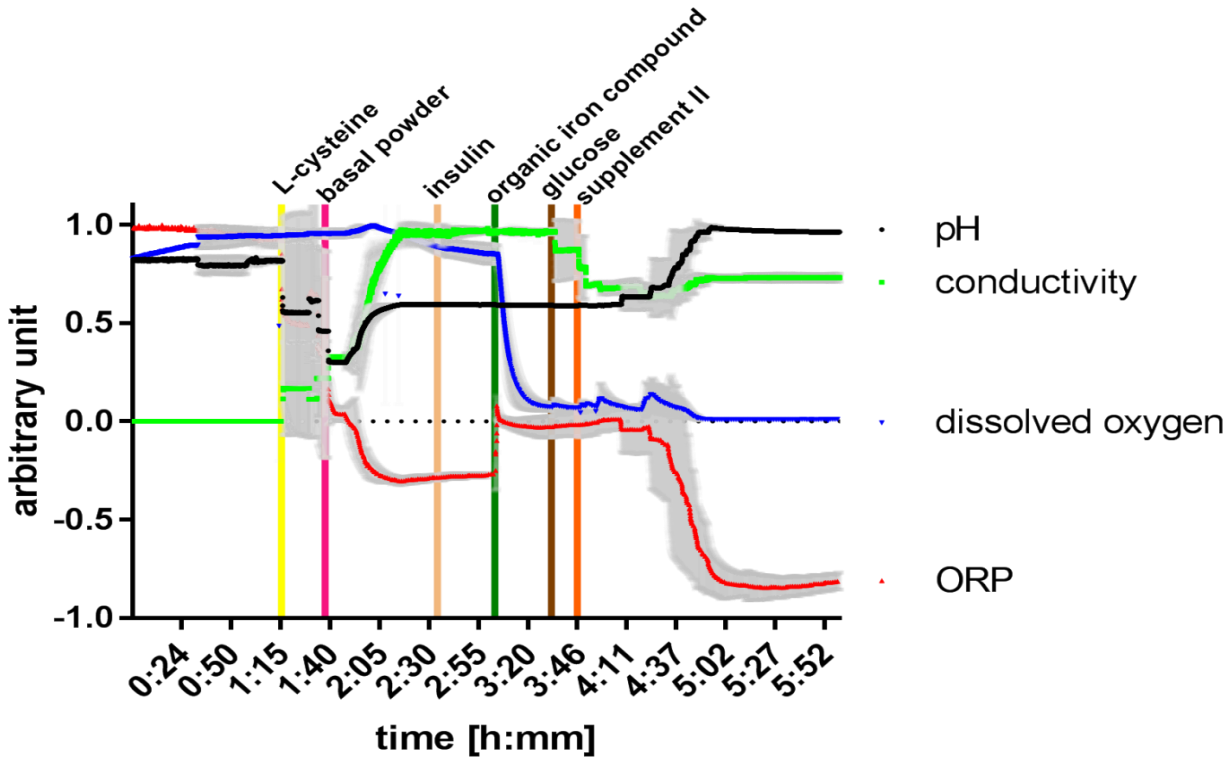

Figure 17: Parallel comparison of univariate sensors during medium preparation. Plotted is the mean of the three standard preparations normalized to the maximum with standard deviations (SD) shown in transparent grey. The vertical colored lines symbolize an approximated average compound addition time point.

Evaluation of dissolution of powders using a particle probe

The focused beam reflectance measurement (FBRM) technology has been described in literature for the measurement of particle chord length in medium dissolution kinetics estimation.[478] The online probe has been evaluated on its capability to judge whether a powder was completely dissolved during media preparation. Furthermore, the particle profiles were analyzed with a focus on batch to batch comparability. As shown in Figure 18 A and B the L-cysteine addition does not add many particles in comparison to maximum particle count appearing during preparation. At least on the chosen scale it cannot be distinguished from water. When the basal powder is added, the number of measured particles increases significantly. It reaches quickly a maximum of approximately 60 counts/s (Figure 18 A and B). It is very interesting to note that right after the addition of basal powder there is almost no increase in particle count observable (Figure 18 C). This is expected, due to the before described effect that basal powder builds up a thick layer of wet powder on the surface. If no additional shear force is applied (e.g. stirring with spatula or increased stirring rate) the powder only starts to dissolve after wetting is sufficient to break down the lumps. After 20 min of stirring the thick layer started to break up what can be seen by an increase of particle counts. In Figure 18 A and B a blue arrow points at a particle population with a chord length from 50 to 100 µm. These particles only occur when the thick layer on the surface breaks apart and small lumps are getting into the solution that keep on dissolving as they are stirred. The typical chord length for the particles with the highest abundancy in model medium 1 range from 1 to approximately 50 µm (Figure 18 C and D). This particle population remains more or less constant over the entire medium preparation until the pH adjustment is started (Figure 18 D). This observation leads to the conclusion that there must be some compounds in the basal powder that are not soluble in the acidic pH range during medium preparation.

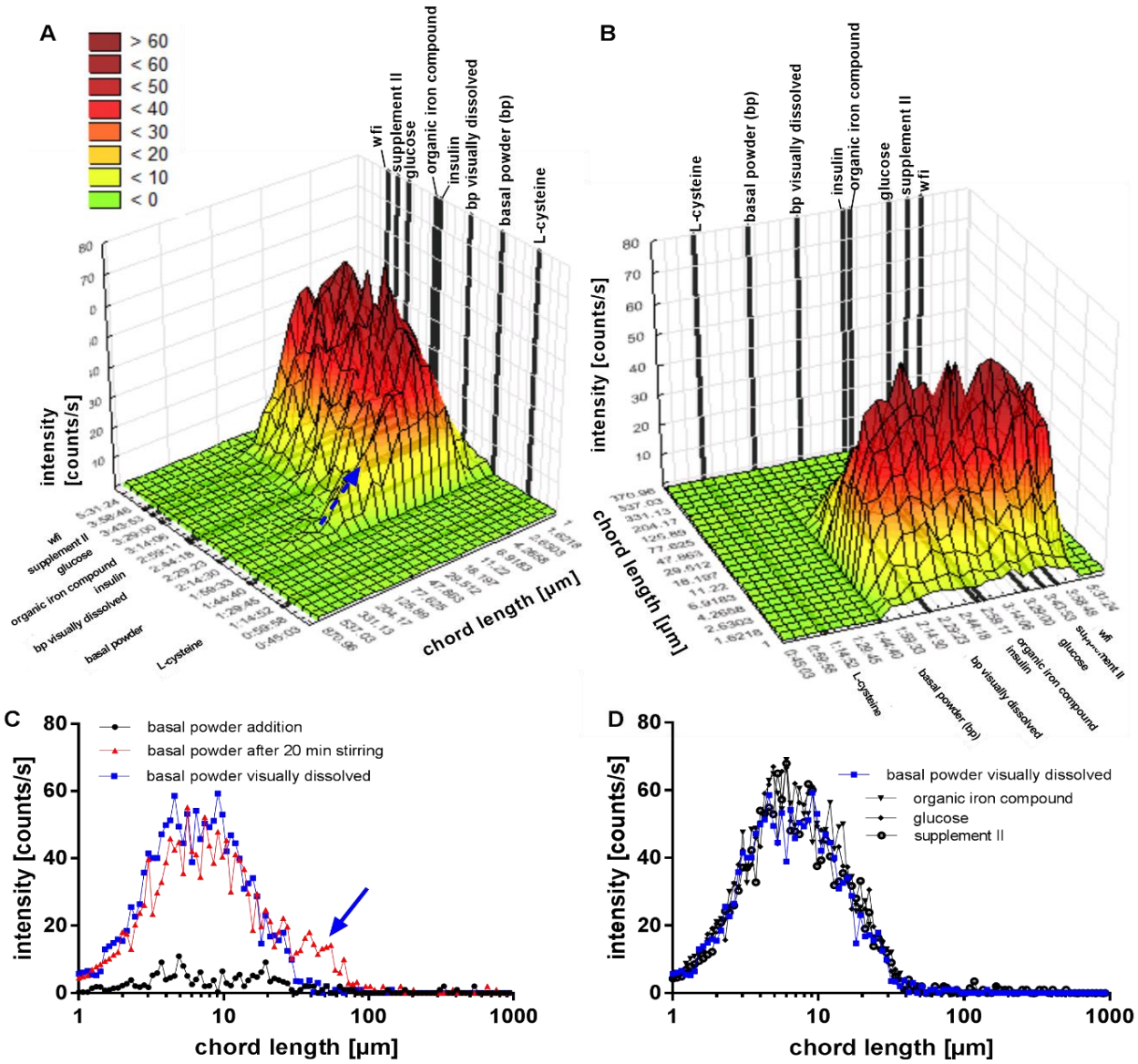

Figure 18: Particle size distribution of model medium 1 during preparation. A) and B) 3D Sequential Graphs of model medium 1 preparation. The black lines mark the addition time points of medium compounds on the x axis. The blue dashed arrow in A) points out a population of particles with a high chord length that appears with the addition of basal powder. After a little while these big particles disappear. B) shows the 3D graph from a different angle pointing out that there is no significant change in particle population with short chord length (< 4 µm). C) and D) show the intensity of particle size measured as chord length at chosen time points during medium preparation. C) focuses on basal powder addition showing that there is no signal right after addition. Again, the blue arrow shows a particle population of long chord length that disappears after approximately 30 min when the medium under preparation was visually clear. D) points out that the addition of any following medium compound didn´t change the particle size distribution.

When the NaOH is added these particles dissolve and remain in solution (Figure 19 A). The graph shows that the dissolution of particles happened very abruptly when a pH of approximately 5.5 was reached. After the pH adjustment the particle count is very low (1 count/second) and the counts for the particle profile are approximately 10 times lower compared to visually dissolved before NaOH titration has started. However, when the particle profile of after medium preparation is compared to pure water at the beginning it is obvious that even completely clear medium after preparation contains more particles than WFI (Figure 19 B). As explained in the introduction, filtration is a common approach to sterilize CDM. Since sterility is absolutely critical for successful cell cultivation each kind of filter clogging that may make a filter change necessary is considered as absolutely high risk. Thus, it would be desirable for cell culture medium development to have a tool that can predict filterability from a particle distribution. However, the predictive power of

particle count on filterability can be very elusive. A high number of big particles does for example not necessarily lead to filtration issues. If the filter cake building up remains permeable there will not be an impact on filter performance. In contrast, particles in the submicron size category that perfectly fit into the filter's pores are likely to cause bad filter performance and might be the most problematic for filterability. Standard filter membranes used for medium sterilization have a pore size of 0.1 or 0.2 µm. However, particles in this size range cannot be detected by the FBRM technology because it is limited to particles bigger than 1 µm. During medium preparation the particle size distribution measured with FBRM can give a good hint when powder particles are dissolved. This is true if each compound added dissolves right after addition. When looking at the profile of model medium 1 this is not the case because after basal powder addition each following compound addition gets masked by the high remaining particle count from the basal powder addition.

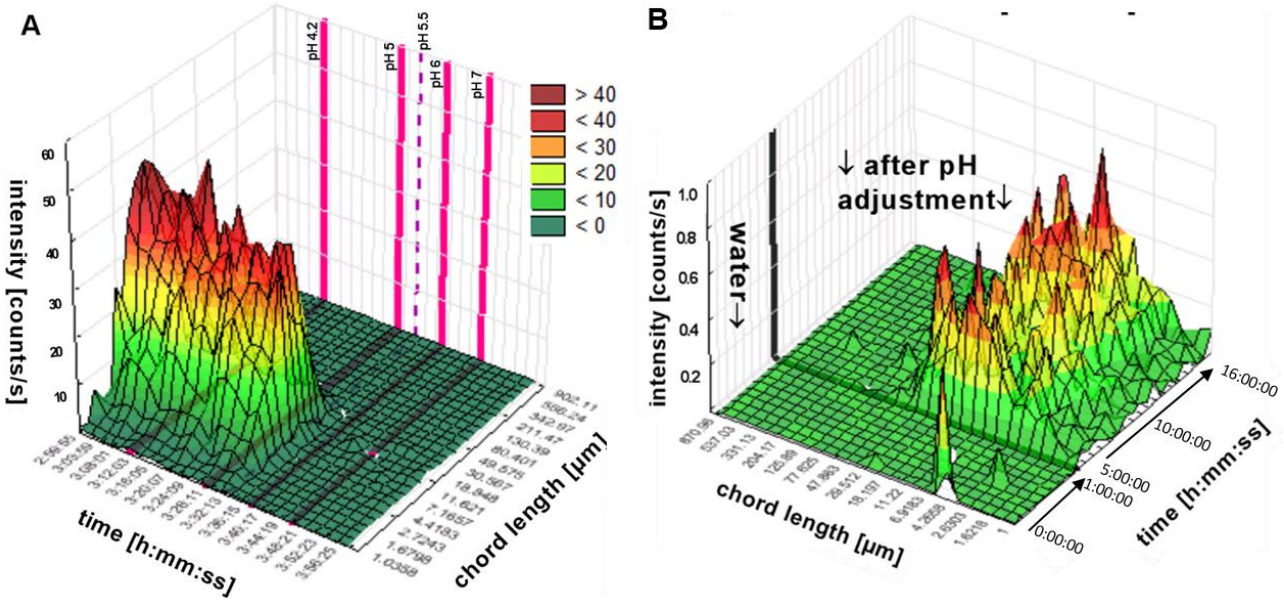

Figure 19: Particle size distribution during pH adjustment in model medium 1. A) shows the 3D sequential graph of the particle population during NaOH titration. The solid pink lines mark the pH that has been reached at the specific time points by base addition in intervals of one unit. Additionally, a pink dashed line has been added to mark the time point when particles dissolve. B) In this part the whole preparation part has been cut out of the 3D graph to compare the particle profile of readily prepared medium to pure WFI. The frontier between WFI particle size distribution and medium after preparation is symbolized by the bold black line.

Effect of preparation temperature and basal powder composition on particle distribution

As shown by the investigations of model medium 1 in the previous chapter, the FBRM principle measures particle populations during medium preparation. A common and simple strategy to improve powder dissolution is to increase temperature. In order to investigate the impact of temperature and the chemical composition on dissolution time model medium 1 was prepared at different temperatures and with different basal powders. Preparation in the coldroom at 2-8°C was compared to standard preparation conditions at 35°C. An interesting and important side effect for the characterization of CDM is that the low temperature should slow down chemical reactions as will be discussed in the following chapter.

As the focus in model medium 1 preparation was on comparable sampling, the basal powder was not shattered and pushed under surface with a spatula. When particle count is plotted against time this led to very little or no particles bigger than 150 µm right after basal powder addition (Appendix Figure 67). The media prepared at 35°C showed few particles ≥150 µm right after addition for a short time. But especially the medium prepared at 2-8°C had a very stable basal

powder layer that did not release particles ≥150 µm. The big particles observed in the standard temperature preparations quickly broke down to particles with chord length of 50 to 150 µm due to shear forces (Figure 20 A). After a short peak, this particle population further broke down until it remained constant (metal free with exception of Na salts) or almost completely disappeared (less than 10 counts/s for standard and metal free plus NaCl). In contrast, the medium prepared in coldroom showed a constant increase of particles with chord length of 50 to 150 µm. This underlines the assumptions that particles that break out of the moist basal powder layer on liquid surface are of this particle size population. In contrast to the biggest particles measured (≥50 µm), the profile of the smallest particles (1-50 µm) looked different (Figure 20 B and C). It has been explained that some of the compounds in model medium 1 only completely dissolved when a pH of 5.5 was reached. Thus, a constant particle population is observed after big lumps break down due to shear forces. An equilibrium of aggregation and dissolution processes forming a suspension can be assumed when the particle populations are stable and a plateau in particle count is reached. As shown in Figure 20 B and C the media prepared at standard preparation temperature showed a constant increase of particle count over time for approximately 10 min with a short peak and a subsequent decrease to the final level. The plateau is reached already in less than 16 minutes for particles smaller than 50 µm. In contrast, the preparation at 2 to 8°C reached a plateau only after 1 hour and 20 minutes. Additionally to the longer time for stable particle population formation there is a higher total count of particles per second. This is expected because dissolution processes are endothermic reactions with slower kinetics at decreased temperature and with a specific activation energy. If the required energy level to dissolve some compounds is not reached the suspended particle count remains higher. This makes the medium prepared at 2-8°C a suspension before pH adjustment with even more particles compared to standard preparation. The comparison of model medium 1 preparations at 2-8°C to standard preparations at 35°C showed that differences in dissolution behavior due to temperature variation can be measured with FBRM.

Additionally to temperature, the effect of chemical composition of model medium 1 on dissolution behavior was also investigated. Metal free basal powder and metal free basal powder with the exception of sodium salts was compared to the standard basal powder. Figure 20 A shows a different particle population behavior for metal free basal powder with Na salts in comparison to standard and completely metal free basal powder. After 30 min a stable population with approximately 100 counts/s was observed. This indicated a different dissolution behavior. For the intermediate sized particles of 10 to 50 µm the distribution pattern of both modified basal powders looks very comparable to standard chemical composition (Figure 20 B). However, when comparing profiles of particles with ≤10 µm chord length the final count/s is double as high for modified chemical composition as for standard powder (Figure 20 C). It is interesting to note that for all particle categories from 1 µm to 150 µm the metal free basal powders reach the apex faster than the preparation with standard powder. This simple experiment with 3 different basal powders shows that chemical composition can impact particle break down and dissolution behavior. Furthermore, the data shows that FBRM is in principle capable of analyzing CDM prepared at different temperatures and with alternative chemical composition.

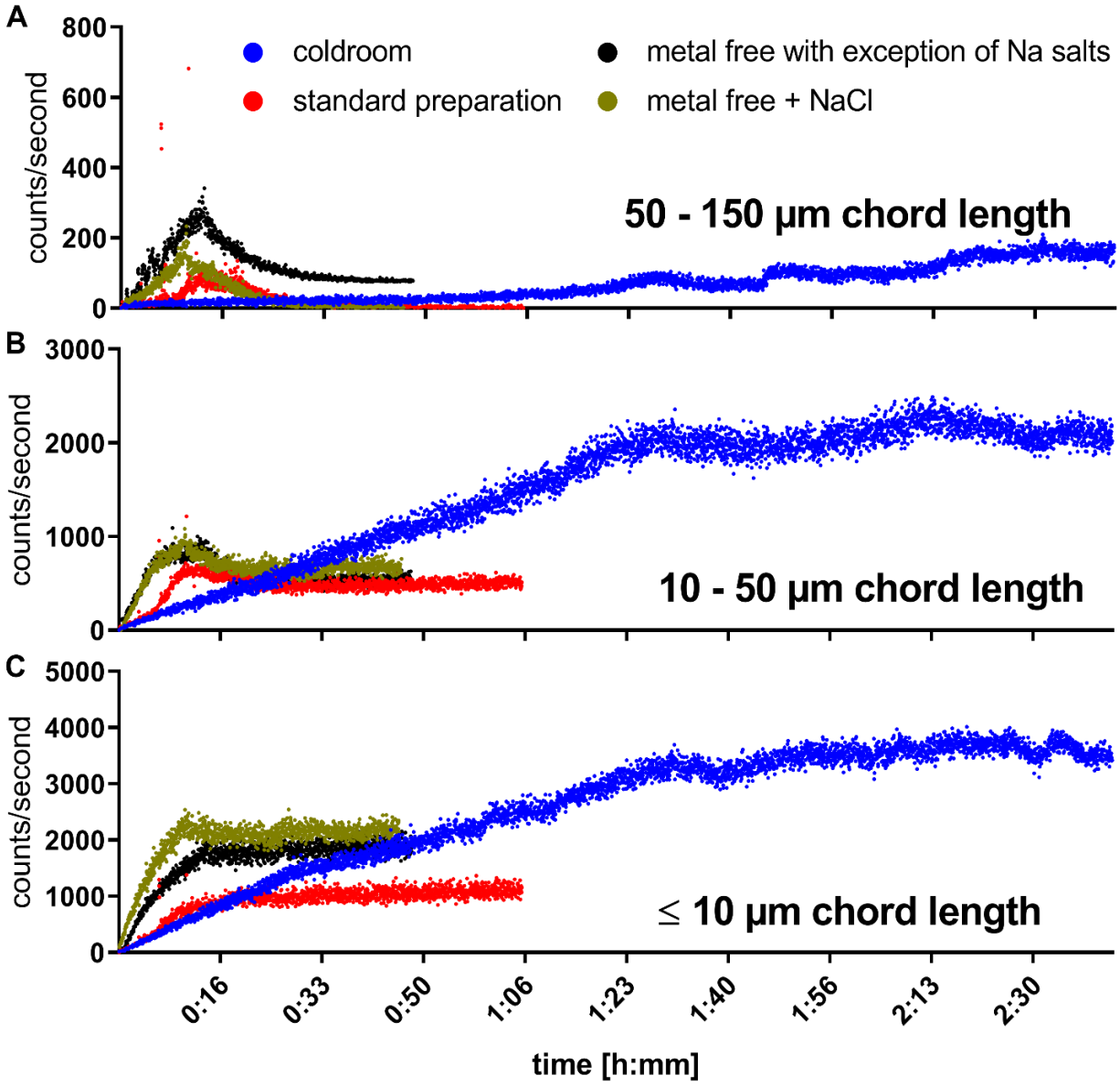

Figure 20: The particle counts per second plotted over time after basal powder addition in model medium 1 preparation. The particle frequency is the cumulated counts per second of the respective size range. A) shows the particles with chord length from 50 to 150 µm, B) shows particles with chord length between 10 and 50 µm, and C) shows particles with chord length smaller than 10 µm.

The experiments with model medium 1 proved the principle that effects of temperature on medium dissolution could be measured with FBRM. As the temperature difference between 2-8°C and 35°C is rather big and since such low temperatures are not realistic for standard medium preparation a follow up experiment with a process relevant temperature range was designed. For this purpose model medium 2 was used as the particle profile measured with FBRM showed in total lower intensity over time and basal powder compounds dissolved after approximately 10 min (Figure 21). It is interesting to note that the comparison of these two media recipes shows that FBRM profiles of different media recipes can be easily distinguished.

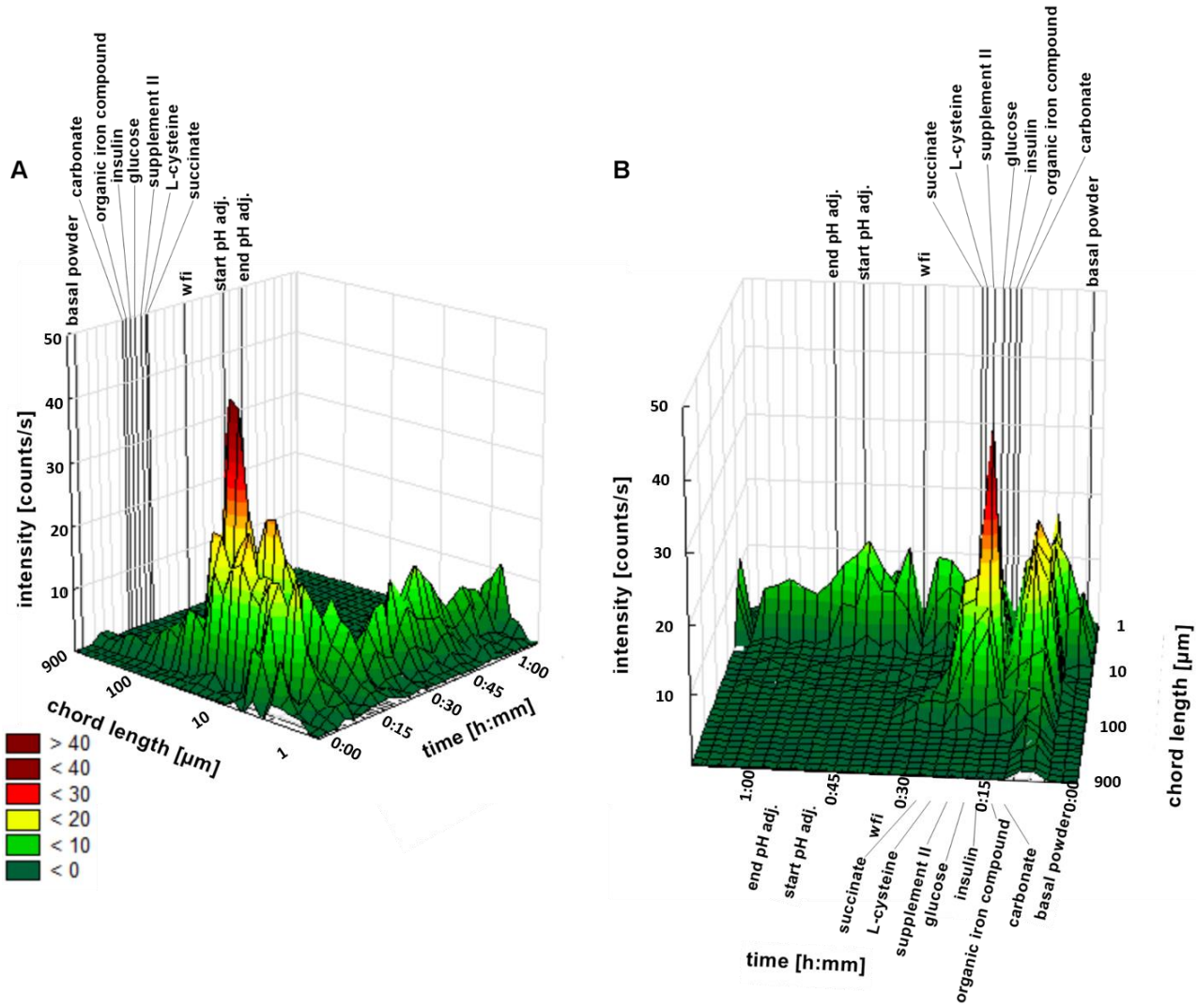

Figure 21: Particle size distribution of model medium 2 during preparation. A) and B) show the 3D sequential graph from two different angles. The black lines mark the addition time points of medium compounds on the x axis.

The fact that no undissolved compounds from basal powder addition were hiding all the following additions like in model medium 1 made model medium 2 a much better candidate to investigate batch to batch variation. Of special interest was if differences in preparation temperature in a range from 25°C to 40°C can be monitored with FBRM technology (Figure 22). Furthermore, the impact of this temperature range on chemical behavior was of interest and will be discussed later in this work. Especially in large scale it is not always technically feasible to exactly match a specific temperature setpoint. Therefore, ranges are defined for the target temperature in standard operating procedures (SOP´s) that are typically derived from assumptions. Thus, the focus of this experiment was on the impact of temperatures above and below the target of preparation temperature range on the dissolution kinetics and chemical behavior. This is of special interest for the scientific evaluation of empiric temperature ranges defined in SOP´s and to estimate the impact of deviations in the case of trouble shooting activities.

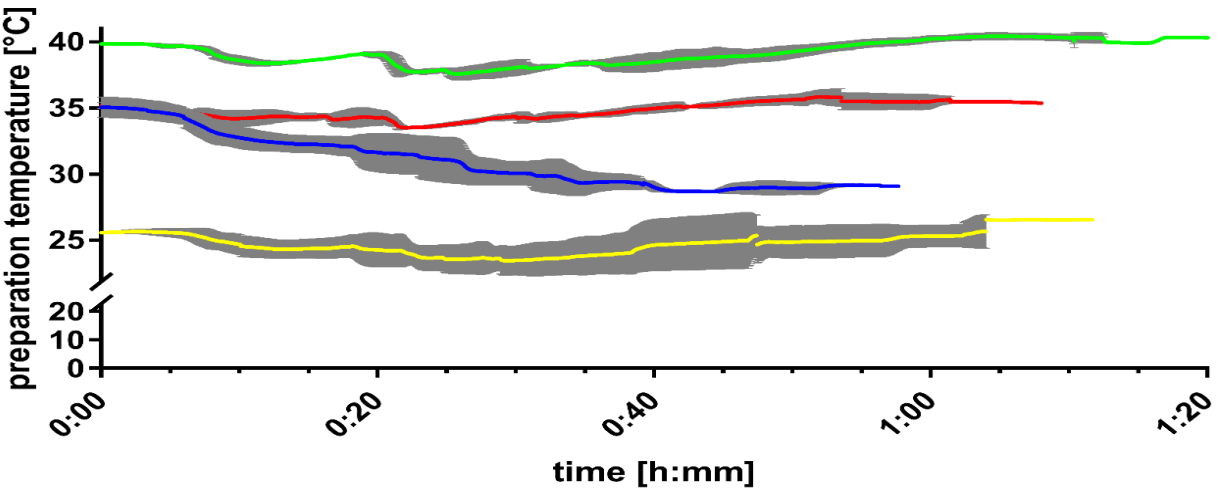

Figure 22: Temperature measured during medium preparation. Each line shows the mean of three independent preparations. The standard deviation of each preparation temperature condition is plotted in grey. Yellow: 25°C target temperature with further temperature control; Blue: 35°C starting temperature without further temperature control; Red: 35°C target temperature with further temperature control; Green: 40°C target temperature with further temperature control.

In order to further investigate if preparation temperature differences relevant for medium make up in small- and large scale could be monitored using FBRM technology the dissolution kinetics after basal powder addition were observed (Figure 23 and Figure 68 in appendix). Figure 68 in appendix shows that the particle size distribution after basal powder addition of model medium 2 is including chord length of the entire measurement spectrum of the FBRM probe (1-1000 µm). However, by absolute counts per second the small particles (≤150 µm) are predominant. By comparing the four preparation temperatures in Figure 23 no trend with preparation temperature can be observed. The standard deviations of the plotted mean value of the three individual preparations show such a big overlap in a random pattern that the preparations have to be considered identical due to high data variability. One could argue that high variability could be introduced by shattering of the powder layer on the surface with a spatula. However, shattering was done for a maximum of 1 minute by manually pushing powder under the surface. Consequently, it can be expected that particles generated by this uncontrolled process must be very big in size. Furthermore, the spatula was used for a short and very specific time, so it is not expected to have a big impact on overall data variability. The high comparability of all preparation temperatures is confirmed by the particle size distribution of chord length ≤ 150 µm (Figure 23 A, B and C). The FBRM data has revealed that the basal powder dissolution with the applied powder addition procedure and defined power input is finished after 10 min with high reproducibility. This can be seen by the low particle count (≤ 200 counts/second) with low standard deviation in Figure 23 A, B and C after 10 minutes of mixing after basal powder addition. The determined time needed for basal powder dissolution is important for the improvement of model medium 2 preparation protocol with fact based specific stirring times and will help to improve reproducibility in the plant. The robustness of basal powder dissolution to the investigated temperature range is an advantageous result for media development because it provides scientific understanding of dissolution kinetics and allows to determine a bigger temperature range for medium preparation under GMP. This will give flexibility in the media production without affecting the dissolution steps. Additionally to basal powder dissolution behavior, the impact of preparation temperature on chemical composition is of major interest and will be discussed in the following chapters.

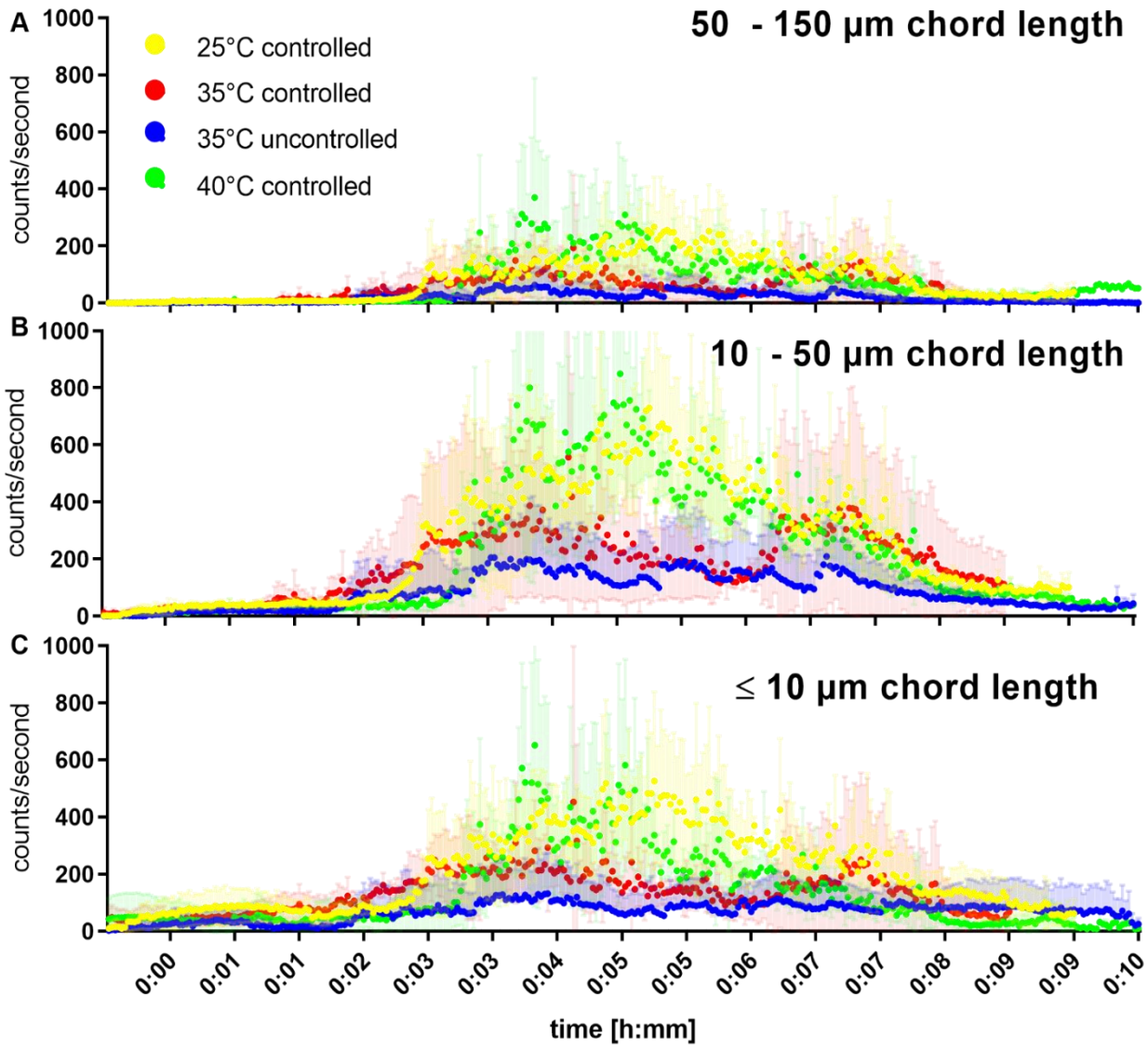

Figure 23: The particle counts per second over time after basal powder addition in model medium 2 preparation. The particle frequency is the cumulated counts per second of the respective size range. A) shows the particles with chord length from 50 to 150 µm, B) shows particles with chord length between 10 and 50 µm, and C) shows particles with chord length smaller than 10 µm.

As FBRM data analysis of basal powder addition showed high robustness to temperature, the next step was to understand if the entire model medium 2 recipe preparation did also not show temperature sensitivity. For this purpose, the data of the 12 independently prepared cell culture media at 4 different preparation temperatures with the same recipe were analyzed using principal component analysis (PCA). Because two preparation tanks were used in parallel also two different FBRM probes had to be used. Therefore, first a model was generated for each probe individually to get a feeling how comparable the two systems would be. The Figure 69 and Figure 70 in the appendix show that the majority (more than 80%) of variance in the particle distribution data monitored with FBRM during preparation is explained by principal components (PC) 1 and 2. As can be seen in the loadings plot (particle size versus principal components) for both probes used, the PC 1 and 2 behave very comparably. Therefore a model with all the data included and two PC´s was generated (Figure 71 and Figure 72). As shown in Figure 71 B the Q residuals and especially T-squared hotellings are very high. This means that the variability in the model is still very high and that the data of the particle profiles during preparation is not well represented by the PCA model. Figure 71 A in appendix shows that the data of the two probes used is having only

little data coverage offset so the poor model cannot be explained by differences of the two probes. Comparing the patterns for both PC´s in Figure 72 also confirms that there is no trend with the probe used. Looking at the particle profiles based on PCA (Figure 72 and Figure 71 C) revealed no trend with preparation temperature in the FBRM data. Finally, it is important to emphasize that no model could be found that describes patterns in the FBRM data measured during model medium 2 preparation at different temperatures. The fact that no patterns could be found underlines that there is no real difference in the data and the PCA model confirms what can be concluded by visual data interpretation. The particle size distributions over the entire time range of model medium 2 preparation is robust to the tested temperature range. In other words, dissolution kinetics of model medium 2 is comparable from 24 to 40°C.

In summary, the FBRM technology has been found suitable to distinguish between different preparation temperatures and chemical compositions of model medium 1. This was possible even though the chemical properties of model medium (basal powder composition and recipe order) with the high particle number masked all powder additions and a dissolution was only achievable with pH adjustment. The proof of principle for temperature effect detection on dissolution behavior was achieved with a big 30°C temperature difference. The effect of process relevant temperature ranges (25 to 40°C) on dissolution behavior of model medium 2 was not present. This is emphasizing the robustness of model medium 2 dissolution behavior on temperature variability. Furthermore, this information is highly beneficial for the definition of temperature ranges in process descriptions.

Conclusions on the usefulness of evaluated online probes for the routine application

The conductivity and pH probes are very valuable to judge the time point when basal powder dissolution is complete in medium preparation. This can be useful in a large scale stainless-steel tank where foaming and a powder cap on the solution can hinder the visual judgement of basal powder dissolution. Furthermore, visual judgement is very subjective and depends on operator, but probe signals do not. Both probe types have the limitation that they show signal response to specific compounds only. pH probe is limited to either bases or acids and if working in a strongly buffered system as the medium small amounts of base and acid may not even be detected. The conductivity can only give information about the dissolution of compounds that either increase or decrease the transportability of charge (in the investigated model medium 1 L-cysteine, basal powder and glucose). The dissolved oxygen probe is rather not useful to judge powder dissolution because it shows no clear response to the addition of most powders and is strongly impacted by oxygen diffusion and effects that can happen during powder addition. Nevertheless, it revealed an important insight that there is a strongly oxygen consuming reaction going on after organic iron compound addition that keeps the feed medium at 0% DO afterwards. Thus, this probe is very useful in medium development to gain understanding of CDM preparation. The ORP is an interesting tool that shows pretty much a direct response to the addition of each chemical compound. However, as explained earlier it reaches equilibria slowly. Therefore, it is not useful to judge if a powder is completely dissolved or not during preparation. The univariate sensors are beneficial when a protocol for medium makeup needs to be established and when it comes to scale-up or transfer between different manufacturing sites to guarantee that key chemical properties are identical. A similar conclusion can be made for the multivariate FBRM sensor. It showed a very slow dissolution kinetic of basal powder at extremely low temperature for media make up (2-8°C) and revealed different dissolution properties of chemically distinct basal powders. In medium development it can add information of how the particle size distribution looks like when the visually noticeable particles are broken. Thus, it can contribute information for the development of medium preparation protocols. If several replicate data sets of the

preparation of one medium recipe with comparable addition time points are available, the average time for particles reaching constant level after compound addition can be determined (even in different preparation vessels). This can be helpful to define time ranges the ideal medium preparation should have for a distinct CDM recipe. But even though the probe can measure the particle level present after medium preparation it cannot predict the medium filterability due to its limitations for particles smaller than 1 µm.

When it comes to long term batch to batch comparability between media preparations the univariate probes must be evaluated differently. The usage of these probes in many batches prepared the same way (mounting of probes and time intervals between powder additions) would be necessary. Then, some statistical approaches on a high number of replicates would be necessary to estimate which of the probes is the most useful to judge the comparability between media preparations. Along with that, a correlation to cell culture performance would be necessary to conclude on medium quality. However, doing this kind of work was beyond the scope of this thesis.

Another possible application of the probes could be the detection of a forgotten powder addition, but this would have to be tested in separate experiments. Additionally, other control strategies may be easier to implement and worked effective in the past.

All five probes tested during medium make up were shown to have their advantages and drawbacks. For the decision when the next recipe position needs to be added the FBRM probe is the most useful if the powders dissolve during preparation. This would exclude the applicability on media like model medium 1 where the majority of components only dissolve when pH is adjusted and the threshold of pH 5.5 is reached. An impact of process relevant temperature ranges on dissolution patterns was not detected but there could be still an impact on media chemistry. For better batch to batch comparison more online information about the chemistry going on during medium preparation is needed. Therefore, the application of different measurement principles as Raman spectroscopy [572, 573] or near infrared (NIR) spectroscopy [574] would be an option.

3.2.2 Chemical stability during medium preparation – comparison of univariate sensor signals with chemical compound concentration

The monitoring of DO during routine medium preparation revealed a drastic DO drop happening in model medium 1 preparation after organic iron compound addition (Figure 13). As mentioned earlier, robust bioprocess development requires chemically stable medium with reproducible properties at the end of preparation. Because such a dramatic oxygen drop during medium preparation is an obvious indicator of chemical reactivity the impact on chemical composition could be tremendous. For that reason, it is of high importance to understand the influence on the CDM composition and if essential compounds get depleted or if potentially toxic compounds get generated. The goal of gaining knowledge about such chemical reactions in CDM preparation is to have basic knowledge for developing control strategies (either avoiding reactions or control them so the output of medium preparation is reproducible). Therefore, model medium 1 was prepared under different conditions and with different basal powder composition. The preparation in the cold room at 2-8°C and the preparation under nitrogen gassing were conducted with the aim to slow down or to prevent the responsible reactions. Furthermore, an identification of reactive compounds by comparing the physico-chemical and chemical profiles to a standard preparation was of interest. Additionally to changing physical parameters, an approach with simplified medium basal powders has been tested. Because the medium recipe includes several

metal ions which are known to be good catalysts of redox reactions due to redox cycling between oxidation states, all the metal containing compounds were eliminated.[575] Since the reduction of sodium (Reaction 1) has a very negative standard redox potential in acidic aqueous solutions at 25°C (E^0=-2.714 V) it is very unlikely that this reaction happens under the conditions present during medium preparation:

$$Na^+_{(aq)} + e^- \leftrightharpoons Na_{(s)} \; (Reaction\ 1)$$

Therefore, additionally to the basal powder with all metal salts eliminated there was a second mixture that involved all the sodium salts but no other metal salts. The following subchapters discuss chemical behavior during the medium preparation of these test cases and where differences may come from.

Univariate probe readings in water for injection (WFI) and factors impacting accuracy and precision

Conductivity in WFI is the same for all experiments (Figure 16 and Figure 24 D). This is not surprising because there are no ions dissolved in WFI that can transport charge and the signal is close to zero. The specification level of WFI in the European Pharmacopeia is 0.6 – 4.7 µS/cm^{-1}.[576] The distilled water that was used for all the medium preparations described in this thesis easily fulfilled this criterion with 1 – 2 µS/cm^{-1} before the first compound addition. In the same time this low reading in the medium preparation tank is a confirmation for the sufficient cleaning procedure.

In contrast to conductivity the pH measured in pure water has higher variation with a mean value of 5.5 and a standard deviation (SD) of 0.15 pH (Figure 24 C). The specifications of the applied Hamilton EasyFermPlus Arc 120 probe is given with a reading at zero point of 0±20 mV and a sensitivity of 57 to 59 mV/pH slope. If we consider these parameters the pH meters sensitivity will be 1/57x0.2=0.035 pH.[577] However, overemphasizing the resolution and accuracy of pH can be misdirecting. Several factors can impact pH reading as for example temperature, stirring, cross sensitivity to other ions like e.g. sodium and suspension effect.[577-579] Therefore, it is reasonable for the discussed experiments to assume an accuracy of ± 0.1 pH units. For example, the in and out diffusion of gas to a stirred system at the open atmosphere as the applied medium preparation tank cannot be controlled. Because fresh water usually has a pH between 6 and 7 the reaction of CO_2 with water will form $CO_{2(aq)}$ or H_2CO_3 (Reaction 2).[580] The formed carbonic acid then dissociates and acidifies the water (Reaction 3):

$$H_2O + CO_{2\,(aq)} \leftrightharpoons H_2CO_{3\,(aq)} \; (Reaction\ 2)$$

$$H_2CO_{3\,(aq)} \leftrightharpoons H^+ + HCO_3^- \; (Reaction\ 3)$$

Because the described experiments were intensive in preparation time it was not possible to perform the different preparations in one series. Therefore, it is possible that the conditions in the WFI system were slightly different from day to day. It for example has the option to tap the water at different temperatures. Generally, the solubility of gases in liquids decreases with temperature. This is also true for carbon dioxide.[581] Depending on how far the WFI has been heated by the previous user it is possible that more or less gas is dissolved in the water in the storage vessel. This is also a possible explanation for different starting DO values in pure WFI (Figure 24 B). As mentioned, the starting pH of WFI of all prepared media is very comparable but there were two preparations that had outstanding values (pH 5.81 standard preparation 1 and

5.25 coldroom preparation). This can possibly be accounted for by differences in carbon dioxide content due to temperature related gas solubility and/or probe accuracy.

The average ORP reading in pure water of all experiments was +263 mV ± 32.5 mV (Figure 24 A). The main half reaction in water accounting for redox potential is:[582]

$$O_2 + 4H_3O^+ + 4e^- \leftrightharpoons 6H_2O \ (Reaction\ 4)$$

This reaction clearly shows the dependency of ORP in pure water on hydrogen ion concentration and DO concentration: a lower pH results in a higher ORP (Figure 14 and Figure 15 standard preparation 1 and 3).[571] Also, a lower oxygen concentration (Figure 13 and Figure 15 standard preparation 1) causes a decreasing redox potential. This explains the variance of readings in WFI. Thus, the measured values are well comparable with literature (+250 mV for distilled water).[582]

The already mentioned effect of gas diffusion over time becomes visible for most of the experiments when looking at DO values that slightly increased when WFI was stirred in the tank. In the case of nitrogen gassing preparation condition the steep decrease of DO just before the first compound addition marks the time point when the nitrogen gassing has been switched on (Figure 24 B green line).

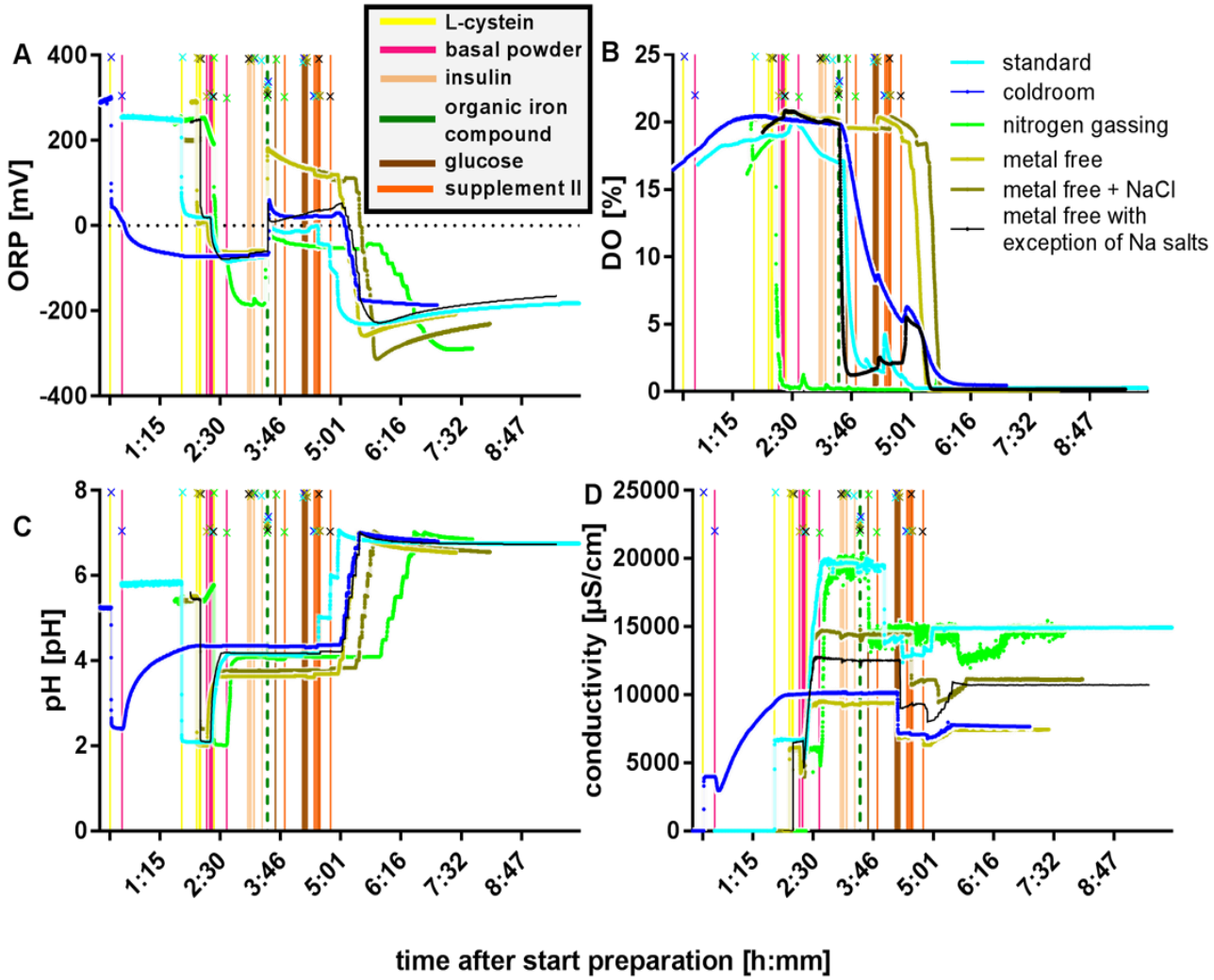

Figure 24: Univariate sensor signals during preparation of model medium 1 at different conditions and with different basal powder composition.The vertical lines in the color assigned to the compounds in the legend show the addition time point. The crosses in the color of the preparation symbolize which addition belongs to which preparation. A) shows oxidative reductive potential, B) shows dissolved oxygen, C) shows pH and D) shows the conductivity.

L-Cysteine HCl addition

The first compound dissolved for model medium 1 preparation is L-cysteine HCl. Therefore, all the measured values are accountable to L-cysteine at the concentration used in the medium. The effect on DO by the powder addition is negligible (Figure 24 B). Except for the preparation under nitrogen gassing the DO increase keeps going on with the same slope as for pure water. It can be assumed that DO has not reached equilibrium and diffusion of oxygen into the medium continues. The still present increase of DO over time after L-cysteine addition shows that there is no or minimal oxygen consumption and if it can be compensated by diffusion. As expected, the signals of pH, conductivity and ORP show a response on the compound addition. The signal of the ORP sensor depends on diffusion rate of molecules and reaction rates of redox reactions in solution and on the probe surface. Thus, it can take a long time until the ORP reading gets constant after a fast initial response. The reaction rate of chlorine on the surface of platinum sensing element for example is sensitive to the oxide film.[583-585] David Ezra Green reported a value of + 30 mV of cell potential at standard conditions for cysteine measured against a calomel electrode at various concentrations and over a wide pH range from 4 to 8.[586] Even though such a wide pH and concentration range of 1 to 10 mM was investigated it does not cover the observed pH 2.2 (SD ± 0.15 pH) caused by HCl form of cysteine used for medium preparation. However, the value for E_0 was considered a good approximation and thus used to calculate the expected potential of 11 mV with the following formula.

$$E_h = E_0 - \frac{RT}{F} pH - \frac{RT}{F} logRSH$$

The average measured ORP for L-cysteine HCl in WFI in the preparation of model medium 1 was 19 mV (SD ± 15 mV). Considering the explained factors of uncertainty, the theoretical calculated value and the measured value are very well comparable. The application of conversion factors has made sure that values are compared with the same reference electrode system (0.2412 mV calomel electrode and 0.205 mV Ag/AgCl 3.5 M KCl).[587, 588] An exception to the good comparability to literature was the preparation under nitrogen gassing. As mentioned, the steep drop of DO marks the time point when nitrogen gassing finally was switched on in this experiment (Figure 24 B). The L-cysteine was added to WFI when a DO of 0.3% was reached. Due to the passivation effects of oxygen on the platinum ORP ring element it is likely that oxygen film removal takes longer than stripping oxygen out of the liquid (See steep slope in Figure 24 A right before the yellow line marked with a green cross).[584, 585] Nevertheless, the addition of L-cysteine further decreased ORP. In contrast to all the other preparations the first constant value was reached at -64 mV. The decrease of ORP is likely to be caused by displacement of oxygen with inert nitrogen. As explained, the main half reaction in pure water accounting for ORP value is hydronium ion and oxygen forming water. When the oxidizing compound is replaced by inert nitrogen there is no electron acceptor remaining in the system. Therefore, the entire system changes from oxidizing (more positive ORP) to reducing (more negative ORP). This causes the nitrogen gassing system to rather donate electrons than accepting them from compounds entering.

For the conductivity all the different preparation conditions are very comparable after cysteine addition. The only exception is the solution at 2-8°C. This is well in accordance with the expectation because the lower temperature slows down diffusion of ions that can carry charge.

It is interesting to note that after dissolution in water the L-cysteine concentration measured with dMRM is only at 60% of expected theoretical concentration for all the six investigated preparation conditions (Figure 26). As the method validation has shown that L-cysteine has poor accuracy

and reproducibility, this value must therefore be considered relative. There were two sampling time points after each compound addition in a narrow time window with the goal to give a hint on method variability within the experiment. The fact that L-cysteine addition to water has minimal impact on DO is a hint that at these conditions the oxidation rate is very low, or oxidation is not happening. Even though there is L-cystine found in concentrations of 100 µM after L-cysteine addition there is no increase in concentration in the next two measurement points. This suggests that L-cystine is an impurity in L-cysteine HCl powder. As long L-cystine concentration is below solubility limit it is not critical for process robustness because it is commonly used in mammalian cell culture and L-cystine transporters are known.[268, 589]

Basal powder addition

In model medium 1 preparation, the second recipe position is the basal powder addition (Figure 24 magenta vertical lines). The negative slopes of DO observed after basal powder addition in standard preparations after the peak value has been reached (Figure 13 and Figure 24) are a hint on oxygen consumption upon basal powder dissolution in the L-cysteine solution. The experiments were designed with the goal to slow down or prevent oxygen consuming reactions. As DO levels after basal powder addition remained constant for metal free or metal reduced basal powders and cold room preparation this was achieved (Figure 24 B). Other than the before discussed air trapping effects, DO was comparable for all conditions but standard after basal powder addition (Figure 24).

It is interesting to note that after basal powder addition ORP is the same for all media apart from nitrogen gassing preparation condition. As explained earlier, the more negative ORP in the nitrogen gassing experiment is caused by oxygen displacement. The difference in pH after basal powder addition is very slight, but present. According to the probe signals in Figure 24 C hydrogen concentration is lowest in cold room preparation. This can be explained by little dissociation of acids at low temperature. Generally, the pH readings for standard preparation, cold room, metal free basal powder with sodium salts and nitrogen gassing are comparable. The two preparations performed with metal free basal powder were more acidic compared to previous group. Because no additional acids were added to this basal powder it can be assumed that the removal of some buffering compounds caused this effect.

The conductivity after basal powder addition is showing extensive difference between preparation conditions. The standard preparation and the preparation under nitrogen gassing have the same level after powder dissolution. The noisiness of signal under nitrogen gassing is resulting from gas bubbles attaching to the flat surface of the probe tip where the dipoles are mounted. The lowest conductivity was measured for the metal free basal powder. This was expected because missing metal ions that are forming at dissolution are good carriers of charge. The effect of temperature on charge transportation is so strong that the normal basal powder under coldroom conditions has such low conductivity as metal free basal powder. When sodium chloride is added to metal free basal powder with the target to mimic Na concentration from normal medium, the conductivity is even higher than in the preparation with Na containing salts. This can be caused by Na salts that complex the sodium ions better than completely dissociating chloride.

The concentrations for most of the compounds in model medium 1 remain constant over the preparation time (Appendix Figure 73 to Figure 77). The medium compound concentrations measured with LC-QqQ-MS show robustness of model medium 1 to preparation conditions because most values are close to expectation within the method variability. In the same time this

confirms the method suitability for medium preparation control. The range of QC samples gives a good estimation of method variability of the measured batches for the respective compounds (left pane of Appendix Figure 63 to Figure 65). Additionally, these samples guarantee the system suitability. Most of the compounds showed stable concentration values within the LC-QqQ-MS method variability over the course of preparation. That means the concentrations were not impacted by none of the compound additions. The fact that many of the medium compounds were considered stable over preparation time does not necessarily mean that these compounds cannot be involved in chemical reactions. Due to the fact that the method shows variability some small trends in compound decrease may not be detected. Especially small changes in concentration of compounds that are present in high concentrations in media, as for example amino acids, may not be detected due to method variability.

Thiamine, L-cysteine and pyridoxine concentration profiles are comparable during medium preparation in the time window from basal powder addition to pH adjustment (Figure 25, Figure 26 and Figure 27). In this time frame the concentrations in metal free basal powders were higher for the three compounds by approximately 20 to 50%. It is very likely that the lower pH for metal free basal powder (pH 3.6) and metal free basal powder with sodium chloride (pH 3.7) in comparison to the other preparations (standard 4.1, coldroom 4.3, nitrogen gassing 4.1 and metal free including sodium salts 4.2) in combination with basal powder matrix impacts this effect. ESI ionization is known to show pH dependent ionization efficiencies.[534] Interestingly, there are some compounds that are sensitive to pH and others which show no pH dependent ionization efficiency. Furthermore, compounds were identified that responded by increasing ionization efficiency on lower pH by two orders of magnitude in a very narrow pH range (0.5 units). As Liigand *et al.* conducted experiments in positive mode the effects should be comparable. Even though it must be emphasized that this work does not represent the compounds discussed in this thesis. Thus, the mechanisms should be considered as generally possible but not certain. A higher proton concentration at low pH increases the charge to mass ratio in the charged droplets during gas phase analyte ion formation in ESI source making some compounds more susceptible to ionization.[530] Even though the three compounds are very different in structure (Figure 2 and Figure 11) they have in common that reports about their ability to complex metal ions exist. In contrast to thiamine pyrophosphate, where metal complexation is most likely limited to the pyrophosphate, the bivalent metal ion interacts with the nitrogen of pyrimidine ring of thiamine hydrochloride.[324, 326] Both the dependency on pH and the capability to complex metal ions more or less combined may impact the outstanding behavior of these three compounds in model medium 1 samples measured with LC-QqQ-MS. However, to better understand the pH effect on analysis result further experiments with varying pH and more simple solutions would be necessary. The possible impact of pH on ionization efficiency of some compounds must always be considered when drawing conclusions on chemical reactivity if data is solely based on LC-QqQ-MS data.

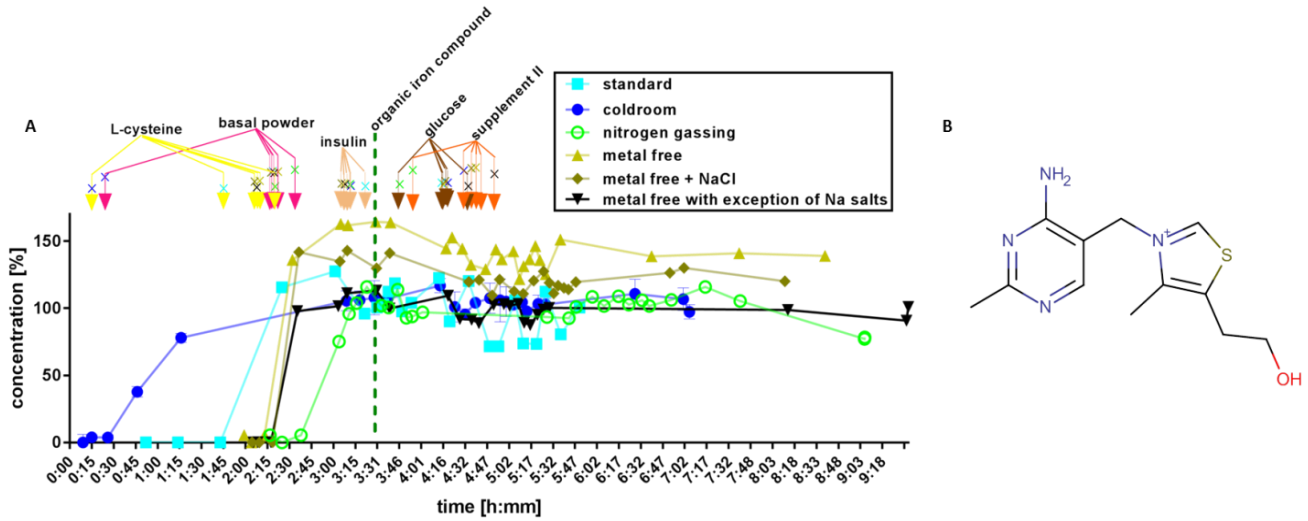

Figure 25: A) Thiamine concentration profiles during CDM preparation. The metal free basal powders show apparently higher concentration level (method variability determined by range in QC samples is 7%). B) Structure of thiamine showing the pyrimidine ring which can complex metal ion.

The addition of a compound or compound mixtures to the medium under preparation adds new potential reaction partners as the mixture becomes more complex. Furthermore, key chemical parameters as ORP or pH can change upon compound addition and thus change reaction conditions. Therefore, some of the compounds show different concentration after basal powder addition. An example is the interesting behavior of L-cysteine concentration (Figure 26 A). Whereas the relative concentration of L-cysteine added to WFI is at 50 to 60 % for all preparation conditions the concentration becomes apparently different after basal powder addition for completely metal eliminated mixtures. After basal powder addition the measured concentration was 80% for metal free and metal free plus sodium chloride preparation (red arrow Figure 26 A). The increased relative values for the two changed basal powder compositions were observed until the pH was adjusted. A behavior observed for all preparation conditions was a trend of decreasing L-cysteine concentration after organic iron compound addition. pH adjustment to 7 caused L-cysteine concentrations that were not detectable by LC-QqQ-MS.

As mentioned, the ionization efficiency of some compounds is dependent on pH and it is generally higher with lower pH.[534, 590] The reason for solutions with the metal free basal powders showing increased L-cysteine values remains unclear. For some extent the slightly lower pH in these two preparation conditions with metal free basal powder may have improved ionization efficiency. However, if pH was the main reason for signal increase of L-cysteine in metal free preparations the concentrations of the compound dissolved in water at pH 2 (Figure 24 C) is expected to show increased values as well. This observation hints at the possibility that metal free basal powder does not contain an ionization suppressing compound that is present in basal powder with sodium containing salts and of course in the standard basal powder. In combination with lower pH this may be a reason for the different concentration values measured with LC-QqQ-MS. Another possible explanation could be that normal medium includes bivalent metal ions that can cause metal complexation with L-cysteine and therefore suppress ionization efficiency in the ESI source. An increasing pH due to basal powder addition would support this process due to partial L-cysteine deprotonation. However, the majority of the thiol group remains in protonated form due to its pK_a of ~8.5.[269] The non-detectable concentrations after pH adjustment may have been caused by matrix conditions as well. If for example pH is adjusted to neutral at the end of medium preparation the thiol group of cysteine ionizes to a negatively charged thiolate group after deprotonation. This enhances cysteine reactivity to electrophiles, the

oxidation by reactive oxygen and nitrogen species and increases the affinity to metal ions. This chemical behavior could be an explanation for non-detectable L-cysteine after pH adjustment.

The L-cystine concentration looks comparable after basal powder addition for all preparation conditions (Figure 26 B). With the given method variability it is difficult to judge if it is higher in the metal free basal powder preparations. As the ORP of metal free preparation is comparable to standard at this state of medium preparation (Figure 24 A), the concentration of the L-cysteine redox partner in metal free preparations should be considered comparable for all preparation conditions after basal powder addition. Thus, L-cystine concentration is neither impacted by chemically different conditions after basal powder addition nor by thereof resulting matrix effects in LC-QqQ-MS measurement.

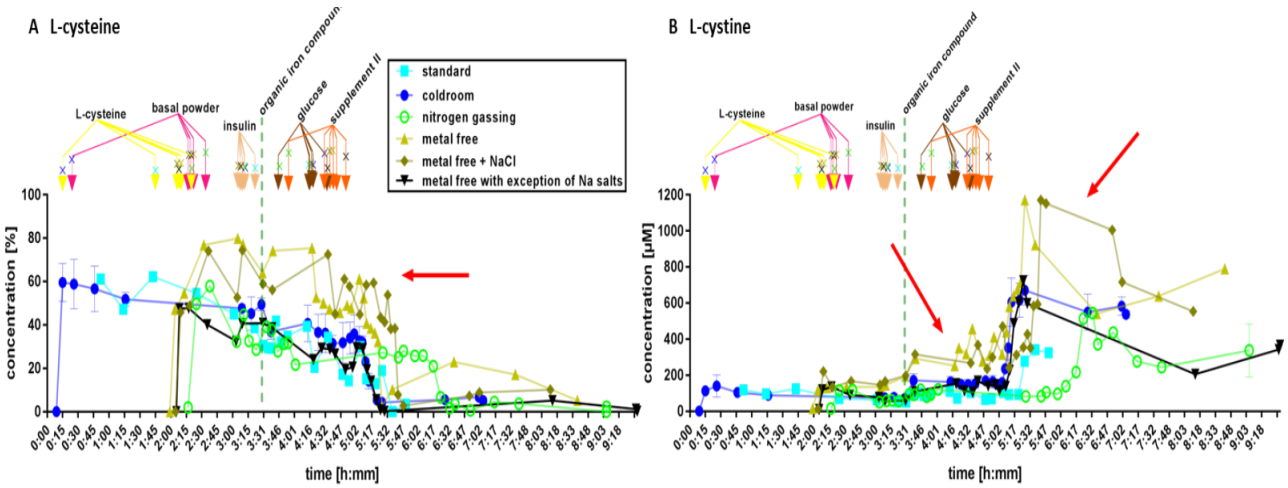

Figure 26: L-cysteine (A) and L-cystine (B) concentration profiles over the time of medium preparation. Shown are six independent medium preparations with standard conditions and raw material (turquoise rectangle), with standard raw material at 2-8°C in the coldroom (blue circles), with standard raw material under oxygen exposure prevention by nitrogen gassing (green circles), with standard conditions and metal free basal powder (ochre triangles), with standard conditions and metal free basal powder and NaCl added to reach the Na concentration as in standard raw material and with a metal reduced powder that still contained all the Na salts (black triangles). The arrows on the top of the graph symbolize the addition time point of medium recipe positions. The arrow symbolizing a specific medium preparation condition is marked with a cross in the color of the respective preparation. All the data of the six independent preparations were aligned on the time scale to the organic iron compound addition time point. The red arrow in A shows the increased L-cysteine level after metal free basal powder addition. The first red arrow in B points on the increased L-cystine level after organic iron compound addition. The second red arrow in B points on the increased L-cystine formation during pH adjustment in the metal free basal powder preparations.

In addition to L-cysteine, the vitamin B6 group shows sensitivity to the experiment conditions right after their addition with basal powder (Figure 27). It is interesting to note that pyridoxine and pyridoxamine levels are increased in metal free basal powders (Figure 27 B and C) while in the same time the level of pyridoxal is decreased for these two preparations (Figure 27 A). As shown by redox potential upon basal powder addition the ORP is – 80 mV (Figure 24 A). Accordingly, increased pyridoxine and decreased pyridoxal concentration measured with dMRM LC-QqQ-MS data suggests the reduction of pyridoxal happening (Figure 27 D). In contrast, in the metal free preparations the entire system should be electron accepting after organic iron compound addition. At this state of medium preparation an oxidation from pyridoxine to pyridoxal is expected for this redox couple. However, organic iron compound addition seems to have no impact on Vitamin B6 concentration. As there is an excess of pyridoxal in comparison to pyridoxine also less favorable reactions can happen. Additionally, the ORP reading is not absolute. As mentioned earlier it is rather a characteristic measure of a total system. Frank Sessa has reported of systems that have been impacted by pH that led to negative ORP readings for NaOH persulfate solutions.[571] This does not mean that the strong oxidizing agent persulfate does no

longer act as an oxidant. This example shows that ORP is not an absolute predictor of whether compounds are getting oxidized or reduced. It is rather an estimator of the overall direction since reduction and oxidation are always happening in competition. Therefore, it is not excluded that the reaction shown in Figure 27 D continues with positive ORP reading. Alternatively, it is also possible that ORP was not positive enough to invert it. Furthermore, it is very important to keep in mind that even though LC-QqQ-MS measurements are highly specific by their principle the ionization efficiency can be strongly impacted by matrix as discussed for L-cysteine. As shown in Figure 27 F, pyridoxine can for example complex bivalent metal ions. If such a complex remains stable during chromatography it will certainly impact the MS signal. Thus, in this specific case the increased concentrations measured with MRM must be interpreted carefully. Since the ORP reading was positive with the addition of OICA for metal free basal powders it would have been interesting to include 4-pyridoxic acid in the dMRM LC-QqQ-MS method to investigate if the expected reaction shown in Figure 27 E has occurred. This is especially true for metal free basal powder preparations after organic iron addition. As mentioned, pyridoxamine shows a significantly higher concentration in the metal free basal powder preparations (Figure 27 C). Since it is not a constituent of basal powder it must have formed as a reaction product. This reaction is preferentially happening under conditions in metal free basal powder. Chemical transamination can happen with a multitude of amine bearing compounds. Because of the high amino acid and peptide concentration it is likely that one of these compounds acts as the amine group donor. In literature model systems demonstrate pyridoxal 5´-phosphate transamination by L-phenylalanine and the amino acid reaction products kynurenines under metal catalysis.[336, 337, 341] Even though reported as agent with high transaminating potential, L-glutathione can be excluded as the source of amino group in model medium 1 since its concentration remains stable during preparation (Figure 31).[338] As significant pyridoxamine concentration increase has only been observed for metal free basal powders there must be a mechanism that happens without metal catalysis or metal impurities are present in basal powders. Indeed, the measurements of the basal powder manufacturer confirmed that minimal traces of chromium, iron, zinc, manganese and mercury were in the basal powders (Cr 0.001, Fe 0.006, Zn 0.007 ppm measured with ICP-MS; K 0.82 ppm measured with ICP-OES for metal free basal powder and Cr 0.001, Fe 0.005, Zn 0.011, Mn 0.001, Hg 0.001 ppm measured with ICP-MS; K 1.023 ppm measured with ICP-OES for the metal free basal powder containing sodium salts, Appendix Figure 78). For example, manganese was reported to be an efficient catalysator of Schiff-base oxidation and it would have been interesting to see if an addition had increased the pyridoxamine formation.[322] The very minor increase of pyridoxamine after organic iron compound addition in model medium 1 prepared under standard conditions suggests an alternative iron dependent mechanism that is not happening if temperature is too low or oxygen is eliminated (Figure 27 C). The role of metal ions in pyridoxal transamination is to stabilize intermediates like aldimine Schiff base chelates.[339] However, depending on condition this metal complexation could protect pyridoxal from transamination by the formation of a stable complex. This complex formation may have prevented pyridoxamine formation in metal free basal powder with exception of sodium salts in contrast to the standard condition. Furthermore, the neutral ORP and the reduced conductivity in this experiment may have been a non-favorable transamination condition upon OICA addition.

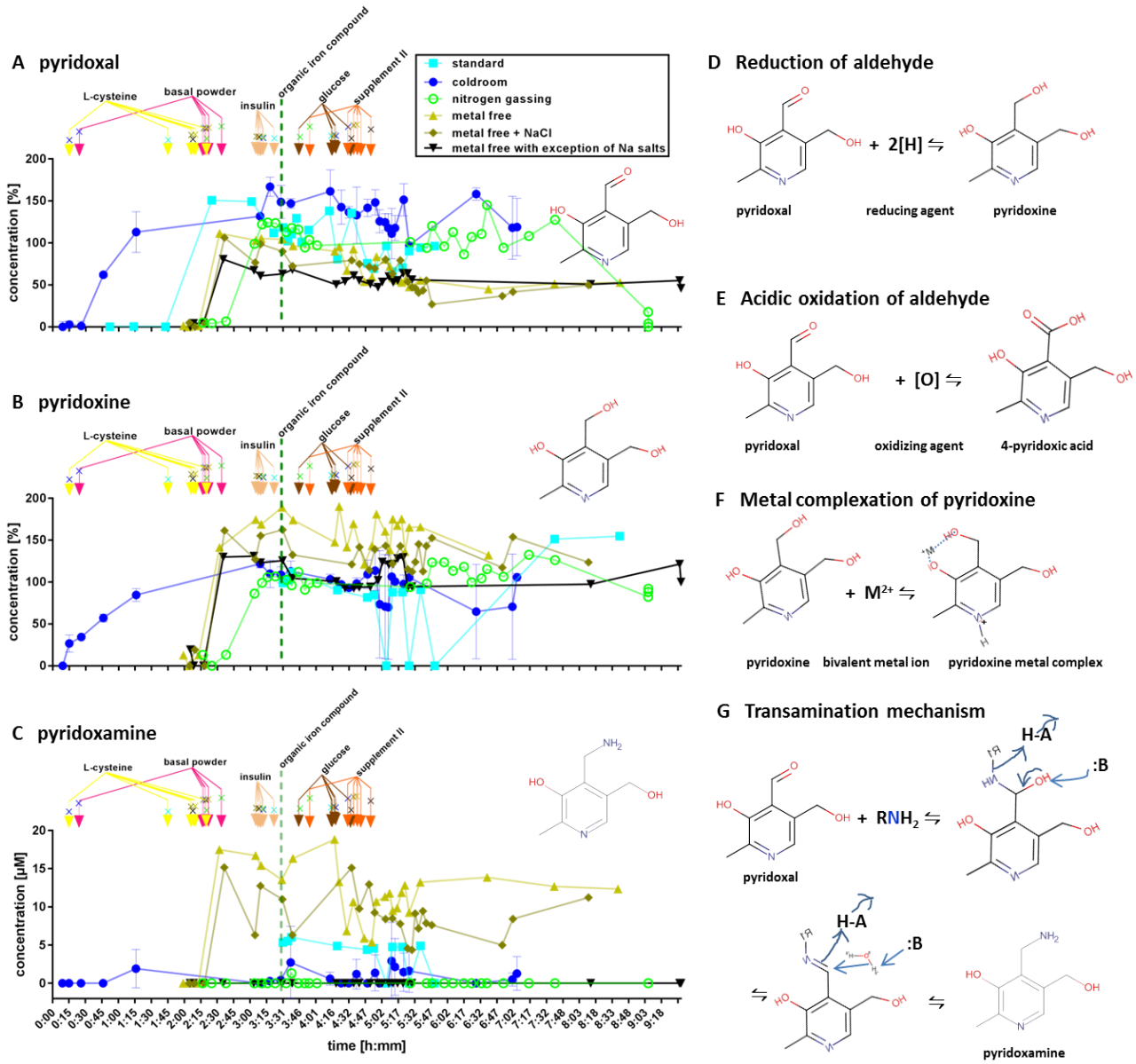

Figure 27: The concentration profiles of B6 vitamins pyridoxal (A), pyridoxine (B) and pyridoxamine (C) during medium preparation measured with LC-QqQ-MS. Pyridoxal has a wide range (~30% for QC samples). But there is a clear tendency for lower concentrations in metal free basal powders. Metal free preparations show apparently higher values for pyridoxine concentration than other experiments (15% range in QC samples). The range for pyridoxamine is 2 µM in QC samples. Therefore, the seen concentration difference is bigger than method variance. D, E, F and G show possible reaction mechanisms for B6 vitamins in CDM.

The three examples of Thiamine, L-cysteine and the Vitamin B6 group show the complexity of chemical mechanisms happening during medium preparation and measurement. Even though the LC-QqQ-MS dMRM measurement mode is highly specific by principle, effects like ion suppression or ionization efficiency can impact the readout. The question if for example differences between metal free basal powders and standard basal powder or basal powder containing sodium salts are mainly due to different chemical reaction profiles in medium or caused by effects on ionization in ESI MS would need to be addressed in follow up studies with a focus on matrix composition. In the end, it is probable that both chemical effects in the CDM and during LC-MS measurement are happening and impact the results.

Insulin addition

The next compound added after basal powder was insulin as a stock solution. The addition has no impact on pH (Figure 24). By closely looking at signals from conductivity and ORP probe from coldroom and metal free with exception of sodium salts preparation, tiny peaks after insulin addition can be seen. Since the changes are so small in comparison to overall alterations occurring during medium preparation, they may be accounted to concentration gradients caused by adding the stock solution. Also, the impact on DO signal is minimal. Because there was a slight negative slope after basal powder addition it is not possible to assess if DO has not equilibrated due to basal powder addition or if insulin has an impact on this parameter. Generally, it is likely that insulin does not impact signals of univariate sensors because it is a small protein with two closed disulfide bonds and no extremely reactive residues. Indeed, Kaplan *et al.* found that at low concentrations the reactivities of functional amino acid residues of insulin were negligible.[591] In comparison to other small polar compounds of CDM insulin is a rather big molecule. Because of chromatographic conditions and MS instrument properties it was not included in dMRM.

Organic iron compound addition

As discussed in the introduction, adding and maintaining iron in CDM in a bioavailable form can be challenging. Therefore, a ferric iron complex, named organic iron compound A (OICA), was used to prepare the investigated media. When OICA gets dissolved in water at the concentration that is used for model medium 1 preparation it lowers pH to 3.66 (Appendix Figure 79). Since the dissolved basal powders of the investigated preparations already had a pH between 3.5 and 4 the addition of OICA to the well buffered basal powders did not impact pH reading. Interestingly, OICA addition does not show an effect on conductivity apart from little negative spikes. The little negative spikes can be caused by the formation of little gas bubbles that can be observed after OICA addition. Solutions from iron salts are known to be able to transport charge. Generally, all compounds dissociating into ions upon dissolution should be able to transfer charge and increase conductivity.[592, 593] The lack of increasing conductivity upon OICA addition is a hint for the efficient complexation of iron by the ligand of OICA because the complex is not charged. Therefore, the paired ions contribute little or nothing to the solutions conductivity.[594] Contrarily to conductivity, the addition of OICA does show an apparent increasing effect on ORP signal after dissolution. At the time OICA is added to the medium a reducing environment is present in all preparations (-60 mV, Figure 24 A). High ferric iron concentration in contrast to ferrous iron concentration is predicted to result in a high redox potential.[595] Thus, the ferric iron gets reduced to ferrous iron in the CDM until equilibrium is reached. Furthermore, for most of the preparations a level around neutral ORP is reached. As described earlier, the oxygen displacement reduces ORP reading in the nitrogen gassing condition. Consequently, it shows the most reducing ORP reading after OICA addition (-35 mV). The most apparent effect of OICA addition on ORP is observed in the preparations with metal free basal powder. There, ORP jumps from -60 mV to highly oxidizing environment of ~150 mV. Because several compounds were removed from metal free basal powder it can be concluded that there must have been some that act as redox buffer. The chemical properties of some of those will be discussed in the next section. The most drastic reaction on OICA addition was shown by the DO probe. For all the media preparations with standard basal powder and the basal powder without metal but sodium salts DO drops within less than a minute to zero. As expected, the addition shows no additional effect on DO profile in the nitrogen gassing preparation. The DO drop in coldroom preparation is much slower in comparison to all the other preparations with DO drop. This is very likely caused by the cold temperature slowing down chemical reactions. The consumption of all the dissolved oxygen by the CDM upon the addition of OICA is a clear sign for a chemical reaction happening already during preparation. From a

process development point of view uncontrolled chemical reactions such as this are highly undesirable. Due to little opportunities in the large scale medium preparation tank to control physical parameters like for example temperature and pressure the chemical reactions can result in unequal reaction product concentration from batch to batch. If educts and products of a chemical reaction are known, no side reactions are happening that form toxic product and if the batches are comparable a chemical reaction in CDM may still be acceptable for a robust process. However, many reaction mechanisms, especially with the participation of iron, generate radicals which may start further unknown chemical reactions that can form reaction products that could either benefit or harm the cell culture. Generally, unknown chemical reactions in CDM bear a high risk of introducing undesired variability into the bioprocess. Since the excluded compounds of metal free basal powders were known, the impacted oxygen consumption behavior in these two compound mixtures were a great opportunity to increase the highly important understanding of this unknown reaction mechanism and will therefore be discussed in section *3.2.3. The quantitative measurement of OICA ligands is one approach to understand how this compound impacts the chemical behavior of model medium 1*. One ligand of OICA is a constituent of the basal powders as the pure compound and could be included into the positive mode LC-QqQ-MS method. Considering the high variability for this analyte the concentration was as expected before OICA addition (Figure 28). The addition of the same amount of OICA to all media increased the concentration to a comparable level in all preparations. Because OICA is a complex with an unknown stability constant it is not surprising that a certain portion dissociates into ferric iron and its ligands. The dissociated ligands are responsible for the concentration increase after OICA addition shown in Figure 28. If the OICA compound gets released in solution, under chromatographic conditions or in the ion source cannot be answered with this experimental setup. However, it is interesting to note that the concentration of the ligand of OICA is comparable in all experimental conditions. This leads to the conclusion that the ligand is not directly involved in differing oxygen consumption behavior of metal free basal powder experiments.

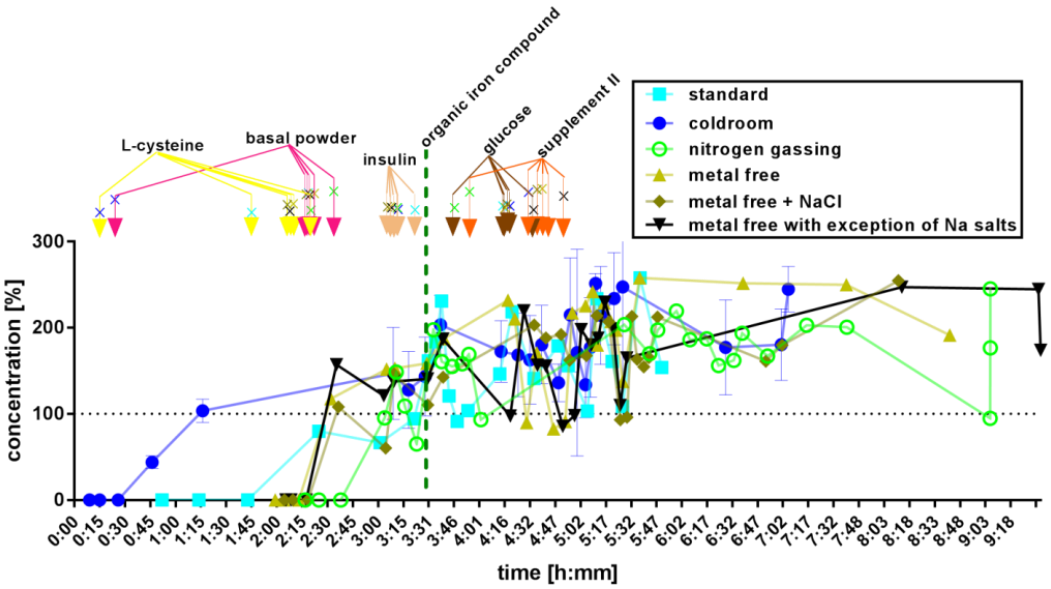

Figure 28: The concentration profile of OICA compound over the preparation time. The dotted line at 100% marks the expected concentration of basal powder. The addition of organic iron compound adds up approximately another 100% of OICA compound to the basal powder. Range in r chart is 40% representing the very high variability in measurement results.

Another interesting effect shown by the dMRM measurements is the different L-cystine concentration in metal free media after organic iron compound addition (Figure 26 B first red arrow). Due to the elimination of compounds, as for example pyruvate, the redox potential is not as well buffered as for standard basal powder (Figure 24 A). Therefore, organic iron compound addition increases ORP and creates an oxidizing environment. Pyruvate is known to form complexes with iron and reduce iron(III) in a pH range of three to four with slower kinetics at higher pH.[260] Because of the lack of effects such as the one described for pyruvate the metal free basal powder preparations became oxidizing systems. At oxidizing ORP iron is mainly present at oxidation state Fe^{3+}. The excess of catalyzing ferric iron added by organic iron compound addition starts L-cysteine oxidation.[402] In contrast, the preferred oxidation state of iron in non-metal free preparations with acidic pH and almost neutral ORP is Fe^{2+}. Thus, the L-cysteine oxidation is not promoted by OICA in standard basal powder preparations.

Glucose addition

The second biggest recipe position by mass is glucose. The DO signal showed some little peaks of increased concentration right after powder addition (Figure 24). The increased DO lasted only for a few minutes. As explained before, big amounts of powder can trap air and pull it under the surface of the CDM under preparation. The air getting released upon glucose dissolution forms air bubbles that can gather at the sensor tip and therefore increase DO reading. This lasts for a short time until either the oxygen gets consumed by chemical reactions or the bubbles rise to the surface and get dispensed due to shear forces in the stirred tank. A significant negative effect of glucose addition on conductivity could be observed. This is because of the many hydroxyl groups of the glucose molecule. These can form a stable lattice with other glucose molecules when the compound is in the solid state. Since the breaking of the hydrogen bonds in the dissolution process takes energy from the environment the addition of glucose to CDM is cooling the solution (Appendix Figure 66). The mentioned hydroxyl groups cannot only form hydrogen bonds between glucose molecules but also between glucose molecule and water. This leads to the formation of a water shell around each molecule of glucose and a subsequent decrease in entropy in the solvent (Figure 29 A). Because of the water immobilized in water shells, the ions that carry charges are less mobile in the solvent which causes the conductivity to drop after glucose dissolution. It has for example been shown that the complexation of metal by the glucose decreases cation mobility in the medium which might have an effect on the conductivity.[254, 255] Another study has shown that carbohydrates as sucrose, fructose and glucose can change thermodynamic properties of $CuCl_2$ due to its destructing effects on water structure.[596]

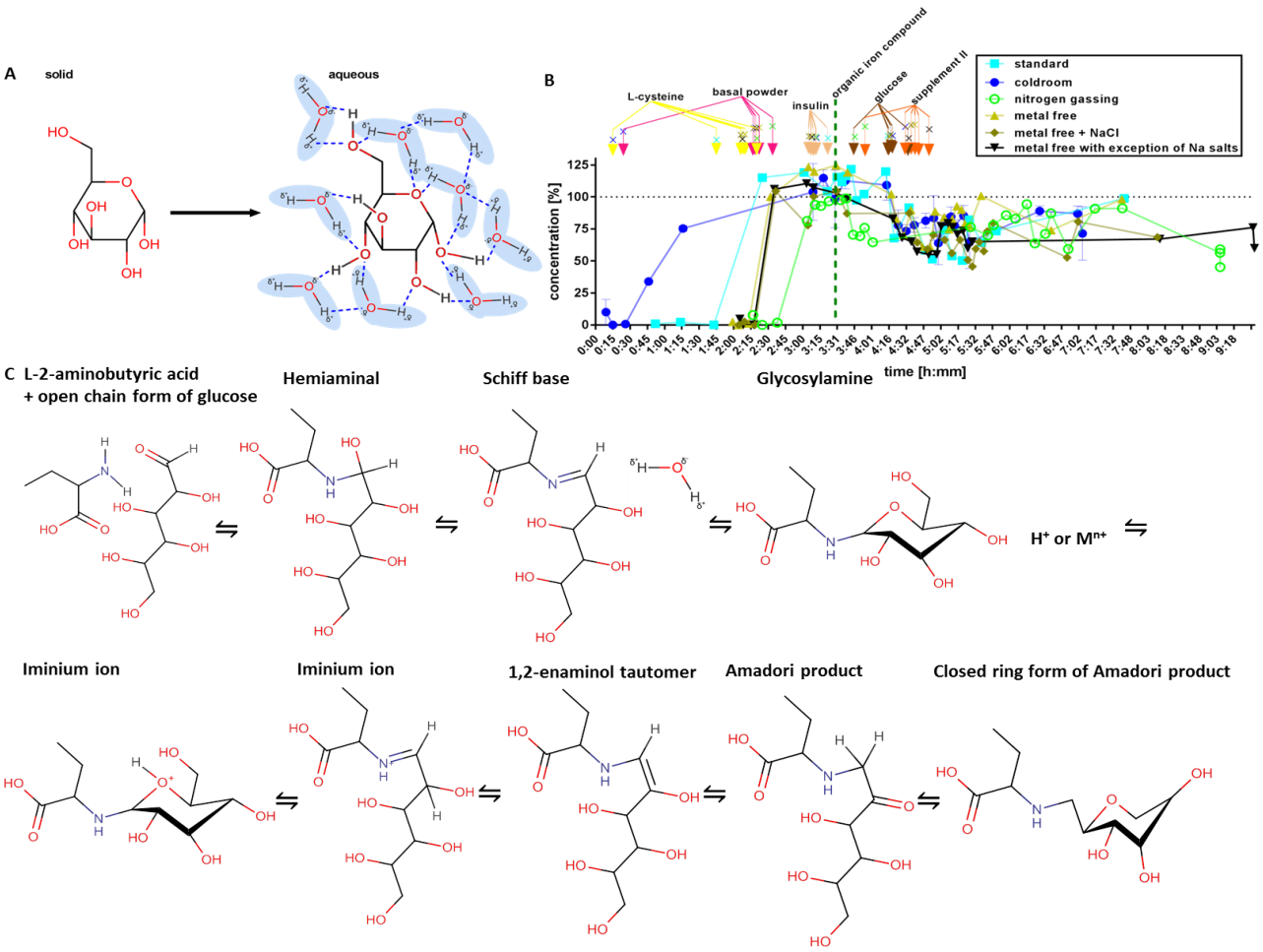

Figure 29: Chemical consideration of glucose during medium preparation. A) The glucose molecule has a lot of open hydroxyl groups that allow H-bonding. B) The concentration profile of L-2-aminobutyric acid shows a strong and sudden decrease of approximately 25% after glucose addition (Range of 15%). C) Glycation mechanism of L-2-aminobutyric acid.

Figure 29 B shows the concentration profile of L-2-aminobutyric acid during medium preparation. The graph confirms that the expected concentration is accurately measured during medium preparation until the glucose addition. Each preparation condition shows a sudden decrease from 100% ± 15% to approximately 75%. From this time point on, the concentration remains at this level suggesting that the reaction behind this L-2-aminobutyric acid concentration decrease has found equilibrium or ran out of educt. This very direct response on addition is a strong hint on a chemical reaction involving glucose. A commonly occurring and well described reaction mechanism between reducing sugar, such as glucose, and primary amine is a non-enzymatic, multi-step browning reaction. It has been first described in 1912 by Maillard.[251] The initial stage of this reaction is glycation that is characterized by the reaction of a carbonyl group and a primary amino group forming a ketoamine or fructosamine. The product of this first reaction step was named Amadori product after the person who first described it.[252] Briefly explained, the reaction mechanism starts with a nucleophilic attack of a primary amine on the open ring form of glucose that is present at 0.002% in aqueous solution (Figure 29 C).[248] This attack leads to Schiff base formation which can spontaneously cyclize to form N-substituted Glycosylamine. Since this molecule is not stable it either degrades into the educts glucose and L-2-aminobutyric acid or it rearranges to the stable Amadori product. In order to confirm the hypothesis of L-2-aminobutyric acid glycation, an identification of L-2-aminobutyric fructosamine with high resolution MS by comparing the theoretical to the observed mass or the development of an appropriate MRM method with standard compounds would be the method of choice. As described by Troise *et al.*, Amadori products and small polar molecules as amino acids show poor retention in reversed

phase chromatography.[505] Whereas their method requires ion pairing reagents, mixed mode chromatography described in this work has the potential to achieve comparable retention of Amadori products and amino acids. Another straight forward approach to identify the reaction product would be for example the usage of isotopically labelled educts followed by high resolution MS. As described, in principle any primary amine of for example the various amino acids present in the CDM could undergo glycation. A potential reason why this is not clearly seen in dMRM data (Appendix Figure 73 to Figure 77) is that method variability may mask the relatively to absolute concentration very small concentration decrease. In the same time susceptibility to glycation differs from amino acid to amino acid showing that quantitative differences could also result thereof.[249]

Supplement II addition

The addition of BI proprietary compound Supplement II does not show any significant effect on univariate sensors during medium preparation (Figure 24). For a biopharmaceutical company such as BI, it is very important to demonstrate to authorities that the proprietary medium compounds are present in the expected concentration and are sufficiently stable during manufacturing and storage. The developed LC-QqQ-MS dMRM method shows specificity and accuracy for supplement II as demonstrated by the spontaneous response on the addition and the measurement of expected supplement II concentration (Figure 30 A). The supplement II compound A is not a compound of model medium 1 basal powder (Figure 30 B). The values obtained before supplement II addition are therefore false positive identifications. After supplement II addition there is only a minimal trend to increased concentration. However, these values are still showing such high variability and are so close to LoQ that concentration still can be considered close to zero. This shows that supplement II is sufficiently stable over the time of medium preparation. Supplement II compound B in contrast is part of the basal powder (Figure 30 C). The addition of supplement II to the medium does not impact the expected concentration of this compound, again confirming that it does not decompose during the medium preparation.

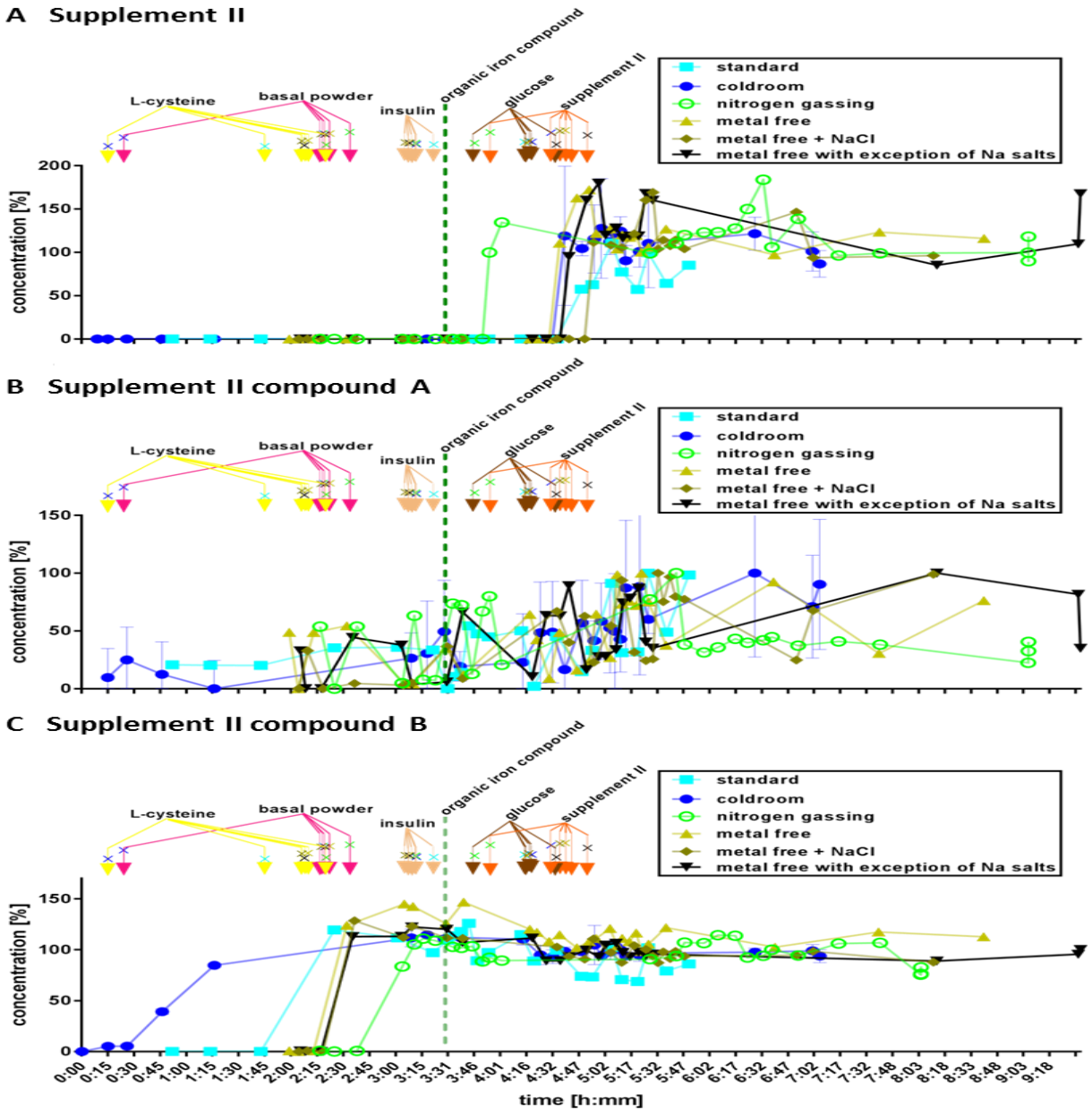

Figure 30: Supplement II concentration profile over time. A) The main compound shows 100% concentration after addition. The high range of 40% determined for this analyte shows high variability. B) Supplement II compound A is not part of the basal powder composition of model medium 1. Therefore, data was normalized to the highest value. The range determined for this analyte was 4%. High variability in this graph is due to values around LoQ. C) Supplement II compound B is also a component of basal powder. The range determined for the measurement series of model medium 1 was 8%. The data shows that the expected concentration is met with high measurement variability.

Base addition to adjust to final pH

As the first compound dissolved in model medium 1 is L-cysteine in the HCl form, the pH of the medium under preparation is acidic (between pH 2 and 4). For adjusting pH from acidic to neutral sodium hydroxide was used. The steps in the online pH profile show the stepwise titration to target pH 7 (Figure 24 C). The same step by step behavior can be observed in the ORP signal. The redox potential decreases upon NaOH addition due to shifting reaction equilibria in reactions where protons or hydroxide ions are involved. Because the measured redox potential is an energy that is transferred in a half reaction along with the electrons, there would be no change in redox potential upon pH adjustment if protons or hydroxide ions were not involved in the main reactions responsible for the ORP. Because NaOH is a strong base it readily dissociates into Na^+ and OH^-. Hydroxide ion is considered a one-electron reducing agent that lowers the ORP reading

during pH adjustment.[597] The decreased conductivity after water fill step is increased by the addition of NaOH due to the effect of ions carrying charge. In the same time the base addition lowers DO. For all the preparations where OICA addition has shown a DO drop and no nitrogen bubbling was applied this decrease is comparably moderate (from ~5% to ~0% DO). But for the preparations with metal free basal powder this DO drop by pH adjustment is as dramatic as for preparations with normal basal powder when OICA is added. Because the oxygen consumption upon NaOH addition is happening in each preparation condition investigated it can be assumed that the underlying reaction mechanism is different to oxygen consumption upon OICA addition.

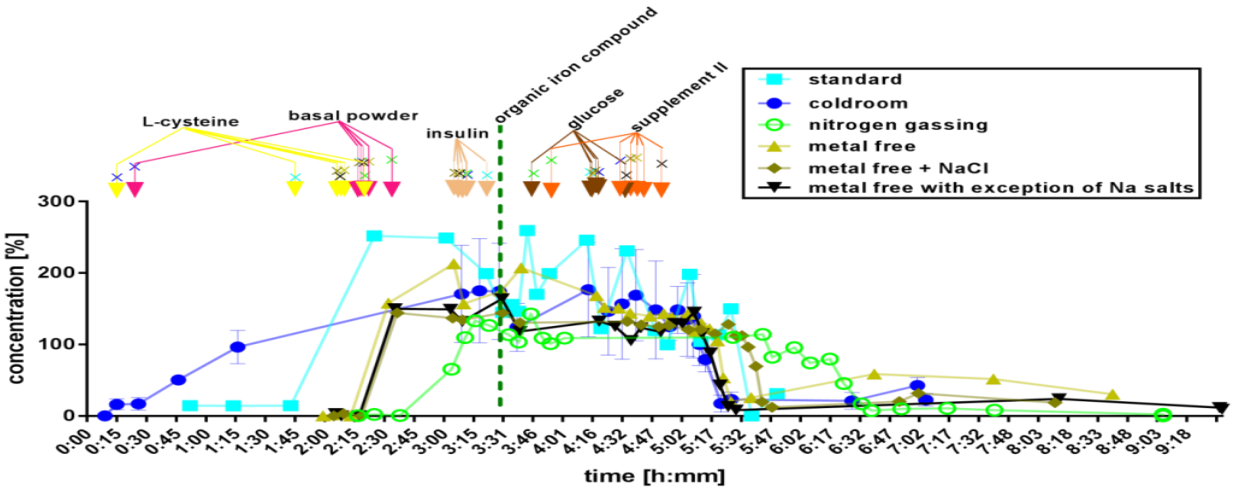

Figure 31: Concentration profile of reduced glutathione (GSH) over the time of medium preparation. The fact that GSH shows low accuracy in the method validation is likely caused by pH 7 in samples used for these experiments.

As shown in appendix Figure 73 to Figure 77 the pH has no impact on concentration of most media compounds. However, as can be seen in Figure 31 the impact of base addition on reduced glutathione is apparent. Even though glutathione is present in both standard and metal free basal powder at a concentration very close to LoQ the measured effect of pH adjustment was significant. The fact that the concentration is so close to LoQ also explains why accuracy is rather poor and there is high variability. Nevertheless, the pH adjustment causes a decrease of glutathione concentration to not detectable. Reduced glutathione shows four pK values.[598] The –SH and $-NH_2$ possess high pKa values with 8.7 and 9.6 respectively.[599] At the pH values occurring over the medium preparation those functional groups remain protonated all the time. In contrast, the carboxy-terminus and the carboxy group of glutamic acid have a pKa of 3.5 and 2.1 respectively. This means that with pH adjustment to neutral these groups get deprotonated. Since the used MS has a mass accuracy of 0.1 u over the mass range and a mass resolution of 1.2 u this deprotonation of two groups is already enough to shift the precursor ion out of detection window. The very well-known oxidation of glutathione to glutathione disulfide is unlikely under the present conditions in model medium 1 due to several reasons. It has been shown by several authors that any thiol-disulfide redox system can only be oxidized directly when anionic thiolate is present.[600] However, it is not completely excluded that glutathione oxidation can take place. For example, in case hydrogen peroxide gets formed by photochemical reactions or Fenton reaction. The photochemical hydrogen peroxide formation has been shown for groundwater and surface waters with clear correlation to dissolved organic carbon without known impact of biological systems.[460] It has to be mentioned that the authors do not explicitly define the identity of dissolved organic carbon. If hydrogen peroxide was formed in the medium under preparation even at pH 6, oxidation of reduced glutathione to for example oxidized glutathione would be possible.[601] But a comparable oxidation rate as demonstrated by Finley *et al.* would only be

expected if hydrogen peroxide was formed in equimolar ratio to reduced glutathione. Furthermore, the anionic thiolate does not necessarily have to stem from a reduced glutathione but may also come from other compounds as for example L-cysteine.

The increase of pH during adjustment generates conditions that are expected to shift the ratio of Fe^{2+} to $Fe(OH)_3$ or complexed ferric iron. The very likely increased Fe^{3+} concentration before pH adjustment in metal free basal powder preparations explains why L-cystine concentration is increased in comparison to other preparation conditions (Figure 26 B second red arrow). As soon as pH adjustment starts all the other preparation conditions also show an obvious L-cystine increase to 600 to 800 µM. After final pH of 7 was reached and no more base was added the ORP equilibrated and the ratio of iron oxidation state was expected to move back to more reducing. This subsequently would lead to L-cystine reduction to L-cysteine explaining the decrease of L-cystine concentration after pH adjustment for all preparation conditions.

3.2.3 Identification of oxygen consuming reaction after organic iron compound addition during medium preparation

As described under *Evaluation of univariate sensors to monitor dissolution of powders in medium preparation* and *Organic iron compound addition* the addition of organic iron always resulted in oxygen consumption leading to almost zero DO. Because the effect of dissolved oxygen decrease during medium preparation was so dramatic (from ~100% DO to ~0%) it raised the concern of the presence of a reaction with the potential to significantly impact the chemical composition of the medium. Especially the fact that the chemical reaction responsible was unknown makes it almost impossible to take the right means to quantitatively control turnovers of educts in order to provide batch to batch comparability and process robustness. One prerequisite to judge the criticality of this reaction and to enable the development of a control strategy is the characterization of the oxygen consumption during model medium 1 preparation.

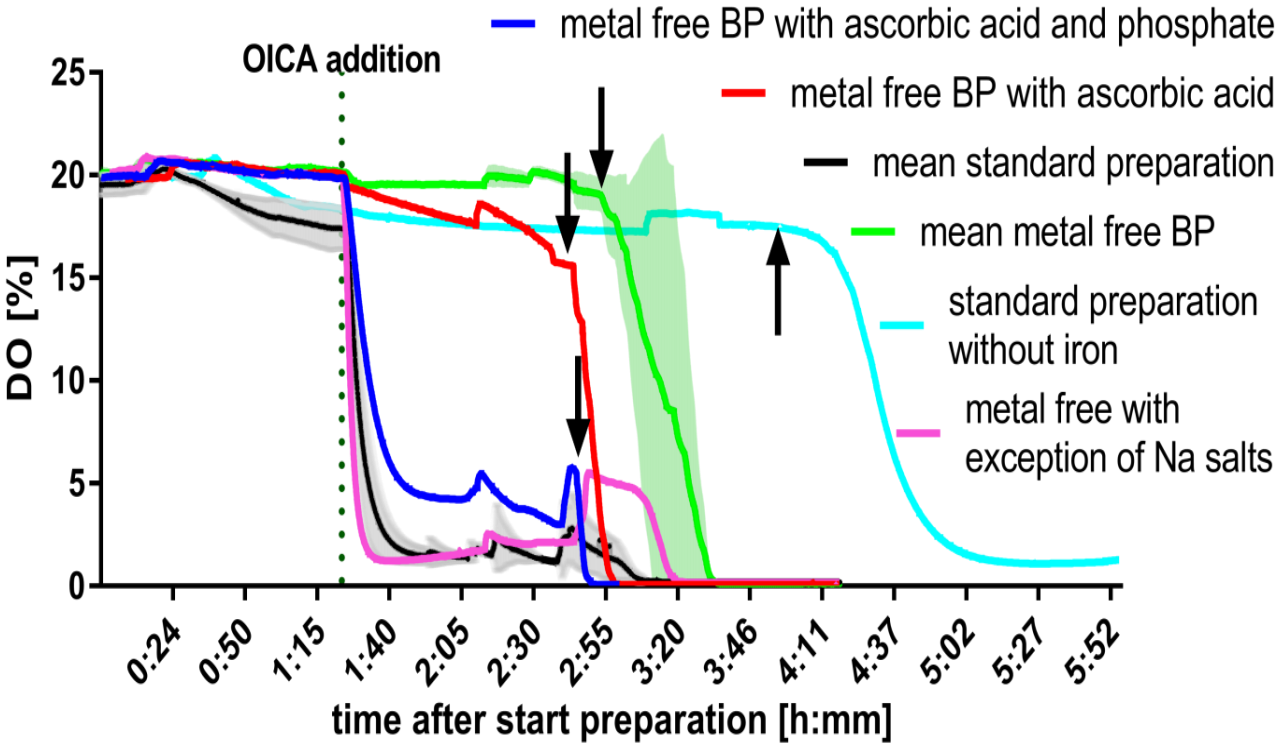

Figure 32: Simplified matrix experiments. The grey and green shade of metal free BP and standard preparation show the 3 SD range of replicate preparations (n=2 and n=3 respectively). The black arrows show the time points when pH adjustment was started.

The routinely used iron salt in CDM development at BI is OICA. Since it is a complex organic salt of ferric iron, a control experiment was used to increase certainty that the effect of oxygen consumption upon OICA addition was coming from iron and not from any counter ions or impurities. The replacement of OICA with other ferric iron salts showed that OICA was exchangeable with for example $FeCl_3$ (Appendix Figure 80). A preparation without additional iron addition to the solution did not result in oxygen consumption (Figure 32 turquoise). This shows that iron was a key reactant or catalyst in the oxygen consuming reaction. As explained earlier, (*3.2.2 Chemical stability during medium preparation – comparison of univariate sensor signals with chemical compound* concentration) a simplified medium matrix approach was used to reduce complexity of chemical reaction environment. Interestingly, the entirely metal free basal powder (Appendix Figure 78) did not show an oxygen consumption upon OICA addition (Figure 24 and Figure 32 green). In contrast, the metal free basal powder with sodium salts showed the oxygen consumption just as drastic as in the standard preparations. This behavior meant that a key ingredient responsible for reaction with oxygen was a sodium salt. In order to identify the involved compounds, the most suspect ones with the highest concentration in medium recipe were added one at a time. Since this did not clearly identify one single compound a series of empirical experiments with combinations of compounds was conducted. They showed that the addition of sodium phosphates and ascorbic acid to metal free basal powder led to the oxygen consuming behavior of standard basal powder and metal free basal powder with the exception of sodium salts. The addition of ascorbic acid only to metal free basal powder was not sufficient to mimic oxygen consumption behavior in standard medium (Figure 32 red).

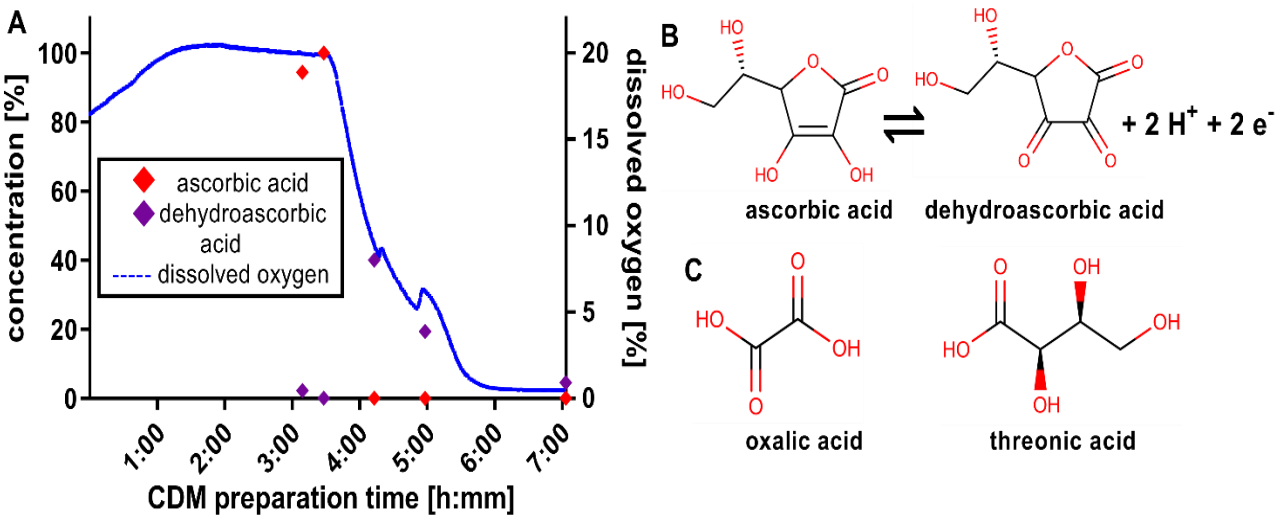

Figure 33: Ascorbic acid oxidation. A) shows the DO profile aligned with the ascorbic acid and dehydroascorbic acid concentrations in the cold room standard medium preparation. B) The redox couple ascorbic acid and dehydroascorbic acid. C) Degradation products of dehydroascorbic acid.

The fact that oxygen consumption was accompanied by ascorbic acid oxidation could be shown with LC-QqQ-MS measurements (Figure 33 A). Because ascorbic acid needs to be measured in negative mode it was not included in the CDM dMRM. The coldroom experiment was ideal to measure reactants due to slowed down kinetics at lower temperatures. The results measured with MS confirm that ascorbic acid was present in the CDM prepared in coldroom at the expected concentration. Upon OICA addition the ascorbic acid concentration decreased to under detection limit and in parallel the concentration of its oxidized form dehydroascorbic acid increased. The oxidation reaction of ascorbic acid to dehydroascorbic acid follows a 1:1 molar ratio (Figure 33 B). However, there is no stoichiometric turnover measured with the MS method. This is very likely caused by different ionization efficiencies of the two analytes. Furthermore, the bell shape of

dehydroascorbic acid suggests that it is an intermediate and this is a second reason why a stoichiometric ratio is not expected. Ascorbic acid is known as reducing agent and antioxidant that can be oxidized by for example hydrogen peroxide.[127] But simultaneously it can also have prooxidant effects for example by reducing metal ions which subsequently generate free radicals.[602, 603] The addition of ferric iron with OICA is very likely causing an ascorbic acid mediated Fenton reaction:

$$Fe^{3+} + AscH_2 \leftrightharpoons Fe^{2+} + Asc^- + 2H^+ \ (Reaction\ 5)$$

$$Fe^{2+} + O_2 \leftrightharpoons Fe^{3+} + O_2^- \ (Reaction\ 6)$$

$$2O_2^- + 2H^+ \leftrightharpoons H_2O_2 + O_2 \ (Reaction\ 7)$$

$$H_2O_2 + Fe^{2+} \leftrightharpoons Fe^{3+} + OH\bullet + OH^- \ (Reaction\ 8)$$

The reactive oxygen species generated from Fenton reaction are very potent in promoting radical mediated chemical reactions. Such uncontrolled reactions are highly undesirable during media preparation.

After pH adjustment, the dehydroascorbic acid concentration also decreases to not detectable levels. This means that there could be other ascorbic acid degradation products as for example oxalic acid, threonic acid, oxalyl L-threonate, cyclic oxalyl L-threonate or free oxalate (Figure 33 C).[316, 604] The observation that dehydroascorbic acid decreases after pH adjustment may suggest that degradation reactions get activated by base addition. It is interesting to note that both oxidation states of ascorbic acid are almost zero at the end of preparation.

As mentioned earlier, the sole addition of ascorbic acid to metal free basal powder was not enough to match oxygen consumption behavior of the standard preparations. This suggests that a reaction cascade was the underlying mechanism. The combination of compounds added to metal free basal powder causing the most comparable oxygen consumption behavior was ascorbic acid and phosphate salts (see blue line Figure 32). This is very surprising because phosphate is generally considered a redox insensitive element due to the highly endergonic nature of the reduction reaction.[605] Its reduction requires more electrons than normally available. At the addition time point of OICA the ORP is slightly negative (-60mV, Figure 24). Han *et al.* have shown that phosphate ($H_2PO_4^-$) reduction to phosphite ($H_2PO_3^-$) is preferred when low ORP is present in environment.[606] Another interesting observation is the positive correlation of iron phosphate complexes with phosphite concentration. However, studies on ferric phosphate complex formation made working pH of below 2.3 necessary because at higher pH an almost white precipitate was encountered.[607-610] Therefore, the formation of iron phosphate complexes at pH present in medium is not likely at high concentrations. Besides, the precipitation of phosphate by the addition of ferric iron is a commonly used principle to reduce phosphate load in wastewater.[421] However, it has to be emphasized that during medium preparation no precipitates were observed. The role of phosphate in the oxygen consuming reaction during medium preparation remains elusive. Literature mainly hints at phosphate being unlikely to participate in redox reactions. However, there are also some studies which report similar observations as described in this thesis. Elvehjem reported that the presence of pyrophosphate activated oxygen consumption in his cysteine and copper reaction systems.[611] In some experiments the presence of pyrophosphate accelerated oxidation rates by almost a factor of three. It is interesting to note that the paper shows that the used phosphate buffer alone is not inducing an oxidation rate as high as pyrophosphate added to the buffer. This allows either the conclusion that phosphate buffer alone is inhibiting or that pyrophosphate is accelerating the

oxidation of cysteine. The observation that the addition of a copper sulfate solution to phosphate buffer lead to immediate precipitate formation, whereas the same amount of copper added to pyrophosphate solution did not, shows the high specificity of this reaction system to pyrophosphate. The oxygen uptake accelerating effect of phosphate in CDM is comparable with the effect of pyrophosphate on cysteine oxidation observed by Elvehjem. However, in the same time the results discussed here are contradictory to the quoted paper because phosphate buffer was discussed as inhibitory on oxidation. Since the spontaneous formation of pyrophosphate from phosphates in CDM is not likely, the similar effects observed in model medium 1 seem to be subject to different reaction mechanisms.

Reinke *et al.* reported that the addition of 100 mM phosphate buffer at pH 7.4 to their reaction system of microsomes increased the formation of free radical metabolites including H_2O_2. [612] The group could show that increasing phosphate concentration (0 to 100 mM) increased ferric iron reduction rate from 6.1 ± 0.4 nmol/min/mg to 21.7 ± 0.3 nmol/min/mg without dependency on pH or osmotic potential. The increasing effect on radical formation was dependent on reducing agent NADPH. Without it no reduction of Fe^{3+} was observed. The importance of iron for this mechanism could be shown by inhibiting the reaction by adding either Fe^{2+} or Fe^{3+} chelator. Chelation of both iron ions led to obviously reduced radical formation. Even though the reactions described by Reinke *et al.* were carried out with an enzymatic system, the data clearly shows that phosphate can indirectly influence certain free radical forming reactions. The reason phosphate buffer is usually used in free radical reaction investigations is that it has poor reactivity with most radicals. Additionally to phosphate affecting ferric ion reduction also reports of increased rates of ferrous ion autoxidation in phosphate buffer (50 mM, pH 7.2) exist.[405, 613] This shows that under certain conditions phosphate buffer can promote redox cycling of iron into both reducing and oxidizing direction. In order to get deeper understandings of iron phosphate cycling in the medium iron chelation experiments as described by Reinke *et al.*, variations of phosphate concentrations in CDM and further simplified matrix experiments could shed more light on the reaction mechanism causing oxygen consumption in CDM. Additionally, it would be interesting to test if other phosphate compounds as tested by Rasmussen *et al.* induce the same redox cycling or if some of these induce less redox reactions by either more efficiently chelating ferric ion or less chelation leaving the iron to its meant chelators.[373] In a second test it would be necessary to investigate if these compounds would increase or maintain the bioavailability of phosphate and in the same time provide the buffering properties.

As mentioned before, the addition of phosphates and ascorbic acid caused an highly comparable oxygen consumption behavior but did not exactly match the oxygen consumption profile of standard basal powder (DO profile after OICA addition not within SD range of standard preparation in Figure 32). One of the compounds excluded from metal free basal powders is sodium pyruvate. This compound is known for a long time as hydrogen peroxide scavenger and has also been used as antioxidant in cell culture.[256, 257, 614] Therefore, it is likely that pyruvate plays an important role in the described ROS generating reaction. If it is not present, it is possible that other scavengers not as potent (e.g. other keto acids) overtake the role. This may lead to an accumulation of intermediates and thus an inhibition of the oxygen consuming reaction that gets started by ascorbic acid and phosphates in metal free basal powder.

Thus, a reaction mechanism similar to the one described by Reinke *et al.* is postulated for the oxygen consuming reaction in investigated model medium 1 (Figure 34 A).[612] In a first step a reducing agent, ascorbic acid, promotes the reduction of ferric iron. As discussed earlier, this mechanism is accelerated by phosphate due to most likely a complexation effect. The then produced hydrogen peroxide will be neutralized by the reaction with pyruvate (Figure 34 B).[258, 259] The hydrogen ions released in this reaction and the degradation product carbon dioxide can be the cause for acidification of CDM to 6.8 after adjustment to pH 7.

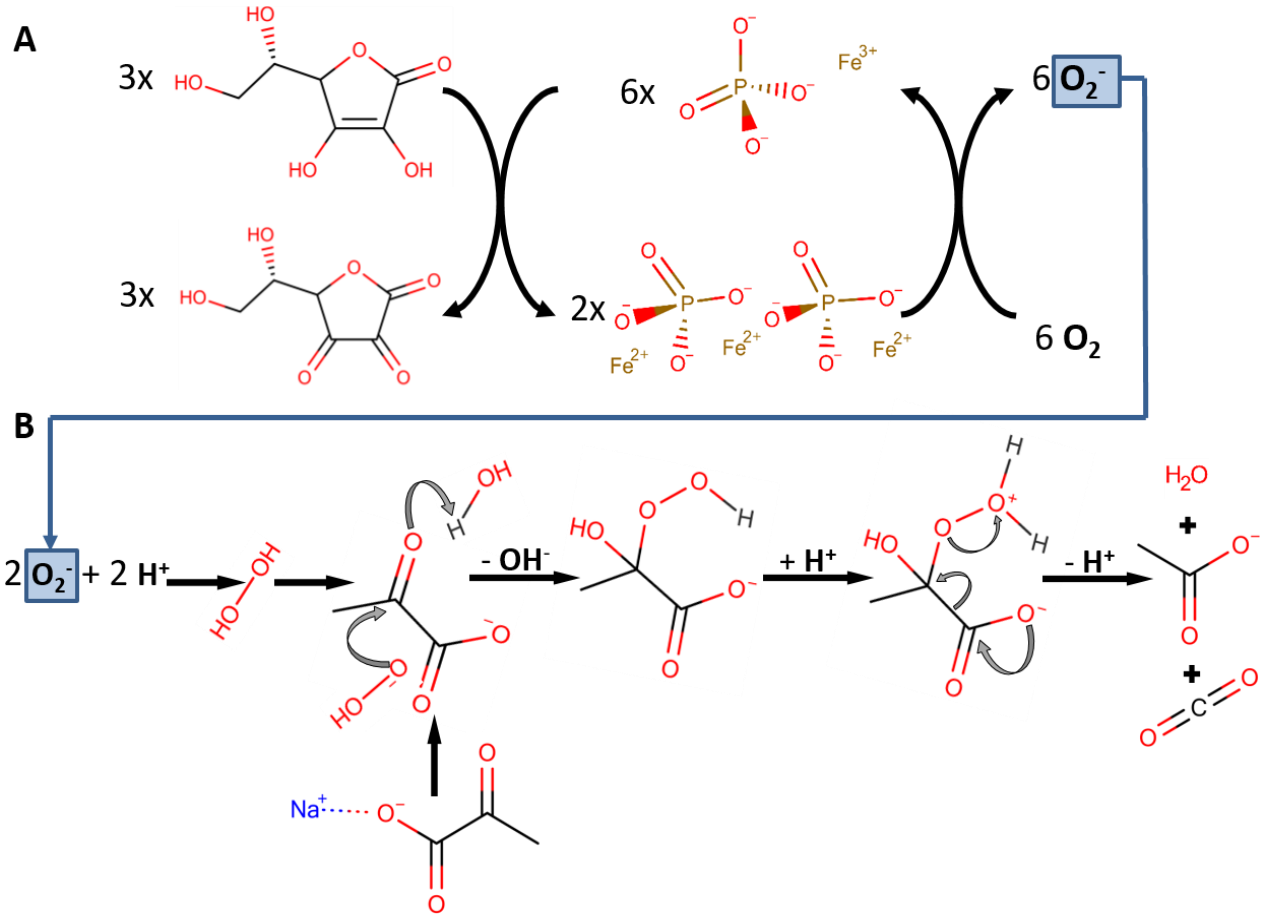

Figure 34: Hypothetical reaction mechanism of oxygen consuming reaction during model medium 1 preparation. Reaction pathways adapted from Asmus *et al.* and Reinke *et al.*[258, 612] A) Ascorbic acid oxidation catalyzed by iron-phosphate complex. B) Reduction of pyruvate as final electron acceptor.

If ascorbic acid was not present in CDM other compounds may overtake its role. For example cysteine and glutathione are also known to autoxidize.[405] An autoxidation describes an oxidation reaction such as the Fenton type reaction discussed for ascorbic acid (Reaction 5 to 8). In that type of mechanisms, no catalyst is altering the speed of the reaction but the substance that induces the reaction is oxidized only by the exposure to oxygen of the air or of the liquid.

Concluding remarks on the chemical characterization of CDM during medium preparation

This work shows that the hydration of CDM is chemically very complex. The approaches discussed describe possibilities to monitor and start to understand certain effects. This data shows promising chemical insights in CDM preparation, especially due to the complex medium composition and the multitude of physical and chemical effects impacting the solution. For a full understanding further advances in analytical development are necessary. Also, simplified media compositions would increase the potential for understanding of chemical reactivity during medium preparation.

The developed LC-QqQ-MS dMRM method is capable to generate data that sheds light on several mechanisms happening during medium preparation. From an analytical point of view, an increase in method accuracy would help and identify smaller changes e.g. in amino acid concentration. For proving hypothesized reaction pathways an inclusion of the reaction end product to the dMRM method would be the most straight forward option. Another very good way to identify reaction products is isotopic labelling of reaction educts.

The chemical characterization of model medium 1 during preparation has revealed several interesting insights. As most of the compounds were stable over medium preparation L-cysteine, thiamine, vitamin B_6, L-2-aminobutyric acid and glutathione showed sensitivity to medium preparation conditions. The most outstanding chemical effect during preparation is the oxygen consuming reaction. The applied media matrix simplification approach has revealed iron, ascorbic acid and phosphates as the main reactants. This and the hypothetical reaction pathway will allow cell culture media scientists to control the reaction in future media development.

3.3 Feed Medium Storage

The planning and organization of multi-bioreactor facilities is a complex and difficult task that requires a high amount of flexibility. Thus, storage of hydrated CDM is inevitable. This is even more true for small-scale than for large-scale. Therefore, effects of storage on the chemical composition of media is of inherent interest for the bioengineer with a focus on robust and reproducible bioprocesses.

3.3.1 The stability of components during feed medium storage at room temperature

Fed-batch cultivation is a commonly used process format in at scale biotherapeutic protein manufacturing. A typical CHO cell cultivation process takes around 14 days, with continuous feeding starting in the first couple of days. For this specific feeding strategy, the vessels containing the feed medium are sterile coupled to the bioreactor in local proximity. Because the target temperature in cultivation is around 37°C the rooms where the equipment is installed are usually not temperature controlled. Therefore, feed medium is exposed to ambient temperature during the cultivation. Even though the feed medium is stored at 2-8°C for longer term storage, the cells are actually fed with medium that was exposed to elevated temperatures in the laboratories where the bioreactors are installed. Thus, feed medium composition alteration that occurs due to storage at room temperature is highly process relevant.

Up to date, the osmolality and pH after preparation are the only parameters measured for CDM quality control. In order to get a glimpse into CDM composition from preparation over a 28 day storage period the model medium 2 prepared at 4 different preparation temperatures (Figure 22) was stored in two commonly used vessel materials (glass and plastic containers). The stored medium was sampled at several process relevant time points and measured with CDM LC-QqQ-MS dMRM in 6 independent batches with the samples randomized between the batches. The data was first analyzed with PCA to get a broad overview of the least stable compounds over time. A model with four principal components (PC´s) explained 58.31% of variability in the data. PC2 and PC3 mainly describe batch to batch variability due to batch 1 and batch 5 respectively (Figure 35 and Figure 36). The PCA is sensitive to small changes in the data that were not detected in the inter- and intraday precision experiments during method validation. As discussed earlier, the method validation showed robustness for these parameters. The statistical significance of this observation was confirmed by One-way ANOVA (Figure 36). A small summary P value is a measure for the improbability of the observed differences being random. The P values for both PC2 and PC3 are < 0.0001. This means that not all batches in these populations have the same or a similar mean (Figure 36 F and G). As opposed to this, the PC1 and PC4 P values are large which is confirming that these principal components are not impacted by batch to batch variability and solely describe a time effect (Figure 36 E and H). Furthermore, the overlap of means graphically visualize the descriptive P value. It has to be mentioned that a batch to batch variability was described by the PCA model even though each individual data set was normalized to the respective QC samples. The variability in PC2 is mainly attributed to extraordinary concentrations of calcium pantothenate, putrescine, riboflavin and nicotinamide that could not be corrected by normalization to QC sample. In the same way the variability in batch 5 can be tracked back to L-proline, L-valine, L-isoleucine and L-leucine.

.

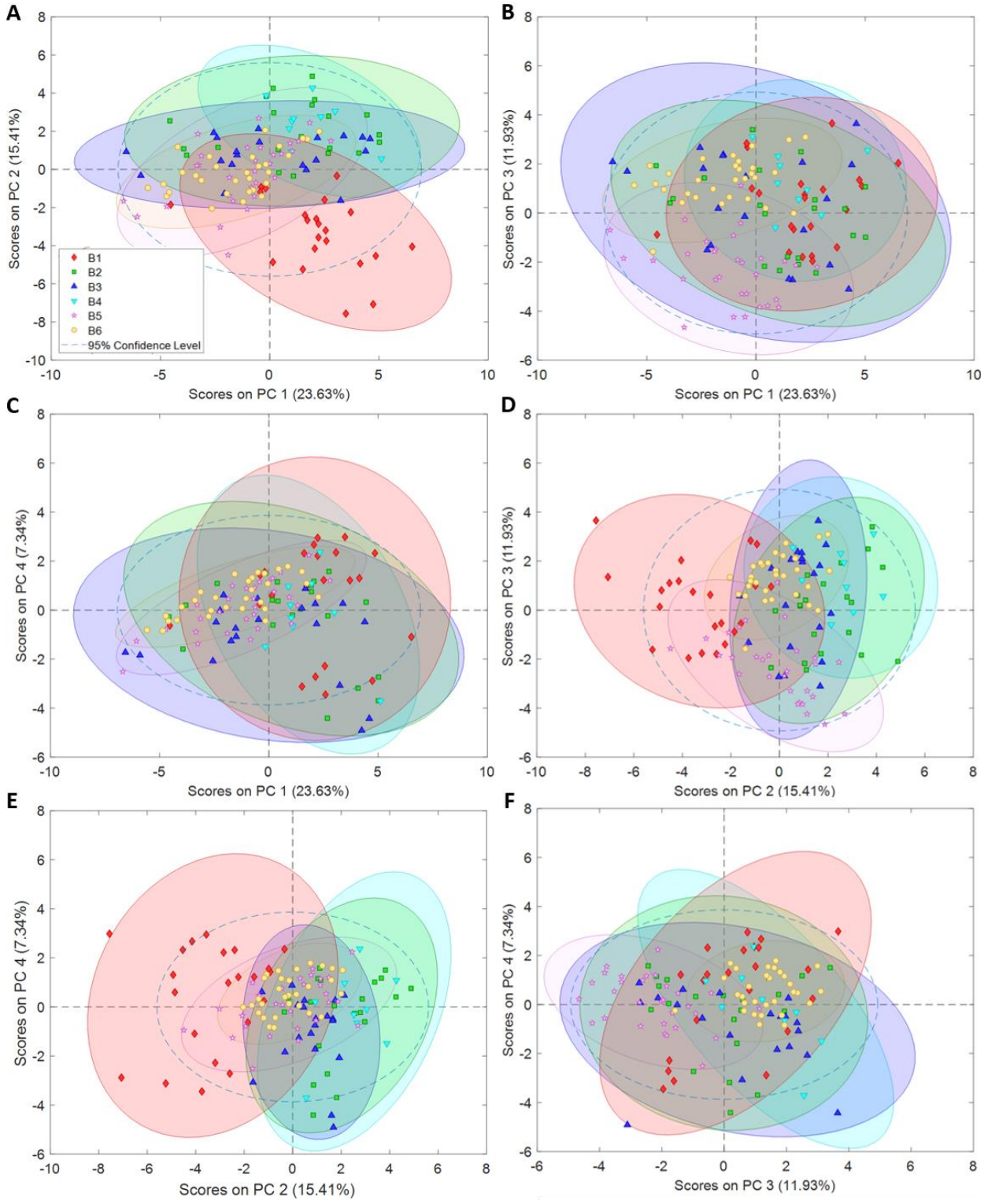

Figure 35: PCA analysis of model medium 2 stored over time (B1=batch 1, B2=batch 2, B3=batch 3, B4=batch 4, B5=batch 5 and B6=batch 6).The graphs show that the principal components 2 and 3 explain variability in the data due to batch. A) PC1 plotted against PC2. PC2 shows distinct properties of batch 1. B) PC1 plotted against PC3. PC3 shows differences in batch 5. C) PC1 versus PC4 shows overlapping ellipses and data populations. This shows that these PC´s are not impacted by batch to batch variability. D) PC2 versus PC3, E) PC2 versus PC4 and F) PC3 versus PC4.

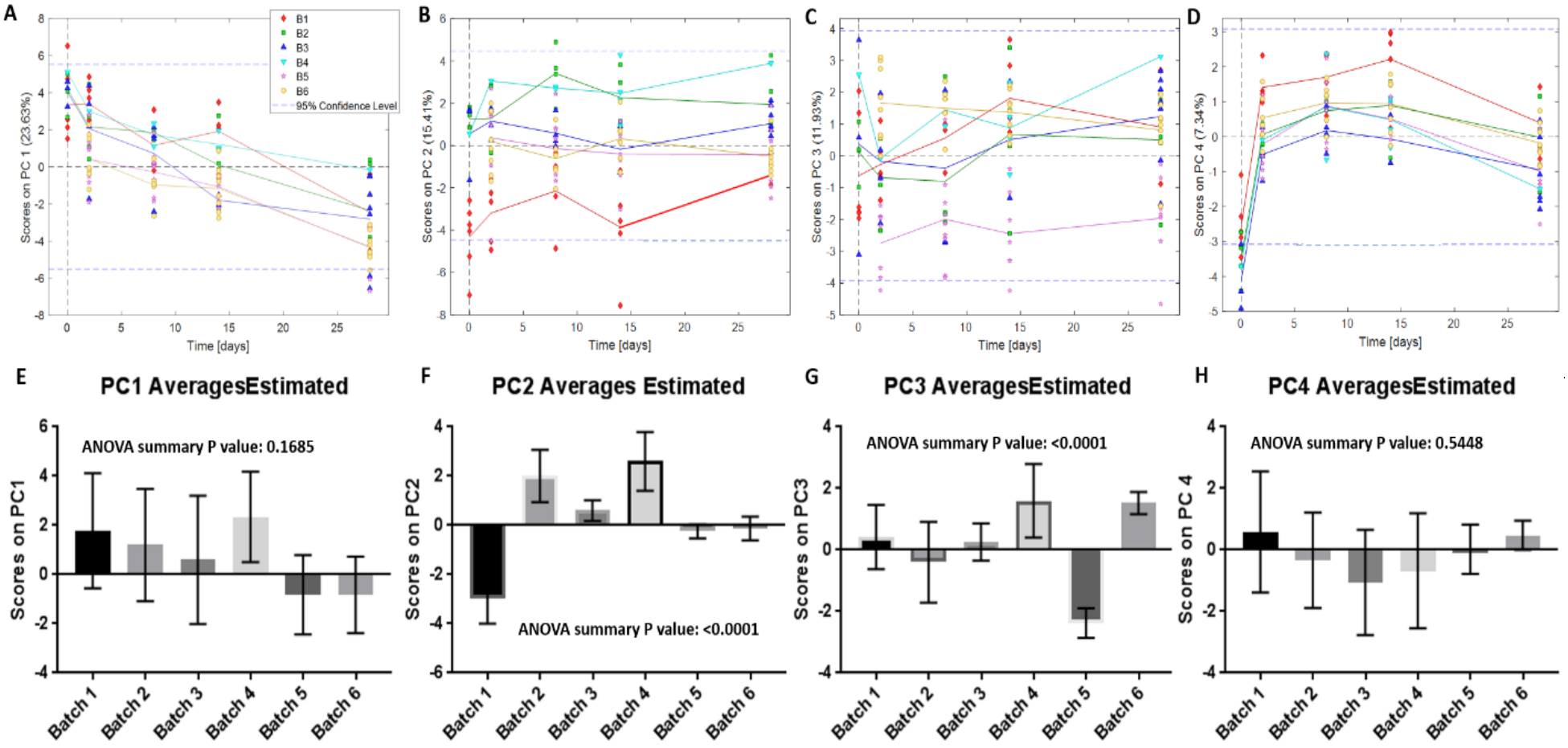

Figure 36: ANOVA testing proofs that there is no batch effect in PC1 and PC4. A), B), C) and D) show time plotted versus the scores of PC´s 1 to 4. The color legend shows the data categorized by batch the data has been measured in (B1=batch 1, B2=batch 2, B3=batch 3, B4=batch 4, B5=batch 5 and B6=batch 6). If the data categorized by batch shows similar behavior, this means that the batch effect in the respective PC is negligible (PC1 and PC4). The plots E), F), G) and H) show the result of the data of plots A-D analyzed by One-Way ANOVA which compares the variability among group means with the variability within the groups. A large P value means that there is a weak relationship between group membership and the variables (Batch 1 to 6). If the overall P value is small, then it is unlikely that the differences observed are random. As both PC2 and PC3 show P<0.0001 it is confirmed that not all the populations plotted by batch have the same mean. In contrast, the P values of PC1 and PC4 are big.

PC1 and PC4 clearly do not describe batch variability and even though variation accounted for by PC4 is small in comparison to PC2 and PC3, it is still there and important to describe the data (Figure 35 and Figure 36). The overlapping ellipses in Figure 37 A show that there is neither an effect of medium preparation temperature nor of storage vessel material (Figure 37 B) on chemical composition of analyzed media. The preparation temperature varied between 25°C and 40°C did not show an impact on the concentrations of analyzed compounds over preparation and storage time. This is well in accordance with the observation that particle profile measured with FBRM during preparation did not show any apparent differences due to preparation temperature during preparation (See chapter *Effect of preparation temperature and basal powder composition on particle distribution*). The comparability between 3 L scale model (Figure 37 - 25°C controlled, 35°C uncontrolled, 35°C controlled and 40°C controlled) and standard laboratory scale preparation method at 35°C in Erlenmeyer flasks without temperature control was demonstrated by the overlap of ellipses. This confirmed comparability between scales used in process development for medium preparation, increased confidence for chemical comparability in scale-up and increased the freedom in medium preparation scale-up at BI. Furthermore, storage in the vessel materials plastic and glass did not show any difference on CDM composition over time (Figure 37 B). This is important information for process development because cultivation at different scales requires altering vessel sizes which is coming typically with different materials. For example, feed media for micro-bioreactor cultivations are usually stored in glass bottles, whereas medium size reactors are normally coupled with feed media stored in plastic bottles as Biotainers. At large scale feed medium is commonly stored in plastic bags which are made of different plastics than the described bottles. However, these different plastics should have comparable properties with respect to air permeability.

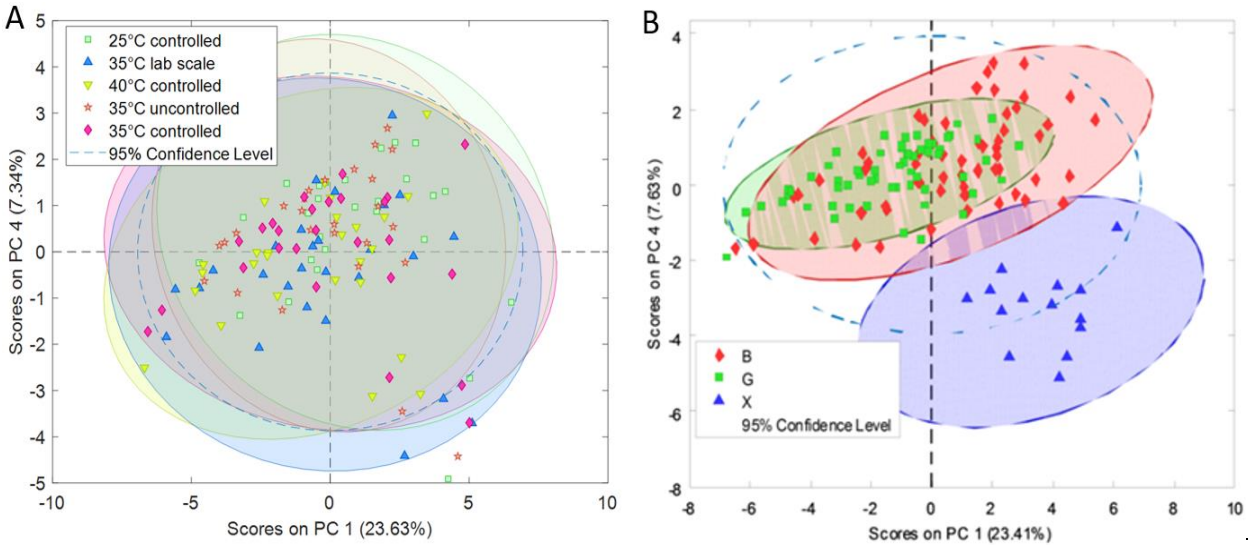

Figure 37: Scores plot of PC1 and PC4 shows that there is no effect of preparation temperature or storage vessel on chemical composition of CDM measured by dMRM. The completely overlapping confidence ellipses in A) show that preparation temperature does not impact compound concentrations after preparation and storage. B) shows the data plotted by storage vessel, whereas the blue triangles marked with X represent data points measured right after preparation. The red diamonds show media stored in plastic vessels (B=biotainer) and the green squares show media stored in glass bottles (G=glass). Compound concentrations measured in CDM stored in plastic show slightly bigger variation but the complete overlap with concentrations measured from media stored in glass vessels shows that there is also no effect of storage vessel on CDM composition.

The average CHO cell cultivation in fed-batch mode takes 8 to 14 days. During this time, the feed medium must be sufficiently stable at room temperature. The concentrations plotted versus time did not reveal prominent instabilities for most of the CDM ingredients such as the amino acids (Figure 38). The graphs in Figure 38 suggest that some amino acid concentration profiles like L-serine, L-ornithine, L-asparagine, L-threonine, L-lysine, L-aminobutyric acid, L-methionine, L-arginine, L-histidine, and L-phenylalanine imply that there could be a slight decrease in concentration over time. Nevertheless, the wide standard deviations calculated from triplicates do not allow a reliable conclusion on stability effects of these compounds over time. If concentration was impacted over storage time it would be very small (one digit percent range). Considering the high nominal concentrations of amino acids in media (Appendix Table 15) the supply of the running cell culture would not be impacted. If these minor concentration changes could be confirmed, it would be of interest to identify products or educts of chemical reactions. With that knowledge the criticality on cell culture can be estimated and if necessary, strategies against the critical chemical reactions can be developed. In contrast to for example amino acids, compounds like thiamine, cyanocobalamin, pyridoxal, supplement II compound A, OICA compound, L-cystine, L-cysteine and L-hydroxyproline showed obvious concentration changes over the storage time.

As mentioned earlier, the PCA is capable to highlight minor changes in a data set. Therefore, the PCA model with LC-QqQ-MS data was investigated for time effects. Figure 39 A shows that PC1 and PC4 describe a time dependent concentration behavior. PC1 describes chemical reactions that start slowly from the beginning until the end of storage (Figure 39 D) and PC4 explains a fast media aging progress after preparation lasting until day 2 (Figure 39 G). Because PC2 and PC3 mainly describe batch to batch variability they can be excluded from a time effect consideration (Figure 39 E and F). The PCA model confirmed the impression that many amino acids exhibit a slight concentration decrease over the entire storage duration (loadings on PC1, Figure 39 B). Besides these minor changes, the PCA model also underlines the main CDM compounds with reduced stability over the analyzed time frame. Amongst them are slowly changing compounds (thiamine, cyanocobalamin, L-cystine, Supplement II compound A and OICA compound), mainly described by PC1 and fast changing compounds described by PC4 (L-cysteine, pyridoxal and pyridoxamine).

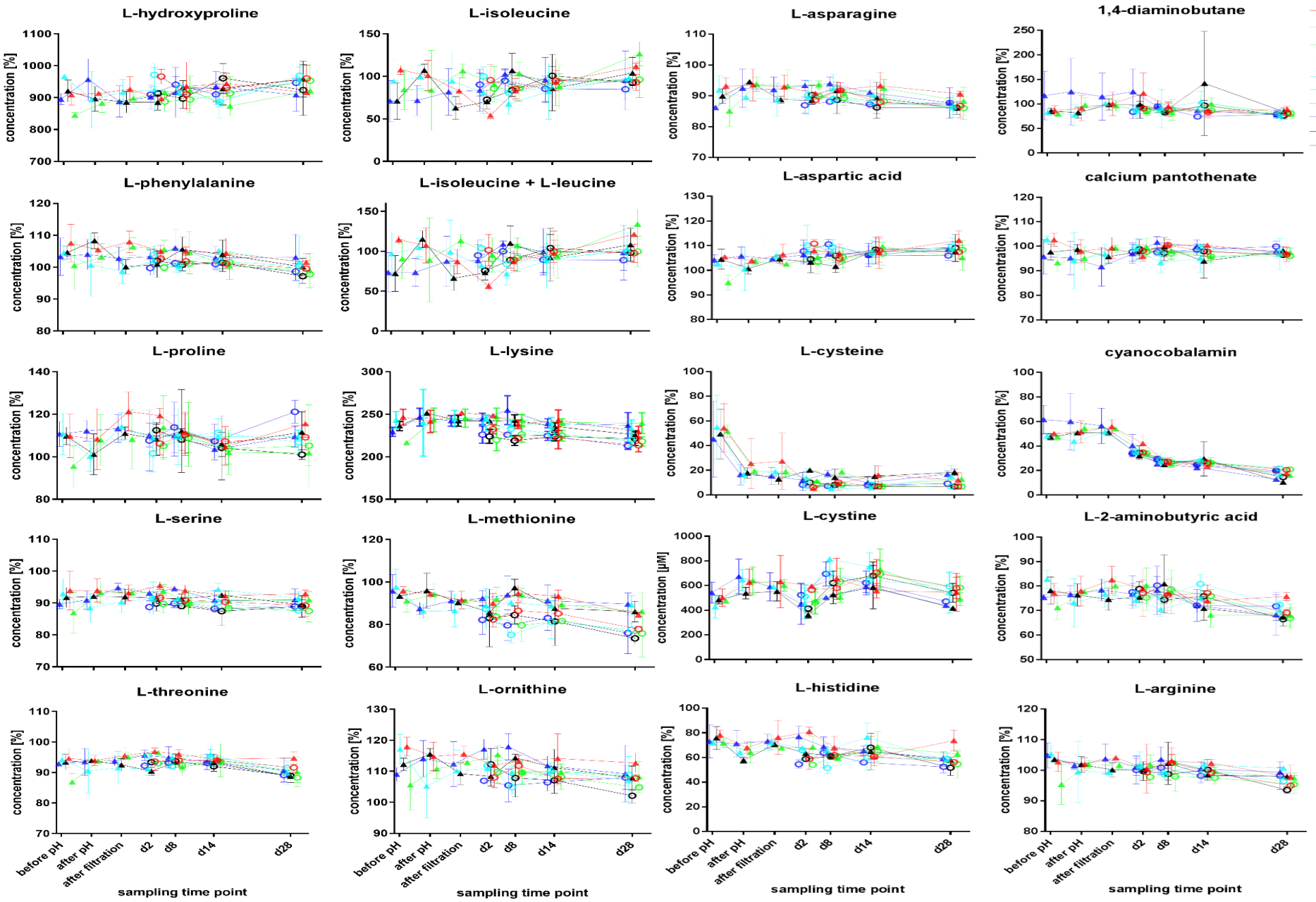
L-hydroxyproline
L-isoleucine
L-asparagine
1,4-diaminobutane
L-phenylalanine
L-isoleucine + L-leucine
L-aspartic acid
calcium pantothenate
L-proline
L-lysine
L-cysteine
cyanocobalamin
L-serine
L-methionine
L-cystine
L-2-aminobutyric acid
L-threonine
L-ornithine
L-histidine
L-arginine
concentration [%]
concentration [µM]
before pH
after pH
after filtration
d2
d8
d14
d28
sampling time point
25Y B
25Y G
35L B
35L G
35N B
35N G
35Y B
35Y G
40Y B
40Y G

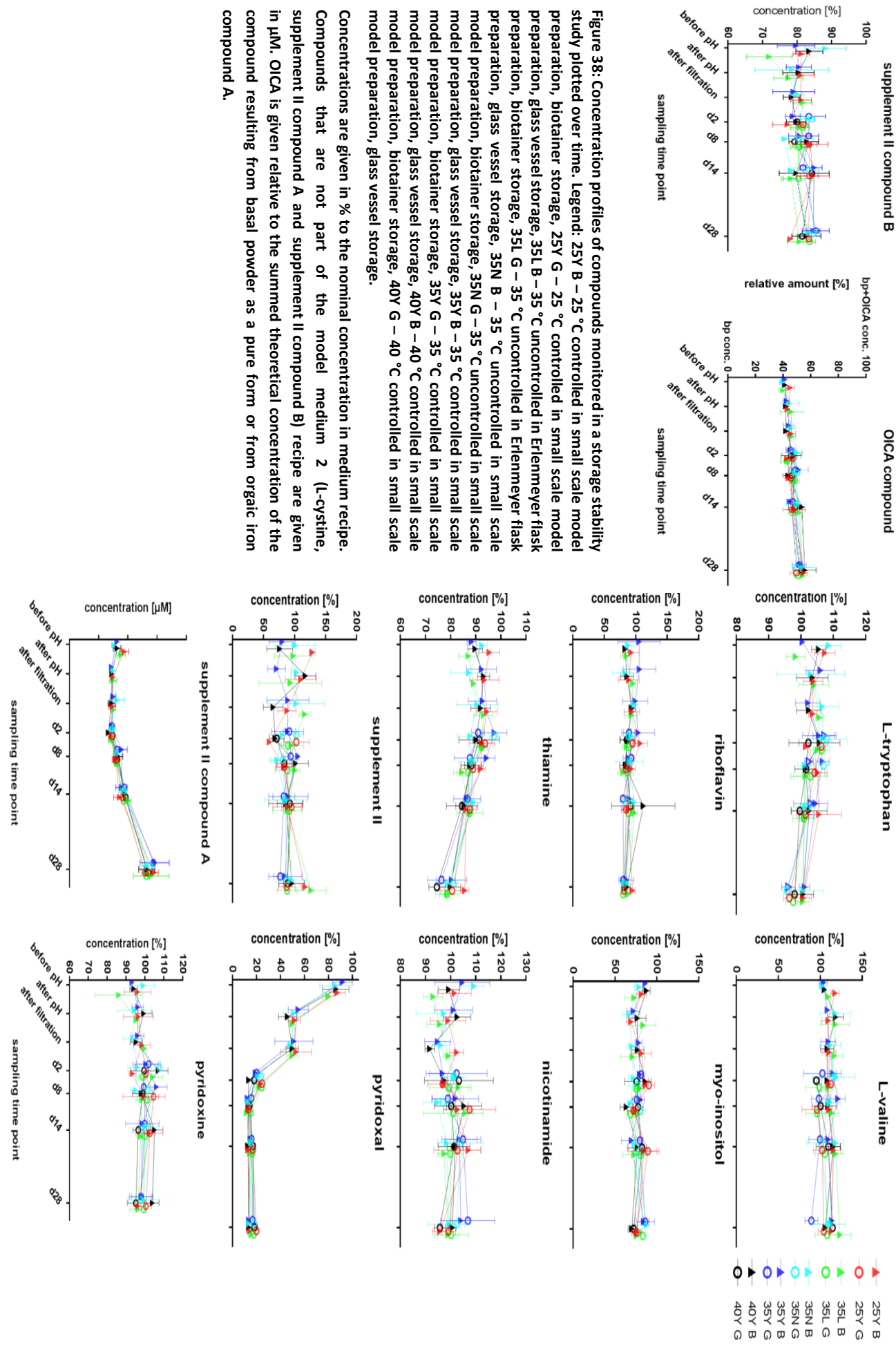

Figure 38: Concentration profiles of compounds monitored in a storage stability study plotted over time. Legend: 25Y B – 25 °C controlled in small scale model preparation, biotainer storage, 25Y G – 25 °C controlled in small scale model preparation, glass vessel storage, 35L B – 35 °C uncontrolled in Erlenmeyer flask preparation, biotainer storage, 35L G – 35 °C uncontrolled in Erlenmeyer flask preparation, glass vessel storage, 35N B – 35 °C uncontrolled in small scale model preparation, biotainer storage, 35N G – 35 °C uncontrolled in small scale model preparation, glass vessel storage, 35Y B – 35 °C controlled in small scale model preparation, biotainer storage, 35Y G – 35 °C controlled in small scale model preparation, glass vessel storage, 40Y B – 40 °C controlled in small scale model preparation, biotainer storage, 40Y G – 40 °C controlled in small scale model preparation, glass vessel storage.

Concentrations are given in % to the nominal concentration in medium recipe. Compounds that are not part of the model medium 2 (L-cystine, supplement II compound A and supplement II compound B) recipe are given in µM. OICA is given relative to the summed theoretical concentration of the compound resulting from basal powder as a pure form or from orgaic iron compound A.

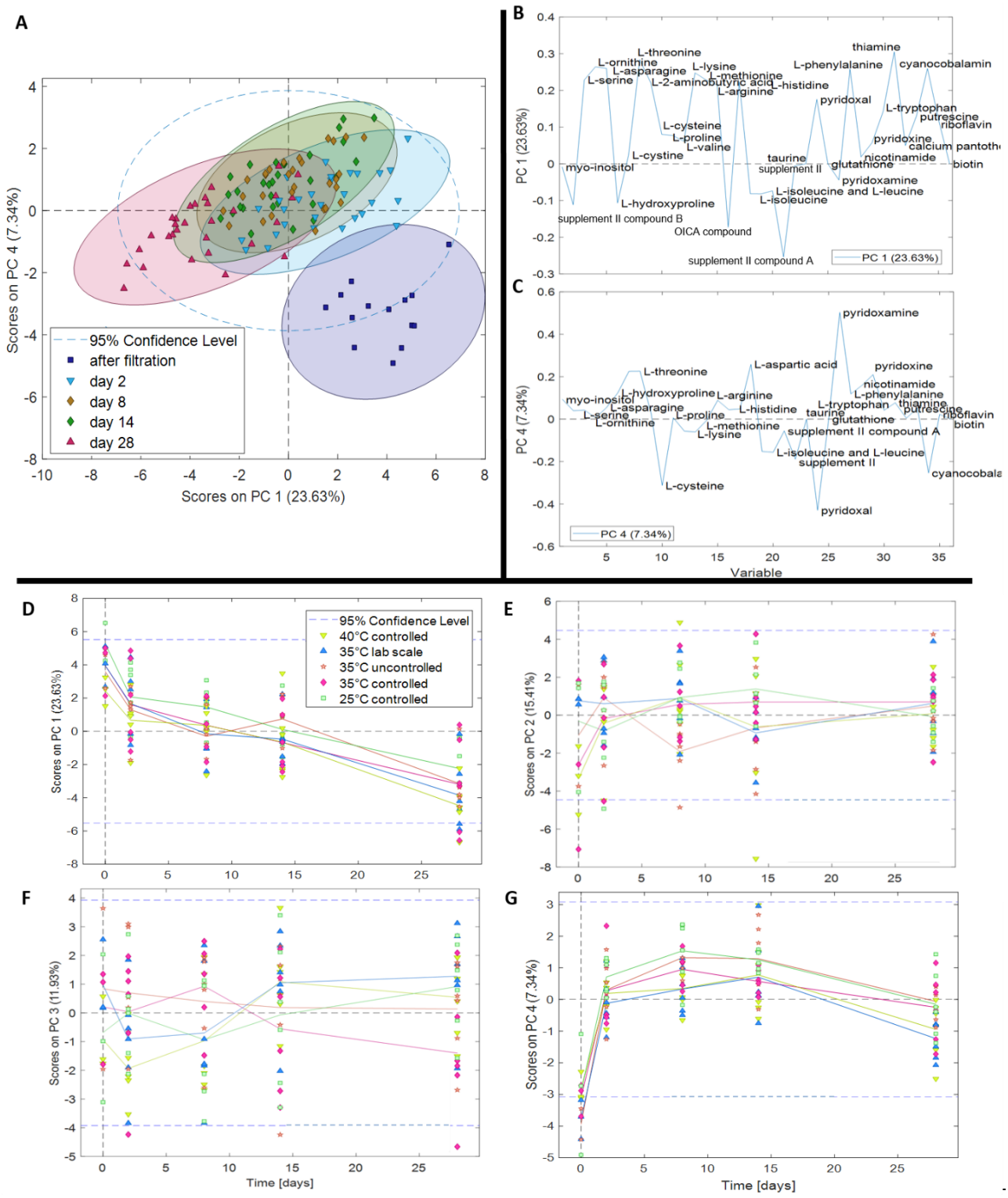

Figure 39: CDM compound composition is changing over time. A) The score plot of PC1 versus PC4 shows a time dependent behavior. B) The loadings on PC1 show compounds that decrease over time (positive values) and compounds that increase over time (negative values). Amongst several amino acids thiamine, cyanocobalamin and pyridoxal decreased over time, whereas supplement II compound A and OICA compound showed slightly increased concentrations over time. C) The main loadings on PC4 come from pyridoxamine, pyridoxine (increasing concentration) and from pyridoxal, L-cysteine and cyanocobalamin (decreasing concentration). D) Shows the scores of PC1 plotted versus time. The graph depicts that PC1 explains slow concentration decreases happening over the entire storage time. E) and F) show that there is no time effect but only a batch effect. G) A very fast concentration alteration between day zero and day 2 is described by PC4.

The biologically active form of vitamin B6, pyridoxal 5´phosphate, is a cofactor in more than 160 enzymes mainly catalyzing transamination reactions.[615] The investigated model medium 2 contains the B6 as pyridoxine and pyridoxal. As shown in Figure 40 A and Figure 38 pyridoxine remained stable over the entire storage duration. On the contrary, the pyridoxal concentration showed an apparent concentration decrease to 10% of expected concentration after 8 days storage at room temperature. In the same time, pyridoxamine showed an increase from 50% to 140% on day 8. Chemical transamination of pyridoxal is a reaction mechanism that explains the concentration increase of pyridoxamine. The source for amine group in CDM can be variable and many potentially transaminating agents are constituent of CDM recipes. For example, L-glutathione or other amino acids in combination with metal catalysis could participate in these kind of reactions.[338, 339] Furthermore, Kurauchi *et al.* investigated a reaction in which transamination was shown to be dependent on photo induced decarboxylation. The model described in the paper contained pyridoxal 5´phosphate and the amino acid L-phenylalanine in potassium phosphate buffer and was incubated at room temperature and pH 7. However, as the model medium 2 prepared in small scale model was light protected, and comparability to lab scale has been demonstrated, a light induced reaction mechanism is unlikely. Another group of transaminating compounds under metal catalysis was identified as kynurenines.[336, 337] For the simple reason that amino acids are used at high concentration in CDM, it is likely that multiple amino acids or degradation products such as kynurenines are involved in pyridoxamine formation from pyridoxal during preparation and storage. The fact that pyridoxamine concentration seems to decrease after day 8 may be due to a nucleophilic attack of the aldehyde group of glucose on its primary amine.[335] This reaction would for example generate 4-pyridoxic acid. Generally, the inter-transformation of pyridoxal and pyridoxine is not considered critical for cell culture because, as any rodents, CHO cells should possess salvage pathways and are therefore able to uptake all vitamin B6 sub-forms.[616-618]

Thiamine decreased over the 28 days of storage, but the loss does not exceed 20% to nominal concentration (Figure 40 B). Therefore, the risk of thiamine degradation impacting cell culture performance is negligible. A well-known degradation mechanism of thiamine is oxygen induced degradation to thiochrome.[325, 328] Furthermore, no toxic effect of thiochrome on cell culture is known.

In contrast, the cyanocobalamin showed a decrease of 40% to nominal concentration already during preparation (Figure 40 B). Over the storage period, it further degraded to 20% of expectation. Oxidation of cyanocobalamin to hydroxocobalamin was described in the presence of ascorbic acid.[331] Abu-Soud *et al.* described the depletion of cyanocobalamin through oxidation with HOCl.[330] Interestingly, hydrogen peroxide, that can for example be generated by the autoxidation of L-cysteine, has a comparable oxidation potential and could therefore induce similar reaction mechanisms.[614] Since cyanocobalamin decreases by more than 60% over the storage time an impact on cell culture process is likely.

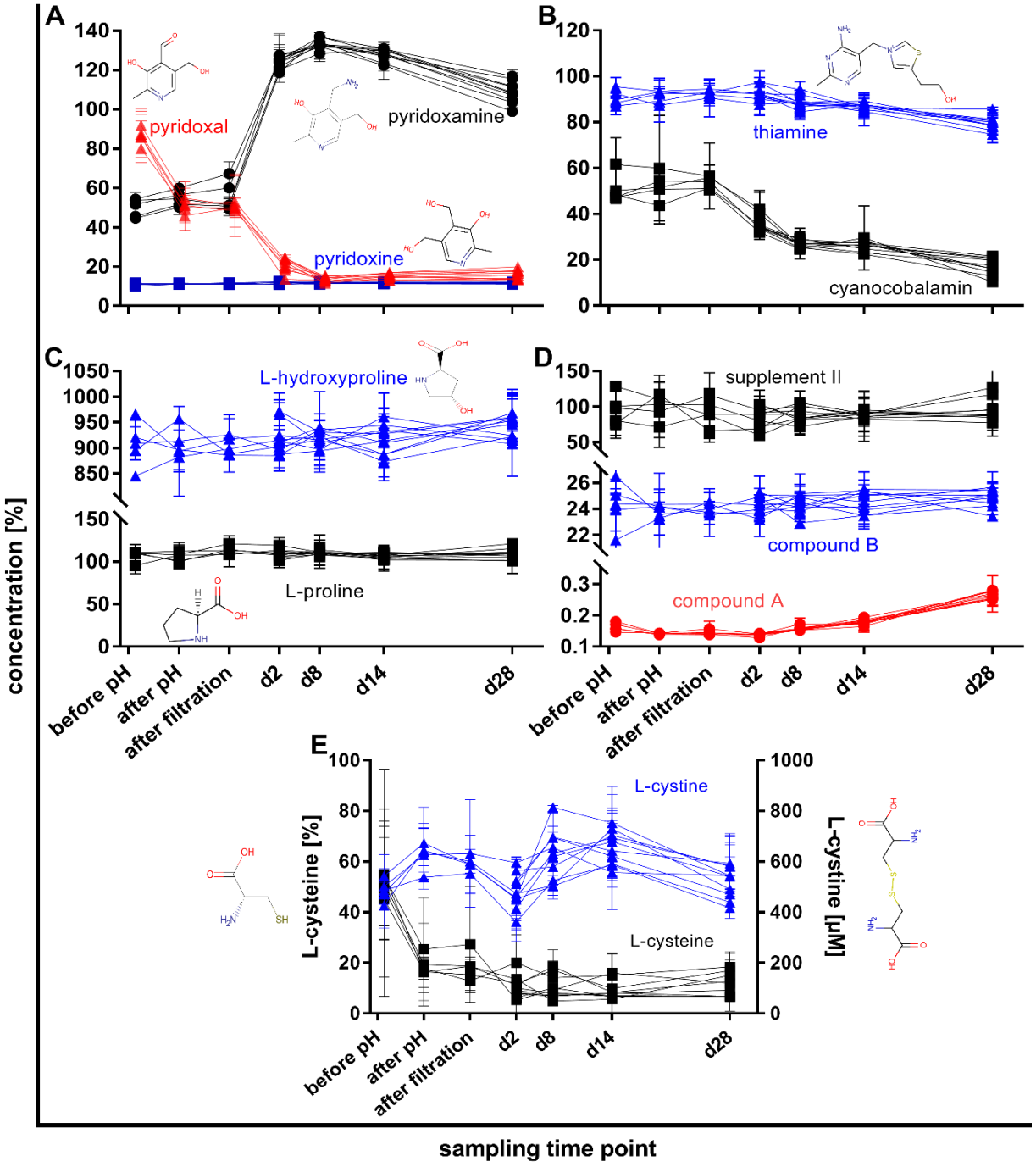

Figure 40: Compounds which have an apparently impacted stability over storage time. The concentration profiles of compounds were analyzed on the following sampling time points: before pH adjustment, after pH adjustment and after filtration during preparation and the media were sampled during storage on various days (Day(d)2, d8, d14 and d28). If not other indicated, the measured concentrations were normalized to their expected values. A) All B6 vitamin sub-forms were normalized to the expected concentration of pyridoxal. The concentration profile shows pyridoxine being stable over storage time, whereas pyridoxal showed a significant decrease and pyridoxamine an increase. B) Both thiamine and cyanocobalamin showed apparent concentration decrease over storage time. C) Both L-proline and L-hydroxyproline had rather stable concentration over preparation and storage. However, the L-hydroxyproline concentration was increased by approximately 900% to expectation. D) Supplement II and its constituent compounds were stable over storage time. All three compounds were normalized to expected concentration of supplement II. A negligible increase of supplement II compound A starting from day 8 could be observed. E) L-cysteine significantly decreased over preparation and remained stable over storage. In contrast, the oxidation product L-cystine increased over storage before it finally decreased.

PCA analysis confirmed that L-proline and L-hydroxyproline were showing no major concentration change over storage time (Figure 39 B and C). Both compounds were stable during pH adjustment at the end of medium preparation. Although both L-proline and L-hydroxyproline were neither impacted by storage duration nor by medium preparation the L-hydroxyproline concentration was found to be 900% above expected concentration. As described by Osberger *et al.*, an oxidation of L-proline could be responsible for the L-hydroxyproline increase.[399] Since the L-hydroxyproline concentration did not change over time it can be assumed that the high concentration is already present in the basal powder. This would be well in accordance with observations from model medium 1 investigations during medium preparation (Appendix Figure 74 F). Even though L-hydroxyproline is among commonly used amino acids in CDM its positive effect on cell culture remains rather elusive. If the assumption that it comes as an impurity with L-proline proves right, it is one compound that could be eliminated from basal powder formulation.[268, 619, 620]

Supplement II was shown to be stable during medium preparation and storage (Figure 40 D). This observation also keeps true for Supplement II compound B. In contrast, the supplement II compound A showed a minimal decrease over time. This was also covered by the PC1 in PCA (Figure 39 B). Since this increase is $\leq$1% compared to supplement II target concentration it is considered negligible and most likely not impacting cell culture performance.

L-cysteine is considered to act as an antioxidant but in the same time it can react with oxygen in metal catalyzed mechanisms to generate reactive species.[614] The compound was already identified during method development in both CDM and artificial matrix as rather unstable. As observed during the medium preparation experiment with model medium 1, model medium 2 revealed a significant decline of L-cysteine concentration between before and after pH adjustment (Figure 40 E). After preparation, the concentration remained stable at approximately 20% of the expected concentration. The autoxidation of L-cysteine is not only catalyzed by iron[402, 614] or copper[621, 622] but also by other metals as for example cobalt.[292] In the same time, the L-cysteine oxidation can generate thyil or hydroxyl radicals and hydrogen peroxide.[614, 623, 624] Subsequently, it can also be oxidized by hydrogen peroxide or react with other compounds such as pyridoxal.[342, 625] As shown by these many examples of reactions involving L-cysteine, the actual reaction underlying its poor recovery is almost impossible to estimate. An important observation made was the accompanying increase of oxidized L-cysteine dimer L-cystine during preparation (Figure 40 E). The instability of L-cysteine, in combination with the L-cystine concentration increase during media preparation, is a clear indicator for L-cysteine oxidation happening amongst other reactions. It is interesting to note that a minimum of L-cystine concentration was observed on day 2 after filtration. One possible explanation could be that gas diffusion stabilized the pH slightly below 7 (6.7 to 6.8) and this shifted reaction equilibria due to reduced L-cystine solubility.[626] In agreement with Königsberger *et al.* the L-cystine concentration reached a maximum of 800 µM over the following 12 days of storage in CDM which has been determined as maximum soluble concentration in physiologic salt solutions. The L-cystine concentration reaches a maximum after 8 days of storage, followed by concentration decrease over the following 14 days. The fact that the decrease in L-cystine is not accompanied by L-cysteine concentration increase leaves the fate of L-cystine open. One possibility is that it is an intermediate of an entire oxidation cascade and gets further oxidized to cysteine monoxide, cystine dioxide or cysteic acid.[627] Furthermore, L-cystine and also L-cysteine itself participate in metal complex formation.[403, 628] Another possible reaction explaining the decrease of L-cystine is reduction to L-cysteine. Even though reductions are unlikely to happen at ambient air it cannot be excluded due to negative ORP of model medium 2 after preparation (Figure 24). Since the

concentrations measured for L-cystine are very small in comparison to L-cysteine concentration it would be of no consequence on concentration levels of reduced form and would be covered by method variability.

The storage stability analysis with LC-QqQ-MS revealed interesting learnings that should be considered in future media development strategies. For example, media developers could remove pyridoxal and only deliver the B6 vitamin in the more stable pyridoxine form to the cells. Furthermore, the impact of stability issues observed for thiamine and cyanocobalamin on cell culture should be investigated. The results also suggest that the expensive compound L-hydroxyproline does not need to be added to CDM basal powders and the BI proprietary compound supplement II shows excellent stability properties. Finally, the low stability of L-cysteine should draw more attention because it is an essential compound to CHO cell culture and it shows high reactivity with potential accompanying radical formation.

3.3.2 The formation of reaction products during feed medium storage

As shown by the stability issues of a couple of CDM compounds, for knowledge driven stable CDM development it is important to understand the underlying reaction products and mechanisms. In order to investigate and characterize unknown compounds, the standard approach usually would be to start with untargeted analytics. Typical examples are high resolution MS, NMR or 2D fluorescence followed by attempts to isolate the compounds and identify them. However, if suspect compounds are known or can be guessed due to gained knowledge also targeted approaches have high potential to be successful.

Therefore, a literature research with the goal to identify CDM associated reaction products was conducted. As a result, compounds such as lumichrome, N-formylkynurenine, 5-hydroxy-L-tryptophan, DL-O-tyrosine, L-citrulline, DL-methionine sulfoxide, 3-hydroxy-DL-kynurenine, hydroxocobalamin, L-methionine sulfone, L-cysteic acid, L-cysteinsulfinic acid and 3-aminopropionamide were identified as potential degradation products in CDM.[477, 629, 630] Due to the application of the mixed mode chromatography method, these compounds could be easily implemented as analytes in the by then existing LC-QqQ-MS dMRM method. Since degradation product formation is most likely after storage, the model medium 2 samples of day 28 were measured with this reaction product supplemented dMRM method. The comparison of signals measured in CDM to reference standard (Figure 41) displays the qualitative identification of lumichrome, N-formylkynurenin, 5-hydroxy-L-tryptophan, DL-O-tyrosine, L-citrulline and DL-methionine sulfoxide. The comparability of retention time between standard and model medium 2 sample and the molecule specific transitions give high certainty for right positive identification. It is interesting to note that rather low levels of the riboflavin photolysis product lumichrome were detected. This confirms the beneficial effect of light protection during CDM preparation and storage.[308] Riboflavin photosensitized product of tryptophan degradation, N-formylkynurenine, was shown to negatively impact cell culture.[309, 631] The other identified degradation products such as 5-hydroxy-L-tryptophan, DL-O-tyrosine and DL-methionine sulfoxide are described as oxidation products of amino acids. For example, L-citrulline may result from oxidative deamination of L-arginine.[632]

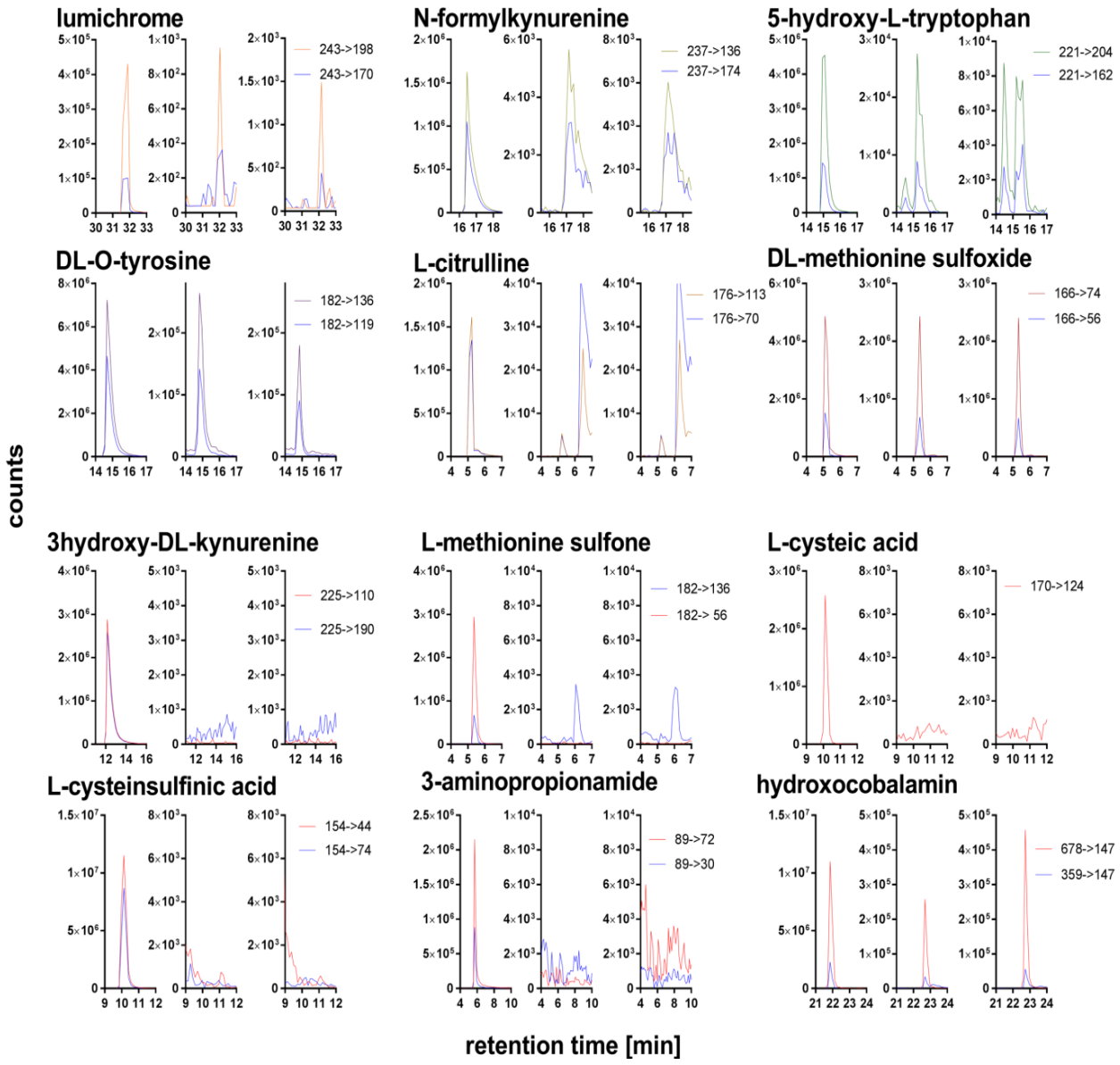

Figure 41: LC-QqQ-MS method supplemented with potential CDM reaction products identified in literature. The three graphs under the compound name show (from left to right) the EIC of standard reference compound, model medium day 28 prepared at 25°C and 40°C. The comparison of extracted ion chromatograms shows the proven compounds (lumichrome to DL-methionine sulfoxide) and the disproved compounds (3-hydroxy-DL-kynurenine to hydroxocobalamin). Since both the precursor ions 678 and 359 *m/z* and the product ion 147 *m/z* are also used for cyanocobalamin quantification, the presence of hydroxocobalamin remains elusive. The fact that cyanocobalamin elutes under normal conditions at 22.7 min and the hydroxocobalamin standard is expected to elute at 22 min further suggests that hydroxocobalamin was not present in stored CDM.

3.3.3 The formation of precipitate over the course of feed medium storage

After the 28-day storage of model medium 2 in plastic and glass containers a certain volume of each vessel was filtered over a filter membrane. A discoloration and clogging of the filters suggested that a precipitate formation occurred in the CDM over time (Figure 42 A). This was a surprising insight as the CDM were visually clear and no solid precipitate could be seen in the liquid. As shown in Figure 42, the membranes with precipitate of CDM prepared at 40 °C were darker in comparison to CDM prepared at lower temperatures. This difference in color perception can either mean the material is of different composition or there is simply more material on the membranes. The same is true for precipitate harvested from glass vessels versus precipitates from Biotainer stored media. As a higher volume was available from Biotainer storage, a bigger volume was filtered over the membranes and therefore the more material could be responsible for the darker color. Figure 42 B shows the results of a weight per volume analysis. The data confirm that higher preparation temperature increased the precipitate formation by quantity. The same trend can be observed for both media stored in glass and in plastic vessels. The fact that precipitate weight by volume measured from glass storage is at the lower border of Biotainer error bars is very likely caused by the mentioned smaller available medium volume. The quantitative data does not give absolute certainty to judge if difference in coloration between the varied preparation temperatures is solely caused by more material or if the composition is also different. Even though the amount precipitated from CDM is low (0.02 to 0.04 g/L) it can still be critical to cell culture robustness. Especially if precipitates form with compounds that are essential for cells and are effective at low concentrations in CDM this can be very unfavorable because it is assumed that non-soluble compounds are not bioavailable to eukaryotic expression systems.

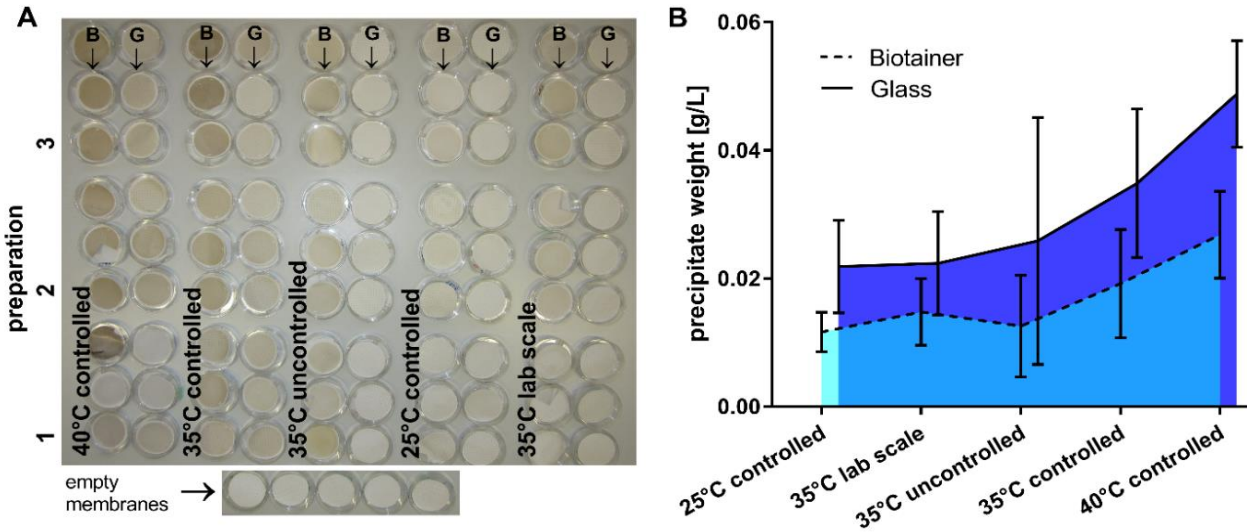

Figure 42: Solid reaction products filtered out of model medium 2 after 28 days of storage. A) 0.2 µm filter membranes with filter cakes after drying in desiccator. The precipitates collected from media prepared at high temperatures showed darker hue compared to preparations at 25°C. B – precipitat from CDM stored in Biotainers; G – precipitate of CDM stored in glass bottles. B) The membranes were scaled and the mass of dried solid per volume of filtered CDM is plotted. An increasing amount of precipitate per volume with high preparation temperature is depicted.

In order to get a better overview and understanding of the occurrence of such an event of precipitation, other CDM were filtered. Interestingly, the color spectrum of different precipitates found in CDM is very broad (See Figure 43). In some of the media the particles could be seen in the liquid. In one instance, the precipitate formation was discovered as a thick particle population in the tubing leading to the bioreactor (Figure 43 A). In other CDM the particles were observed as clouds of solid material floating through the feed medium bags (Figure 43 B, C and E). Another stored CDM showed particles as little white speckles in a plastic Biotainer (Figure 43 D). One

experimental medium preparation in small scale model showed a turbidity right after preparation (Figure 43 F). The most obvious particles found were of glittering appearance and reflected the flash light of the camera (Figure 43 K). In most of the other examples visually no precipitate could be observed (Figure 43 H-L). The presented examples show that even if visually no solid material can be seen in CDM liquid this does not necessarily mean that there is no solid present that is bigger than the 0.2 µm filter membrane pore size. It is interesting to note that the medium shown in Figure 43 A and F was prepared in the same batch but filled into different storage vessels. Medium of Biotainer shown in Figure 43 A was filtered 6 days before medium stored in bag. Thus, the time seems to have a significant impact on the appearance of the precipitate. An impact of storage vessel still cannot be excluded. Additionally, the quantity of solid material recovered per liter medium is very small and thus hard to correctly measure. Weighting on a highly sensitive instrument gave values from the one-digit mg/L area to a maximum of approximately 45 mg/L (Figure 42 B). For some media shown in Figure 43 the amount of precipitate was too small to be assessed due to scale range and lack of replicate. Furthermore, the size of the particle aggregates and the amount seen in the liquids was not predictive of filter clogging behavior. Sometimes, visually completely clear media clogged the filters immediately. Whereas, big visual precipitate did most often not impact filtration performance for a long time. In comparison to the totally dissolved amount of compounds, the masses measured for the precipitates are negligible. However, it must not be forgotten that some compounds are effective and essential for cell culture in trace amounts. If precipitation is an indicator for chemical degradation of essential compounds, the mechanism can still be negative for process robustness or lead to the production of toxic compounds.

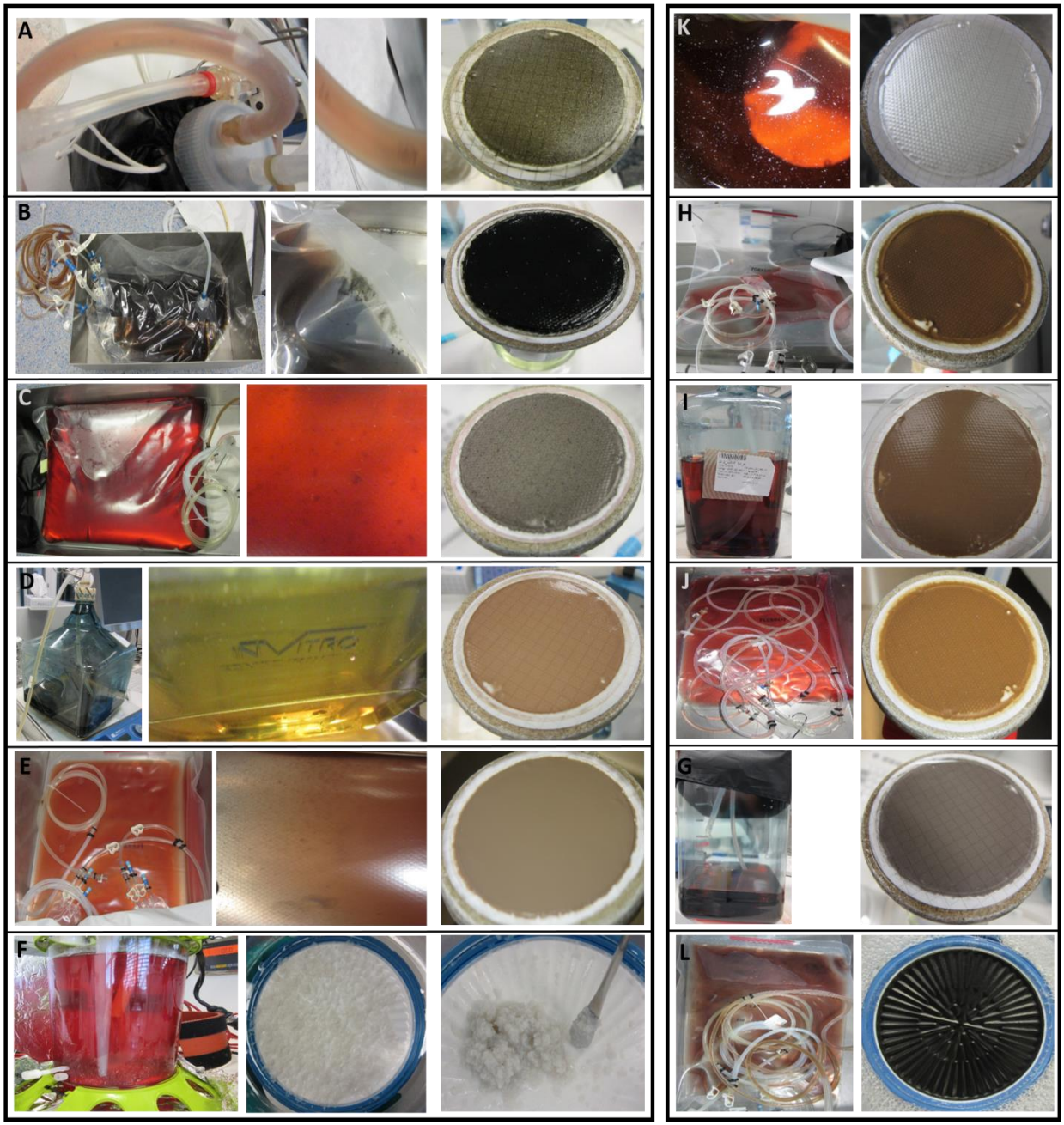

Figure 43: Coloration of precipitates collected from different CDM. All the media shown were filtered over disc filter membranes (0.2 µm, Merck Millipore). An exception were F) and L) where a Stericup filtration system (0.22 µm pore size, capacity 1 L, Merck Millipore) was used. Photographs were taken of the moist filter cake right after filtration and washing with pure water. The variability in color could be caused by either different composition of multi component precipitates or by different identity of pure components.

3.3.4 Identification of precipitate found in feed medium

As precipitate formation could harm cell culture robustness and impacts each filtration process step, an identification of solid material is of high interest for process development. Therefore, a precipitate collected from model medium 2 was analyzed in a first step with Fourier transform infrared spectroscopy (FTIR). The spectra collected from two independent collaborating laboratories look comparable (Figure 44 A and B). Searches against spectra databases showed that the spectra obtained from precipitate material were consistent with proteinaceous material. Since both whey protein and human placenta extract are not used in CDM and contact can be excluded, these data base matches cannot be considered as an identification. Thus, a different protein source must be considered.

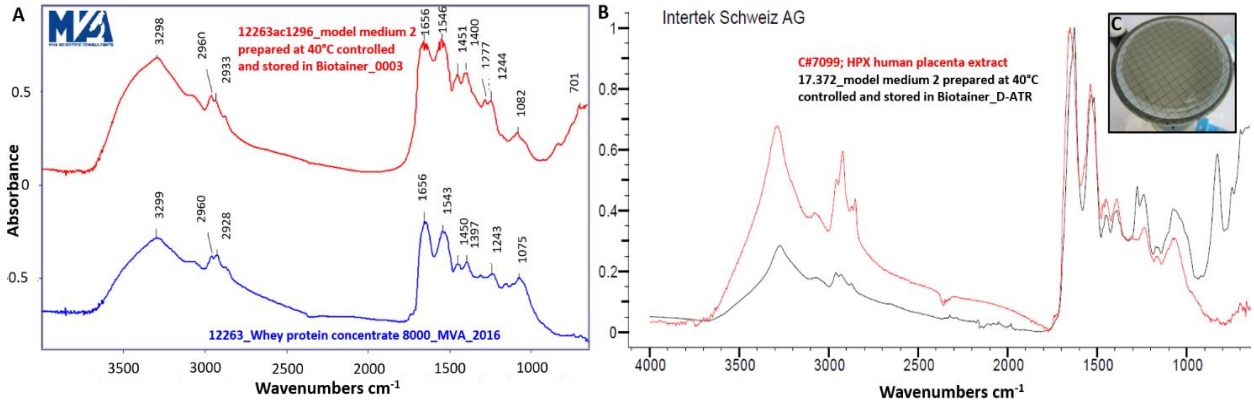

Figure 44: Fourier-transform infrared spectroscopy (FTIR) spectra of precipitate sample and reference Spectra. A) FTIR spectrum of precipitate filtered out of model medium 2 prepared at 40°C and stored in Biotainer (red) and a polyamide extracted from whey reference spectrum (blue) measured at collaborating laboratory 1. B) FTIR spectrum of the same precipitate sample measured at collaborating laboratory 2. The precipitate spectrum is shown in black and the reference protein spectrum (extract from human placenta) is shown in red. C) The picture inlet shows the visual appearance of the filter membrane after collection and purification with water of which identical pieces have been sent to each contract research organization.

A commonly used protein in CHO cell culture is insulin which functions as growth factor in CDM.[443] In the case of insulin, already catalytic amounts of free thiols have been shown to cause concentration dependent irreversible breakdown that is accompanied by disulfide isomerization.[633] The unfolding of insulin increases the vulnerability for thiolates binding metal, as e.g. iron, with high affinity.[269, 634]

In order to further identify the precipitates from model medium 2 an investigation with a Raman microscope has been conducted. Getting a spectrum from the precipitate has generally been difficult because of high fluorescence, little resistance to high laser power, interference of the background and the impossibility to scraping material off the filter membrane due to strong attachment. However, as shown in Figure 45 A, B, C and D spectra of two samples could be obtained. Comparing these spectra with insulin spectra (Compare Figure 45 C and D with E) the local maximum at 2935±5 can be found in all spectra. This Raman shift region is typical for υ(C-H) bonds which are abundant in protein. Another band common in all three spectra is observed at Raman shift 1000 cm^{-1}. This signal is typical for υ(CC) aromatic ring chain vibrations as found for example in phenylalanine. Comparison of precipitate spectra to published insulin Raman spectra or a direct overlay with the insulin reference spectrum could not clearly identify insulin in the precipitate spectra (Figure 45 F and G).[635-639] Comparison of precipitate spectra to features in insulin Zn^{2+} crystals did not reveal more similarity.[640] Even though Raman microscopy could not identify insulin, it is still very likely that it is a constituent of the investigated precipitates. Furthermore, it has to be mentioned that the conformational change that led to precipitation is expected to change Raman spectra and thus comparison to reference powder is difficult.

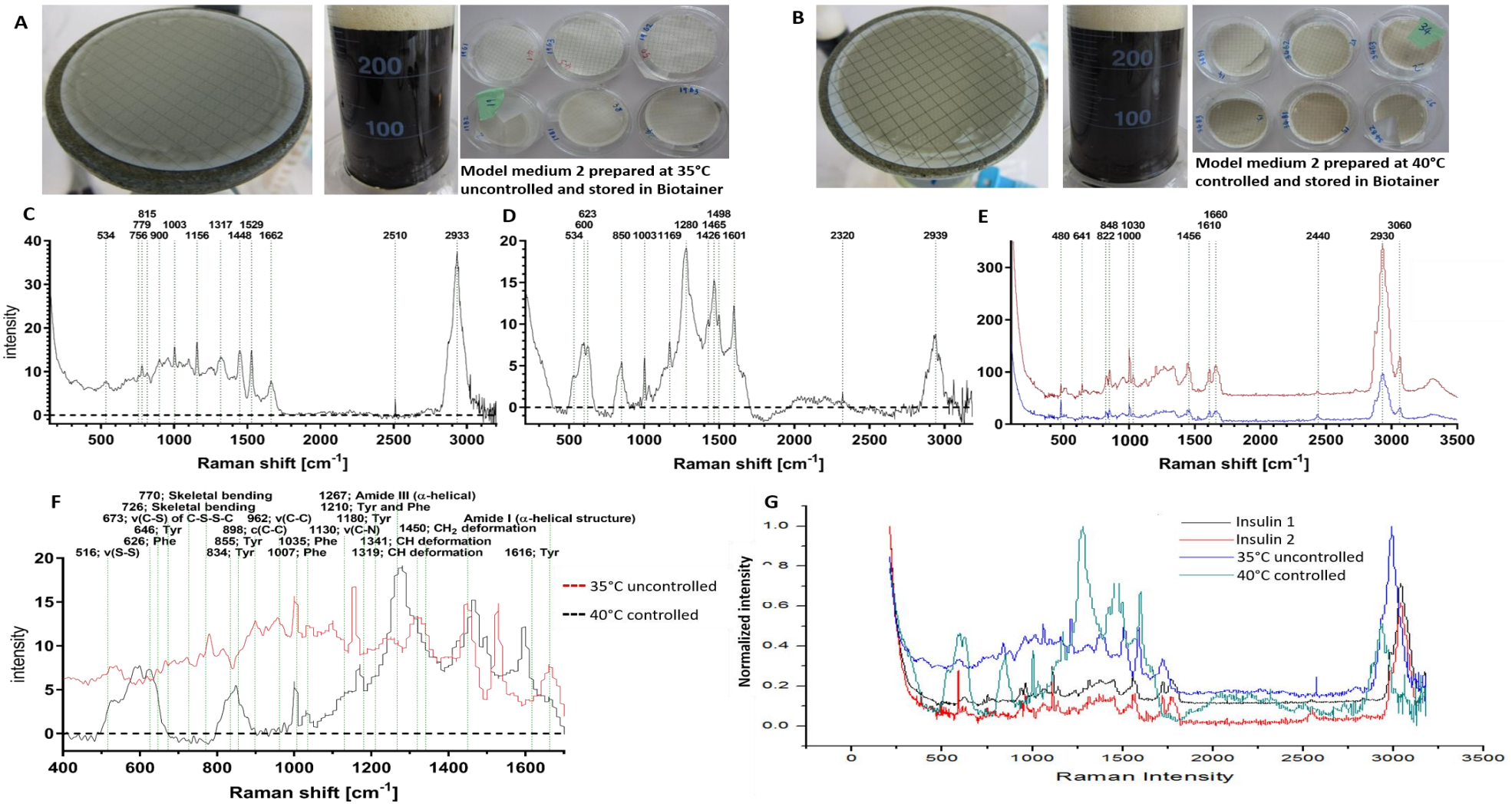

Figure 45: Investigation of precipitates from model medium 2 with Raman microscopy. A) and B) show precipitate right after filtration, the color of CDM after storage and the dried precipitate that was measured with Raman microscopy. C) Raman spectrum of sample shown in B. The local maxima in Raman spectrum are marked with dotted green lines and labelled. D) Raman spectrum of sample shown in A. The local maxima in Raman spectrum are marked with dotted green line and labelled. E) Reference spectra taken from solid insulin of two different vendors that are typically used in CDM development. The local maxima in Raman spectrum are marked with dotted green lines and labelled. F) Comparison of CDM precipitates with assigned Raman spectral features of insulin described in literature.[636] The dotted green lines mark the insulin peaks assigned by Ortiz *et al*. G) Overlay of measured insulin reference spectra and model medium 2 precipitates.

The elemental composition of precipitate measured with SEM-EDX both at a collaborating laboratory and BI internally further confirmed the proteinaceous composition of the material because mainly elements that are typical for protein were found (Figure 46 A, B and C show that sample mainly contains carbon (C), nitrogen (N), oxygen(O) and Sulfur(S)). A detailed analysis with the SEM identified material of different visual aspect in the precipitate on the filter (images in Figure 46 C and D). The EDX spectra in Figure 46 C and D show that the material is mainly composed of magnesium (Mg), silicon (Si) and O. These elements are for example typical for talc which is not soluble in water. The formation of some low abundance talc particles later found as inclusions in precipitate may have initiated the precipitation process of other compounds in CDM. Alternatively, it might have been co-precipitated by other mechanisms leading to the proteinaceous material on the filter membranes.

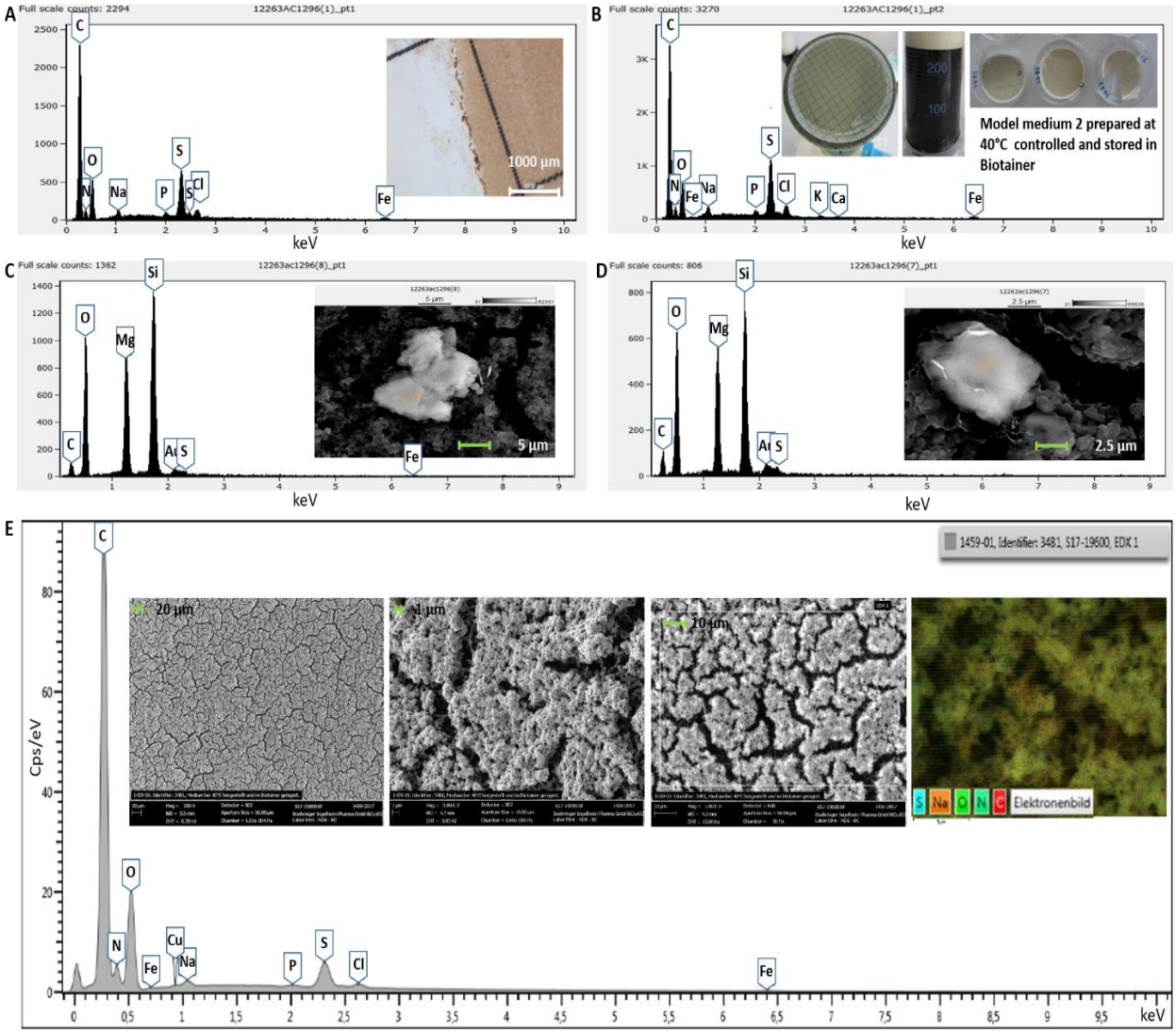

Figure 46: SEM-EDX analysis of model medium 2 precipitate prepared at 40°C and stored in Biotainer. A) and B) show spectra measured by collaborating laboratory 1. The brown precipitate is mainly composed of carbon (C), nitrogen (N), oxygen (O) and Sulfur (S). The elements sodium (Na), phosphorus (P), chlorine (Cl), potassium (K), calcium (Ca) and iron (Fe) were detected with very low intensities. C) and D) show a section of the filter mounted on a carbon tape and coated with gold sputters. Therefore, the signal of gold (Au) and carbon in spectra is very likely caused by sample preparation. The particles found as traces (less than 1% by volume) shown in image inlays (SE detector) were mainly composed of magnesium (Mg), silicon (Si) and oxygen. E) results of internal laboratory confirm the elemental composition. Additionally, high resolution pictures of brown caked precipitate material on filter membrane are shown (SE and AsB detector). The electron image demonstrates the homogeneous distribution of the elements.

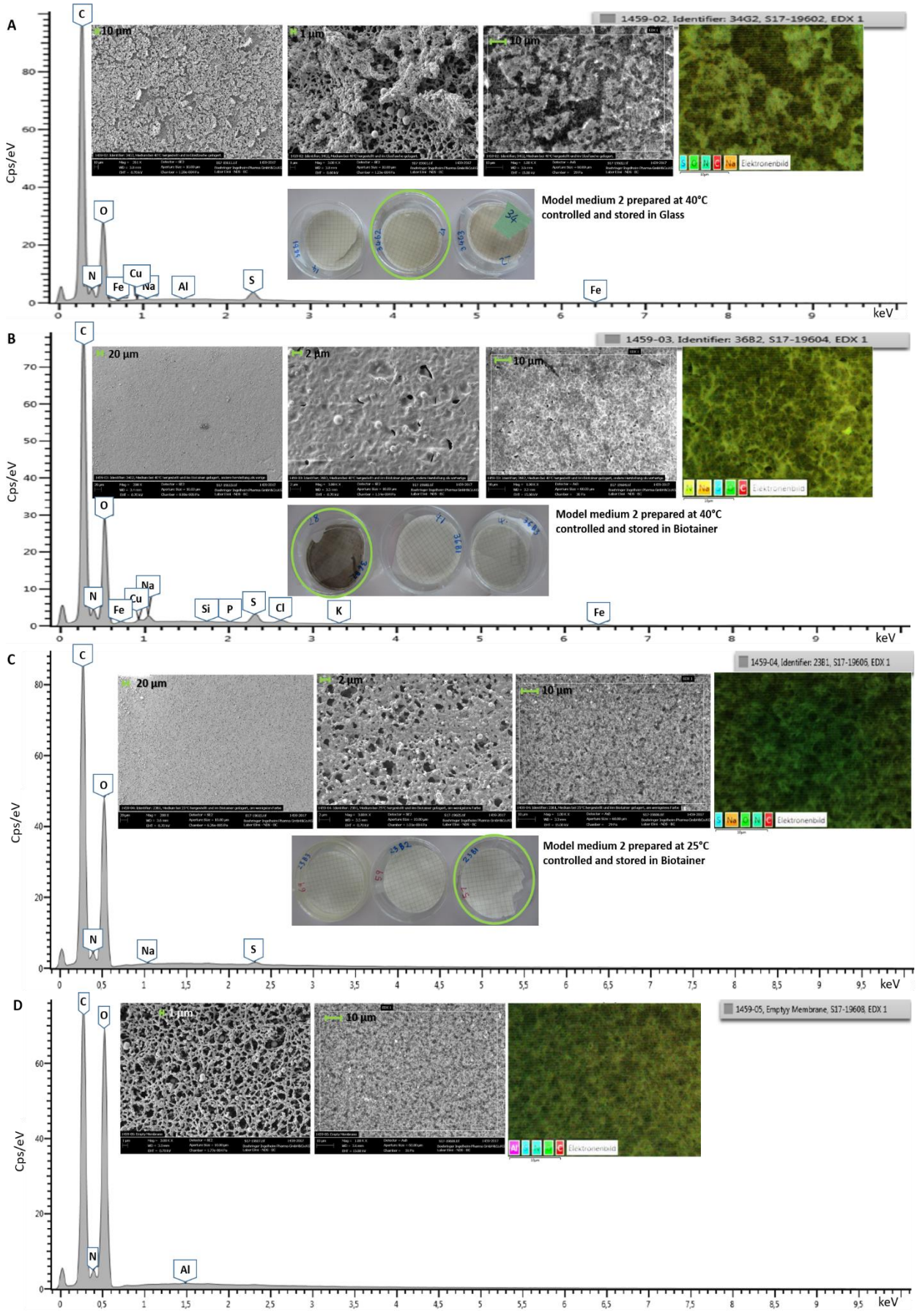

Figure 47: EDX spectra, SEM images (SE detector), electron images (AsB detector) and images of dried precipitates of A) Model medium 2 prepared at 40°C and stored in glass vessel, B) another preparation at 40°C and stored in Biotainer, C) preparation at 25°C and storage in Biotainer and D) empty membrane washed with pure water.

Besides the identity of the precipitate, also the reason for the different appearance with altering preparation temperature or storage vessel was of interest (Figure 42). Therefore, the precipitates of model medium 2 prepared at different temperatures and stored in glass and plastic containers were investigated with SEM-EDX. Figure 47 A shows precipitate of medium prepared at the same conditions but stored in glass vessel instead of plastic (Figure 46 and Figure 47 B and C). The comparison of SEM images shows that the filter membrane of CDM stored in glass vessel is less densely covered. This is expected because less volume was left over in glass vessels and therefore less volume was filtered. The elemental composition of precipitate is basically the same as in Biotainer storage. Figure 47 B shows the results of SEM-EDX analysis of an outstandingly dark precipitate of a preparation at 40°C. The filter membrane is densely covered and the EDX spectrum shows elements not detected in other samples of this experiment (Si, K, Cl). Additionally, the Na peak seems to be higher than in other samples. This could be a hint that additional salts or metal complexes are responsible for the darker color in this precipitate. In contrast, precipitates collected from preparations conducted at 25°C were generally much brighter. However, the SEM-EDX analysis revealed a densely covered filter membrane (Figure 47 C). The elemental composition was much less versatile in comparison to preparations at high temperature. It is of special interest that no metals like iron or copper could be detected. This further underlines that the higher metal content could be responsible for the darker hue of precipitates collected from high temperature preparations. Finally, analysis of an empty filter membrane that was washed with water confirms that only measurements of elements C, N, O and Al can be impacted by filter membrane background.

The brown precipitates extracted from CDM other than model medium 2 were also investigated with Raman spectroscopy. In contrast to model medium 2, three of these CDM spectra showed high similarity to the insulin reference spectra (Figure 48 A, B, C and D). Raman shifts of 2930, 3060, 1610, 1000, 822 and 848 have been identified in all four spectra. The Raman shift of 848 is also present in the reference spectrum of blank membrane and can therefore be accounted to background signal (Figure 62). It is important to mention that the insulin reference spectra were measured of crystalline insulin on aluminum covered slides and not on cellulose membrane. The similarity of spectra is a hint that the conformation of insulin precipitated from media must have remained in a comparable state to raw material. Furthermore, it is interesting to note that the CDM age at the day of filtration was between 11 and 20 days. This confirms that the precipitation not only occurs in very old medium but can already happen during cultivation. To better understand how fast precipitation happens specific kinetics experiments would be necessary. Additionally, these clear insulin identifications in CDM precipitate allow the hypothesis that the protein identified in model medium 2 must have been chemically changed in a way that makes it extremely difficult to obtain useable Raman spectra.

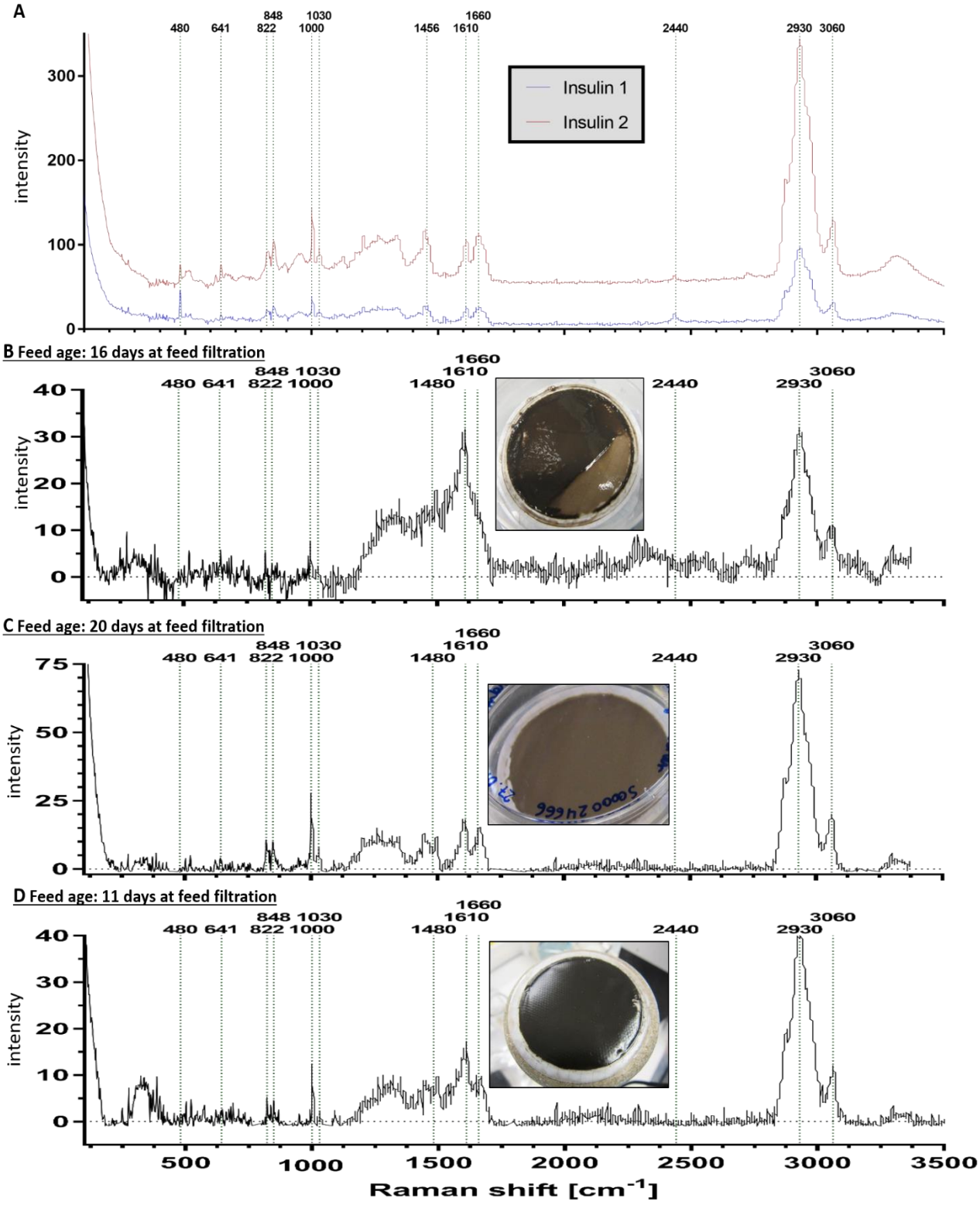

Figure 48: Raman spectra of brownish precipitates. A) Reference spectra taken from solid insulin of two different vendors that are typically used in CDM development. The local maxima in Raman spectrum are marked with dotted green lines and respective labels. B) Raman spectrum of brown precipitate filtered out of 16-day old feed CDM. The local maxima of insulin Raman reference spectra are marked with dotted green lines. C) Raman spectrum of brown precipitate filtered out of 20-day old feed CDM. The local maxima of insulin Raman reference spectra are marked with dotted green lines. D) Raman spectrum of brown precipitate filtered out of 11-day old feed CDM. The local maxima of insulin Raman reference spectra are marked with dotted green lines.

Another brown precipitate has been investigated. At the end of cultivation it has been discovered as small brown flakes in the dark red medium (Figure 49 A). Precipitate with similar appearance has been collected from other preparations (Figure 49 B). The color is very similar, but slight differences in hue are observable. Investigations with the Raman microscope revealed white inclusions (Figure 49 C and D). Comparison of measured Raman spectrum with spectra published by Fran Adar identifies the white crystals as cystine (Figure 49 E).[641] Very typical is the band at 495 cm^{-1} which is originating from the disulfide bond. A more detailed comparison to spectra published in literature confirmed the identity of white crystals as cystine (Figure 49 F).[642] L-cystine is known for its low solubility and is therefore a likely initiator of precipitation mechanisms.[626] Interestingly, cystine has not been found in any of the other precipitates described. This is noteworthy, because due to its low solubility it is usually the first suspect for precipitation in CDM. Additionally, the cystine found in the investigated medium is not the only precipitate composite. SEM-EDX results of precipitate from three different preparations show the versatile elemental composition (Figure 49 G, H, I). The elements C, N, O, Fe, Na, Mg, Al, P, S, Cl, K, Ca and Cu have been identified. The K-series images in Figure 49 H show local inclusions of Ca, Mg, P and Al. This shows that not only cystine is present as local inclusion but also salts can be expected as distinct populations in the precipitate. Thus, this precipitate group is not one distinct chemical compound forming solids but complex mixtures of different chemical origin. The fact that compounds that initiate the precipitation process are almost indiscernible of co-precipitation underlines the complexity of this chemical mechanism.

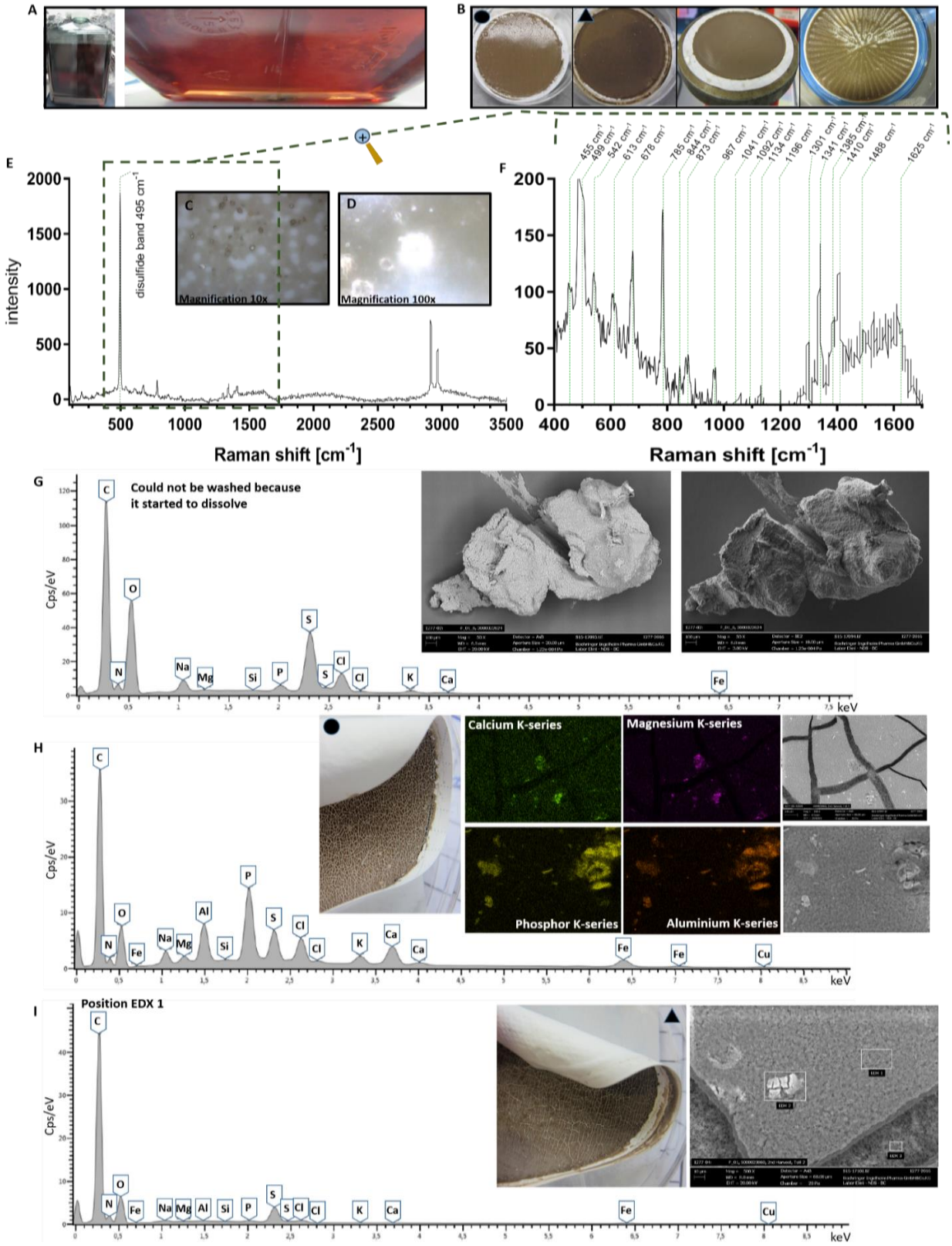

Figure 49: Cystine as ingredient of precipitate identified. A) appearance of CDM at day of precipitate filtration. B) Precipitate of several independent CDM preparations after usage and filtration. C) and D) amplified image of dried precipitate. E) Raman spectrum measured with 532 nm, 1 mW, 50 µm pinhole, no FC. Spectrum was measured on white area shown in D). Comparison of spectrum with Fran Adar identifies compound as cystine.[641] F) Zoom of a specific wavenumber range. Green dotted lines represent the bands described of Guangyong Zhu *et al.*.[642] G) SEM images (SE detector) and EDX spectrum of precipitate scratched off filter membrane. H) Picture of dried precipitate, chosen images of K-series, SEM images of respective location (AsB and SE detector) and EDX spectrum of third brown precipitate. I) Picture of dried precipitate SEM image and EDX spectrum of fourth brown precipitate.

A third population of brown precipitates was isolated from three independently prepared media developed for differing BI projects. The color ranged from bright ochre to dark greyish brown (Inserts in Figure 50 show precipitates after filtration). The Raman spectra of all three samples showed distinct bands at 480, 1426, 1526, 2436 and 2949 cm^{-1}. A spectral database search gave a high match (>99%) of all spectra with yellow iron oxide PY42, which is a pigment used by the painting industry. It is known under historic or marketing names as Dry Ochre, Goethite, Limonite, Antique Dandelion and others.[643] Chemically it is referred to as Fe_2O_3 monohydrate (CAS 51274-00-1). In more common terms, this chemical formula is rust and is expected to originate from ferric iron oxidation in CDM. Strategies to prevent formation of this precipitate could be to reduce iron content, usage of stronger chelators or balancing of redox potential.

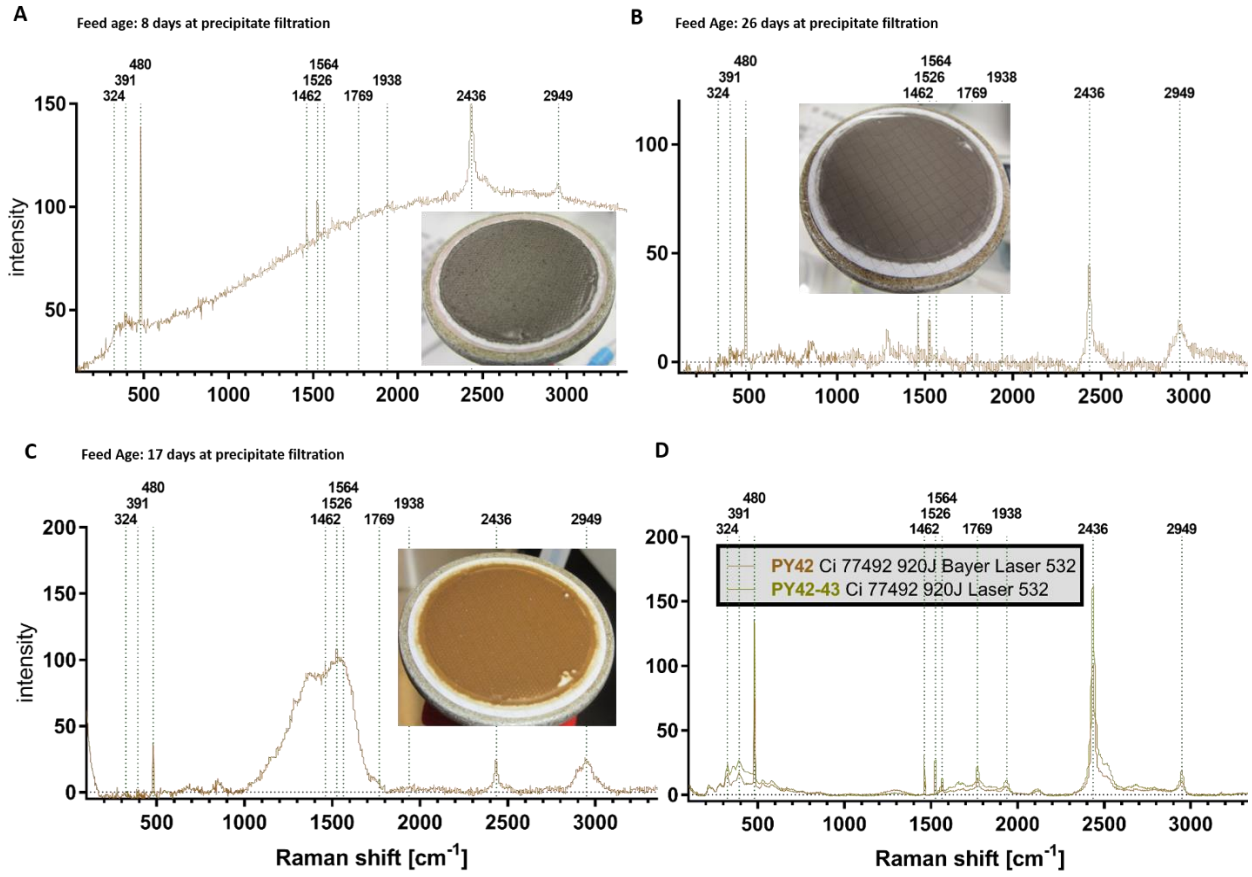

Figure 50: Raman spectra of three precipitates. Local maxima are marked with green dotted lines. The respective Raman bands are labelled on top of each graph. Raman spectra were taken with 0.5 mW laser power, 532 nm wavelength and 50 µm slit width. A) grey-brown precipitate. B) Darker grey-brown precipitate of the same medium recipe as A, but different preparation. C) Ochre colored precipitate of different medium. D) Reference spectra from Thermo Raman library of yellow iron oxide PY42.

Another very interesting population of precipitates is shown in Figure 51. The pitch-black material was observed in three independent media preparations. The solid has been shown to be very fluorescent and absorbing in the same time. Attempts to obtain Raman spectra always ended with burnt material. The only analysis that produced useful spectra was SEM-EDX. The only elements found in all three samples were C, N, O, Fe, Cu, Al and S, whereas some proportion of the signal of C, Cu and Al can come from the sample holder. However, the samples certainly contain significant amounts of C, O, Fe and S.

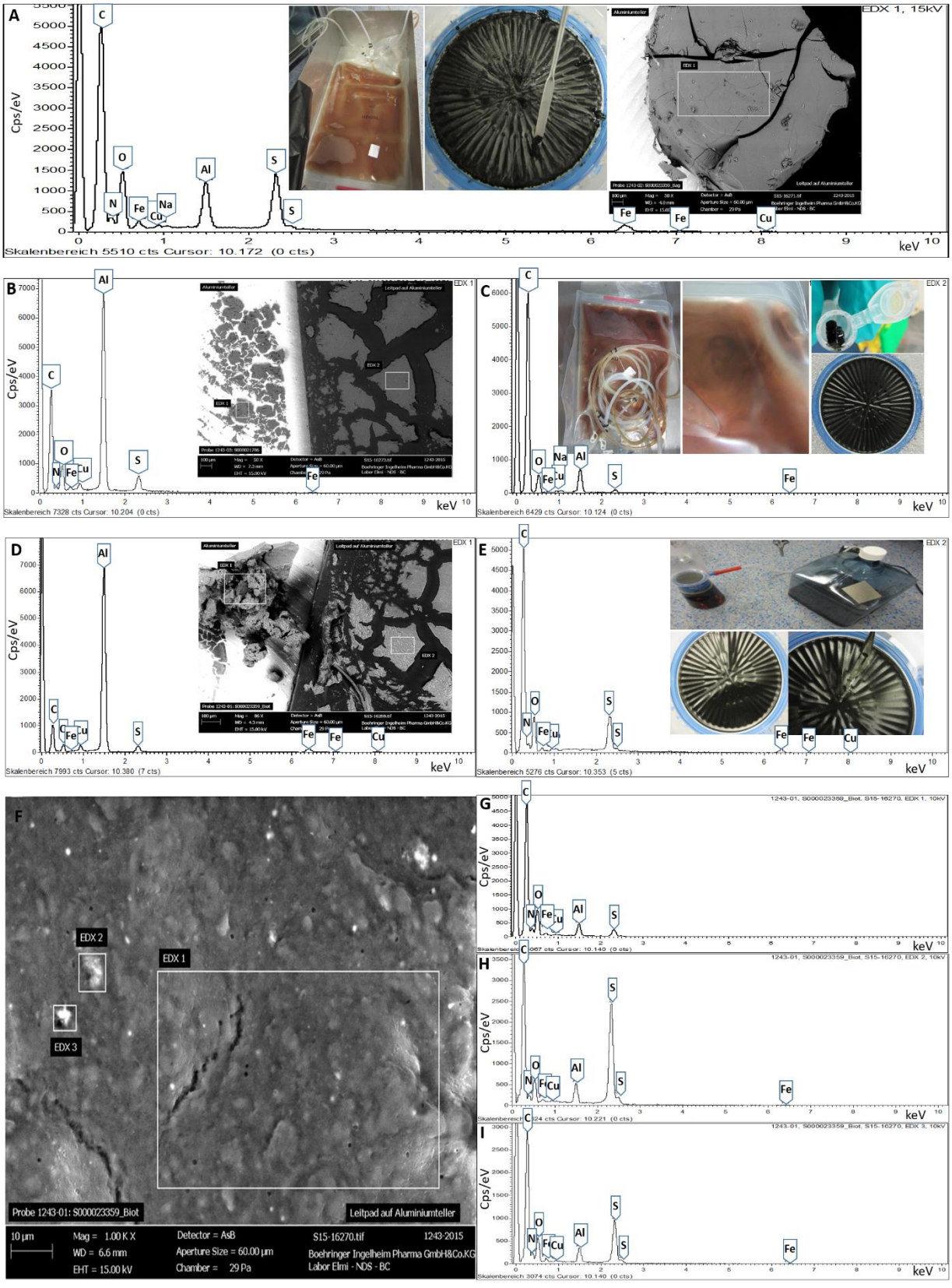

Figure 51: Black precipitate investigations. A) Photo of first liquid medium and washed precipitate at day of filtration, SEM image of sample prepared on aluminum and coal pad and EDX spectrum measured at position EDX1. B) SEM image of sample prepared on aluminum and on coal pad. EDX spectrum is measured at position EDX1 on aluminum background. C) Image of second liquid medium and filtered precipitate on harvest date. EDX spectrum measured at position EDX2 on coal pad. D) SEM image of sample prepared on aluminum and on coal pad. EDX spectrum is measured at position EDX1 on aluminum background. E) Image of third liquid medium and filtered precipitate on harvest date. EDX spectrum measured at position EDX2 on coal pad. F) SEM image (AsB detector) of investigated detail of precipitate of third medium with positions EDX1 to 3. G) to I) The respective EDX spectra of EDX1, EDX2 and EDX3 are shown (Top to bottom).

The visually most outstanding precipitate collected from feed media was discovered as a very fine sediment at the bottom of medium storage bottles (Figure 52 A). Upon shaking, the particles readily suspended and floated as sparkling clouds through the darkened feed medium. The little particles resembled glimmer in a snow globe. The light reflecting property remained after filtration. The filter cakes generated the impression as the filter membranes were covered with pearl-white. In a first attempt to identify the precipitate Raman spectra were taken (Figure 52 B and C). The collection of the Raman spectrum did not present any issue. A spectral data base search gave a surprising result. The highest percentage matches with reference spectra shown in Figure 52 D were Sulfur (99.6%) and iron sulfide (99.56%). This was not expected, because sulfur is known to exhibit bright yellow or any yellowish hue. Similarly, iron sulfide is known to be of dark grey to almost black color. Since the color of precipitate and Raman spectra contradicted each other further analytical techniques were applied. A high-resolution picture taken with electron microscope of the precipitate material showed that the filter cake was constituted of many little needles or platelets (Figure 53 A). If in solution, these approximately 10 µm big particles are responsible for the light reflection and sparkling effect. An EDX spectrum of the material revealed that it was constituted of the elements C, S, O, Na, Al, Si, P and Fe. However, the by far most intense signal was Sulfur (Kα 2.307 keV). The individual pictures of the K-series show that carbon is mainly located on the sample holder but in minimum amounts in the sample itself (Figure 53 B carbon K-series). The bright green coloration of the entire sample in the Sulfur K-series image (Figure 53 B) confirms that the main element present was Sulfur. Furthermore, the material was investigated with another orthogonal method, ICP-OES. Especially for ICP-OES big quantities of material were necessary. Therefore 2 L feed medium were prepared in order to generate as much precipitate as possible. It was possible to extract 115 mg out of the medium (Figure 53 C). The analysis with ICP-OES confirmed the findings of SEM-EDX and Raman that the precipitate was mainly constituted of sulfur (Figure 53 D). The elements Na, Al and Fe found by SEM-EDX could also be detected by ICP-MS. Furthermore, the elements Ca, As, Ba, Ce, Co, Cr, Cu, Mg, Mn, Mo, Ni, Pb, Pd, Sb, Se, Sn, Ti, V, Zn and Zr could be measured. However, most of these compounds were proven to be present in minute amounts only. It is interesting to note that iron was measured by ICP-MS as the highest concentrated impurity in the Sulfur sample. This and other impurities could be responsible for the discoloration of Sulfur and the silver appearance. If the iron sulfide suggested by Raman was the main constituent of the silver precipitate a much higher iron concentration in both SEM-EDX and ICP-MS would have been expected. The reason is that in this mineral iron and Sulfur make up 50% to the crystal lattice each. Thus, it is highly likely that the main compound responsible for silver precipitate formation is elemental Sulfur with metal impurities as confirmed by ICP-OES and ICP-MS.

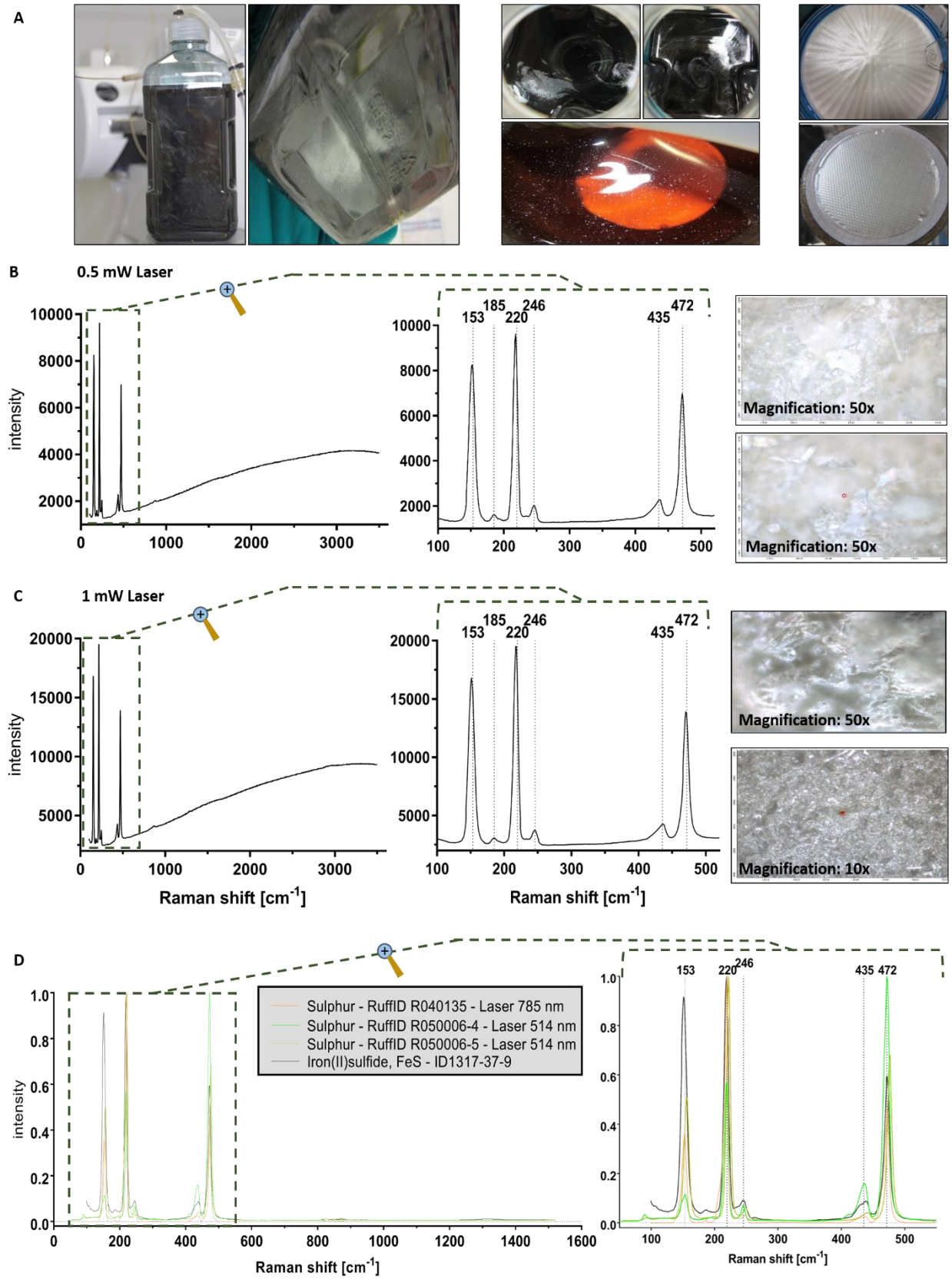

Figure 52: Silver precipitate observed in CDM feed medium and subsequent analysis with Raman microscopy. A) The silver precipitate was discovered at the bottom of medium stored in Biotainer bottles. After shaking, the material floated as silver sparkling clouds through the liquid. The very small sparkling particles were also observable during filtration. After filtration the membranes were covered with a shiny silver layer of precipitate. B) and C) show Raman spectra of samples measured with 532 nm wavelength and 50 µm pinhole, a zoom into the region of interest and microscope images with given magnification. Silver precipitate spectra matched by 99.6% with sulfur and 99.56% with iron sulfide in a search against the Thermo Raman spectral database. D) Reference spectra of different Sulfur samples and an iron sulfide Raman spectrum are shown. The right side shows a magnification of 50 to 550 cm^{-1} Raman shift region.

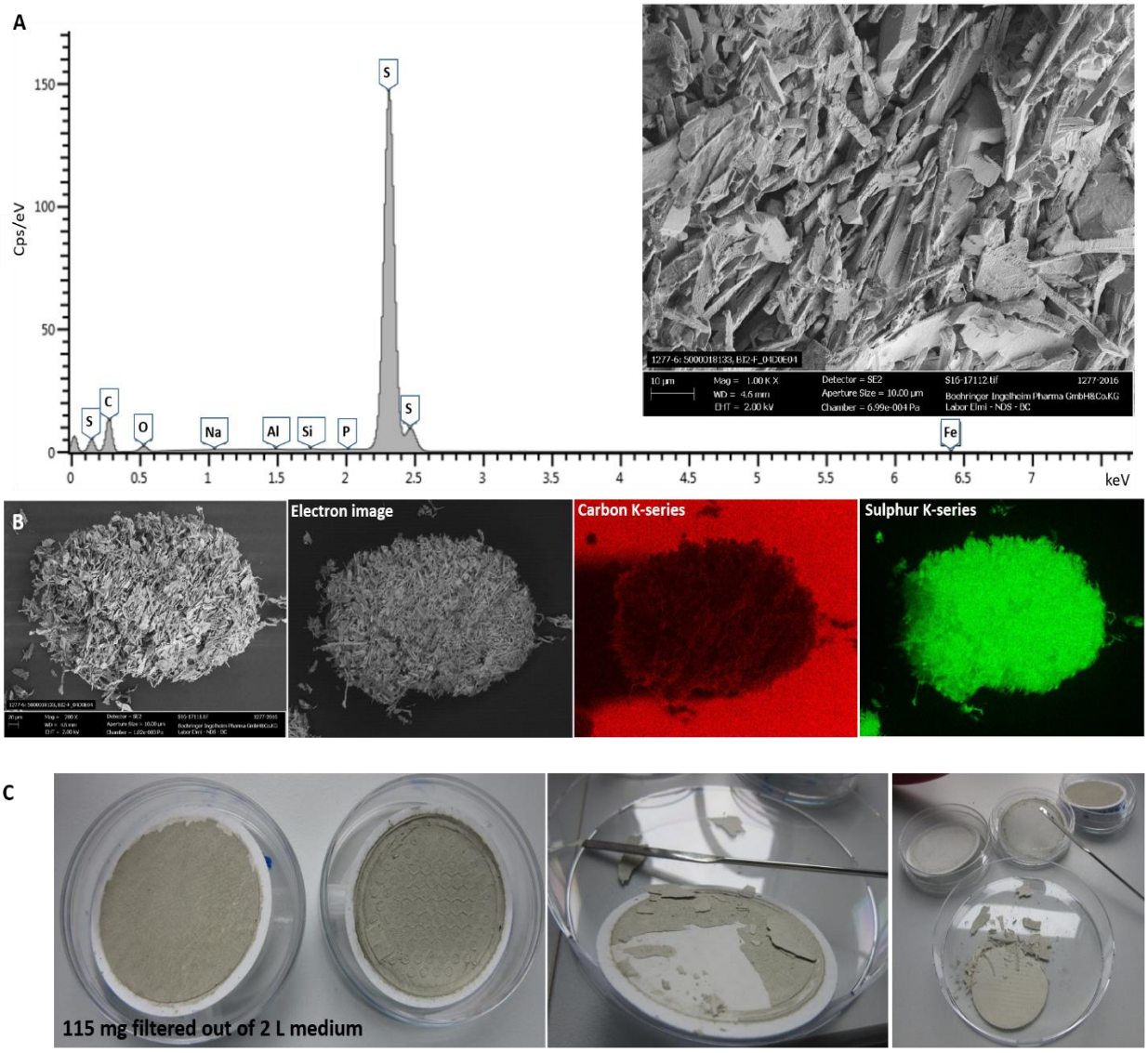

D	Test	Result	Test	Result	Test	Result	Test	Result	Test	Result	Test	Result
	Ca	57 mg/kg	Cd	<0.01 mg/kg	Hg	<0.05 mg/kg	Ni	5.0 mg/kg	Sb	0.02 mg/kg	W	<0.1 mg/kg
	Ag	<0.5 mg/kg	Ce	0.02 mg/kg	Ir	<0.1 mg/kg	Pb	0.28 mg/kg	Se	110 mg/kg	Zn	3.7 mg/kg
	Al	57 mg/kg	Co	0.35 mg/kg	Li	<0.01 mg/kg	Pd	0.01 mg/kg	Sn	0.4 mg/kg	Zr	2.1 mg/kg
	As	0.2 mg/kg	Cr	7.8 mg/kg	Mg	21 mg/kg	Pt	<0.05 mg/kg	Ti	4.3 mg/kg	Na	60 mg/kg
	Au	<0.05 mg/kg	Cs	<0.01 mg/kg	Mn	3.1 mg/kg	Rh	<0.01 mg/kg	Tl	<0.5 mg/kg	P	<125 mg/kg
	B	<0.5 mg/kg	Cu	13 mg/kg	Mo	0.4 mg/kg	Ru	<0.01 mg/kg	V	0.13 mg/kg	S	101% w/w
	Ba	0.5 mg/kg	Fe	381 mg/kg								

Figure 53: Confirmation of sulfur being the main constituent of silver precipitate by SEM-EDX, ICP-MS and ICP-OES. A) high resolution SEM image of silver precipitate and the respective EDX spectrum. B) SEM image of entire investigated particle of silver precipitate and electron image with the K-series pictures of carbon and Sulfur. C) High quantity collection for ICP-OES analysis. A total amount of 115 mg could be filtered out of medium. D) Results of ICP-MS (Elements Ca to Na) and ICP-OES (Elements P and S). Results marked with < were below limit of detection and therefore these elements were assumed to be not detected.

3.3.5 Experiments to elucidate mechanisms of silver precipitate formation.

After the identification of Sulfur as the main constituent of the silver precipitate the question remaining was how elemental Sulfur could get into the CDM or how it could be formed. The compound contributing the most sulfur in the investigated medium due to its high concentration was L-cysteine. Thus, it was the most likely source of the sulfur precipitate. Furthermore, it was the main compound bearing a thiol group making thiol chemistry very likely. Therefore, L-cysteine with radioactively labelled Sulfur-35 was spiked into medium known for silver precipitate formation after preparation. Sulfur-35 is known as a low energy beta emitter which makes it ideal to track the fate of Sulfur and in the same time the external dose hazard to exposed persons is minimal. The graph in Figure 54 A shows the behavior of radioactivity in stored feed medium that was centrifuged after sampling. Visually the first silver sparkles could be observed on day 13. After that sampling day, significant amounts of silver precipitates were observed that could be even seen on the vessel walls after centrifugation. Starting from day 21 the radioactivity in the supernatant started to decline and in the same time the radioactivity in the dissolved precipitate increased. This trend continued approximately to day 39 and seems to have reached a plateau afterwards. In contrast, the control (Figure 54 B) showed the expected behavior of a medium with either no precipitation or no precipitations that include the 35S-L-cysteine. The radioactive Sulfur-35 remained in solution as it was not part of the precipitate observed as little black pellet from day 4.

It is interesting to note that at the end of storage, the total measured radioactivity of precipitate and supernatant sum up to the 91% radioactivity in silver precipitate forming medium (Figure 54 A). As the sample handling was done the exact same way for control and medium generating silver precipitate it is proven that sample handling did not cause any radioactivity loss because the values measured in the beginning and at the end of the control experiment remain constant.

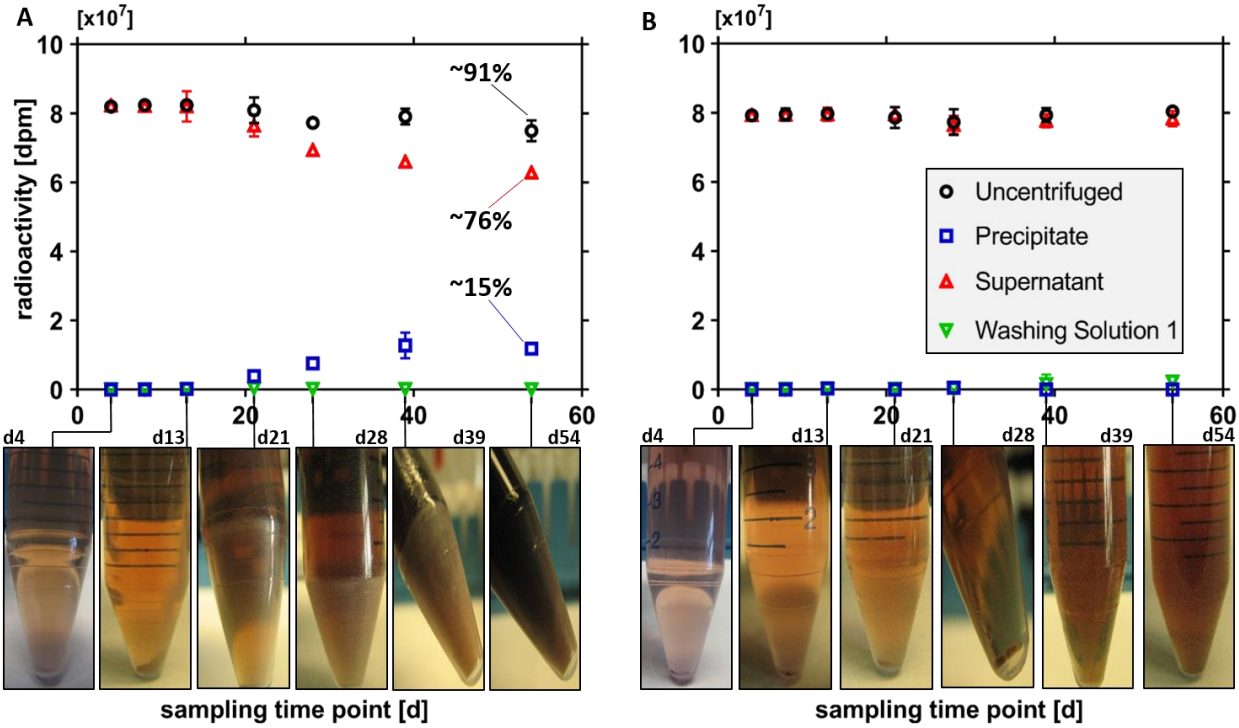

Figure 54: 35S-L-cysteine in CDM stored over prolonged time. The radioactivity was measured over time in the untreated sample (uncentrifuged), in the supernatant after centrifugation, in the washing solution used to wash precipitate after supernatant removal and in the precipitate dissolved in DMSO. All points were calculated out of triplicates. A) Chemically defined feed medium forming silver precipitate: the discoloration of medium over time and silver precipitate layer on vessel wall are illustrated by pictures taken on the respective sampling day. B) Control medium that was not expected to have L-cysteine involved in precipitation mechanism. A brown precipitate has already been observed on day 4 on the bottom of centrifuge vessel.

The observation that total radioactivity summed up at the end of the experiment was not 100% raised the question where the 9% of radioactivity could have been lost. The decrease of radioactivity in uncentrifuged sample starts in the same time when an increase in radioactivity was observed in precipitate (Figure 54 A day 21). Therefore, it may be an accompanying phenomenon to precipitate formation. A possible explanation for the loss of Sulfur-35 would be gas formation and diffusion through the sterile filter. Thus, several lead acetate strips were put into a tubing attached to the exhaust sterile filter of a stored medium. Lead acetate forms black precipitate upon contact with hydrogen sulfide. Surprisingly, the exhaust gases of stored medium under slight overpressure caused the indicator paper to become black already after 1 day (Figure 55). The discoloration of test paper continued slightly over the subsequent storage days but didn´t lead to completely black paper on day 11. This observation confirmed the likelihood that the 9% radioactivity loss in experiment with 35S-L-cysteine can be explained by gas diffusion.

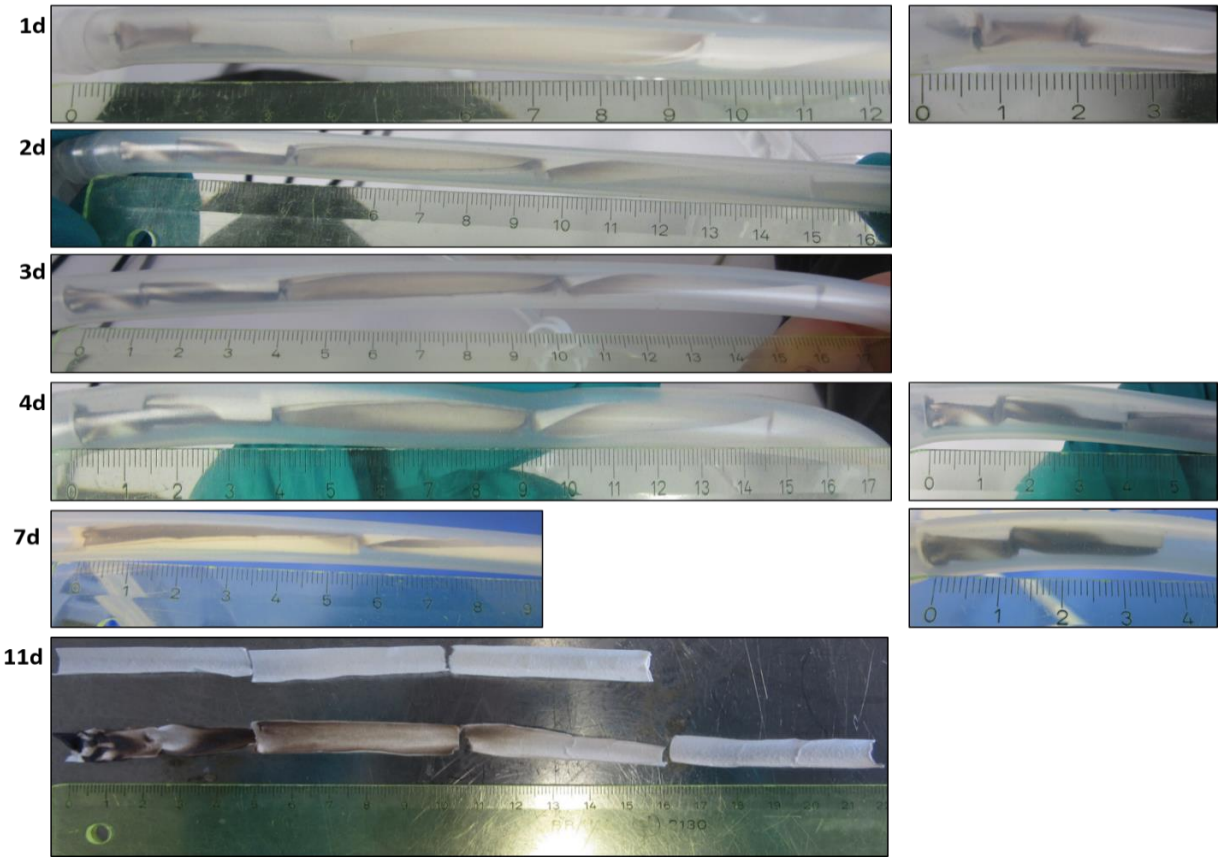

Figure 55: Lead acetate paper in the exhaust tubing of CDM under storage photographed over time (1 day (d), 2d, 3d, 4d, 7d and 11d). Pictures on the right side show magnified pictures of specific areas on the respective day. Experiment was taken down on day 11. Therefore, the indicator paper from the tubing (4 papers on bottom) were compared to unspent control papers (three papers on top).

Currently, H_2S is a topic of active research because it is one of the most recently described gasotransmitters.[644-646] It plays pathophysiological roles in for example anti-inflammation, anti-oxidant, neuromodulation and vasoregulation. Therefore, H_2S donors have been described as compounds interesting for research purposes and as potential drug candidates or pro-drugs. [647, 648] However, besides its physiological roles H_2S gas is well known for its toxic effects by inhalation that can even lead to death.[649, 650] The main mode of action responsible for toxicity is respiratory chain inhibition by HS^-. Hydrogen sulfide ion blocks cytochrome oxidase by binding to ferric iron in the catalytic center. A multitude of enzymatic reaction pathways forming hydrogen sulfide from cysteine in nature have been described. Amongst the organisms described to have H_2S forming enzymatic cascades species of all kingdoms can be found. For example oral bacteria,[651] *Escherichia coli*,[652] *Salmonella* species[653] and sulfate reducing bacteria[654, 655] have been described to produce the gas as a waste product of their catabolism. Furthermore, it has been shown that the enzymatic reactions were reversible and can for example be used to produce isotopically labelled cysteine. [656] Higher kingdoms as fungi, plants and mammals have also been proven to possess H_2S producing enzymatic pathways.[646, 657-659] Due to the widespread distribution of hydrogen sulfide producing mechanisms in the kingdoms of life it is also not surprising that the gas plays a role in a multitude of technologies as for example wine fermentation, dental treatments, pathology and wastewater treatment.[422]

The fact that hydrogen sulfide can be formed of cysteine chemically has already been reported in the early 19th century. However, all these early reports found in an intensive literature search describe experiments that used temperatures at water boiling point. For example, heating of neutralized cysteine hydrochloride solution to 100°C resulted in the decomposition products

cystine, hydrogen sulfide and ammonia.[660] Furthermore, the formation of sulfenic and sulfinic acid was suspected. Interestingly, a similar decomposition study of cystine revealed in addition to cysteine and hydrogen sulfide also elemental sulfur as reaction product. Joseph Routh therefore concluded that there must be two different breakdown mechanisms for cysteine and cystine. Metzler and Snell investigated transamination reactions between pyridoxal and cysteine at 100°C in 0.1 M acetate buffer at pH 5.[343] The standard reaction catalyst used has been aluminum. But it has been shown that ferric iron, ferrous iron and copper were as effective in catalyzing the reaction. The degradation products ammonia and pyruvate have been measured. A hydrogen sulfide formation has been noticed by the characteristic odor. The authors suggested an intermediate Schiff base that is stabilized by complexation with a metal ion (Figure 56). They suggest that a shift of the double bond and α-hydrogen migration could induce the transamination and the splitting out of H_2S.

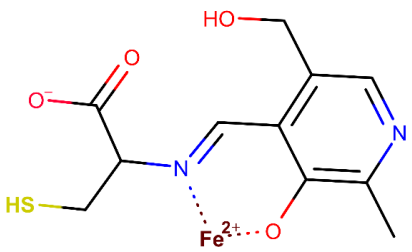

Figure 56: Hypothetical intermediate in hydrogen sulfide forming reaction mechanism from L-cystein and pyridoxal.

Another similar study describes H_2S formation as a consequence to equimolar boiling of glucosamine and cysteine at 100°C.[661] A reductive cleavage of the C-S bond by enaminol that has been formed by Strecker degradation is considered the decisive reaction step in hydrogen sulfide formation from cysteine. Further degradation mechanisms of cysteine have been suggested based on results of radiolysis experiments.[662] These studies have been mainly conducted to compare the off-odor of meat to specific amino acids. The amino acids methionine, cysteine and cystine have been irradiated by electron beam irradiator at 5 g/L in 100 mM citrate phosphate buffer at pH 6. A multitude of volatile degradation products have been identified with headspace GC-MS and H_2S has been discussed as important intermediate being involved in the formation of volatile sulfurous compounds. Dong Uk Ahn *et al.* explained that the cleavage of the $-CH_2$-SH bond can happen either by attack of aqueous electron (e^-_{aq}), hydrogen radical (H•) or hydrogen atom (H^+). Both e^-_{aq} and H• are chemical species mainly known for radiolysis experiments.[663, 664] Since the little plastic bottles used for CDM storage during silver precipitate formation experiments were tightly wrapped with aluminum foil such products typical for irradiation are rather unlikely. Therefore, an attack of hydrogen atom forming H_2S and alanine is much more likely.[665] Experiments with atomic hydrogen generated by electrical discharge with a subsequent transport into aqueous solution containing cysteine have shown that small but well detectable amounts of H_2S have been formed.[666] However, if alanine was formed due to cleavage of H_2S it should be possible to measure a concentration increase in CDM forming silver precipitate. It must also be said that due to the complexity of CDM it is also possible that H_2S forming mechanisms in CDM are more complicated. For example a combination of mechanisms described in Figure 56 and Figure 57 or even more complicated pathways with further CDM compounds involved could be possible.

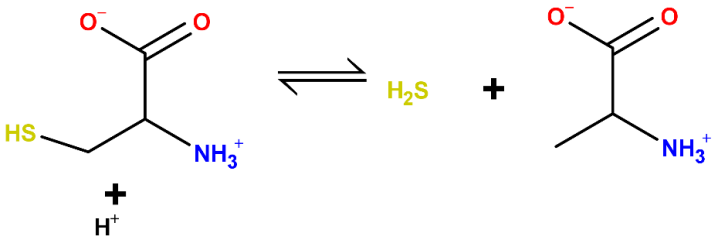

Figure 57: Potential mechanism forming H_2S from cysteine. The hydrogen sulfide is potentially cleaved off by an attack of proton on the thiol group.

In aqueous solution, the equilibria of sulfides is determined by two concentration dependent equilibria reactions:[667]

$$H_2S = H^+ + HS^-; \quad K_1 = \frac{(H^+)(HS^-)}{(H_2S)} \; (Reaction\ 9)$$

$$HS^- = H^+ + S^{2-}; \quad K_2 = \frac{(H^+)(S^{2-})}{(HS^-)} \; (Reaction\ 10)$$

Since stored CDM usually exhibits a pH of 6.8 to 7 the weak acid H_2S with a pk_a value of 6.98 can be expected to be present to approximately 50% in the HS^- form.[645] Since the pk_{a2} value of hydrogen sulfide was described to be 19±2 the likelihood of sulfide anion S^{2-} formation at pH 6.8 can be assumed to be very low. Therefore, some portion of the H_2S formed will presumably diffuse as gas out of the CDM. Kenneth Y. Chen investigated the complex kinetics of aqueous sulfide oxidation by O_2.[667] The investigated reactions have been shown to be kinetically highly dependent on pH and the specific reaction rate has two maxima at approximately pH 8 and 11. He proposed the following reaction pathway for solutions at neutral, slightly acidic or slightly alkaline pH:

$$HS^- + O_2 \leftrightharpoons HS\bullet + O_2^- \; (Reaction\ 11)$$

$$HS\bullet + O_2 \leftrightharpoons HO_2 + S \; (Reaction\ 12)$$

$$HS\bullet + O_2^- \leftrightharpoons S + HO_2^- \; (Reaction\ 13)$$

$$HS^- + (x-1)S \leftrightharpoons H^+ + S_x^{2-}, x\ can\ be\ 2-5 \; (Reaction\ 14)$$

The solubility of elemental sulfur in water is generally very low. Reported values range from $5x10^{-6}$ M to only $1.9(\pm0.6)x10^{-8}$ mole S_8 kg^{-1} for rhombic sulfur.[667, 668] Therefore, some portion of the oxidized sulfur precipitates as elemental sulfur. The mass of the precipitate collected out of 2 L stored medium was calculated as 12% of the sulfur of L-cysteine (Figure 53 C). As mentioned before, quantitative yield of silver precipitate was extremely low. An enormous amount of medium had to be prepared to collect at least 115 mg of precipitate to reduce the measurement error in weighing. Considering these difficulties in quantitative work with this material the calculated value of 12% sulfur found in solid form is well in accordance with the 15% radioactivity measured in silver precipitate (Figure 54 A).

Subsequently, the hydroperoxyl formed in reaction 12 may disproportionate by the following reaction:[669]

$$2HO_2 \leftrightharpoons H_2O_2 + O_2 \ (Reaction\ 15)$$

Furthermore, reaction equilibrium of reaction 16 is far on the right side at approximately neutral pH in CDM.[670]

$$H_2O_2 \leftrightharpoons HO_2^- + H^+ \quad pk_a = 11.6 \ (Reaction\ 16)$$

Up to date, all the CDM forming silver precipitate had the trait that they contained an exceptionally high pyruvate content. Therefore, it is possible that antioxidants such as pyruvate play an important role as radical scavengers to balance reactions in favor of the formation of elemental sulfur (Figure 58). The pyruvate would presumably shift the reaction equilibria of reactions 12 and 13.

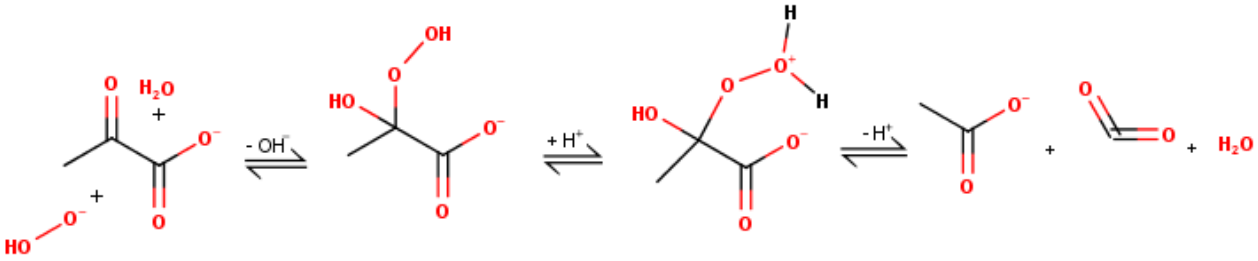

Figure 58: Pyruvate scavenging the hydroperoxide anion.

When no or too little antioxidant like pyruvate is present in the CDM it is possible that the sulfanyl formed in reaction 9 finds a different reaction partner. Iron is highly concentrated in CDM developed for high titer in CHO cell cultivation. The pH and ORP of CDM are usually in a range that Fe^{2+} is predominant during preparation and storage.[671] Even though the iron is usually added in a complexed form to CDM and complexed ferric iron has been shown to be prevented from taking part in redox reaction it is still highly possible that a certain amount of iron is present as Fe^{2+}.[413] Therefore, a hypothetical reaction occurring in the absence of radical scavenger is the following described by Harmandas *et al.*:

$$Fe^{2+} + HS^- \leftrightharpoons FeS + H^+ \ (Reaction\ 17)$$

The investigation of silver medium precipitate revealed a new reaction mechanism in CDM. It emphasizes the complicated and versatile chemistry of L-cysteine in the medium matrix and improves understanding of conditions that lead to instability. This will benefit media development in the future by providing L-cysteine in a stable and bioavailable form.

5 Summary

5.1 Concluding remarks

The versatile results discussed in this thesis range from development and implementation of analytics suitable for CDM to detailed investigations of distinct chemical behavior. Thus, the most important learnings from the characterization of chemically defined cell culture medium for the cultivation of CHO cells are summarized in the following section.

Method development for the quantification of CDM compounds

At the time this work has been started reports about methods describing monitoring tools for CDM were very limited. Indeed, up to date the only parameters measured upon CDM preparation to indicate quality and reproducibility at Boehringer Ingelheim are pH and osmolality. Considering the high risk that bad quality media bears to harm cell culture performance and the high investment costs of 1 to 3 million € per fed batch run at the 18000 L scale the efforts to improve CDM understanding and preparation robustness are obvious.

The superior specificity and sensitivity of LC-QqQ-MS dMRM triple quadrupole technology makes it ideal for CDM compound quantification. The method developed has been validated for 37 important CDM compounds. For most of the media recipes this is approximately 50% of recipe positions. Considering the versatility of CDM compounds in their chemical nature this is already a very high coverage that gives insight into the chemical behavior of the nutrient solutions. The applicability of the developed method for samples drawn during CDM preparation or storage has been demonstrated. Furthermore, the mixed mode chromatography has the advantage to retain both small polar compounds and also larger molecules with a more hydrophobic character. Therefore, it can be easily supplemented at any time with additional compounds of interest. This makes the method highly flexible for running media development or trouble shooting activities. Additionally, it could be used to prove 6 CDM related reaction products that are of interest to estimate the grade of oxidation in future process development.

Analytical on-line technologies and chemical reactions during CDM preparation

In routine 18000 L production volume cultivation the preparation tanks are made of stainless steel and already simple questions during powder hydration like when is the powder dissolved and when can the subsequent compound be added are difficult to estimate. Therefore, in future process development with a strong focus on robustness a good and reliable on-line monitoring tool giving information about complete powder dissolution of each compound and batch comparability will be indispensable. In the course of this thesis pH, ORP, DO, conductivity and FBRM on-line probes have been used for chemical characterization of CDM during preparation. All the technologies investigated revealed their strengths and weaknesses for medium preparation monitoring and none of these has been found to fulfill all expectations. The experiment described in chapter *3.2.2 Chemical stability during medium preparation – comparison of univariate sensor signals with chemical compound concentration* shows that major chemical differences of basal powder composition could be detected by ORP, DO, pH and conductivity. However, process variation like different preparation temperatures in 5°C steps were not detected in the specific experimental condition by FBRM. This indicates that the dissolution behavior of the measured particle population is robust. If FBRM technology is applied in medium recipes with conditions throughout preparation that allow the compounds to dissolve right after addition the readout gives an estimation when solids break down to particles ≥1 µm and when the next compound may be added. Even though the principle of directly measuring particles is ideal to

estimate the state of compound dissolution the FBRM technology is limited by its lower limit of detection range. Additionally, it is sensitive on incident flow angle, mounting position in the tank and the kind of powder addition. In order to characterize a newly developed CDM recipe a preferably complete set of probes is recommended as each measurement principle allows conclusions on different chemical parameters. For a routine batch to batch comparability monitoring tool, for example after process transfer to manufacturing scale, conductivity is the most suitable of the sensors evaluated in this thesis. The reasons are it shows fast reaction to most of the CDM compound additions and is simple and robust to handle.

The value of characterizing many chemical parameters during medium preparation has been emphasized by the discovery of a tremendously oxygen consuming chemical reaction in CDM upon iron addition. Each unknown chemical reaction is not under control because the impact of educts and products on cell culture robustness cannot be assessed and the risk for process robustness is difficult to estimate. Even though to date it is not realistic to characterize each single chemical reaction taking place in a complex multi component mixture like CDM, at least the major reactions with such outstanding traits should be investigated in more detail. The approach with simplified basal powder mixtures enabled to limit the compounds responsible for the oxygen consumption upon iron addition. This example underlines that simplified basal powders or grouping of chemical compounds can be promising to either conclude on chemical reactions occurring in CDM or to decrease reactivity during preparation and storage. Due to this strategy the oxygen consuming reaction upon iron addition to basal powder could be restricted to an oxidation of ascorbic acid that is very likely accelerated by phosphate. The presumably emerging radicals could be scavenged by compounds such as pyruvate. Furthermore, the investigation of metal free basal powders showed that further oxygen consuming reaction mechanisms upon pH adjustment were present in CDM.

The study of simplified basal powders during preparation further revealed that the chemical composition of CDM impacts key chemical parameters as pH, redox potential, dissolved oxygen and conductivity. The application of the dMRM method developed showed that compounds like L-cystine reacted with a concentration increase upon iron addition. Others like thiamine, vitamin B6 and L-cysteine were either matrix dependent in MS measurement or had an impacted stability profile. Another interesting observation was the effect of glucose addition on L-2-aminobutyric acid concentration. The concentration decrease upon glucose addition suggests that the expected glycation reactions are happening in CDM.

A further major concern in present day CDM preparation, especially in large scale, is the control of preparation temperature. Since currently used manufacturing plants are equipped with medium preparation tanks made of stainless-steel without temperature control option the controllability of preparation temperature will remain limited in the future 10 to 20 years. Therefore, understanding the impact of CDM hydration temperature on chemical composition is of high interest. The results of a chemical composition investigation of media prepared at different temperatures clearly shows that this critical parameter does not alter CDM composition. Thus, an impact of preparation temperature in a range from 25 to 40°C on cell culture robustness is highly unlikely. In improbable events of process deviations this finding helps to specify trouble shooting activities.

The versatile results of CDM behavior during preparation emphasize the chemical complexity of CDM. This underlines the need to investigate chemical balances in complex mixtures to better understand the key raw material of bioprocesses.

Chemical characterization of CDM during and after storage

As modern cell culture facilities are filled to capacity they are run with high efficiencies and minimized warehousing of hydrated CDM. However, in order to increase flexibility it is still inevitable to store the liquid formulations for some time. Even though the standard storage temperature for liquid medium is 2-8°C a prolonged exposure to room temperature for example during cell cultivation in fed-batch processes is typical. Therefore, cell culture medium characterization experiments were conducted in liquid feed medium at room temperature.

The regular sampling of feed medium during storage showed that the concentrations of measured CDM compounds were not impacted of the storage vessel materials glass and plastic. The independence of vessel material is of great importance during process development where different scale cultivations require different format storage vessels. Another important observation was that in particular L-cysteine, L-proline, vitamin B6, thiamine and cyanocobalamin were unstable during medium preparation and storage. These findings bring a better understanding of the maturation of CDM and show that these compounds should be in focus during future media development. For example, oxidation products like L-hydroxyproline could be completely removed from basal powders. Vitamin B6 could be added in the stable pyridoxine form only and cyanocobalamin and thiamine should be tested if they are really essential for CHO cells. Furthermore, L-cysteine should be investigated for more stable derivatives or if a balance could be found with antioxidant compounds. The investigation of reaction products identified in literature proved the 6 oxidation products lumichrome, N-formylkynurenine, 5-hydroxy-L-tryptophan, DL-O-tyrosine, L-citrulline and DL-methionine sulfoxide being formed during medium storage. Knowledge about reaction products allows investigations for their impact on cell culture. The example of lumichrome as an oxidation product of tryptophan that harms cell culture performance clearly shows the importance to understand reaction mechanisms in CDM.[309] Understanding the impact of reaction products is important to understand effects that are negative for cell culture. But in the same time there could be degradation products that are beneficial and positively impact medium development. If such cases exist, they would be as interesting for cell culture engineers.

Another phenomenon happening during cell culture media storage is the formation of solid precipitates. Understanding the identity of these precipitates and the underlying reaction mechanisms will further benefit the chemical understanding of CDM. The industry will especially benefit from this if the mechanisms that form precipitates in CDM are so deeply understood that they and the subsequent blockage of filters and loss of nutrients can be avoided. A first step in that endeavor is the establishment of suitable analytical tools. Over the course of this thesis FTIR, Raman microscopy, SEM-EDX, ICP-MS and ICP-OES have been found to be suitable tools to gain information. However, special care has to be taken on sample preparation and handling. By application of these tools proteinaceous material could be identified in a multitude of solid precipitates. Raman spectra of some of these precipitates could be clearly matched to insulin. Another distinct identification of precipitate forming material was iron oxide. Furthermore, a silver precipitate could be identified as elemental sulfur with three orthogonal methods. This undoubtable precipitate identification with ICP-OES, SEM-EDX and Raman spectroscopy allowed to postulate a potential reaction mechanism responsible for silver precipitate formation.

5.2 Outlook

The presented experiments and the analytics applied on CDM topics reveal a detailed understanding of chemical processes happening during preparation and storage. However, CDM compositions are highly complex, recipes are very versatile and storage conditions can vary between processes. Therefore, key points for the most interesting follow up experiments are listed.

Reaction product characterization:

- Application of high resolution non-targeted mass spectrometry analytics with advanced statistical approaches and a very big data base. The MS-detector would be preferably run in MS^n multiple stage mode to allow for a potential compound identification based on fragment ion spectra. For unknown compound identification ideally the comparison of aged with directly after preparation frozen CDM should be strived to.
- In the case the comparison of aged and non-aged media samples reveals significant differences and a database search does not give a suggestion for chemical identity a preparative chromatography isolating and enriching the compound of interest could be promising. The enriched compound could then be further analyzed with Raman, fluorescence spectroscopy, NMR spectroscopy or other tools. Furthermore, fractionated reaction products would allow for testing effects on cell culture.
- The addition of more hypothetical reaction products to the LC-MS method developed for this thesis would improve the chemical understanding of CDM. Examples are glycation products of amino acids and other compounds capable of Schiff base formation, more B6 degradation products, oxidation and reduction products of L-cystine and L-cysteine and thiamine degradation products. In order to supplement literature-based compound identification a full scan MS approach with high specificity followed by supplementation to the targeted MRM MS could be promising. If reaction products found by this approach could be fully identified and if reference compound would be available this would be even better.
- Completion of cell culture medium precipitate data base with Raman spectra (Identity), ICP-MS results (metal impurities), redox potential of precipitated media, compound concentration in recipe and amount precipitate per volume medium. Draw further conclusions out of data base which factors impact precipitation. The possibility to draw conclusions on instability inducing mechanisms will improve media development options.
- Investigation of precipitate formation kinetics. Application of alternative analytics like dynamic light scattering (DLS) or nanoparticle tracking analysis (NTA). If precipitate formation is very fast (within minutes during or after preparation) the medium should be developed further to prevent sterile filter blockage.
- The precipitates isolated at the end of feed medium storage time partially possess highly filter blocking properties. Therefore, investigations about the fate of precipitate during cultivation and harvest would be of interest. If the precipitate gets removed by centrifugation together with cells and cellular debris no impact on harvest performance should be expected. However, if precipitate particles are too small to get removed, blockages of depth filters and in final filters must be feared.
- All the experiments presented in this thesis have been performed with feed media. Mainly because they have a higher likelihood to degrade due to high compound concentrations and prolonged storage time. But with the knowledge of potential mechanisms the production media should also be investigated for chemical stability.

Medium development:

- Monitoring of preparations with presented on-line probes should be followed up, at least once before transfer to production plant. Additionally, more tools like on-line fluorescence probes or NMR probes should be investigated to find a suitable on-line monitoring tool.
- Usage of the silver precipitate forming medium recipe to screen for scavengers and antioxidants that avoid sulfur formation. Monitor compounds with developed dMRM method and high resolution non-targeted approaches.
- Removal of unnecessary compounds such as L-hydroxyproline. Investigation of the role of L-glutathione in CDM (increased and removed). Removal of pyridoxal and only usage of more stable form pyridoxine.
- Take media known for iron oxide formation and test if decreasing the iron salt concentration prevents precipitation.

6 Material and Methods

6.1 Chemicals, reagents and equipment

The material used in this thesis is listed in the following tables. Chemicals and reagents are listed in Table 9, the consumables used in everyday work are listed in Table 10, the instruments used for analytic work are listed in Table 11 and the programs used for data pre-processing and statistical analysis are listed in Table 12.

Table 9: Chemicals and Reagents

Chemicals and reagents	Manufacturer
L-arginine HCl, L-asparagine monohydrate, L-aspartic acid, L-isoleucine, L-leucine, L-lysine HCl, L-methionine, L-phenylalanine, L-threonine, L-tryptophan and L-valine	Kyowa Hakko Europe GmbH, Düsseldorf, Germany
L-histidine HCl monohydrate and L-cysteine HCl monohydrate	SA Ajinomonto OmniChem NV, Tokio, Japan
L-proline, taurine, L-cystine, L-ornithine HCl and L-serine and L-hydroxyproline, cyanocobalamin, calcium pantothenate, pyridoxal HCl, pyridoxine HCl, pyridoxamine, biotin, riboflavin, thiamine HCl, nicotinamide, myo-inositol, L-2-aminobutyric acid, L-glutathione, 4-aminobenzoic acid, 1,4-diaminobutane 2 HCl, 7,8-dimethylalloxazine (Lumichrome), 3-hydroxy-DL-kynurenine, DL-methionine sulfoxide, 5-hydroxy-L-tryptophan and L-cysteinesulfinic acid monohydrate, Cell Free Amino Acid Mixture 13C, 15N and di-β-alanine-13C6,15N2 calcium salt, ammonium formate	Sigma Life Science, St. Louis, USA
L-citrulline and L-cysteic acid	TCI Deutschland GmbH, Eschborn, Germany
3-aminopropanamide	ChemBridge Corp., San Diego, USA
L-methionine sulfone and DL-o-tyrosine	Lancaster, Lancashire, UK
hydroxocobalamin	Bosche Scientific, New Brunswick, USA
N-formylkynurenine	Oxchem corporation, Illinois, USA
CDM basal powder	SAFC, Sigma Aldrich. St. Louis. USA
LC/MS grade methanol, water and formic acid	Fluka, Sigma Aldric, St. Louis, USA
Sodium hydroxide solution	BMH Chemikalienhandel GmbH, Ostrach, Germany
Cysteine, L [35S], $HSCH_2CH(NH_2)COOH$; M.W.: 121.2; Specific activity 1075 Ci/mmol	American Radiolabeled Chemicals Inc., St Louis, USA

Table 10: Consumables

Consumable	Manufacturer
2 mL / 1.5 mL Eppendorf® Safe-Lock Tubes	Eppendorf AG, Hamburg, Germany
10 / 20 / 100 / 200 / 1000 µL Eppendorf epT.I.P.S	Eppendorf AG, Hamburg, Germany
1-10 mL Eppendorf epT.I.P.S	Eppendorf AG, Hamburg, Germany
15 / 50 mL Falcon™ conical centrifuge tube	Thermo Fisher Scientific, Waltham, Massachusetts, USA
EZ-Pak ® Membrane Filter (Mixed Cellulose Esters filter, Sterile; White gridded; 47 mm; 0.45 µm)	Merck Millipore, Merck KGaA, Darmstadt, Germany
Cell Culture Dish w/2mm Grid 430196; 60 mm x 15 mm Style; Tissue Culture Treated, Polystyrene; Nanopyrogenic, Sterile	Corning Inc., Corning, New York, USA
2 mL crimp top white glass vials with insert	Agilent technologies Inc., Santa Clara, California, USA
11 mm blue PTFE caps with red rubber septa	Agilent technologies Inc., Santa Clara, California, USA
125 mL and 1 L Nalgene™ Polycarbonate Biotainers™	Thermo Fisher Scientific, Waltham, Massachusetts, USA
250 mL glass bottles	DURAN group GmbH, Wertheim, Germany
Scherzo SM-C18 150 x 2 mm, 3 µm particle size	Imtakt USA, Philadelphia, Pennsylvania, USA
Millipack 60 or 100 with 0.03 m2 and 0.05 m2 respectively, Durapore PVDF-membrane with 0.1 µm pore size	Merck Millipore, Merck KGaA, Darmstadt, Germany

Table 11: Instruments

Instrument	Manufacturer
Mobius® 3-L Single-use Bioreactor	Merck Millipore, Merck KGaA, Darmstadt, Germany
ME 5-OCE scale	Sartorius AG, Göttingen, Germany
Micro scale MC1	Sartorius AG, Göttingen, Germany
DO probe Visiferm 225 mm	Hamilton Messtechnik GmbH, Höchst, Germany
pH probe Easyferm plus Arc 120	Hamilton Messtechnik GmbH, Höchst, Germany
Conductivity probe Conducell 4USF Arc PG 120	Hamilton Messtechnik GmbH, Höchst, Germany
ORP probe EasyFerm plus Arc 120	Hamilton Messtechnik GmbH, Höchst, Germany
FBRM probe ParticleTrack™ D600L	Mettler-Toledo Inc., Columbus, Ohio, USA

Instrument	Manufacturer
6410 triple quadrupole MS with ESI source	Agilent technologies Inc., Santa Clara, California, USA
1260 series binary HPLC system	Agilent technologies Inc., Santa Clara, California, USA
Scanning electron microscope SUPRA 55 VP	Zeiss Microscopy GmbH, Oberkochen, Germany
Energy dispersive x-ray spectrometer N-Max 80 EDX	Oxford Instruments, High Wycombe, England
JEOL JSM-6490LV SEM coupled to a Noran System 7 (MVA scientific consultants)	Thermo Fisher Scientific, Waltham, Massachusetts, USA
Varian 3100 FT-IR spectrometer	Varian Inc. Nowadays Agilent technologies Inc.
DXR™ 2 Raman-microscope	Thermo Fisher Scientific, Waltham, Massachusetts, USA
7500cx ICP-MS (Solvias AG)	Agilent technologies Inc., Santa Clara, California, USA
5110 ICP-OES (Solvias AG)	Agilent technologies Inc., Santa Clara, California, USA
LS 6500 scintillation system	Beckman Coulter Inc., Brea, California, USA
5415 R centrifuge	Eppendorf AG, Hamburg, Germany
5810 R refrigerated centrifuge	Eppendorf AG, Hamburg, Germany

Table 12: Software for raw data acquisition and data analysis.

Data analysis software	Manufacturer
Excel	Microsoft Corporation, Redmond, Washington, USA
MassHunter B.06.00	Agilent technologies Inc., Santa Clara, California, USA
GraphPad Prism 7.03	GraphPad Software, La Jolla, California, USA
Matlab R2016b	MathWorks, Natick, Massachusetts, USA
PLS_Toolbox 8.0.2	Eigenvector Research, Wenatchee, Washington, USA
Minitab®17.3.1	Minitab Inc., State College, Pennsylvania, USA
Hamilton device manager	Hamilton Messtechnik GmbH, Höchst, Germany
iC FBRM Particle Track software	Mettler-Toledo Inc., Columbus, Ohio, USA
Omnic™ Spectra™	Thermo Fisher Scientific, Waltham, Massachusetts, USA

6.2 CDM handling

6.2.1 Small scale medium preparation tank model

The cell culture medium preparation is a fundamental part of experiments with the goal to characterize chemical CDM properties. In order to have similar mixing properties to large scale medium preparation tanks and to guarantee as high reproducibility in probe signals due to fixed mounting position as possible, a small scale single-use bioreactor was used (Mobius®) in the majority of experiments described. It is equipped with a three blade marine impeller which is driven by an engine mounted on the plastic head plate. The plastic material allowed easy experiment specific adjustments to the head plate. For example, additional probe mounting ports for medium preparation characterization were installed.

Since the FBRM probe manufacturer defines an optimum angle in its guidelines for the solution to flow on the probe an identical mounting device for the shaft of the probe was attached to both small scale systems. Additionally, by keeping the depth by which the probe dipped in the solution and the maintenance of constant stirring speed the risk of suspension agitation impacting measurement results was minimized.[511] The sensitivity of FBRM probes to dirt on the probe surface made a check measurement in pure water necessary. Only if minimal counts/second (≤5 counts per second for all particle sizes) the measurement was started. If background signal was too high the sapphire glass of probe tip was intensively cleaned with tooth paste, scouring milk or organic solvents to remove persistent dirt.

The univariate probes (DO, pH, ORP and conductivity) were operated with the Hamilton device manager software. The Hamilton Arc system allows the user to continuously write data for the described sensors in parallel. DO and pH probes were calibrated each time before usage. Calibration was not necessary for conductivity and ORP sensor. Usually, freshly tapped WFI contained about 14-15 %-vol of DO. As soon as the agitation was started, DO slowly increased up to about 20 %-vol. When this value was reached and approximately stable the medium preparation and parameter monitoring was started.

6.2.2 Cell culture medium preparation in small scale model

Medium preparation started by filling 80 % WFI of the targeted final volume of 2.9 L into the small scale model. Then, the head plate with stirrer and mounted engine was placed on the reactor. The probes were mounted in specific positions. Next, the thermometer was installed and the Finesse® software for temperature control and stirring rate adjustment was switched on. The medium preparation temperatures were chosen in a process relevant temperature window. The standard condition for medium preparation is a starting temperature of 35°C with no further temperature control during preparation. If not highlighted differently the temperature was set to 35 °C and stirring rate was 485 rpm for the entire preparation. The stirring rate was kept the same for all experiments. Compounds were added following the medium preparation recipes saved in the BI internal labware informative system (LIMS). The medium recipes described in this thesis contained 5 – 10 powder additions including basal powder. Since the goal of preparing model medium 1 in this model system was to investigate the effect of single compound additions on parameters such as pH, DO, ORP and conductivity the total preparation time was expanded. Usually, a subsequent powder addition was done when the previous powder added was visually dissolved. For experiments with model medium 2 the standard preparation times were applied. When the last compound was added to the medium under preparation a fill up step to final volume was done. For well-established media recipes the exact volume of WFI needed to reach final volume was known. If the medium recipe was still under development a standard approach

of adding the theoretically missing 20% WFI of total volume was used. The last step in medium preparation was the pH adjustment with NaOH to 7. This was done with the online pH probe mounted in the small scale model. After specific time intervals 500 µL samples were taken between compound additions and were frozen immediately on dry ice. Keeping comparable time intervals for sampling was important to ease the comparison between the different preparations.

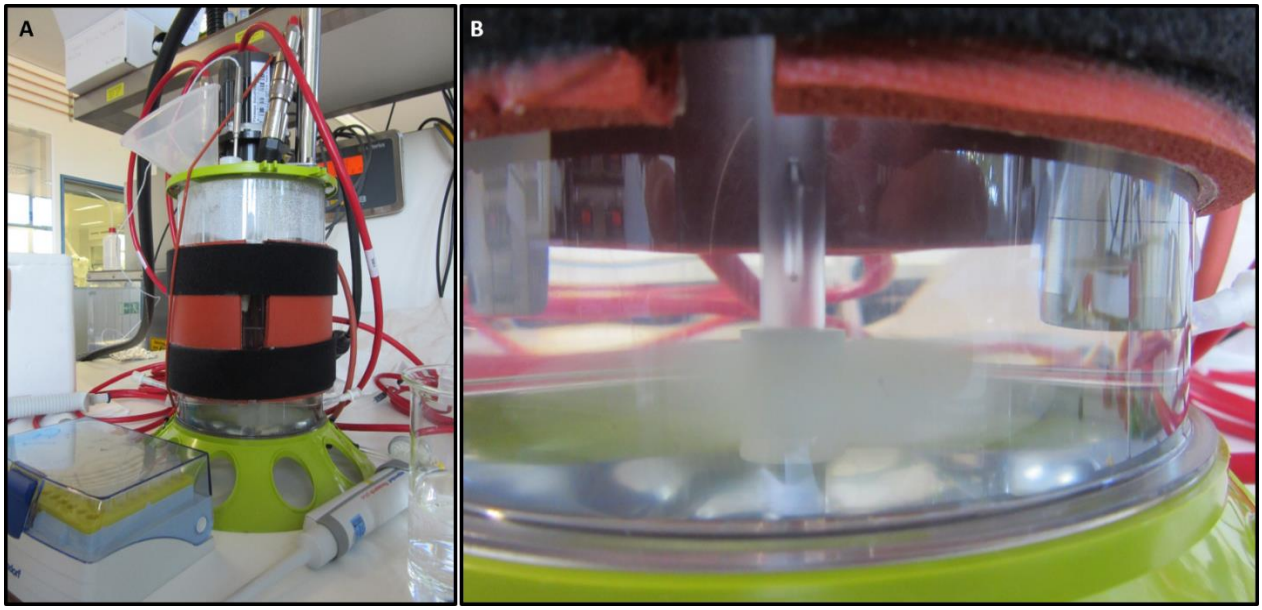

Figure 59: Medium preparation in small scale model. A) Mounting of probes and equipment for sampling shown. B) Position of probes in tank in relation to stirrer.

6.2.3 Cell Culture Medium preparation in conical flask

Under specific circumstances the preparation of medium in the small scale model was not suitable. For example, raw materials for isotopical labelling experiments are very expensive and therefore minimum volumes of medium were prepared. In comparison to the small scale model tank the CDM recipe does not change. This includes the addition order of compounds and the relative amounts per volume. The smaller scale brings challenges like mixing with stir bar that cannot be set to a specific power input per volume. Also, the usage of probes is very restricted due to missing possibilities to mount them. Since precision in weighing of small powder masses is limited, the minimal volume of medium prepared was 500 mL. At this scale pH adjustment with NaOH was done with a standard pH-meter.

Figure 60: Medium preparation in Erlenmeyer flask.

6.2.4 Storage of medium

Whether CDM storage impacts chemical composition of model medium 2 was investigated with the standard vessel formats for feed medium. After sterile filtration the CDM was filled into routinely used 1 L Nalgene® Biotainer® and 250 ml glass bottles (Figure 61 A and B). During storage all vessels were wrapped with aluminum foil to protect the CDM from light. To maintain CDM sterile during storage the bottles were opened only under a laminar flow. For sampling the CDM was mixed by shaking and the needed volume was poured into sampling vessels.

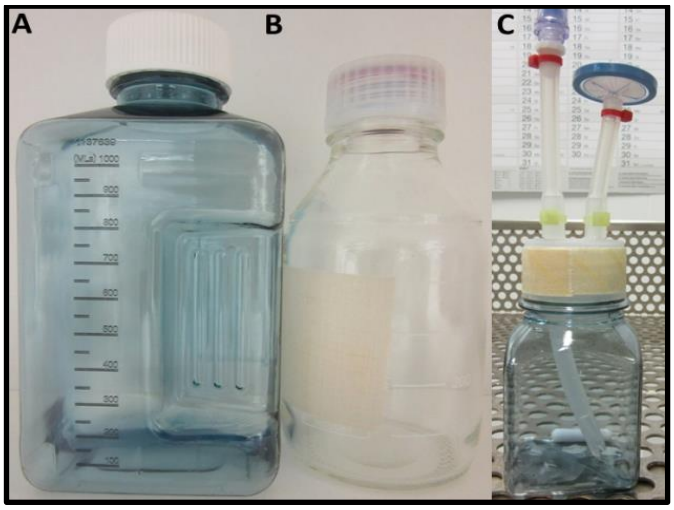

Figure 61: CDM storage vessel formats to investigate feed media over storage time. A) shows Nalgene Biotainer B) shows glass bottle and C) shows small Biotainer format equipped with stir bar for CDM suspension and sampling port to maintain medium sterility.

In case only small volumes of CDM could be prepared and sampling was necessary during storage time specially prepared storage vessels have been used. After mounting the special vessel setup with tubes for sampling and stir bar it was sterilized in an autoclave (Figure 61 C). Filling CDM after sterile filtration into vessel was done under laminar flow. Sampling was conducted after resuspension by stir bar with a syringe through the sterile sampling tube at ambient conditions. This was important because access to laminar flows that were qualified for usage with radioactive material was limited. Samples were drawn with a syringe through sampling port after intensive mixing with stir bar. At each sampling process the first filled syringe was discarded due to dead volume remaining in sampling tubing.

6.2.5 Handling of precipitate

After prolonged periods of storage, media were filtered over mixed cellulose membranes with a funnel filter. Afterwards, the membrane was washed with at least 50 to 100 mL LC-MS H2O. A spatula was used to put the washed filter membrane with precipitate into cell culture dishes for storage. In order to prevent the membrane from sticking to the storage vessel the cell culture dish was previously equipped with 200 µL pipette tips. Generally, the membranes were directly put in desiccator for drying (silica gel in bottom and dried under vacuum with protection from light at room temperature). In exceptional cases (e.g. no capacity in desiccator to dry or the need to continue the experiment at later time) the membranes were stored in freezer at negative 70°C in cell culture dish wrapped with parafilm before they were dried in desiccator. After drying, the filter membranes were weighted three times on a ME 5-OCE scale to guarantee sufficient drying (weight did not decrease anymore from time to time).

The filtration of precipitate was the preferred procedure to separate solids from liquid medium because it allowed to process comparably big volumes in a reasonable amount of time. Furthermore, the discoloration of filter surface allowed for a visual comparison of precipitates. In case the volume of available medium was limiting and quantification by mass was not of primary interest the more labor intensive and error prone centrifugation was used. This was generally conducted by spinning 15 mL of suspended medium at maximum speed for 30 minutes at 2-8°C in conical 15 mL polypropylene centrifugation tubes. Afterwards, the supernatant was removed carefully with a pipette in several steps to not break up the very loose precipitate pellets. Usually the last 100 – 500 µL of medium supernatant could not be removed because that would have ruptured the pellet and too much material would have been lost in the waste. In order to avoid background issues during analysis two washing steps by adding 2 mL of WFI or LC-MS grade water to the remaining 100 – 500 µL supernatant have been applied. After each filling up step with washing solvent, the spinning down and removing of supernatant procedure has been repeated.

6.3 Analytical methodologies applied to CDM

6.3.1 Theoretical structure similarity considerations of CDM compounds

Structure similarity index calculation of media components was performed based on the 2D Tanimoto Similarity on the NCBI PubChem webpage.[672, 673] Data visualization in dendograms was realized with Minitab®17.3.1.

6.3.2 Dynamic multiple reaction monitoring with triple quadrupole LC-MS method development and measurements

A targeted LC-QqQ-MS method with the goal to monitor as many organic cell culture medium compounds as possible in parallel has been developed. The dynamic multiple reaction monitoring method has been elaborated to get a method that hints at unstable compounds and thereof resulting reaction products.

Standard preparation A solution with all the compounds of Table 3 was prepared in LC/MS grade water under constant stirring at room temperature as reference stock solution. The compound concentrations were chosen to cover the concentration ranges expected from model medium 1 and 2. With regard to analysis throughput a single reference stock solution has been aimed at. This avoids a high number of calibration curve injections to the LC-QqQ-MS system that would be impossible to handle. However, chemical stability of such a complex solution must be controlled. To prevent chemical reactions as much as possible stock solution aliquots were frozen at -80°C immediately after preparation.

An internal standard (IS) mix has been prepared of 436.6 µL of 20 mM cell free amino acid mixture (^{13}C ^{15}N), 15 µL of 103.2 mM di-β-alanine-$^{13}C_6{}^{15}N_2$ calcium salt and 39 µL of 39.4 mM MES. Quality control samples (QC) were aliquoted from freshly prepared and directly frozen (-80°C) model medium 2. In order to investigate matrix effect, an artificial matrix was produced with all medium components not included in the validated dMRM method (e.g. trace elements, carbohydrates, inorganic salts). Due to confidentiality reasons, individual compound identities and concentrations of artificial matrix components cannot be specified further.

Sample preparation For LC-QqQ-MS analysis, CDM samples frozen at -80°C were thawed at RT under constant protection from light exposure for 1 to 2 hours. The absence of solids in samples made centrifugation or filtration unnecessary. Samples were diluted 1:10 with LC/MS grade water and added to the IS mix in a 3:4 ratio.

LC-QqQ-MS measurement Per batch a Calibration curve, QC standards and 30 samples were measured in random order. The batch size was limited to a maximum of 30 samples, to minimize compound degradation in the autosampler at 2 -8°C. After every five samples pure water was injected as blank. The method was developed with a Scherzo SM-C18 150 mm x 2 mm I.D. column, with 3 µm particle size. Chromatographic separation was achieved at 37°C with mobile phase A (5 mM ammonium formate) and mobile phase B (80:20 methanol/water (v/v), 0.025% v/v formic acid). The injection volume was set to 2 µL and the gradient profile is displayed in Table 13. Maximal column pressure was set to 250 bar.

Liquid chromatography (LC) has been performed with an Agilent 1260 infinity series system with a binary pump. The LC was coupled to an Agilent 6410 triple quadrupole mass spectrometer equipped with an ESI source. Nitrogen was used as curtain and collision gas. Nebulizer pressure was set to 50 psi at a flow rate of 8.5 L/min. The auxiliary gas temperature was maintained at 350 °C. Inlet capillary voltage and electron multiplier voltage were adjusted to 3.3 and 1 kV,

respectively. Data were acquired using MassHunter B.06.00 software. The mass spectrometer was operated in positive dynamic multiple reaction monitoring (dMRM) mode and set to unit resolution. MS/MS product ion spectra for each analyte were recorded using direct injection of single compound references into the ESI source. Reference compounds were dissolved in a mixture of water/methanol 50:50 (v/v). The cell accelerator voltage (CAV) was set to 7 V, while fragmentation voltage (UF) and collision energy (CE) were optimized for each transition. Retention times, transition pairs and MS/MS acquisition parameters for each analyte are shown in Table 3.

Table 13 Chromatographic gradient for dMRM method. Mobile phase A was 5 mM ammonium formate in water and mobile phase B was a 80:20 methanol/water (v/v) mixture with 0.025% v/v formic acid. Maximum column back pressure was set to 250 bar.

time [min]	mobile phase A [vol.%]	mobile phase B [vol.%]	flow rate [mL/min]
0	95.0	5.0	0.18
4	77.5	22.5	0.18
5	74.5	25.5	0.18
6	71.5	28.5	0.18
7	68.5	31.5	0.18
15	49.3	50.7	0.18
30	0.0	100.0	0.18
32	0.0	100.0	0.18
33	95.0	5.0	0.18
36	95.0	5.0	0.80
40	95.0	5.0	0.80
40.5	95.0	5.0	0.18

Method validation In order to investigate the developed LC-QqQ-MS method in more detail a validation after scientific quality standards has been conducted. If possible, all the described method validation parameters were performed according to the FDA guidelines for industry.[558]

Selectivity Method interferences were evaluated through signal analysis with SNR≥3 as cut-off criterion for artificial matrix analysis. Based on the high number of compounds included in the method (≥ 50% coverage of CDM compounds) preparation of blank matrix for individual compounds was not feasible. Matrix effect assessment was thus performed by comparing the reference stock solution spiked into the artificial medium matrix and into water (1:2 dilution). This was done for solutions at 5 different concentration levels (1:10, 1:50, 1:100, 1:500 and 1:100). The norm of the correlation matrix and the percent difference in absolute values was used to estimate the impact of the matrix effect. With differences below 30% and correlation norms ≤0.98, an impact of the matrix was rejected. It has to be noted that ion suppression caused by coeluting analytes was not investigated.

Calibration curves Calibration curves for each component were obtained by analyzing freshly thawed aliquots of the reference stock solution at 15 dilution levels (1:1.5:1.33:1.25:1.4: 1.28:1.38:1.48:1.35:1.5:1.33:2:2.5:2:2). Serial dilution of the stock was performed in water. Based on the measurement time and the variety of analyte concentrations in cell culture medium, multiple dilution levels ensuring linear calibration curves were not feasible for all compounds. To

solve this problem, either quadratic or power regression models were used. For regression model decision, comparison of R^2 values of forced linear fit and heteroscedasticity test was performed. The chi-square distribution test calculated after Breush, Pagan and Koenker in Matlab was used to determine if heteroscedasticity affected the calibration data.[1] If the calculated pValue was ≤0.05, the null hypothesis of homoscedasticity was rejected and heteroscedasticity assumed. For low R square (forced linear fit) and distinctively higher R square for power or quadratic fit linear regression was rejected.

Accuracy and Precision Method accuracy was assessed through comparison of measured analyte concentrations in QC samples with known concentration levels of model medium 2. The measurement was considered accurate when deviations of ≤ 15% between known and measured analyte concentrations could be demonstrated. For inter-batch comparability, accuracy of QC samples was determined for each batch and plotted on a Xbar-R chart. Intra- and inter-day precision was evaluated as coefficient of variation (CV). For this purpose, compound concentrations in QC samples were determined over 6 days with three replicates per day. Sample comparability was ensured through single sample preparation (aliquots frozen at -80°C) and aliquot thawing just prior to measurements. The method was considered precise when CV was ≤5%.

Sensitivity and carryover The lower limit of quantification (LLOQ) was determined according to the mathematical equation $LLOQ = 10 \times \frac{s}{b}$, where b depicts the calibration graph slope and s the standard deviation of intercept. For limit of detection (LOD) determination, $LOD = 3.3 \times \frac{s}{b}$ was assumed.[556] Logarithmic transformation of the calibration curve was performed for compounds with power regression type. For quadratic regression, SNR ≥3.3 and SNR ≥10 were set as criteria for LOD and LLOQ respectively. Carryover was assessed by comparison of analyte peak areas of blank injections measured after and before QC samples and reported as the difference relative to peak area in replicate QC samples.

Reproducibility and stability Reproducibility was determined by QC sample incorporation within each measurement batch. Coefficients of variation below or equal to 20% were considered acceptable. Furthermore, compound stabilities within the measurement time were examined for both QC and calibration curve samples.

6.3.3 FTIR spectroscopy

Fourier transform infrared microspectroscopy (FTIR) analysis was performed in two collaborating laboratories. MVA incorporated used an Olympus BX-51 compound microscope coupled to a SensIR IlluminatIR FTIR spectrophotometer.
Intertek AG in Switzerland used an Attenuated Total Reflectance (ATR) – FTIR approach. The IR spectra of the samples were recorded on a Varian 3100 FT-IR Spectrometer.

6.3.4 Raman Microscopy

All the precipitate analyzed were filtered on mixed cellulose ester filter membranes. Since the layer of precipitate was usually too thin to be scratched off the membranes the dried solid precipitate has been analyzed directly on the filter membrane. Having the material of interest in a pure layer would have been advantageous for the Raman analysis. In order to be able to distinguish signal of the filter membrane from the precipitate, a pure membrane has been measured on an aluminum foil wrapped slide (Figure 62). All slides used have been wrapped in aluminum foil in order to prevent the glass to mask the Raman signal of the sample. In a first step the sample was focused with either a 50x or 100x objective. All results shown were measured with

the 532 nm wavelength laser. For CDM precipitate samples the laser power was generally set between 0.2 and 2 mW to prevent burning. Standard settings for slit width and pinhole were 50 µm. Investigative analysis as baseline subtraction and data base searches have been conducted in the Thermo software used to control the instrument (Omnic™ Spectra™). After raw data acquisition and matching to Thermo data base the spectra have been exported in *.csv format. Plotting and analysis was done later with GraphPad Prism 7.03 software.

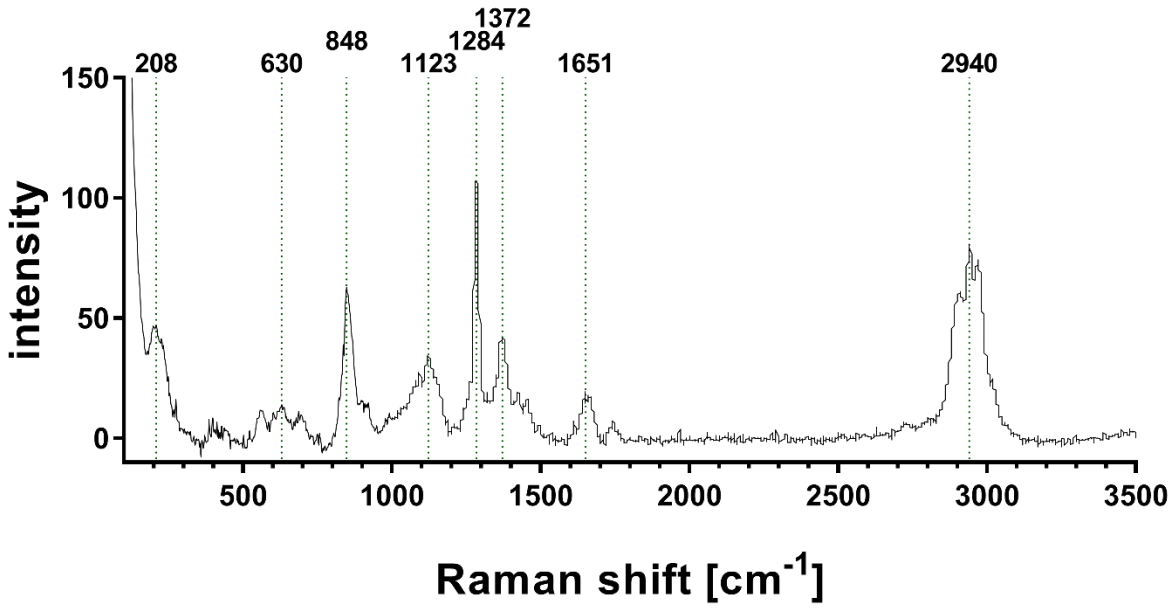

Figure 62: Blank filter membrane measured on aluminum foil wrapped slide. The reference spectrum was used to judge if sample spectra were impacted by mixed cellulose ester background.

6.3.5 Scanning electron microscopy – energy dispersive x-ray (SEM-EDX)

Scanning electron microscopy coupled with energy dispersive x-ray detector (SEM-EDX) was performed in a collaborating laboratory within BI. The samples were prepared by excising little pieces of the filter membrane with the dried filter cake. Subsequently, the little pieces were mounted on aluminum sample holders with sticky coal pads. The samples were first investigated with the high-resolution secondary electrons detector (SE). The microscopic investigations with the SE-detector gave good knowledge of the sample topology and the fine-structural composition. In a second step, the sample was scanned with a back-scattered-electrons detector (BSE). The BSE-detector type allows conclusions on elemental composition because elements with higher order number reflect electrons more efficiently due to their bigger nuclei than elements with lower order number. Therefore, elements with lower order number appear darker in the image. BSE-detector is marked in the images of the results and discussion part as angular selective backscattered (AsB). Both SE-detector and BSE-detector images are shown as results. BSE-detector images are coupled with K-series images highlighting local hotspots of specific elements.

The EDX analysis has been performed on local, representative fields marked in the AsB images with white rectangles. The exciting electron beam causes the elements with elemental order number ≥5 to emit x-rays with element specific energy [keV]. The EDX measurements with high local resolution have been conducted with a process time of 5 and an acceleration voltage of 10-25 kV. For the interpretation of EDX spectra the elements of the sample holder have to be considered as background.

6.3.6 Inductively coupled plasma mass spectrometry (ICP-MS) and inductively coupled plasma optical emission spectroscopy (ICP-OES)

All the ICP-MS and ICP-OES analysis have been conducted externally at the contract research organization Solvias AG in Kaiseraugust. The precipitate on filter membrane was dissolved with acid (HCl, H_3PO_4 or HNO_3). The dissolution has been conducted in quartz glass vessels with PTFE caps that were carefully rinsed with acid and water. Afterwards, the sample material was dissolved in digestion apparatus with high pressure autoclave and microwave heating. The measurement has been conducted with settings proprietary to Solvias AG. The data has been provided in elemental concentrations in mg/kg or w/w.

6.3.7 Conditions for radioactivity measurements – liquid scintillation counting (LSC)

All samples were determined for 14C-radioactivity using a LS 6500 multi-purpose scintillation counter (Beckman Coulter). The sample aliquots were transferred into a mini-Vial and filled up with 4.5 ml LSC-cocktail (Ultima Gold).

All parameters for the measurement were documented on the protocol and were as follows:

Count conditions:

Nuclide C-14

Count time **2 min**

Count unit **dpm**

Quench set:

Quench limits (low) **29.062**

Quench limits (high) **198.56**

Background subtract **Off**

Low CPM threshold **Off**

Count region **0.0 – 156.0 kEV**

Count corrections:

Color quench correction On

The samples were measured in the C-14 protocol because of the lack of S-35 LSC-Standards. The energy and the counting yield of these isotopes are nearly the same (C-14: 96%, S-35: 97%).

6.4 Experiments

6.4.1 Empirical approach to characterize reactions contributing to DO drop during model medium 1 preparation

In a first step, the model feed medium 1 was characterized as deep as possible to collect more information around the oxygen consuming reaction. Therefore, the standard medium was characterized with all the available on-line probes DO, ORP, conductivity, pH and FBRM in order to collect a broad data base. In a second step, a simplified matrix approach was used to further investigate the oxygen consumption during medium preparation. As the oxygen consumption was initiated with OICA addition it was assumed that metal salts play a fundamental role in the reaction. Subsequently, two different metal free basal powders were designed and ordered. Both powders were based on model medium 1 recipe. The basal powder that contained sodium salts was designed by eliminating all metal other than sodium. This means that for example compounds like cyanocobalamin or copper sulfate have been eliminated. For completely metal free basal powder also compounds such as ascorbic acid sodium salt or sodium chloride were eliminated. In order to confirm the absence of metals in simplified matrix powders the manufacturer has performed ICP-MS analysis.[475] In a pH adjustment step the medium was treated with NaOH. Thus, sodium concentration measured can be expected very high. The simplified matrix media were prepared in the small scale medium preparation tank with the same monitoring tools used for standard recipe. Individual powder addition time points have been elongated in order to give the chemical parameters time to equilibrate from addition to addition. With the goal to guarantee comparability between simplified matrix experiments and model medium 1 preparations with standard powder under standard conditions, with nitrogen gassing, or at 2-8°C in the cold room the addition time points have been kept constant if possible. The medium sampling was also harmonized between the experiments. After each powder addition two samples have been drawn right after addition and just before the addition of the next compound. Samples were immediately frozen on dry ice to prevent side reactions and stored at -70°C until analysis. Samples were analyzed with the developed dMRM method. Analytics for ascorbic acid were performed in the laboratories of Biofidus AG in Bielefeld, Germany. The method has not been validated and therefore the results need to be considered qualitatively.

6.4.2 Storage stability study of model medium 2

The small scale model was equipped with a heating jacket. Therefore, it was possible to control temperature at values higher than room temperature. As the standard preparation condition in development and commercial manufacturing is 35°C a temperature range around this target was of interest. As normal medium preparation tanks are not equipped with temperature control options the medium usually cools down during preparation. Thus, one test case was 35°C starting temperature without activated temperature control and another test case was 35°C starting temperature with activated heating at this set point. The most elevated preparation temperature was at constantly 40°C. Since active cooling was not possible the lowest temperature investigated was room temperature. All the preparation conditions were conducted in small scale model in triplicate preparations. An exception was the 35°C starting temperature without temperature control. In addition to the triplicates prepared in small scale model the condition was also tested in triplicate in Erlenmeyer flask preparation to include the standard development preparation scale into the experimental design. In contrast to the small scale model, the Erlenmeyer flask was not equipped with FBRM and DO probes. Another difference between the two preparation vessels was the absence of light protection during preparation in standard laboratory scale. The 15 media preparations were conducted within two subsequent days. As two identical small scale models were available two preparations could be performed in parallel.

After preparation the medium was sterile filtered and filled into the storage vessels under sterile conditions. The 2.9 L CDM prepared were distributed as aliquots of 3x 750 mL in Biotainer® plastic vessels and in 3x 250 mL glass bottles. The storage containers were closed under the laminar flow hood and stored with light protection at RT for 28 days. Each of the 15 preparations was sampled before pH-adjustment, after pH-adjustment and immediately after sterile filtration. Further 1 mL samples were taken during the storage period on day 2, 8, 14 and 28. Samples were taken under sterile conditions and samples were immediately frozen at -70°C.

6.4.3 Silver precipitate formation investigations

A major finding of the investigation of precipitate identities was the formation of elemental sulfur. In most of the CDM the major sulfur containing compound is cysteine, as is in the medium investigated. Therefore, it has been hypothesized that the silver sulfur precipitate may come from cysteine degradation. In order to test this hypothesis a medium, identical to the media where the silver precipitate has been isolated from for identification, was prepared. The key difference to standard media was the addition of S-35 L-cysteine to a 420 mL aliquot of the finally prepared CDM with a final activity of 0.013 MBq/mL. This aliquot supplemented with radioactive L-cysteine was split after sterile filtration under a sterile hood approved for work with radioactive material into three identical 125 mL Biotainer® vessels for storage. The remaining 250 mL of medium was not supplemented with radioactive material and was treated the same way as radioactive samples in order to have a non-radioactive control. As an additional control a medium that was known for forming minimal precipitate with presumably no cysteine participation was prepared the same way as silver precipitate forming medium. The readily prepared medium was protected from light with aluminum foil for storage and sampled on day 0, 4, 8, 13, 21, 28, 39 and 50. Samples were drawn with a syringe through the sampling port. The 10 mL medium sample was filled into Falcon™ conical centrifugation tubes and spun down in a suitable centrifuge at maximum speed for 1 hour. Afterwards, the supernatant was removed carefully without disrupting the precipitate on the vessel walls, precipitate was washed and finally dissolved in DMSO. All samples were measured with scintillation counter.

7. References

1. Krattenmacher, F., T. Heermann, A. Calvet, B. Krawczyk, and T. Noll, (2019). ***Effect of manufacturing temperature and storage duration on stability of chemically defined media measured with LC-MS/MS***. Journal of Chemical Technology & Biotechnology, **94**(4): p. 1144-1155.
2. Verma, A.S., S. Agrahari, S. Rastogi, and A. Singh, (2011). ***Biotechnology in the realm of history***. Journal of pharmacy & bioallied sciences, **3**(3): p. 321-323.
3. Wiles, A.E.D., (1946). ***THE MANUFACTURE OF PENICILLIN***. Journal of the Institute of Brewing, **52**(3): p. 113-116.
4. Reichstein, T. and A. Grüssner, (1934). ***Eine ergiebige Synthese der l-Ascorbinsäure (C-Vitamin)***. Helvetica Chimica Acta, **17**(1): p. 311-328.
5. Scott, C.H.B.a.D.A., (1923). ***THE PREPARATION OF INSULIN***. (57): p. 709-723.
6. Scott, D.A. and C.H. Best, (1925). ***The Preparation of Insulin***. Industrial & Engineering Chemistry, **17**(3): p. 238-240.
7. Fraser, L. ***Cloning Insulin - Genentech Defining Moments***. 2016; Available from: https://www.gene.com/stories/cloning-insulin.
8. Goeddel, D.V., D.G. Kleid, F. Bolivar, H.L. Heyneker, D.G. Yansura, et al., (1979). ***Expression in Escherichia coli of chemically synthesized genes for human insulin***. Proc Natl Acad Sci U S A., **76**(1): p. 106-10.
9. Junod, S.W., (2007). ***Celebrating a Milestone: FDA's Approval of First Genetically-Engineered Product***. This article originally appeared in the "History Corner" column of the September-October 2007 - issue of Update magazine, the bimonthly publication of the Food and Drug Law Institute.
10. Hofemeister, J., (1988). ***Achievements in application of recombinant DNA technology for creation of industrial microorganisms***. Zentralblatt fur Mikrobiologie, **143**(8): p. 551-560.
11. AlDeghaither, D., B.G. Smaglo, and L.M. Weiner, (2015). ***Beyond peptides and mAbs--current status and future perspectives for biotherapeutics with novel constructs***. J Clin Pharmacol, **55 Suppl 3**: p. S4-20.
12. Kontermann, R.E. and U. Brinkmann, (2015). ***Bispecific antibodies***. Drug Discovery Today, **20**(7): p. 838-847.
13. Muik, A., I. Kneiske, M. Werbizki, D. Wilflingseder, T. Giroglou, et al., (2011). ***Pseudotyping Vesicular Stomatitis Virus with Lymphocytic Choriomeningitis Virus Glycoproteins Enhances Infectivity for Glioma Cells and Minimizes Neurotropism***. Journal of Virology, **85**(11): p. 5679.
14. Muik, A., C. Dold, Y. Geiß, A. Volk, M. Werbizki, et al., (2012). ***Semireplication-competent vesicular stomatitis virus as a novel platform for oncolytic virotherapy***. Journal of Molecular Medicine, **90**(8): p. 959-970.
15. Muik, A., L.J. Stubbert, R.Z. Jahedi, Y. Gei β , J. Kimpel, et al., (2014). ***Re-engineering Vesicular Stomatitis Virus to Abrogate Neurotoxicity, Circumvent Humoral Immunity, and Enhance Oncolytic Potency***. Cancer Research, **74**(13): p. 3567.
16. Tober, R., Z. Banki, L. Egerer, A. Muik, S. Behmüller, et al., (2014). ***VSV-GP: a Potent Viral Vaccine Vector That Boosts the Immune Response upon Repeated Applications***. Journal of Virology, **88**(9): p. 4897.
17. MordorIntelligence. ***BIOPHARMACEUTICALS MARKET , SEGMENTED BY PRODUCTS (MONOCLONAL ANTIBODIES, RECOMBINANT GROWTH FACTORS, PURIFIED PROTEINS, RECOMBINANT PROTEINS, RECOMBINANT HORMONES, SYNTHETIC IMMUNOMODULATORS, VACCINES), BY APPLICATION, BY GEOGRAPHY- GROWTH, TRENDS, AND FORECAST (2019 - 2024)***. 2019; Available from: https://www.mordorintelligence.com/industry-reports/global-biopharmaceuticals-market-industry.
18. Mathaes, R. and H.-C. Mahler, (2018), ***Next Generation Biopharmaceuticals: Product Development***, in *New Bioprocessing Strategies: Development and Manufacturing of Recombinant Antibodies and Proteins*, B. Kiss, U. Gottschalk, and M. Pohlscheidt, Editors. Springer International Publishing: Cham. p. 253-276.

19. EvaluateLtd. ***EvaluatePharma - World Preview 2018, Outlook to 2024***. 2018; Available from: http://info.evaluategroup.com/rs/607-YGS-364/images/WP2018.pdf.
20. Irani, V., A.J. Guy, D. Andrew, J.G. Beeson, P.A. Ramsland, et al., (2015). ***Molecular properties of human IgG subclasses and their implications for designing therapeutic monoclonal antibodies against infectious diseases***. Molecular Immunology, **67**(2, Part A): p. 171-182.
21. Vidarsson, G., G. Dekkers, and T. Rispens, (2014). ***IgG subclasses and allotypes: from structure to effector functions***. Frontiers in immunology, **5**: p. 520-520.
22. Janeway CA Jr, T.P., Walport M, et al. , (2001), ***Immunobiology: The Immune System in Health and Disease. -The structure of a typical antibody molecule.*** 5th edition ed. New York: Garland Science.
23. Singh, S., N.K. Kumar, P. Dwiwedi, J. Charan, R. Kaur, et al., (2018). ***Monoclonal Antibodies: A Review***. Current clinical pharmacology, **13**(2): p. 85-99.
24. Mayrhofer, P. and R. Kunert, (2019). ***Nomenclature of humanized mAbs: Early concepts, current challenges and future perspectives***. Human antibodies, **27**(1): p. 37-51.
25. Houde, D., Y. Peng, S.A. Berkowitz, and J.R. Engen, (2010). ***Post-translational modifications differentially affect IgG1 conformation and receptor binding***. Molecular & cellular proteomics : MCP, **9**(8): p. 1716-1728.
26. Jennewein, M.F. and G. Alter, (2017). ***The Immunoregulatory Roles of Antibody Glycosylation***. Trends Immunol, **38**(5): p. 358-372.
27. Zheng, K., M. Yarmarkovich, C. Bantog, R. Bayer, and T.W. Patapoff, (2014). ***Influence of glycosylation pattern on the molecular properties of monoclonal antibodies***. mAbs, **6**(3): p. 649-658.
28. Kuriakose, A., N. Chirmule, and P. Nair, (2016). ***Immunogenicity of Biotherapeutics: Causes and Association with Posttranslational Modifications***. Journal of immunology research, **2016**: p. 1298473-1298473.
29. Jefferis, R., (2016). ***Posttranslational Modifications and the Immunogenicity of Biotherapeutics***. Journal of immunology research, **2016**: p. 5358272-5358272.
30. Walsh, G., (2010). ***Biopharmaceutical benchmarks 2010***. Nature Biotechnology, **28**: p. 917.
31. Walsh, G., (2014). ***Biopharmaceutical benchmarks 2014***. Nature Biotechnology, **32**: p. 992.
32. Walsh, G., (2018). ***Biopharmaceutical benchmarks 2018***. Nature Biotechnology, **36**: p. 1136.
33. Goh, J.B.N., Say Kong, (2017). ***Impact of host cell line choice on glycan profile***. Critical Reviews in Biotechnology, **38**(6): p. 851-867.
34. Fischer, S., R. Handrick, and K. Otte, (2015). ***The art of CHO cell engineering: A comprehensive retrospect and future perspectives***. Biotechnology Advances, **33**(8): p. 1878-1896.
35. Jayapal, K.P., K.F. Wlaschin, W.S. Hu, and M.G.S. Yap, (2007). ***Recombinant protein therapeutics from CHO Cells - 20 years and counting***. Chemical Engineering Progress, **103**(10): p. 40-47.
36. Kim, J.Y., Y.G. Kim, and G.M. Lee, (2012). ***CHO cells in biotechnology for production of recombinant proteins: current state and further potential***. Appl Microbiol Biotechnol., **93**(3): p. 917-30. doi: 10.1007/s00253-011-3758-5. Epub 2011 Dec 9.
37. Kunert, R. and D. Reinhart, (2016). ***Advances in recombinant antibody manufacturing***. Applied Microbiology and Biotechnology, **100**(8): p. 3451-3461.
38. Tejwani, V., M.R. Andersen, J.H. Nam, and S.T. Sharfstein, (2018). ***Glycoengineering in CHO Cells: Advances in Systems Biology***. Biotechnology Journal, **13**(3): p. 1700234.
39. EuropeanMedicinesAgency, (2015), ***Praxbind - International non-proprietary name: idarucizumab***, in *Assessment report*.
40. Reinhart, D., L. Damjanovic, C. Kaisermayer, W. Sommeregger, A. Gili, et al., (2019). ***Bioprocessing of Recombinant CHO-K1, CHO-DG44, and CHO-S: CHO Expression Hosts Favor Either mAb Production or Biomass Synthesis***. Biotechnology Journal, **14**(3): p. 1700686.
41. Wilson, A.W. and P.J. Neumann, (2012). ***The cost-effectiveness of biopharmaceuticals: a look at the evidence***. mAbs, **4**(2): p. 281-288.
42. Hu, W.-S., (2013), ***Cell Culture Bioprocess Engineering***.
43. Boehringer-Ingelheim_Pharma_GmbH_&_Co_KG. ***Boehringer Ingelheim Invests in Europe: Pharma Company Expands Biopharmaceutical Production at Vienna Site***. 2015; Available

from: https://www.boehringer-ingelheim.com/press-release/boehringer-ingelheim-invests-europe-pharma-company-expands-biopharmaceutical.

44. Fan Y., L.D., Andersen M.R., (2017), ***Fed-Batch CHO Cell Culture for Lab-Scale Antibody Production. In: Picanço-Castro V., Swiech K. (eds) Recombinant Glycoprotein Production. Methods in Molecular Biology,***. Vol. 1674. Humana Press, New York, NY.
45. Bielser, J.-M., M. Wolf, J. Souquet, H. Broly, and M. Morbidelli, (2018). ***Perfusion mammalian cell culture for recombinant protein manufacturing – A critical review***. Biotechnology Advances, **36**(4): p. 1328-1340.
46. Li, F., N. Vijayasankaran, A.Y. Shen, R. Kiss, and A. Amanullah, (2010). ***Cell culture processes for monoclonal antibody production***. mAbs, **2**(5): p. 466-479.
47. Hong, J.K., M. Lakshmanan, C. Goudar, and D.-Y. Lee, (2018). ***Towards next generation CHO cell line development and engineering by systems approaches***. Current Opinion in Chemical Engineering, **22**: p. 1-10.
48. Omasa, T., M. Onitsuka, and W.D. Kim, (2010). ***Cell engineering and cultivation of chinese hamster ovary (CHO) cells***. Current pharmaceutical biotechnology, **11**(3): p. 233-240.
49. Yang, W.C., J. Lu, C. Kwiatkowski, H. Yuan, R. Kshirsagar, et al., (2014). ***Perfusion seed cultures improve biopharmaceutical fed-batch production capacity and product quality***. Biotechnology Progress, **30**(3): p. 616-625.
50. Xie, L. and D. Wang, (1994), ***Fed-batch cultivation of animal cells using different medium design concepts and feeding strategies***. Vol. 43. 1175-89.
51. Xie, L. and D.I.C. Wang, (1997). ***Integrated approaches to the design of media and feeding strategies for fed-batch cultures of animal cells***. Trends in Biotechnology, **15**(3): p. 109-113.
52. Lu, F., P.C. Toh, I. Burnett, F. Li, T. Hudson, et al., (2013). ***Automated dynamic fed-batch process and media optimization for high productivity cell culture process development***. Biotechnology and Bioengineering, **110**(1): p. 191-205.
53. Walther, J., J. Lu, M. Hollenbach, M. Yu, C. Hwang, et al., (2019). ***Perfusion Cell Culture Decreases Process and Product Heterogeneity in a Head-to-Head Comparison With Fed-Batch***. Biotechnology Journal, **14**(2): p. 1700733.
54. Xu, S., J. Gavin, R. Jiang, and H. Chen, (2017). ***Bioreactor productivity and media cost comparison for different intensified cell culture processes***. Biotechnology progress, **33**(4): p. 867-878.
55. Karst, D.J., F. Steinebach, and M. Morbidelli, (2018). ***Continuous integrated manufacturing of therapeutic proteins***. Current Opinion in Biotechnology, **53**: p. 76-84.
56. Arora, M., (2013), ***Cell Culture Media: A Review***. Vol. 3.
57. Krampe, B. and M. Al-Rubeai, (2010). ***Cell death in mammalian cell culture: molecular mechanisms and cell line engineering strategies***. Cytotechnology, **62**(3): p. 175-188.
58. Albrecht, S., C. Kaisermayer, C. Gallagher, A. Farrell, A. Lindeberg, et al., (2018). ***Proteomics in biomanufacturing control: Protein dynamics of CHO-K1 cells and conditioned media during apoptosis and necrosis***. Biotechnology and Bioengineering, **115**(6): p. 1509-1520.
59. Hwang, S.O. and G.M. Lee, (2008). ***Autophagy and apoptosis in Chinese hamster ovary cell culture***. Autophagy., **4**(1): p. 70-2. Epub 2007 Sep 20.
60. Cummings, B.S. and R.G. Schnellmann, (2004). ***Measurement of cell death in mammalian cells***. Current protocols in pharmacology, **Chapter 12**: p. 10.1002/0471141755.ph1208s25-12.8.
61. Cummings, B.S., L.P. Wills, and R.G. Schnellmann, (2012). ***Measurement of Cell Death in Mammalian Cells***. Current Protocols in Pharmacology, **56**(1): p. 12.8.1-12.8.24.
62. Meredith, J.E., B. Fazeli, and M.A. Schwartz, (1993). ***The extracellular matrix as a cell survival factor***. Molecular Biology of the Cell, **4**(9): p. 953-961.
63. Theocharis, A.D., S.S. Skandalis, C. Gialeli, and N.K. Karamanos, (2016). ***Extracellular matrix structure***. Advanced Drug Delivery Reviews, **97**: p. 4-27.
64. Caron, A.L., R.T. Biaggio, and K. Swiech, (2018). ***Strategies to Suspension Serum-Free Adaptation of Mammalian Cell Lines for Recombinant Glycoprotein Production***. Methods in molecular biology (Clifton, N.J.), **1674**: p. 75-85.

65. Jukić, S., D. Bubenik, N. Pavlović, A.J. Tušek, and V.G. Srček, (2016). ***Adaptation of CHO cells in serum-free conditions for erythropoietin production: Application of EVOP technique for process optimization.*** Biotechnology and Applied Biochemistry, **63**(5): p. 633-641.
66. Costa, A.R., M.E. Rodrigues, M. Henriques, R. Oliveira, and J. Azeredo, (2011). ***Strategies for adaptation of mAb-producing CHO cells to serum-free medium.*** BMC Proceedings, **5**(Suppl 8): p. P112-P112.
67. Shridhar, S., G. Klanert, N. Auer, I. Hernandez, M. Kańduła, et al., (2017), ***Transcriptomic changes in CHO cells after adaptation to suspension growth in protein-free medium analysed by a species-specific microarray***. Vol. 257.
68. Gowtham, Y.K.H., Sarah; Saski, Christopher A, (2014), ***370264 Serum-Free Medium Adaptation of Chinese Hamster Ovary (CHO) Cell Lines: A Transcriptome Analysis Using RNA-Seq***, in *14 AIChE Annual Meeting*. Hilton Atlanta.
69. Gowtham, Y., C. A. Saski, and S. Harcum, (2014), ***Transcriptome analysis of Chinese hamster ovary (CHO) cell lines undergoing serum-free medium adaptation using RNA-Seq***.
70. Sung Kim, H. and G. Lee, (2007), ***Differences in optimal pH and temperature for cell growth and antibody production between two Chinese hamster ovary clones derived from the same parental clone***. Vol. 17. 712-20.
71. Yoon, S.K., S.L. Choi, J.Y. Song, and G.M. Lee, (2005). ***Effect of culture pH on erythropoietin production by Chinese hamster ovary cells grown in suspension at 32.5 and 37.0°C.*** Biotechnology and Bioengineering, **89**(3): p. 345-356.
72. Cook, J.A. and M.H. Fox, (1988). ***Effects of Chronic pH 6.6 on Growth, Intracellular pH, and Response to 42.0°C Hyperthermia of Chinese Hamster Ovary Cells.*** Cancer Research, **48**(9): p. 2417.
73. Brunner, M., P. Braun, P. Doppler, C. Posch, D. Behrens, et al., (2017). ***The impact of pH inhomogeneities on CHO cell physiology and fed-batch process performance – two-compartment scale-down modelling and intracellular pH excursion.*** Biotechnology Journal, **12**(7): p. 1600633.
74. Park, H.J., J.C. Lyons, T. Ohtsubo, and C.W. Song, (1999). ***Acidic environment causes apoptosis by increasing caspase activity.*** British journal of cancer, **80**(12): p. 1892-1897.
75. Lee, G.-H., J.-D. Hwang, J.-Y. Choi, H.-J. Park, J.-Y. Cho, et al., (2011). ***An acidic pH environment increases cell death and pro-inflammatory cytokine release in osteoblasts: The involvement of BAX Inhibitor-1.*** The International Journal of Biochemistry & Cell Biology, **43**(9): p. 1305-1317.
76. Sharma, V., R. Kaur, A. Bhatnagar, and J. Kaur, (2015). ***Low-pH-induced apoptosis: role of endoplasmic reticulum stress-induced calcium permeability and mitochondria-dependent signaling.*** Cell stress & chaperones, **20**(3): p. 431-440.
77. Williamson, J.D. and P. Cox, (1968). ***Use of a New Buffer in the Culture of Animal Cells.*** Journal of General Virology, **2**(2): p. 309-312.
78. Itagaki, A. and G. Kimura, (1974). ***TES and HEPES buffers in mammalian cell cultures and viral studies: Problem of carbon dioxide requirement.*** Experimental Cell Research, **83**(2): p. 351-361.
79. Ritacco, F.V., Y. Wu, and A. Khetan, (2018). ***Cell culture media for recombinant protein expression in Chinese hamster ovary (CHO) cells: History, key components, and optimization strategies.*** Biotechnology progress, **34**(6): p. 1407-1426.
80. Hogiri, T., H. Tamashima, A. Nishizawa, and M. Okamoto, (2018). ***Optimization of a pH-shift control strategy for producing monoclonal antibodies in Chinese hamster ovary cell cultures using a pH-dependent dynamic model.*** Journal of Bioscience and Bioengineering, **125**(2): p. 245-250.
81. Miermont, A., F. Waharte, S. Hu, M.N. McClean, S. Bottani, et al., (2013). ***Severe osmotic compression triggers a slowdown of intracellular signaling, which can be explained by molecular crowding.*** Proceedings of the National Academy of Sciences of the United States of America, **110**(14): p. 5725-5730.
82. Finan, J.D. and F. Guilak, (2010). ***The effects of osmotic stress on the structure and function of the cell nucleus.*** Journal of cellular biochemistry, **109**(3): p. 460-467.

83. Mager, W.H., A.H. de Boer, M.H. Siderius, and H.P. Voss, (2000). ***Cellular responses to oxidative and osmotic stress.*** Cell stress & chaperones, **5**(2): p. 73-75.
84. Burg, M.B., J.D. Ferraris, and N.I. Dmitrieva, (2007). ***Cellular Response to Hyperosmotic Stresses.*** Physiological Reviews, **87**(4): p. 1441-1474.
85. Han, Y.K., T.K. Ha, S.J. Lee, J.S. Lee, and G.M. Lee, (2011). ***Autophagy and apoptosis of recombinant Chinese hamster ovary cells during fed-batch culture: Effect of nutrient supplementation.*** Biotechnology and Bioengineering, **108**(9): p. 2182-2192.
86. Jäckle, T., C. Hasel, I. Melzner, S. Brüderlein, P.M. Jehle, et al., (2001). ***Sustained hyposmotic stress induces cell death: apoptosis by defeat.*** American journal of physiology. Cell physiology, **281**(5): p. C1716-26.
87. Lee, M.S. and G.M. Lee, (2001). ***Effect of hypoosmotic pressure on cell growth and antibody production in recombinant Chinese hamster ovary cell culture.*** Cytotechnology, **36**(1-3): p. 61-69.
88. Ryu, J.S. and G.M. Lee, (1999). ***Application of hypoosmolar medium to fed-batch culture of hybridoma cells for improvement of culture longevity.*** Biotechnology and bioengineering, **62**(1): p. 120-123.
89. Soo Ryu, J. and G. Min Lee, (1997). ***Effect of hypoosmotic stress on hybridoma cell growth and antibody production.*** Biotechnology and Bioengineering, **55**(3): p. 565-570.
90. Harbour, C., K.S. Low, C.P. Marquis, and J.P. Barford, (1989). ***pH control options for hybridoma cultures.*** Biotechnology Techniques, **3**(2): p. 73-78.
91. Min Lee, G. and J. Koo, (2010). ***Osmolarity Effects, Chinese Hamster Ovary Cell Culture.*** Encyclopedia of Industrial Biotechnology.
92. Bibila, T.A., C.S. Ranucci, K. Glazomitsky, B.C. Buckland, and J.G. Aunins, (1994). ***Monoclonal Antibody Process Development Using Medium Concentrates.*** Biotechnology Progress, **10**(1): p. 87-96.
93. Shen, D., T.R. Kiehl, S.F. Khattak, Z.J. Li, A. He, et al., (2010). ***Transcriptomic responses to sodium chloride-induced osmotic stress: A study of industrial fed-batch CHO cell cultures.*** Biotechnology Progress, **26**(4): p. 1104-1115.
94. Zhu, M.M., A. Goyal, D.L. Rank, S.K. Gupta, T.V. Boom, et al., (2005). ***Effects of Elevated pCO2 and Osmolality on Growth of CHO Cells and Production of Antibody-Fusion Protein B1: A Case Study.*** Biotechnology Progress, **21**(1): p. 70-77.
95. Zou, W., R. Edros, and M. Al-Rubeai, (2018). ***The relationship of metabolic burden to productivity levels in CHO cell lines.*** Biotechnology and applied biochemistry, **65**(2): p. 173-180.
96. Takagi, M., H. Hayashi, and T. Yoshida, (2000). ***The effect of osmolarity on metabolism and morphology in adhesion and suspension chinese hamster ovary cells producing tissue plasminogen activator.*** Cytotechnology, **32**(3): p. 171-179.
97. Kamachi, Y. and T. Omasa, (2018). ***Development of hyper osmotic resistant CHO host cells for enhanced antibody production.*** Journal of Bioscience and Bioengineering, **125**(4): p. 470-478.
98. Lin, J., M. Takagi, Y. Qu, P. Gao, and T. Yoshida, (1999). ***Enhanced monoclonal antibody production by gradual increase of osmotic pressure.*** Cytotechnology, **29**(1): p. 27-33.
99. Oh, S.K., P. Vig, F. Chua, W.K. Teo, and M.G. Yap, (1993). ***Substantial overproduction of antibodies by applying osmotic pressure and sodium butyrate.*** Biotechnology and bioengineering, **42**(5): p. 601-610.
100. Cai, Q., L. Michea, P. Andrews, Z. Zhang, G. Rocha, et al., (2002). ***Rate of increase of osmolality determines osmotic tolerance of mouse inner medullary epithelial cells.*** American Journal of Physiology-Renal Physiology, **283**(4): p. F792-F798.
101. Ryu, J.S., M.S. Lee, and G.M. Lee, (2001). ***Effects of Cloned Gene Dosage on the Response of Recombinant CHO Cells to Hyperosmotic Pressure in Regard to Cell Growth and Antibody Production.*** Biotechnology Progress, **17**(6): p. 993-999.
102. Mironescu, S. and T.M. Seed, (1977). ***Hyperosmotic injury in mammalian cells 2. Surface alterations of CHO cells in unprotected and DMSO-treated cultures.*** Cryobiology, **14**(5): p. 575-591.

103. Yang, J., C. Pan, J. Zhang, X. Sui, Y. Zhu, et al., (2017). ***Exploring the Potential of Biocompatible Osmoprotectants as Highly Efficient Cryoprotectants.*** ACS Applied Materials & Interfaces, **9**(49): p. 42516-42524.
104. Schmelzer, A.E. and W.M. Miller, (2002). ***Effects of osmoprotectant compounds on NCAM polysialylation under hyperosmotic stress and elevated pCO(2).*** Biotechnology and bioengineering, **77**(4): p. 359-368.
105. Ryu, J.S., T.K. Kim, J.Y. Chung, and G.M. Lee, (2000). ***Osmoprotective effect of glycine betaine on foreign protein production in hyperosmotic recombinant Chinese hamster ovary cell cultures differs among cell lines.*** Biotechnology and Bioengineering, **70**(2): p. 167-175.
106. Øyaas, K., T.E. Ellingsen, N. Dyrset, and D.W. Levine, (1994). ***Utilization of osmoprotective compounds by hybridoma cells exposed to hyperosmotic stress.*** Biotechnology and Bioengineering, **43**(1): p. 77-89.
107. Bougouffa, S., A. Radovanovic, M. Essack, and V.B. Bajic, (2014). ***DEOP: a database on osmoprotectants and associated pathways.*** Database : the journal of biological databases and curation, **2014**: p. bau100.
108. Walls, P.L.L., O. McRae, V. Natarajan, C. Johnson, C. Antoniou, et al., (2017). ***Quantifying the potential for bursting bubbles to damage suspended cells.*** Scientific Reports, **7**(1): p. 15102.
109. T Keane, J., D. Ryan, and P. P Gray, (2003), ***Effect of shear stress on expression of a recombinant protein by Chinese Hamster Ovary cells***. Vol. 81. 211-20.
110. Godoy-Silva, R., J.J. Chalmers, S.A. Casnocha, L.A. Bass, and N. Ma, (2009). ***Physiological responses of CHO cells to repetitive hydrodynamic stress.*** Biotechnology and Bioengineering, **103**(6): p. 1103-1117.
111. Chang, K., D. Osborne, R. Ferguson, R.I. Gilmore, D.A. Grismer, et al., (2016), ***(692c) Foam Control in the Mammalian Cell Culture Process through Extrinsic and Intrinsic Methods***, in *AIChE Annual Meeting*. San Francisco.
112. Gille, J.J.P. and H. Joenje, (1992). ***Cell culture models for oxidative stress: superoxide and hydrogen peroxide versus normobaric hyperoxia.*** Mutation Research/DNAging, **275**(3): p. 405-414.
113. Ahn, W.S. and M.R. Antoniewicz, (2011). ***Metabolic flux analysis of CHO cells at growth and non-growth phases using isotopic tracers and mass spectrometry.*** Metabolic Engineering, **13**(5): p. 598-609.
114. Halliwell, B., (2014). ***Cell culture, oxidative stress, and antioxidants: avoiding pitfalls.*** Biomed J, **37**(3): p. 99-105.
115. W. Handlogten, M., M. Zhu, and S. Ahuja, (2018), ***Intracellular Response of CHO Cells to Oxidative Stress and its Influence on Metabolism and Antibody Production***. Vol. 133.
116. Phaniendra, A., D.B. Jestadi, and L. Periyasamy, (2015). ***Free radicals: properties, sources, targets, and their implication in various diseases.*** Indian journal of clinical biochemistry : IJCB, **30**(1): p. 11-26.
117. Ryter, S., H. Kim, A. Hoetzel, J. W Park, K. Nakahira, et al., (2007), ***Mechanisms of Cell Death in Oxidative Stress***. Vol. 9. 49-89.
118. Goel, R. and K.L. Khanduja, (1998). ***Oxidative stress-induced apoptosis – An overview.*** Current Science, **75**(12): p. 1338-1345.
119. Maher, P. and A. Hanneken, (2005). ***The Molecular Basis of Oxidative Stress-Induced Cell Death in an Immortalized Retinal Ganglion Cell Line.*** Investigative Ophthalmology & Visual Science, **46**(2): p. 749-757.
120. Takahashi, A., A. Masuda, M. Sun, V.E. Centonze, and B. Herman, (2004). ***Oxidative stress-induced apoptosis is associated with alterations in mitochondrial caspase activity and Bcl-2-dependent alterations in mitochondrial pH (pHm).*** Brain research bulletin, **62**(6): p. 497-504.
121. Kannan, K. and S.K. Jain, (2000). ***Oxidative stress and apoptosis.*** Pathophysiology : the official journal of the International Society for Pathophysiology, **7**(3): p. 153-163.
122. Halliwell, B., (2003). ***Oxidative stress in cell culture: an under-appreciated problem?*** FEBS Letters, **540**(1): p. 3-6.
123. Pluschkell, S.B. and M.C. Flickinger, (1995). ***Improved methods for investigating the external redox potential in hybridoma cell culture.*** Cytotechnology, **19**(1): p. 11-26.

124. Shinto, S., Y. Matsuoka, M. Yamato, and K.-I. Yamada, (2018). ***Antioxidant nitroxides protect hepatic cells from oxidative stress-induced cell death.*** Journal of clinical biochemistry and nutrition, **62**(2): p. 132-138.
125. Skała, E.S., Przemysław; Różalski, Marek; Krajewska, Urszula; Szemraj, Janusz; Wysokińska, Halina; Śliwiński, Tomasz, (2016). ***Antioxidant and DNA Repair Stimulating Effect of Extracts from Transformed and Normal Roots of Rhaponticum carthamoides against Induced Oxidative Stress and DNA Damage in CHO Cells.*** Oxidative Medicine and Cellular Longevity, **2016**: p. 11.
126. Malhotra, J.D., H. Miao, K. Zhang, A. Wolfson, S. Pennathur, et al., (2008). ***Antioxidants reduce endoplasmic reticulum stress and improve protein secretion.*** Proceedings of the National Academy of Sciences, **105**(47): p. 18525.
127. Buettner, G.R., (1993). ***The pecking order of free radicals and antioxidants: lipid peroxidation, alpha-tocopherol, and ascorbate.*** Arch Biochem Biophys., **300**(2): p. 535-43. doi: 10.1006/abbi.1993.1074.
128. Ha, T.K., A.H. Hansen, S. Kol, H.F. Kildegaard, and G.M. Lee, (2018). ***Baicalein Reduces Oxidative Stress in CHO Cell Cultures and Improves Recombinant Antibody Productivity.*** Biotechnology Journal, **13**(3): p. 1700425.
129. Xue, L., J. Li, Y. Li, C. Chu, G. Xie, et al., (2015). ***N-acetylcysteine protects Chinese Hamster ovary cells from oxidative injury and apoptosis induced by microcystin-LR.*** International journal of clinical and experimental medicine, **8**(4): p. 4911-4921.
130. Yun, Z., M. Takagi, and T. Yoshida, (2001), ***Effect of Antioxidants on the Apoptosis of CHO Cells and Production of Tissue Plasminogen Activator in Suspension Culture***. Vol. 91. 581-585.
131. Chung, S., J. Tian, Z. Tan, J. Chen, N. Zhang, et al., (2019). ***Modulating cell culture oxidative stress reduces protein glycation and acidic charge variant formation.*** mAbs, **11**(1): p. 205-216.
132. Jagannathan, L., S. Cuddapah, and M. Costa, (2016). ***Oxidative stress under ambient and physiological oxygen tension in tissue culture.*** Current pharmacology reports, **2**(2): p. 64-72.
133. Hossler, P., S. McDermott, C. Racicot, and J.C.H. Fann, (2013). ***Improvement of mammalian cell culture performance through surfactant enabled concentrated feed media.*** Biotechnology Progress, **29**(4): p. 1023-1033.
134. Reinhart, D., L. Damjanovic, A. Castan, W. Ernst, and R. Kunert, (2018). ***Differential gene expression of a feed-spiked super-producing CHO cell line.*** Journal of Biotechnology, **285**: p. 23-37.
135. Sani, M., M. Kreukniet, G. Robinson, and F. Baganz, (2014), ***Comparison of feeding strategies for CHO cell cultures process using a single use 24-well miniature bioreactor system (micro-Matrix)***.
136. Kim, D.Y., J.C. Lee, H.N. Chang, and D.J. Oh, (2005). ***Effects of supplementation of various medium components on chinese hamster ovary cell cultures producing recombinant antibody.*** Cytotechnology, **47**(1-3): p. 37-49.
137. Ali, A.S., R. Raju, R. Kshirsagar, A.R. Ivanov, A. Gilbert, et al., (2018). ***Multi-Omics Study on the Impact of Cysteine Feed Level on Cell Viability and mAb Production in a CHO Bioprocess.*** Biotechnology journal.
138. Kuwae, S., I. Miyakawa, and T. Doi, (2018). ***Development of a chemically defined platform fed-batch culture media for monoclonal antibody-producing CHO cell lines with optimized choline content.*** Cytotechnology, **70**(3): p. 939-948.
139. Fan, Y., H.F. Kildegaard, and M.R. Andersen, (2017). ***Engineer Medium and Feed for Modulating N-Glycosylation of Recombinant Protein Production in CHO Cell Culture.*** Methods in molecular biology (Clifton, N.J.), **1603**: p. 209-226.
140. Karengera, E., A. Robotham, J. Kelly, Y. Durocher, G. De Crescenzo, et al., (2018). ***Concomitant reduction of lactate and ammonia accumulation in fed-batch cultures: Impact on glycoprotein production and quality.*** Biotechnology progress, **34**(2): p. 494-504.
141. Lin, H., R.W. Leighty, S. Godfrey, and S.B. Wang, (2017). ***Principles and approach to developing mammalian cell culture media for high cell density perfusion process leveraging established fed-batch media.*** Biotechnology Progress, **33**(4): p. 891-901.

142. Pan, X., M. Streefland, C. Dalm, R.H. Wijffels, and D.E. Martens, (2017). ***Selection of chemically defined media for CHO cell fed-batch culture processes***. Cytotechnology, **69**(1): p. 39-56.
143. Blondeel, E.J.M., R. Ho, S. Schulze, S. Sokolenko, S.R. Guillemette, et al., (2016). ***An omics approach to rational feed: Enhancing growth in CHO cultures with NMR metabolomics and 2D-DIGE proteomics***. Journal of biotechnology, **234**: p. 127-138.
144. Peng, L., X. Yu, C. Li, Y. Cai, Y. Chen, et al., (2016). ***Enhanced recombinant factor VII expression in Chinese hamster ovary cells by optimizing signal peptides and fed-batch medium***. Bioengineered, **7**(3): p. 189-197.
145. Arvia Eleanor Morris, A.V.V., Erika Pineda, (2012), ***Improved feed media***, C. Amgen Inc. Thousand Oaks, Editor.
146. Torkashvand, F., B. Vaziri, S. Maleknia, A. Heydari, M. Vossoughi, et al., (2015). ***Designed Amino Acid Feed in Improvement of Production and Quality Targets of a Therapeutic Monoclonal Antibody***. PLOS ONE, **10**(10): p. e0140597.
147. Cruz, H., C.M. Freitas, P. Alves, J.L. Moreira, and M.J.T. Carrondo, (2000), ***Effects of ammonia and lactate on growth, metabolism, and productivity of BHK cells***. Vol. 27. 43-52.
148. Lao, M.S. and D. Toth, (1997). ***Effects of ammonium and lactate on growth and metabolism of a recombinant Chinese hamster ovary cell culture***. Biotechnology progress, **13**(5): p. 688-691.
149. Freund, N.W. and M.S. Croughan, (2018). ***A Simple Method to Reduce both Lactic Acid and Ammonium Production in Industrial Animal Cell Culture***. International journal of molecular sciences, **19**(2): p. 385.
150. Brunner, M., P. Doppler, T. Klein, C. Herwig, and J. Fricke, (2018). ***Elevated pCO2 affects the lactate metabolic shift in CHO cell culture processes***. Engineering in Life Sciences, **18**(3): p. 204-214.
151. Hong, J.K., S. Nargund, M. Lakshmanan, S. Kyriakopoulos, D.Y. Kim, et al., (2018). ***Comparative phenotypic analysis of CHO clones and culture media for lactate shift***. Journal of biotechnology, **283**: p. 97-104.
152. Luo, J., N. Vijayasankaran, J. Autsen, R. Santuray, T. Hudson, et al., (2012). ***Comparative metabolite analysis to understand lactate metabolism shift in Chinese hamster ovary cell culture process***. Biotechnol Bioeng, **109**(1): p. 146-56.
153. Zagari, F., M. Jordan, M. Stettler, H. Broly, and F.M. Wurm, (2013). ***Lactate metabolism shift in CHO cell culture: the role of mitochondrial oxidative activity***. N Biotechnol., **30**(2): p. 238-45. doi: 10.1016/j.nbt.2012.05.021. Epub 2012 Jun 6.
154. Yuk, I.H., J.D. Zhang, M. Ebeling, M. Berrera, N. Gomez, et al., (2014). ***Effects of copper on CHO cells: insights from gene expression analyses***. Biotechnol Prog, **30**(2): p. 429-42.
155. Tiago M. Duarte, N.C., Laura C. Barreiro, Manuel J. T. Carrondo, Paula M. Alves, Ana P. Teixeira, (2014). ***Metabolic Responses of CHO Cells to Limitation of Key Amino Acids***. Biotechnol. Bioeng., **111**: p. 2095-2106.
156. Yeo, J.H.M., J.C.Y. Lo, P.M. Nissom, and V.V.T. Wong, (2006). ***Glutamine or Glucose Starvation in Hybridoma Cultures Induces Death Receptor and Mitochondrial Apoptotic Pathways***. Biotechnology Letters, **28**(18): p. 1445-1452.
157. Wei, Y.-Y.C., S. Naderi, M. Meshram, H. Budman, J.M. Scharer, et al., (2011). ***Proteomics analysis of chinese hamster ovary cells undergoing apoptosis during prolonged cultivation***. Cytotechnology, **63**(6): p. 663-677.
158. Feng, H., L. Guo, H. Gao, and X.-A. Li, (2011). ***Deficiency of calcium and magnesium induces apoptosis via scavenger receptor BI***. Life sciences, **88**(13-14): p. 606-612.
159. Haryadi, R., S. Ho, Y.J. Kok, H.X. Pu, L. Zheng, et al., (2015). ***Optimization of heavy chain and light chain signal peptides for high level expression of therapeutic antibodies in CHO cells***. PloS one, **10**(2): p. e0116878-e0116878.
160. Nayak, V.S., Z. Tan, P.M. Ihnat, R.J. Russell, and M.J. Grace, (2012). ***Evaporative Light Scattering Detection Based HPLC Method for the Determination of Polysorbate 80 in Therapeutic Protein Formulations***. Journal of chromatographic science, **50**(1): p. 21-25.

161. Brühlmann, D., M. Jordan, J. Hemberger, M. Sauer, M. Stettler, et al., (2015). ***Tailoring recombinant protein quality by rational media design***. Biotechnology Progress, **31**(3): p. 615-629.
162. Gramer, M.J., (2014), ***Product Quality Considerations for Mammalian Cell Culture Process Development and Manufacturing***, in *Mammalian Cell Cultures for Biologics Manufacturing*, W. Zhou and A. Kantardjieff, Editors. Springer Berlin Heidelberg: Berlin, Heidelberg. p. 123-166.
163. Torkashvand, F. and B. Vaziri, (2017). ***Main Quality Attributes of Monoclonal Antibodies and Effect of Cell Culture Components***. Iranian biomedical journal, **21**(3): p. 131-141.
164. Wei, B., K. Berning, C. Quan, and Y.T. Zhang, (2017). ***Glycation of antibodies: Modification, methods and potential effects on biological functions***. mAbs, **9**(4): p. 586-594.
165. Yuk, I.H., B. Zhang, Y. Yang, G. Dutina, K.D. Leach, et al., (2011). ***Controlling glycation of recombinant antibody in fed-batch cell cultures***. Biotechnology and Bioengineering, **108**(11): p. 2600-2610.
166. Vijayasankaran, N., S. Varma, Y. Yang, M. Mun, S. Arevalo, et al., (2013). ***Effect of cell culture medium components on color of formulated monoclonal antibody drug substance***. Biotechnol Prog, **29**(5): p. 1270-7.
167. Velugula-Yellela, S.R., A. Williams, N. Trunfio, C.-J. Hsu, B. Chavez, et al., (2018). ***Impact of media and antifoam selection on monoclonal antibody production and quality using a high throughput micro-bioreactor system***. Biotechnology Progress, **34**(1): p. 262-270.
168. Yuk, I.H., S. Russell, Y. Tang, W.T. Hsu, J.B. Mauger, et al., (2014). ***Effects of copper on CHO cells: Cellular requirements and product quality considerations***. Biotechnol Prog.
169. Kaschak, T., D. Boyd, F. Lu, G. Derfus, B. Kluck, et al., (2011). ***Characterization of the basic charge variants of a human IgG1: effect of copper concentration in cell culture media***. mAbs, **3**(6): p. 577-583.
170. Liu, M., J. Wang, H. Tang, L. Fan, L. Zhao, et al., (2018). ***Cell culture medium supplemented with taurine decreases basic charge variant levels of a monoclonal antibody***. Biotechnology letters, **40**(11-12): p. 1487-1493.
171. Luo, J., J. Zhang, D. Ren, W.L. Tsai, F. Li, et al., (2012). ***Probing of C-terminal lysine variation in a recombinant monoclonal antibody production using Chinese hamster ovary cells with chemically defined media***. Biotechnol Bioeng., **109**(9): p. 2306-15. doi: 10.1002/bit.24510. Epub 2012 Apr 11.
172. Xu, J., M.S. Rehmann, X. Xu, C. Huang, J. Tian, et al., (2018). ***Improving titer while maintaining quality of final formulated drug substance via optimization of CHO cell culture conditions in low-iron chemically defined media***. mAbs, **10**(3): p. 488-499.
173. Hazeltine, L.B., K.M. Knueven, Y. Zhang, Z. Lian, D.J. Olson, et al., (2016). ***Chemically defined media modifications to lower tryptophan oxidation of biopharmaceuticals***. Biotechnology Progress, **32**(1): p. 178-188.
174. He, L., J.X. Desai, J. Gao, L.B. Hazeltine, Z. Lian, et al., (2018). ***Elucidating the Impact of CHO Cell Culture Media on Tryptophan Oxidation of a Monoclonal Antibody Through Gene Expression Analyses***. Biotechnology Journal, **13**(10): p. 1700254.
175. Jefferis, R., (2005). ***Glycosylation of Recombinant Antibody Therapeutics***. Biotechnology Progress, **21**(1): p. 11-16.
176. Leblanc, Y., C. Ramon, N. Bihoreau, and G. Chevreux, (2017). ***Charge variants characterization of a monoclonal antibody by ion exchange chromatography coupled on-line to native mass spectrometry: Case study after a long-term storage at +5°C***. Journal of Chromatography B, **1048**: p. 130-139.
177. Higel, F., A. Seidl, F. Sorgel, and W. Friess, (2016). ***N-glycosylation heterogeneity and the influence on structure, function and pharmacokinetics of monoclonal antibodies and Fc fusion proteins***. Eur J Pharm Biopharm, **100**: p. 94-100.
178. Liu, L., (2015). ***Antibody glycosylation and its impact on the pharmacokinetics and pharmacodynamics of monoclonal antibodies and Fc-fusion proteins***. J Pharm Sci, **104**(6): p. 1866-1884.

179. Gupta, S.K. and P. Shukla, (2018). ***Glycosylation control technologies for recombinant therapeutic proteins.*** Applied microbiology and biotechnology, **102**(24): p. 10457-10468.
180. Pacis, E., M. Yu, J. Autsen, R. Bayer, and F. Li, (2011). ***Effects of cell culture conditions on antibody N-linked glycosylation--what affects high mannose 5 glycoform.*** Biotechnol Bioeng, **108**(10): p. 2348-58.
181. Lee, J.H., Y.R. Jeong, Y.-G. Kim, and G.M. Lee, (2017). ***Understanding of decreased sialylation of Fc-fusion protein in hyperosmotic recombinant Chinese hamster ovary cell culture: N-glycosylation gene expression and N-linked glycan antennary profile.*** Biotechnology and Bioengineering, **114**(8): p. 1721-1732.
182. Bruhlmann, D., A. Muhr, R. Parker, T. Vuillemin, B. Bucsella, et al., (2017). ***Cell culture media supplemented with raffinose reproducibly enhances high mannose glycan formation.*** J Biotechnol, **252**: p. 32-42.
183. Hossler, P., S. McDermott, C. Racicot, C. Chumsae, H. Raharimampionona, et al., (2014). ***Cell culture media supplementation of uncommonly used sugars sucrose and tagatose for the targeted shifting of protein glycosylation profiles of recombinant protein therapeutics.*** Biotechnology Progress, **30**(6): p. 1419-1431.
184. Rathore, A.K., Rajinder; Borgayari, Dipankar ***Impact of Media Components on CQAs of Monoclonal Antibodies***. 2017; Available from: http://www.processdevelopmentforum.com/articles/impact-of-media-components-on-cqas-of-monoclonal-antibodies/.
185. Rathore, A.S., S. Kumar Singh, M. Pathak, E.K. Read, K.A. Brorson, et al., (2015). ***Fermentanomics: Relating quality attributes of a monoclonal antibody to cell culture process variables and raw materials using multivariate data analysis.*** Biotechnology Progress, **31**(6): p. 1586-1599.
186. Mohammad, A., C. Agarabi, S. Rogstad, E. DiCioccio, K. Brorson, et al., (2019). ***An ICP-MS platform for metal content assessment of cell culture media and evaluation of spikes in metal concentration on the quality of an IgG3: κ monoclonal antibody during production.*** Journal of pharmaceutical and biomedical analysis, **162**: p. 91-100.
187. Ehret, J., M. Zimmermann, T. Eichhorn, and A. Zimmer, (2018). ***Impact of cell culture media additives on IgG glycosylation produced in Chinese hamster ovary cells.*** Biotechnology and bioengineering.
188. Gramer, M.J., J.J. Eckblad, R. Donahue, J. Brown, C. Shultz, et al., (2011). ***Modulation of antibody galactosylation through feeding of uridine, manganese chloride, and galactose.*** Biotechnology and Bioengineering, **108**(7): p. 1591-1602.
189. Purdie, J.L., R.L. Kowle, A.L. Langland, C.N. Patel, A. Ouyang, et al., (2016). ***Cell culture media impact on drug product solution stability.*** Biotechnology progress, **32**(4): p. 998-1008.
190. Sandle, T., (2010), ***History and development of microbiological culture media***.
191. Basu, S., C. Bose, N. Ojha, N. Das, J. Das, et al., (2015). ***Evolution of bacterial and fungal growth media.*** Bioinformation, **11**(4): p. 182-184.
192. Soini, J., K. Ukkonen, and P. Neubauer, (2008). ***High cell density media for Escherichia coli are generally designed for aerobic cultivations - consequences for large-scale bioprocesses and shake flask cultures.*** Microbial cell factories, **7**: p. 26.
193. Yao, T. and Y. Asayama, (2017). ***Animal-cell culture media: History, characteristics, and current issues.*** Reproductive medicine and biology, **16**(2): p. 99-117.
194. Eagle, H., (1955). ***The specific amino acid requirements of a mammalian cell (strain L) in tissue culture.*** J Biol Chem., **214**(2): p. 839-52.
195. Eagle, H., (1955). ***Nutrition needs of mammalian cells in tissue culture.*** Science., **122**(3168): p. 501-14.
196. Eagle, H., (1955). ***The specific amino acid requirements of a human carcinoma cell (Stain HeLa) in tissue culture.*** The Journal of experimental medicine, **102**: p. 37-48.
197. Eagle, H., (1955). ***Utilization of Dipeptides by Mammalian Cells in Tissue Culture***. Experimental Biology and Medicine, **89**: p. 96-9.
198. Eagle, H., (1955). ***The minimum vitamin requirements of the L and HeLa cells in tissue culture.*** The Journal of experimental medicine, **102**: p. 595-600.

199. Eagle, H., (1956). ***The salt requirements of mammalian cells in tissue culture.*** Archives of biochemistry and biophysics, **61**: p. 356-66.
200. Eagle, H., V. I Oyama, M. Levy, C. L Horton, and R. Fleischman, (1956). ***The growth response of mammalian cells in tissue culture to L-glutamine and L-glutamic acid.*** The Journal of biological chemistry, **218**: p. 607-16.
201. Eagle, H., V.I. Oyama, M. Levy, and A.E. Freeman, (1957). ***Myo-Inositol as an essential growth factor for normal and malignant human cells in tissue culture.*** J Biol Chem., **226**(1): p. 191-205.
202. Levintow, L., H. Eagle, and K. A Piez, (1957). ***The role of glutamine in protein biosynthesis in tissue culture.*** The Journal of biological chemistry, **227**: p. 929-41.
203. Eagle, H., V. I Oyama, M. Levy, and A. E Freeman, (1957). ***Myo-Inositol as an essential growth factor for normal and malignant cells in tissue culture.*** The Journal of biological chemistry, **226**: p. 191-205.
204. Eagle, H., V. I. Oyama, and M. Levy, (1957). ***Amino acid requirements of normal and malignant human cells in tissue culture.*** Archives of biochemistry and biophysics, **67**: p. 432-46.
205. E. Darnell, J. and H. Eagle, (1958). ***Glucose and glutamine in poliovirus production by HeLA cells.*** Virology, **6**: p. 556-566.
206. A Piez, K. and H. Eagle, (1958). ***The Free Amino Acid Pool of Cultured Human Cells.*** The Journal of biological chemistry, **231**: p. 533-45.
207. Eagle, H., K. A. Piez, R. Fleischman, and V. I. Oyama, (1959). ***Protein Turnover in Mammalian Cell Cultures.*** The Journal of biological chemistry, **234**: p. 592-7.
208. Eagle, H., (1960). ***The Sustained Growth of Human and Animal Cells in a Protein-Free Environment.*** Proc Natl Acad Sci U S A., **46**(4): p. 427-32.
209. Eagle, H., (1960). ***The sustained growth of human and animal cells in a protein-free environment.*** Proceedings of the National Academy of Sciences of the United States of America, **46**: p. 427-32.
210. Eagle, H., K. A Piez, and M. Levy, (1961). ***The intracellular amino acid concentrations required for protein synthesis in cultured human cells.*** The Journal of biological chemistry, **236**: p. 2039-42.
211. Eagle, H., K.A. Piez, and V. I Oyama, (1961). ***The biosynthesis of cystine in human cell cultures.*** The Journal of biological chemistry, **236**: p. 1425-8.
212. P. Cohen, E. and H. Eagle, (1961). ***A simplified chemostat for the growth of mammalian cells—Characteristics of cell growth in continuous culture.*** The Journal of experimental medicine, **113**: p. 467-74.
213. Levintow, L. and H. Eagle, (1962). ***[8] The technique of mammalian cell culture.*** Methods in Enzymology, **5**: p. 77-89.
214. Eagle, H. and K. Piez, (1962), ***Amino acid pools, protein synthesis and protein turnover in human cell cultures***. 694-705.
215. Eagle, H., (1965). ***Metabolic controls in cultured mammalian cells.*** Science (New York, N.Y.), **148**: p. 42-51.
216. A Plotkin, S., H. Eagle, L. Hayflick, D. Ikic, H. Koprowski, et al., (1969), ***Serially Cultured Animal Cells for Preparation of Viral Vaccines***. Vol. 165. 1278-82.
217. A Plotkin, S., H. Eagle, L. Hayflick, D. Ikic, H. Koprowski, et al., (1969). ***Serially Cultured Animal Cells for Preparation of Viral Vaccines.*** Science (New York, N.Y.), **165**: p. 1278-82.
218. Eagle, H., (1971). ***Buffer Combinations for Mammalian Cell Culture.*** Science (New York, N.Y.), **174**: p. 500-3.
219. Ceccarini, C. and H. Eagle, (1971). ***pH as a Determinant of Cellular Growth and Contact Inhibition.*** Proceedings of the National Academy of Sciences of the United States of America, **68**: p. 229-33.
220. M. Croce, C., H. Koprowski, and H. Eagle, (1972). ***Effect of Environmental pH on the Efficiency of Cellular Hybridization.*** Proceedings of the National Academy of Sciences of the United States of America, **69**: p. 1953-6.

221. Eagle, H., (1973). ***The Effect of Environmental pH on the Growth of Normal and Malignant Cells.*** Journal of Cellular Physiology, **82**: p. 1-8.
222. Eagle, H., (1977). ***Media for animal cell culture.*** Methods in Cell Science, **3**: p. 517-520.
223. Froud, S.J., (1999). ***The development, benefits and disadvantages of serum-free media.*** Dev Biol Stand, **99**: p. 157-66.
224. Pumper, R.W. and L.J. Alfred, (1960). ***Growth phases of mammalian cells propagated in a serum-free medium.*** Exp Cell Res., **20**: p. 630-3.
225. Ham, R.G., (1965). ***CLONAL GROWTH OF MAMMALIAN CELLS IN A CHEMICALLY DEFINED, SYNTHETIC MEDIUM.*** Proceedings of the National Academy of Sciences of the United States of America, **53**(2): p. 288-293.
226. McKeehan, W.L., W.G. Hamilton, and R.G. Ham, (1976). ***Selenium is an essential trace nutrient for growth of WI-38 diploid human fibroblasts.*** Proceedings of the National Academy of Sciences of the United States of America, **73**(6): p. 2023-2027.
227. Guilbert, L.J. and N.N. Iscove, (1976). ***Partial replacement of serum by selenite, transferrin, albumin and lecithin in haemopoitec cell cultures.*** Nature, **263**(5578): p. 594-595.
228. Hayashi, I. and G.H. Sato, (1976). ***Replacement of serum by hormones permits growth of cells in a defined medium.*** Nature, **259**(5539): p. 132-134.
229. Chang, T.H., Z. Steplewski, and H. Koprowski, (1980). ***Production of monoclonal antibodies in serum free medium.*** J Immunol Methods, **39**(4): p. 369-75.
230. Barnes, D. and G. Sato, (1980). ***Serum-free cell culture: a unifying approach.*** Cell, **22**(3): p. 649-655.
231. Barnes, D. and G. Sato, (1980). ***Methods for growth of cultured cells in serum-free medium.*** Anal Biochem., **102**(2): p. 255-70.
232. Bottenstein, J., I. Hayashi, S. Hutchings, H. Masui, J. Mather, et al., (1979), ***[6] The growth of cells in serum-free hormone-supplemented media***, in *Methods in Enzymology*. Academic Press. p. 94-109.
233. Murakami, H., H. Masui, G.H. Sato, N. Sueoka, T.P. Chow, et al., (1982). ***Growth of hybridoma cells in serum-free medium: ethanolamine is an essential component.*** Proceedings of the National Academy of Sciences, **79**(4): p. 1158-1162.
234. Chua, F., S.K. Oh, M. Yap, and W.K. Teo, (1994). ***Enhanced IgG production in eRDF media with and without serum. A comparative study.*** J Immunol Methods., **167**(1-2): p. 109-19.
235. Chua, F.K., M.G. Yap, and S.K. Oh, (1994). ***Hyper-stimulation of monoclonal antibody production by high osmolarity stress in eRDF medium.*** J Biotechnol., **37**(3): p. 265-75.
236. Parampalli, A., K. Eskridge, L. Smith, M.M. Meagher, M.C. Mowry, et al., (2007). ***Developement of serum-free media in CHO-DG44 cells using a central composite statistical design.*** Cytotechnology, **54**(1): p. 57-68.
237. Ozato, K., N. Mayer, and D.H. Sachs, (1980). ***Hybridoma cell lines secreting monoclonal antibodies to mouse H-2 and Ia antigens.*** J Immunol., **124**(2): p. 533-40.
238. Reinhart, D., L. Damjanovic, C. Kaisermayer, and R. Kunert, (2015). ***Benchmarking of commercially available CHO cell culture media for antibody production.*** Appl Microbiol Biotechnol, **99**(11): p. 4645-57.
239. Landauer, K., (2014). ***Designing media for animal cell culture: CHO cells, the industrial standard.*** Methods Mol Biol, **1104**: p. 89-103.
240. Landauer, K., H. Woischnig, N. Hepp, B. Greulich, and A. Herrmann, (2011). ***Development of a chemically defined CHO medium by engineering based on a feed solution.*** BMC proceedings, **5 Suppl 8**(Suppl 8): p. P41-P41.
241. Rouiller, Y., A. Périlleux, N. Collet, M. Jordan, M. Stettler, et al., (2013). ***A high-throughput media design approach for high performance mammalian fed-batch cultures.*** mAbs, **5**(3): p. 501-511.
242. McCoy, R.E., N.A. Costa, and A.E. Morris, (2015). ***Factors that determine stability of highly concentrated chemically defined production media.*** Biotechnol Prog, **31**(2): p. 493-502.
243. Ball, P., (2017). ***Water is an active matrix of life for cell and molecular biology.*** Proceedings of the National Academy of Sciences, **114**(51): p. 13327.

244. Mulukutla, B.C., S. Khan, A. Lange, and W.-S. Hu, (2010). ***Glucose metabolism in mammalian cell culture: new insights for tweaking vintage pathways.*** Trends in Biotechnology, **28**(9): p. 476-484.
245. Noh, S.M., S. Shin, and G.M. Lee, (2018). ***Comprehensive characterization of glutamine synthetase-mediated selection for the establishment of recombinant CHO cells producing monoclonal antibodies.*** Scientific Reports, **8**(1): p. 5361.
246. Zhang, J., T. Zhang, L. Jiang, D. Hewitt, Y. Huang, et al., (2012). ***Rapid identification of low level glycation sites in recombinant antibodies by isotopic labeling with 13C6-reducing sugars.*** Anal Chem, **84**(5): p. 2313-20.
247. Zhang, B., Y. Yang, I. Yuk, R. Pai, P. McKay, et al., (2008). ***Unveiling a Glycation Hot Spot in a Recombinant Humanized Monoclonal Antibody.*** Analytical Chemistry, **80**(7): p. 2379-2390.
248. Bunn, H.F. and P.J. Higgins, (1981). ***Reaction of monosaccharides with proteins: possible evolutionary significance.*** Science, **213**(4504): p. 222.
249. Münch, G., D. Schicktanz, A. Behme, M. Gerlach, P. Riederer, et al., (1999). ***Amino acid specificity of glycation and protein–AGE crosslinking reactivities determined with a dipeptide SPOT library.*** Nature Biotechnology, **17**: p. 1006.
250. Kwak, E.J. and S.I. Lim, (2004). ***The effect of sugar, amino acid, metal ion, and NaCl on model Maillard reaction under pH control.*** Amino Acids., **27**(1): p. 85-90. Epub 2004 Feb 27.
251. Maillard, L.-C., (1912). ***Action des acides aminés sur les sucres; formation des méla-noidines par voie methodique.*** Comptes Rendus de l'Académie des Sciences.
252. Amadori, M., (1929). ***The condensation product of glucose and p-anisidine.*** Atti Reale AccadNazlLincei, **9**(4).
253. Syrový, I., (1994). ***Glycation of albumin: reaction with glucose, fructose, galactose, ribose or glyceraldehyde measured using four methods.*** Journal of biochemical and biophysical methods, **28**(2): p. 115-121.
254. Angyal, S.J., (1989), ***Complexes of Metal Cations with Carbohydrates in Solution***, in *Advances in Carbohydrate Chemistry and Biochemistry*, R.S. Tipson and D. Horton, Editors. Academic Press. p. 1-43.
255. Alekseev, Y.E., A.D. Garnovskii, and Y.A. Zhdanov, (1998). ***Complexes of natural carbohydrates with metal cations.*** Russian Chemical Reviews, **67**(8): p. 649-669.
256. Andrae, U., J. Singh, and K. Ziegler-Skylakakis, (1985). ***Pyruvate and related α-ketoacids protect mammalian cells in culture against hydrogen peroxide-induced cytotoxicity.*** Toxicology Letters, **28**(2): p. 93-98.
257. Long, L.H. and B. Halliwell, (2009). ***Artefacts in cell culture: pyruvate as a scavenger of hydrogen peroxide generated by ascorbate or epigallocatechin gallate in cell culture media.*** Biochem Biophys Res Commun, **388**(4): p. 700-4.
258. Asmus, C., O. Mozziconacci, and C. Schöneich, (2015). ***Low-Temperature NMR Characterization of Reaction of Sodium Pyruvate with Hydrogen Peroxide.*** The journal of physical chemistry. A, **119**(6): p. 966-977.
259. Asmus, C.E.H., (2015), ***The reaction pathways of hydrogen peroxide in the presence of scavengers and its transition metal catalyzed oxidation of disulfide bridge containing peptides***, in *Pharmaceutical Chemistry and the Graduate Faculty of the University of Kansas*. University of Kansas.
260. Kim, J.J., T.E. Cummings, and J.A. Cox, (1972). ***Effect of Pyruvate on the Redox Behavior of the Iron (III)-(II) Couple.*** Analytical Letters, **5**(10): p. 703-715.
261. Willems, J.L., A.F.M. de Kort, T.B. Vree, J.M.F. Trijbels, J.H. Veerkamp, et al., (1978). ***Non‐enzymic conversion of pyruvate in aqueous solution to 2,4‐dihydroxy‐2‐methylglutaric acid.*** FEBS Letters, **86**(1): p. 42-44.
262. Zwolak, I. and D. Gołębiowska, (2018). ***Protective activity of pyruvate against vanadium-dependent cytotoxicity in Chinese hamster ovary (CHO-K1) cells.*** Toxicology and industrial health, **34**(5): p. 283-292.
263. Hossler, P., C. Racicot, C. Chumsae, S. McDermott, and K. Cochran, (2017). ***Cell culture media supplementation of infrequently used sugars for the targeted shifting of protein glycosylation profiles.*** Biotechnology Progress, **33**(2): p. 511-522.

264. Leong, D.S.Z., B.K.H. Teo, J.G.L. Tan, H. Kamari, Y.S. Yang, et al., (2018). ***Application of maltose as energy source in protein-free CHO-K1 culture to improve the production of recombinant monoclonal antibody***. Scientific reports, **8**(1): p. 4037-4037.
265. Leong, D.S.Z., J.G.L. Tan, C.L. Chin, S.Y. Mak, Y.S. Ho, et al., (2017). ***Evaluation and use of disaccharides as energy source in protein-free mammalian cell cultures***. Scientific Reports, **7**: p. 45216.
266. Fan, Y., I. Jimenez Del Val, C. Müller, J. Wagtberg Sen, S.K. Rasmussen, et al., (2015). ***Amino acid and glucose metabolism in fed-batch CHO cell culture affects antibody production and glycosylation***. Biotechnology and Bioengineering, **112**(3): p. 521-535.
267. Hosios, Aaron M., Vivian C. Hecht, Laura V. Danai, Marc O. Johnson, Jeffrey C. Rathmell, et al., (2016). ***Amino Acids Rather than Glucose Account for the Majority of Cell Mass in Proliferating Mammalian Cells***. Developmental Cell, **36**(5): p. 540-549.
268. Salazar, A., M. Keusgen, and J. von Hagen, (2016). ***Amino acids in the cultivation of mammalian cells***. Amino Acids, **48**(5): p. 1161-1171.
269. Poole, L.B., (2015). ***The basics of thiols and cysteines in redox biology and chemistry***. Free Radical Biology and Medicine, **80**: p. 148-157.
270. Greenstein, J.P.W., Milton, (1961). ***Chemistry of the Amino Acids***.
271. Dalton, J.B.S., Carl L. A., (1934). ***The solubilities of certain amino acids and related compounds in water, the densities of their solutions at twenty-five degrees, and the calculated heats of solution and partial molal volumes.***
272. Carta, R., (1998). ***Solubilities ofL-cystine,L-tyrosine,L-leucine, and glycine in sodium chloride solutions at various pH values***. The Journal of Chemical Thermodynamics, **30**(3): p. 379-387.
273. Carta, R.T., Giuseppe, (1996). ***Solubilities of L-Cystine, L-Tyrosine, L-Leucine, and Glycine in Aqueous Solutions at Various pHs and NaCl Concentrations***. J. Chem. Eng. Data, **41**: p. 414-417.
274. Remucal, C.K. and K. McNeill, (2011). ***Photosensitized amino acid degradation in the presence of riboflavin and its derivatives***. Environ Sci Technol, **45**(12): p. 5230-7.
275. Šoškić, V., K. Groebe, and A. Schrattenholz, (2008). ***Nonenzymatic posttranslational protein modifications in ageing***. Experimental Gerontology, **43**(4): p. 247-257.
276. Stadtman, E.R., (1993). ***Oxidation of free amino acids and amino acid residues in proteins by radiolysis and by metal-catalyzed reactions***. Annu Rev Biochem, **62**: p. 797-821.
277. Tolosa, S., A. Hidalgo, and J.A. Sanson, (2012). ***Amino acid tautomerization reactions in aqueous solution via concerted and assisted mechanisms using free energy curves from MD simulation***. J Phys Chem B., **116**(43): p. 13033-44. doi: 10.1021/jp307391s. Epub 2012 Oct 22.
278. Weeks, B.M., S.A. Cole, and W.M. Garrison, (1965). ***Reactions of Alanine with the Reducing Species Formed in Water Radiolysis1***. The Journal of Physical Chemistry, **69**(12): p. 4131-4137.
279. Makhnyr, V.M., (1986). ***Chemical modification of the arginine residues of proteins and peptides***.
280. Toi, K., E. Bynum, E. Norris, and H.A. Itano, (1967). ***Studies on the chemical modification of arginine. I. The reaction of 1,2-cyclohexanedione with arginine and arginyl residues of proteins***. J Biol Chem., **242**(5): p. 1036-43.
281. Turras, P., (2008), ***Hydrolysis of L-Arginine - Chemical and Enzymatic Catalysis***, in *Instituto Superior Técnico*. Universidade Técnica de Lisboa.
282. Blank, I., F. Robert, T. Goldmann, P. Pollien, N. Varga, et al., (2005). ***Mechanisms of acrylamide formation: Maillard-induced transformation of asparagine***. Adv Exp Med Biol, **561**: p. 171-89.
283. Catak, S., G. Monard, V. Aviyente, and M.F. Ruiz-López, (2009). ***Deamidation of Asparagine Residues: Direct Hydrolysis versus Succinimide-Mediated Deamidation Mechanisms***. The Journal of Physical Chemistry A, **113**(6): p. 1111-1120.
284. Geiger, T. and S. Clarke, (1987). ***Deamidation, isomerization, and racemization at asparaginyl and aspartyl residues in peptides. Succinimide-linked reactions that contribute to protein degradation***. J Biol Chem., **262**(2): p. 785-94.

285. Gokmen, V. and H.Z. Senyuva, (2006). ***A simplified approach for the kinetic characterization of acrylamide formation in fructose-asparagine model system.*** Food Addit Contam., **23**(4): p. 348-54.
286. Heaton, A.L. and P.B. Armentrout, (2009). ***Thermodynamics and mechanism of protonated asparagine decomposition.*** J Am Soc Mass Spectrom., **20**(5): p. 852-66. doi: 10.1016/j.jasms.2008.12.027. Epub 2009 Jan 9.
287. Heaton, A.L. and P.B. Armentrout, (2008). ***Thermodynamics and Mechanism of the Deamidation of Sodium-Bound Asparagine.*** Journal of the American Chemical Society, **130**(31): p. 10227-10232.
288. Heaton, A.L., R.M. Moision, and P.B. Armentrout, (2008). ***Experimental and Theoretical Studies of Sodium Cation Interactions with the Acidic Amino Acids and Their Amide Derivatives.*** The Journal of Physical Chemistry A, **112**(15): p. 3319-3327.
289. Heaton, A.L., S.J. Ye, and P.B. Armentrout, (2008). ***Experimental and theoretical studies of sodium cation complexes of the deamidation and dehydration products of asparagine, glutamine, aspartic acid, and glutamic acid.*** J Phys Chem A., **112**(15): p. 3328-38. doi: 10.1021/jp800439j. Epub 2008 Mar 21.
290. Hidalgo, F.J., R.M. Delgado, J.L. Navarro, and R. Zamora, (2010). ***Asparagine decarboxylation by lipid oxidation products in model systems.*** J Agric Food Chem., **58**(19): p. 10512-7. doi: 10.1021/jf102026c.
291. Stephenson, R.C. and S. Clarke, (1989). ***Succinimide formation from aspartyl and asparaginyl peptides as a model for the spontaneous degradation of proteins.*** J Biol Chem., **264**(11): p. 6164-70.
292. Abdel-Halim, H.M., (2006). ***Kinetics of the Oxidation of L-Cysteine by trans- and cis-Cobalt(III) and Iron(III) Complexes.*** Z.Naturforsch., **61b**: p. 1346-1350.
293. Albert, A., (1951). ***Quantitative Studies of the Avidity of Naturally Occuring Substances for Trace Metals.***
294. Fedorcsák, I.H.-R., M.; Ehrenberg, L., (1977). ***PREVENTION OF SULFHYDRYL AUTOXIDATION BY A POLYPEPTIDE FROM RED KIDNEY BEANS, DESCRIBED TO BE A STIMULATOR OF RNA SYNTHESIS.*** Experimental Cell Research, **108**: p. 331-339.
295. Kang, S., J. Mullen, L.P. Miranda, and R. Deshpande, (2012). ***Utilization of tyrosine- and histidine-containing dipeptides to enhance productivity and culture viability.*** Biotechnology and Bioengineering, **109**(9): p. 2286-2294.
296. Barrett, S. and S. Jacobia, (2013), ***Cell culture medium comprising small peptides***. Google Patents.
297. Spearman, M., S. Chan, V. Jung, V. Kowbel, M. Mendoza, et al., (2016). ***Components of yeast (Sacchromyces cervisiae) extract as defined media additives that support the growth and productivity of CHO cells.*** J Biotechnol, **233**: p. 129-42.
298. Spearman, M., C. Lodewyks, M. Richmond, and M. Butler, (2014). ***The bioactivity and fractionation of peptide hydrolysates in cultures of CHO cells.*** Biotechnology Progress, **30**(3): p. 584-593.
299. Hecklau, C., S. Pering, R. Seibel, A. Schnellbaecher, M. Wehsling, et al., (2016). ***S-Sulfocysteine simplifies fed-batch processes and increases the CHO specific productivity via anti-oxidant activity.*** J Biotechnol., **218:53-63.**(doi): p. 10.1016/j.jbiotec.2015.11.022. Epub 2015 Dec 2.
300. Mueller, R., I. Joy-Hillesheim, K. El Bagdadi, M. Wehsling, C. Jasper, et al., (2013). ***Improved fed-batch bioprocesses using chemically modified amino acids in concentrated feeds.*** BMC Proceedings, **7**(Suppl 6): p. P46-P46.
301. Zimmer, A., R. Mueller, M. Wehsling, A. Schnellbaecher, and J. von Hagen, (2014). ***Improvement and simplification of fed-batch bioprocesses with a highly soluble phosphotyrosine sodium salt.*** Journal of Biotechnology, **186**: p. 110-118.
302. Büntemeyer, H. and J. Lehmann, (2001), ***The Role of Vitamins in Cell Culture Media***, in *Animal Cell Technology: From Target to Market: Proceedings of the 17th ESACT Meeting Tylösand, Sweden, June 10–14, 2001*, E. Lindner-Olsson, N. Chatzissavidou, and E. Lüllau, Editors. Springer Netherlands: Dordrecht. p. 204-206.

303. Arigony, A.L.V., I.M. de Oliveira, M. Machado, D.L. Bordin, L. Bergter, et al., (2013). ***The influence of micronutrients in cell culture: a reflection on viability and genomic stability***. BioMed research international, **2013**: p. 597282-597282.
304. Collin, R.L., (1957). ***POLYMORPHISM AND RADIATION DECOMPOSITION OF CHOLINE CHLORIDE1***. Journal of the American Chemical Society, **79**(22): p. 6086-6086.
305. Litwin, J., (1992). ***The growth of Vero cells in suspension as cell-aggregates in serum-free media***. Cytotechnology, **10**(2): p. 169-174.
306. Kurano, S., N. Kurano, C. Leist, and A. Fiechter, (1990). ***Utilization and stability of vitamins in serum-containing and serum-free media in CHO cell culture***. Cytotechnology, **4**(3): p. 243-250.
307. Sarkar, B.D., U Fau - Bhattacharyya, S., Bhattacharyya, S Fau; Bose, S. K., (1997). ***Studies on the aerobic photooxidation of cysteine using riboflavin as a sensitizer: evidence for the photogeneration of a superoxide anion and hydrogen peroxide***. Biol Pharm Bull, **20**(8): p. 910-2.
308. Sheraz, M.A., S.H. Kazi, S. Ahmed, Z. Anwar, and I. Ahmad, (2014). ***Photo, thermal and chemical degradation of riboflavin***. Beilstein Journal of Organic Chemistry, **10**: p. 1999-2012.
309. Zang, L., R. Frenkel, J. Simeone, M. Lanan, M. Byers, et al., (2011). ***Metabolomics profiling of cell culture media leading to the identification of riboflavin photosensitized degradation of tryptophan causing slow growth in cell culture***. Anal Chem, **83**(13): p. 5422-30.
310. Melville, D.B., (1954). ***Biotin sulfoxide***. J Biol Chem., **208**(2): p. 495-501.
311. Lauw, S.J.L., R. Ganguly, and R.D. Webster, (2013). ***The electrochemical reduction of biotin (vitamin B7) and conversion into its ester***. Electrochimica Acta, **114**: p. 514-520.
312. Khan, M.M.T. and A.E. Martell, (1967). ***Metal ion and metal chelate catalyzed oxidation of ascorbic acid by molecular oxygen. I. Cupric and ferric ion catalyzed oxidation***. Journal of the American Chemical Society, **89**(16): p. 4176.
313. Bakurdjieva, N., (1966). ***Effect of manganese, nickel, copper and iron on the oxidation of ascorbic acid by the enzymic and non-enzymic way***. C R Acad Bulg Sci, **19**(11): p. 1067-70.
314. Chumsae, C., P. Hossler, H. Raharimampionona, Y. Zhou, S. McDermott, et al., (2015). ***When Good Intentions Go Awry: Modification of a Recombinant Monoclonal Antibody in Chemically Defined Cell Culture by Xylosone, an Oxidative Product of Ascorbic Acid***. Anal Chem, **87**(15): p. 7529-34.
315. Hsieh, Y.H.P. and N.D. Harris, (1993). ***Effect of sucrose on oxygen uptake of ascorbic acid in a closed aqueous system***. Journal of Agricultural and Food Chemistry, **41**(2): p. 259-262.
316. Jansson, P.J., H.R. Jung, C. Lindqvist, and T. Nordström, (2004). ***Oxidative decomposition of vitamin C in drinking water***. Free radical research, **38**(8): p. 855-860.
317. Jiang, D., X. Li, L. Liu, G.B. Yagnik, and F. Zhou, (2010). ***Reaction Rates and Mechanism of the Ascorbic Acid Oxidation by Molecular Oxygen Facilitated by Cu(II)-Containing Amyloid-β Complexes and Aggregates***. The Journal of Physical Chemistry B, **114**(14): p. 4896-4903.
318. Rzymkowski, J., J. Reitstotter, and R. Kalusa, (1951). ***[Oxidation potential of iron and copper ascorbinates compared with that of ascorbic acid]***. Biochem Z, **322**(1): p. 9-15.
319. Sealock, R.R.G., Ruth L.; Sumerwell, William N.; Brierley, John M., (1951). ***THE ROLE OF ASCORBIC ACID IN THE OXIDATION OF L-TYROSINE BY GUINEA PIG LIVER EXTRACTS**** Journal of Biological Chemistry: p. 761-7.
320. Takahama, U., S. Hirota, A. Yamamoto, and T. Oniki, (2003). ***Oxygen uptake during the mixing of saliva with ascorbic acid under acidic conditions: possibility of its occurrence in the stomach***. FEBS Lett., **550**(1-3): p. 64-8.
321. Bilski, P., M.Y. Li, M. Ehrenshaft, M.E. Daub, and C.F. Chignell, (2007). ***Vitamin B6 (Pyridoxine) and Its Derivatives Are Efficient Singlet Oxygen Quenchers and Potential Fungal Antioxidants***. Photochemistry and Photobiology, **71**(2): p. 129-134.
322. Hill, J.M. and P.J.G. Mann, (1966). ***The oxidation of Schiff bases of pyridoxal and pyridoxal phosphate with amino acids by manganous ions and peroxidase***. Biochemical Journal, **99**(2): p. 454-468.

323. Moorthy, P.N. and E. Hayon, (1975). ***One-electron redox reactions of water-soluble vitamins. III. Pyridoxine and pyridoxal phosphate (vitamin B6)***. Journal of the American Chemical Society, **97**(8): p. 2048-2052.
324. Devi, A.G. and S. Satyanarayana, (1999). ***Potentiometric and 1 H NMR studies of binary and ternary complexes of thiamine hydrochloride with copper (II), zinc (II), nickel (II) or cobalt (II) and various secondary ligands***. NISCAIR-CSIR, India: p. 624-627.
325. Dwivedi, B.K. and R.G. Arnold, (1973). ***Chemistry of thiamine degradation in food products and model systems: a review***. J Agric Food Chem., **21**(1): p. 54-60.
326. Katz, H.B. and K. Kustin, (1973). ***Thiamine pyrophosphate-metal ion complexation: equilibrium and kinetics***. Biochimica et Biophysica Acta (BBA) - General Subjects, **313**(2): p. 235-248.
327. Khurshid, S., (2014), ***Investigations of Ferrous Thiamine Complex by Cyclic Voltammetry***. Vol. 4. 718-726.
328. Lhoest, W.J., L.W. Busse, and C.A. Baumann, (1958). ***Nonenzymatic destruction of thiamine***. Journal of the American Pharmaceutical Association, **47**(4): p. 254-257.
329. Matsukawa, T. and S. Yurugi, (1953). ***On a new derivative of thiamine with cysteine***. Science., **118**(3056): p. 109-11.
330. Abu-Soud, H.M., D. Maitra, J. Byun, C.E.A. Souza, J. Banerjee, et al., (2012). ***The reaction of HOCl and cyanocobalamin: corrin destruction and the liberation of cyanogen chloride***. Free Radic Biol Med, **52**(3): p. 616-625.
331. Ahmad, I., K. Qadeer, S. Zahid, M.A. Sheraz, T. Ismail, et al., (2014). ***Effect of Ascorbic Acid on the Degradation of Cyanocobalamin and Hydroxocobalamin in Aqueous Solution: A Kinetic Study***. AAPS PharmSciTech, **15**(5): p. 1324-1333.
332. Juzeniene, A. and Z. Nizauskaite, (2013). ***Photodegradation of cobalamins in aqueous solutions and in human blood***. J Photochem Photobiol B, **122**: p. 7-14.
333. Prentice, H.L., B.N. Ehrenfels, and W.P. Sisk, (2007). ***Improving Performance of Mammalian Cells in Fed-Batch Processes through "Bioreactor Evolution"***. Biotechnology Progress, **23**(2): p. 458-464.
334. Arribas-Lorenzo, G. and F.J. Morales, (2009). ***Effect of Pyridoxamine on Acrylamide Formation in a Glucose/Asparagine Model System***. Journal of Agricultural and Food Chemistry, **57**(3): p. 901-909.
335. Adrover, M., B. Vilanova, F. Munoz, and J. Donoso, (2005). ***Inhibition of glycosylation processes: the reaction between pyridoxamine and glucose***. Chem Biodivers., **2**(7): p. 964-75.
336. Allegri, G., A. De Antoni, and C. Costa, (1971). ***Non-enzymatic transamination between pyridoxal-5-phosphate and kynurenines in the presence of zinc ions***. Ital J Biochem., **20**(5): p. 139-42.
337. Allegri, G., A. De Antoni, and C. Costa, (1972). ***Catalytic effect of metal ions on non-enzymatic transamination between pyridoxal phosphate and kynurenines***. Ital J Biochem., **21**(5): p. 298-304.
338. Cennamo, C., (1954). ***Non-enzymatic transamination between peptides and pyridoxal***. Naturwissenschaften, **41**(2): p. 39-39.
339. Cennamo, C., (1961). ***[Non-enzymatic transamination between pyridoxal and amino acid esters]***. Boll Soc Ital Biol Sper., **37**: p. 183-7.
340. Franklin, T.A., (1978), ***Metal complexes involving pyridoxine and pyridoxamine***, in *Department of Chemistry*. Brock University.
341. Kurauchi, Y., K. Ohga, M. Moriguchi, and S. Morita, (1980). ***Photoinduced Decarboxylation-dependent Transamination of Pyridoxal 5′-Phosphate-α-Amino Acid Schiff Bases***. Agricultural and Biological Chemistry, **44**(10): p. 2499-2500.
342. Mackay, D., (1962). ***The Mechanism of the Reaction of Cysteine with Pyridoxal 5'-Phosphate***. ARCHIVES OF BIOCHEMISTRY AND BIOPHYSICS, **99**: p. 93-100.
343. Metzler, D.E. and E.E. Snell, (1952). ***Deamination of serine. I. Catalytic deamination of serine and cysteine by pyridoxal and metal salts***. J Biol Chem., **198**(1): p. 353-61.
344. Metzler, D.E. and E.E. Snell, (1952). ***Some Transamination Reactions Involving Vitamin B61***. Journal of the American Chemical Society, **74**(4): p. 979-983.

345. Siegel, F.P. and M.I. Blake, (1965). ***Buffer effects in the nonenzymatic transamination of L-alanine and pyridoxal***. Journal of Pharmaceutical Sciences, **54**(1): p. 155-156.
346. Sato, S., H. Murakami, T. Sugahara, T. Ikegami, K. Yamada, et al., (1989). ***Stimulation of monoclonal antibody production by human-human hybridoma cells with an elevated concentration of potassium or sodium phosphate in serum-free medium***. Cytotechnology, **2**(1): p. 63-67.
347. Wang, S.B., A. Lee-Goldman, J. Ravikrishnan, L. Zheng, and H. Lin, (2018). ***Manipulation of the sodium-potassium ratio as a lever for controlling cell growth and improving cell specific productivity in perfusion CHO cell cultures***. Biotechnology and Bioengineering, **115**(4): p. 921-931.
348. Maralingannavar, V., D. Parmar, T. Pant, C. Gadgil, V. Panchagnula, et al., (2017). ***CHO Cells adapted to inorganic phosphate limitation show higher growth and higher pyruvate carboxylase flux in phosphate replete conditions***. Biotechnology Progress, **33**(3): p. 749-758.
349. Kim, W.H., J.-S. Kim, Y. Yoon, and G.M. Lee, (2009). ***Effect of Ca2+ and Mg2+ concentration in culture medium on the activation of recombinant factor IX produced in Chinese hamster ovary cells***. Journal of Biotechnology, **142**(3): p. 275-278.
350. Cummings, S., J.E. Enderby, G.W. Neilson, J.R. Newsome, R.A. Howe, et al., (1980). ***Chloride ions in aqueous solutions***. Nature, **287**(5784): p. 714-716.
351. Enderby, J.E., (1981). ***Ions in aqueous solutions***. Science Progress (1933-), **67**(268): p. 553-573.
352. Hewish, N.A., G.W. Neilson, and J.E. Enderby, (1982). ***Environment of Ca2+ ions in aqueous solvent***. Nature, **297**(5862): p. 138-139.
353. Varma, S. and S.B. Rempe, (2006). ***Coordination numbers of alkali metal ions in aqueous solutions***. Biophysical Chemistry, **124**(3): p. 192-199.
354. Blake, B., (2003). ***Solubility Rules: Three Suggestions for Improved Understanding***. Journal of Chemical Education, **80**(11): p. 1348.
355. Messer, H.H.M., Elsa J.; Goebel, Nancy K., (1982). ***Removal of Trace Metals from culture Media and Sera for In Vitro Deficiency Studies***. Journal of Nutrition.
356. Rayner, M.H. and K.T. Suzuki, (1995). ***A simple and effective method for the removal of trace metal cations from a mammalian culture medium supplemented with 10% fetal calf serum***. Biometals., **8**(3): p. 188-92.
357. Nargund, S., J. Qiu, and C.T. Goudar, (2015). ***Elucidating the role of copper in CHO cell energy metabolism using 13C metabolic flux analysis***. Biotechnology Progress, **31**(5): p. 1179-1186.
358. Qian, Y., S.F. Khattak, Z. Xing, A. He, P.S. Kayne, et al., (2011). ***Cell culture and gene transcription effects of copper sulfate on Chinese hamster ovary cells***. Biotechnology Progress, **27**(4): p. 1190-1194.
359. Ryll, T., (2003), ***In which the sialic acid content is increased by addition of copper ion to a serum-free medium; can lengthen protein bioavailability and serum half-life***, I. Genentech, Editor. Genentech, Inc.
360. Puig, S. and D.J. Thiele, (2002). ***Molecular mechanisms of copper uptake and distribution***. Curr Opin Chem Biol., **6**(2): p. 171-80.
361. Kim, B.E., T. Nevitt, and D.J. Thiele, (2008). ***Mechanisms for copper acquisition, distribution and regulation***. Nat Chem Biol, **4**(3): p. 176-85.
362. Chaderjian, W.B., E.T. Chin, R.J. Harris, and T.M. Etcheverry, (2005). ***Effect of copper sulfate on performance of a serum-free CHO cell culture process and the level of free thiol in the recombinant antibody expressed***. Biotechnol Prog., **21**(2): p. 550-3.
363. Kang, S., G. Xiao, D. Ren, Z. Zhang, N. Le, et al., (2014). ***Proteomics analysis of altered cellular metabolism induced by insufficient copper level***. J Biotechnol, **189**: p. 15-26.
364. Drapeau, D., J. Snow, G. Hiller, and Y.T. Luan, (2009), ***Use of Copper Glutamate in Cell Culture for Production of Polypeptides***. Wyeth.
365. Camakaris, J., (1995). ***Gene amplification of the Menkes (MNK; ATP7A) P-type ATPase gene of CHO cells is associated with copper resistance and enhanced copper efflux***. Human Molecular Genetics, **4**(11).

366. Ghosh, M.M.O.C., John T.; Engelbrecht, R: S. , (1966). ***Precipitation of iron in aerated ground waters.*** Sanitary Engineering Division.
367. Bai, Y., C. Wu, J. Zhao, Y.H. Liu, W. Ding, et al., (2011). ***Role of iron and sodium citrate in animal protein-free CHO cell culture medium on cell growth and monoclonal antibody production.*** Biotechnol Prog, **27**(1): p. 209-19.
368. Baker, E., S.M. Baker, and E.H. Morgan, (1998). ***Characterisation of non-transferrin-bound iron (ferric citrate) uptake by rat hepatocytes in culture.*** Biochimica et Biophysica Acta (BBA) - General Subjects, **1380**(1): p. 21-30.
369. Kan, M. and I. Yamane, (1984). ***Effects of ferrous iron and transferrin on cell proliferation of human diploid fibroblasts in serum-free culture.*** In Vitro, **20**(2): p. 89.
370. George W. Bates, C.B., Paul Saltman, (1967). ***The Kinetics and Mechanism of Iron(III) Exchange between Chelates and Transferrin I. THE COMPLEXES OF CITRATE AND NITRILOTRIACETIC ACID.*** American Society of Biological Chemists, Inc.
371. Graham, R.M., E.H. Morgan, and E. Baker, (1998). ***Characterisation of citrate and iron citrate uptake by cultured rat hepatocytes.*** J Hepatol., **29**(4): p. 603-13.
372. Kalinowski, D.S. and D.R. Richardson, (2005). ***The evolution of iron chelators for the treatment of iron overload disease and cancer.*** Pharmacol Rev, **57**(4): p. 547-83.
373. Rasmussen, L. and H. Toftlund, (1986). ***Phosphate compounds as iron chelators in animal cell cultures.*** In Vitro Cell Dev Biol., **22**(4): p. 177-9.
374. Silva, A.M., X. Kong, M.C. Parkin, R. Cammack, and R.C. Hider, (2009). ***Iron(III) citrate speciation in aqueous solution.*** Dalton Trans, (40): p. 8616-25.
375. Zu D. Liu, R.C.H., (2002). ***Design of Clinically Useful Iron(III)-Selective Chelators.*** Medicinal Research Reviews, **22**(1): p. 26-64.
376. Chung, M.C.-M., (1984). ***Structure and function of transferrin.*** Biochemical Education, **12**(4).
377. Cammack, R., J. M Wrigglesworth, and H. Baum, (1990), ***IRON-DEPENDENT ENZYMES IN MAMMALIAN SYSTEMS***. 17-39.
378. Eberhardy, S.R., L. Radzniak, and Z. Liu, (2009). ***Iron (III) citrate inhibits polyethylenimine-mediated transient transfection of Chinese hamster ovary cells in serum-free medium.*** Cytotechnology, **60**(1-3): p. 1-1.
379. Gaboriau, F., A. Kreder, N. Clavreul, J.-P. Moulinoux, J.-G. Delcros, et al., (2004). ***Polyamine modulation of iron uptake in CHO cells.*** Biochemical pharmacology, **67**(9): p. 1629-1637.
380. Byrnes, C., Y.T. Lee, E.R. Meier, A. Rabel, D.B. Sacks, et al., (2013). ***Iron dose-dependent differentiation and enucleation of human erythroblasts in serum-free medium.*** J Tissue Eng Regen Med, **18**(10).
381. Clincke, M.-F., E. Guedon, F.T. Yen, V. Ogier, and J.-L. Goergen, (2011). ***Effect of iron sources on the glycosylation macroheterogeneity of human recombinant IFN-γ produced by CHO cells during batch processes.*** BMC Proceedings, **5**(8): p. P114.
382. Kim, B.G. and H.W. Park, (2016). ***High zinc ion supplementation of more than 30 μM can increase monoclonal antibody production in recombinant Chinese hamster ovary DG44 cell culture.*** Applied Microbiology and Biotechnology, **100**(5): p. 2163-2170.
383. Hildebrand, C.E., M.D. Enger, and R.A. Tobey, (1980). ***Comparative studies of zinc metabolism in cultured chinese hamster cells with differing metallothionein-induction capacities.*** Biological Trace Element Research, **2**(4): p. 235.
384. Bhatia, H.Y., Seongkyu, (2018), ***Understanding the zinc induced lactate shift in CHO cell culture at transcriptomics level to improve the protein productionel to improve the protein production***, in *Cell Culture Engineering XVI ECI Symposium Series*.
385. Prabhu, A., R. Gadre, and M. Gadgil, (2018). ***Zinc supplementation decreases galactosylation of recombinant IgG in CHO cells.*** Applied Microbiology and Biotechnology, **102**(14): p. 5989-5999.
386. Wong, V.V.T., K.W. Ho, and M.G.S. Yap, (2004). ***Evaluation of insulin-mimetic trace metals as insulin replacements in mammalian cell cultures.*** Cytotechnology, **45**(3): p. 107-115.
387. Crowell, C.K., G.E. Grampp, G.N. Rogers, J. Miller, and R.I. Scheinman, (2007). ***Amino acid and manganese supplementation modulates the glycosylation state of erythropoietin in a CHO culture system.*** Biotechnology and Bioengineering, **96**(3): p. 538-549.

388. Surve, T. and M. Gadgil, (2015). ***Manganese increases high mannose glycoform on monoclonal antibody expressed in CHO when glucose is absent or limiting: Implications for use of alternate sugars.*** Biotechnology Progress, **31**(2): p. 460-467.
389. Mendel, R.R. and F. Bittner, (2006). ***Cell biology of molybdenum.*** Biochimica et Biophysica Acta (BBA) - Molecular Cell Research, **1763**(7): p. 621-635.
390. Zeng, H., (2009). ***Selenium as an essential micronutrient: roles in cell cycle and apoptosis.*** Molecules (Basel, Switzerland), **14**(3): p. 1263-1278.
391. Zhang, J., D. Robinson, and P. Salmon, (2006). ***A novel function for selenium in biological system: Selenite as a highly effective iron carrier for Chinese hamster ovary cell growth and monoclonal antibody production.*** Biotechnology and Bioengineering, **95**(6): p. 1188-1197.
392. Zwolak, I., (2015). ***Increased Cytotoxicity of Vanadium to CHO-K1 Cells in the Presence of Inorganic Selenium.*** Bulletin of environmental contamination and toxicology, **95**(5): p. 593-598.
393. Hossler, P. and C. Racicot, (2015). ***Targeted Shifting of Protein Glycosylation Profiles in Mammalian Cell Culture through Media Supplementation of Cobalt.*** Journal of Glycobiology, **03**(108): p. 2-9.
394. Prabhu, A. and M. Gadgil, (2019). ***Nickel and cobalt affect galactosylation of recombinant IgG expressed in CHO cells.*** BioMetals, **32**(1): p. 11-19.
395. Permenter, M.G., W.E. Dennis, T.E. Sutto, D.A. Jackson, J.A. Lewis, et al., (2014). ***Exposure to Cobalt Causes Transcriptomic and Proteomic Changes in Two Rat Liver Derived Cell Lines.*** PLOS ONE, **8**(12): p. e83751.
396. Kasten, U., A. Hartwig, and D. Beyersmann, (1992). ***Mechanisms of cobalt(II) uptake into V79 Chinese hamster cells.*** Archives of Toxicology, **66**(8): p. 592-597.
397. Wessjohann, L.A., A. Schneider, M. Abbas, and W. Brandt, (2007). ***Selenium in chemistry and biochemistry in comparison to sulfur.*** Biol Chem., **388**(10): p. 997-1006.
398. Elliott, K.A.C., (1930). ***On the catalysis of the oxidation of cysteine and thioglycollic acid by iron and copper.***
399. Osberger, T.J., D.C. Rogness, J.T. Kohrt, A.F. Stepan, and M.C. White, (2016). ***Oxidative diversification of amino acids and peptides by small-molecule iron catalysis.*** Nature, **537**: p. 214.
400. Pirie, N.W., (1931). ***The oxidation of sulphydryl compounds by hydrogen peroxide: Catalysis of oxidation of cysteine and glutathione by iron and copper.*** Biochemical Journal, **25**(5): p. 1565-1579.
401. Minotti G Fau - Aust, S.D. and A. SD, (1987). ***- The requirement for iron (III) in the initiation of lipid peroxidation by iron (II) and hydrogen peroxide.*** J Biol Chem, **262**(3): p. 1098-104.
402. Taylor, J.E., J.F. Yan, and J.L. Wang, (1966). ***The iron(3)-catalyzed oxidation of cysteine by molecular oxygen in the aqueous phase. An example of a two-thirds-order reaction.*** J Am Chem Soc., **88**(8): p. 1663-7.
403. Tanaka, N.K., I.M.; Stricks, W., (1954). ***Iron-Cysteinate Complexes.***
404. Sutton, H.C. and C.C. Winterbourn, (1989). ***On the participation of higher oxidation states of iron and copper in Fenton reactions.*** Free Radic Biol Med, **6**(1): p. 53-60.
405. Miller, D.M., G.R. Buettner, and S.D. Aust, (1990). ***Transition metals as catalysts of "autoxidation" reactions.*** Free Radical Biology and Medicine, **8**(1): p. 95-108.
406. Borodulin, R.R., C. Dereven'kov Icapital A, D. Burbaev, S.V. Makarov, V.D. Mikoyan, et al., (2014). ***Redox activities of mono- and binuclear forms of low-molecular and protein-bound dinitrosyl iron complexes with thiol-containing ligands.*** Nitric Oxide., **40:100-9.**(doi): p. 10.1016/j.niox.2014.06.005. Epub 2014 Jul 2.
407. Prudent, M. and H.H. Girault, (2009). ***The role of copper in cysteine oxidation: study of intra- and inter-molecular reactions in mass spectrometry.*** Metallomics, **1**(2): p. 157-65.
408. Gautier-Luneau, I., P. Bertet, A. Jeunet, G. Serratrice, and J.L. Pierre, (2007). ***Iron-citrate complexes and free radicals generation: is citric acid an innocent additive in foods and drinks?*** Biometals, **20**(5): p. 793-6.
409. Gautier-Luneau, I., C. Merle, D. Phanon, C. Lebrun, F. Biaso, et al., (2005). ***New trends in the chemistry of iron(III) citrate complexes: correlations between X-ray structures and solution***

species probed by electrospray mass spectrometry and kinetics of iron uptake from citrate by iron chelators. Chemistry., **11**(7): p. 2207-19.

410. Kocha, T., M. Yamaguchi, H. Ohtaki, T. Fukuda, and T. Aoyagi, (1997). ***Hydrogen peroxide-mediated degradation of protein: different oxidation modes of copper- and iron-dependent hydroxyl radicals on the degradation of albumin.*** Biochimica et Biophysica Acta (BBA) - Protein Structure and Molecular Enzymology, **1337**(2): p. 319-326.
411. Winterbourn, C.C., (1995). ***Toxicity of iron and hydrogen peroxide: the Fenton reaction.*** Toxicol Lett., **82-83**: p. 969-74.
412. Welch, K.D., T.Z. Davis, and S.D. Aust, (2002). ***Iron autoxidation and free radical generation: effects of buffers, ligands, and chelators.*** Arch Biochem Biophys., **397**(2): p. 360-9. doi: 10.1006/abbi.2001.2694.
413. Merkofer, M., R. Kissner, R. C Hider, U. T Brunk, and W. Koppenol, (2006), ***Fenton Chemistry and Iron Chelation under Physiologically Relevant Conditions: Electrochemistry and Kinetics***. Vol. 19. 1263-9.
414. Wardman, P. and L.P. Candeias, (1996). ***Fenton chemistry: an introduction.*** Radiat Res., **145**(5): p. 523-31.
415. Buettner, G. and B. Jurkiewicz, (1996). ***- Catalytic metals, ascorbate and free radicals: combinations to avoid.*** Radiat Res, **145**(5): p. 532-41.
416. Aruoma, O.I. and B. Halliwell, (1987). ***Superoxide-dependent and ascorbate-dependent formation of hydroxyl radicals from hydrogen peroxide in the presence of iron. Are lactoferrin and transferrin promoters of hydroxyl-radical generation?*** Biochemical Journal, **241**(1): p. 273-278.
417. von Sonntag, C., (2008). ***Advanced oxidation processes: mechanistic aspects.*** Water Sci Technol, **58**(5): p. 1015-21.
418. Goto, K., H. Tamura, and M. Nagayama, (1970). ***Mechanism of oxygenation of ferrous ion in neutral solution.*** Inorganic Chemistry, **9**(4): p. 963-964.
419. Feng, W. and D. Nansheng, (2000). ***Photochemistry of hydrolytic iron (III) species and photoinduced degradation of organic compounds. A minireview.*** Chemosphere., **41**(8): p. 1137-47.
420. Dodge, C.J. and A.J. Francis, (2002). ***Photodegradation of a ternary iron(III)-uranium(VI)-citric acid complex.*** Environ Sci Technol., **36**(9): p. 2094-100.
421. Fulazzaky, M.A., N.A.A. Salim, N.H. Abdullah, A.R. Mohd Yusoff, and E. Paul, (2014). ***Precipitation of iron-hydroxy-phosphate of added ferric iron from domestic wastewater by an alternating aerobic–anoxic process.*** Chemical Engineering Journal, **253**: p. 291-297.
422. Nielsen, A., T. Hvitved-Jacobsen, and J. Vollertsen, (2008). ***- Effects of pH and iron concentrations on sulfide precipitation in wastewater collection systems.*** Water Environ Res, **80**(4): p. 380-4.
423. Gayer, K.H. and L. Woontner, (1956). ***The Solubility of Ferrous Hydroxide and Ferric Hydroxide in Acidic and Basic Media at 25°.*** The Journal of Physical Chemistry, **60**(11): p. 1569-1571.
424. Murphy, C.B. and A.E. Martell, (1957). ***Metal chelates of glycine and glycine peptides.*** J Biol Chem., **226**(1): p. 37-50.
425. Parry, R.W.D.F.W., (1952). ***Citrate Complexes of Copper in Acid Solutions.***
426. Warner, R.C.W., Ione, (1953). ***The Cupric and Ferric Citrate Complexes.*** **75**: p. 5086 - 5094.
427. Roy, P. and M. Manassero, (2010). ***Tetranuclear copper(ii)-Schiff-base complexes as active catalysts for oxidation of cyclohexane and toluene.*** Dalton Trans, **39**(6): p. 1539-45.
428. Rigo, A., A. Corazza, M. Luisa di Paolo, M. Rossetto, R. Ugolini, et al., (2004). ***Interaction of copper with cysteine: stability of cuprous complexes and catalytic role of cupric ions in anaerobic thiol oxidation.*** Journal of Inorganic Biochemistry, **98**(9): p. 1495-1501.
429. Remelli, M.C., Chiara; Agarossi,Alessandra; Pulidori, Fernando; Mlynarz, Piotr; Kozkowski, Henri, (2000). ***Copper complexes of dipeptides with L-Lys as C-terminal residue: a thermodynamic and spectroscopic study.***
430. Klebanoff, S.J., A.M. Waltersdorph, B.R. Michel, and H. Rosen, (1989). ***Oxygen-based free radical generation by ferrous ions and deferoxamine.*** J Biol Chem., **264**(33): p. 19765-71.

431. Winterbourn, C.C., (2013). ***The biological chemistry of hydrogen peroxide***. Methods Enzymol, **528:3-25.**(doi): p. 10.1016/B978-0-12-405881-1.00001-X.
432. Halliwell, B. and J.M. Gutteridge, (1984). ***Oxygen toxicity, oxygen radicals, transition metals and disease***. Biochem J., **219**(1): p. 1-14.
433. Bakovic, M., M.D. Fullerton, and V. Michel, (2007). ***Metabolic and molecular aspects of ethanolamine phospholipid biosynthesis: the role of CTP:phosphoethanolamine cytidylyltransferase (Pcyt2)***. Biochem Cell Biol, **85**(3): p. 283-300.
434. McGrew, J.T., C.L. Richards, P. Smidt, B. Dell, and V. Price, (2002), ***Lipid Requirements of a Recombinant Chinese Hamster Ovary Cell Line (CHO)***, in *New Developments and New Applications in Animal Cell Technology: Proceedings of the 15th ESACT Meeting*, O.-W. Merten, P. Perrin, and B. Griffiths, Editors. Springer Netherlands: Dordrecht. p. 205-207.
435. Jenkins, N., P. Castro, S. Menon, A. Ison, and A. Bull, (1994). ***Effect of lipid supplements on the production and glycosylation of recombinant interferon-γ expressed in CHO cells***. Cytotechnology, **15**(1): p. 209-215.
436. Rintoul, D.A., L.A. Sklar, and R.D. Simoni, (1978). ***Membrane lipid modification of chinese hamster ovary cells. Thermal properties of membrane phospholipids***. J Biol Chem., **253**(20): p. 7447-52.
437. Fike, R.B., Bruce; Barrett,Shawn, (2011), ***Compositions and methods for stabilizing susceptible compounds***, C.U. Life Technologies Corporation Carlsbad, Editor.
438. MOONEN, K.G., Michael David (2012), ***Stabilized choline solutions and methods for preparing the same***, TAMINCO, Editor.
439. Scott, K.F., F.L. Meyskens, Jr., and D.H. Russell, (1982). ***Retinoids increase transglutaminase activity and inhibit ornithine decarboxylase activity in Chinese hamster ovary cells and in melanoma cells stimulated to differentiate***. Proc Natl Acad Sci U S A., **79**(13): p. 4093-7.
440. Tsopanoglou, N.E., C. Zioudrou, E.C. Tsilibary, and A.S. Charonis, (1995). ***Putrescine: a novel inhibitor of glycosylation-induced cross-links in laminin***. Microcirculation., **2**(3): p. 283-7.
441. Park, S.-J., M.-K. Kwak, and S.-O. Kang, (2017). ***Schiff bases of putrescine with methylglyoxal protect from cellular damage caused by accumulation of methylglyoxal and reactive oxygen species in Dictyostelium discoideum***. The International Journal of Biochemistry & Cell Biology, **86**: p. 54-66.
442. Hasse, K.M., H, (1955). ***Die Reaktionsprodukte der enzymatischen Oxydation von Putrescin und Cadaverin***. Biochemische Zeitrschrift, **327**: p. 296-304.
443. Morris, A.E. and J. Schmid, (2000). ***Effects of Insulin and LongR3 on Serum-Free Chinese Hamster Ovary Cell Cultures Expressing Two Recombinant Proteins***. Biotechnology Progress, **16**(5): p. 693-697.
444. Yandell, C.A., I.P. Butler, A.J. Sheehan, B.J. Wade, A.P. Simula, et al. ***The Effects of Insulin and Long™R3IGF-I on Chinese Hamster Ovary Cells: Cell Survival, Receptor Activation and Second Messenger Pathways***. in *Animal Cell Technology Meets Genomics*. 2005. Dordrecht: Springer Netherlands.
445. Sanfeliu, A., J.D. Chung, and G. Stephanopoulos, (2000). ***Effect of insulin stimulation on the proliferation and death of Chinese hamster ovary cells***. Biotechnology and Bioengineering, **70**(4): p. 421-427.
446. Mendiaz, E., M. Mamounas, J. Moffett, and E. Englesberg, (1986). ***A Defined Medium for and the Effect of Insulin on the Growth, Amino Acid Transport, and Morphology of Chinese Hamster Ovary Cells, CHO-K1 (CCL 61) and the Isolation of Insulin "Independent" Mutants***. In Vitro Cellular & Developmental Biology, **22**(2): p. 66-74.
447. Nakai, M., F. Sekiguchi, M. Obata, C. Ohtsuki, Y. Adachi, et al., (2005). ***Synthesis and insulin-mimetic activities of metal complexes with 3-hydroxypyridine-2-carboxylic acid***. Journal of Inorganic Biochemistry, **99**(6): p. 1275-1282.
448. Saatchi, K., K.H. Thompson, B.O. Patrick, M. Pink, V.G. Yuen, et al., (2005). ***Coordination Chemistry and Insulin-Enhancing Behavior of Vanadium Complexes with Maltol C6H6O3 Structural Isomers***. Inorganic Chemistry, **44**(8): p. 2689-2697.

449. Nejo, A.A., G.A. Kolawole, A.R. Opoku, C. Muller, and J. Wolowska, (2009). ***Synthesis, characterization, and insulin-enhancing studies of unsymmetrical tetradentate Schiff-base complexes of oxovanadium(IV)***. Journal of Coordination Chemistry, **62**(21): p. 3411-3424.
450. Gavrilova, J., V. Tõugu, and P. Palumaa, (2014). ***Affinity of zinc and copper ions for insulin monomers***. Metallomics, **6**(7): p. 1296-1300.
451. Heidemann, R., D. Lütkemeyer, H. Büntemeyer, and J. Lehmann, (1998). ***Effects of dissolved oxygen levels and the role of extra- and intracellular amino acid concentrations upon the metabolism of mammalian cell lines during batch and continuous cultures***. Cytotechnology, **26**(3): p. 185-197.
452. Meyer, A., R.G. Condon, G. Keil, N. Jhaveri, Z. Liu, et al., (2012). ***Fluorinert, an oxygen carrier, improves cell culture performance in deep square 96-well plates by facilitating oxygen transfer***. Biotechnol Prog, **28**(1): p. 171-8.
453. Lowe, K.C., P. Anthony, M.R. Davey, and J.B. Power, (2001). ***Beneficial effects of Pluronic F-68 and artificial oxygen carriers on the post-thaw recovery of cryopreserved plant cells***. Artif Cells Blood Substit Immobil Biotechnol., **29**(4): p. 297-316.
454. Lowe, K.C., (2002). ***Perfluorochemical respiratory gas carriers: benefits to cell culture systems***. Journal of Fluorine Chemistry, **118**: p. 19-26.
455. Lowe, K.C., (1999). ***Perfluorinated blood substitutes and artificial oxygen carriers***. Blood Rev., **13**(3): p. 171-84.
456. Lowe, K.C., (1997). ***Perfluorochemical respiratory gas carriers: applications in medicine and biotechnology***. Sci Prog, **80**(Pt 2): p. 169-93.
457. Min K. Tham, R.D.W.J., Herome H. Modell, (1973). ***Physical Properties and Gas Solubilities in Selected Fluorinated Ethers***. Journal of Chemical and Engineering Data, **18**(4): p. 385-386.
458. Wardrop, J., M.R. Davey, J.B. Power, and K.C. Lowe, (2002). ***Metabolic responses of cultured cells to oxygenated perfluorocarbon***. Artif Cells Blood Substit Immobil Biotechnol., **30**(1): p. 63-70.
459. Gray, D.R., S. Chen, W. Howarth, D. Inlow, and B.L. Maiorella, (1996). ***CO2 in large-scale and high-density CHO cell perfusion culture***. Cytotechnology, **22**(1): p. 65-78.
460. Cooper, W.J.Z., Rod G. , (1988). ***Photochemical Formation of H202 in Natural Waters Exposed to Sunlight***
461. Held, P., (2015). ***An Introduction to Reactive Oxygen Species***. White Paper BioTek(R).
462. Buxton, G.V. ***Critical Review of Rate Constants for Reactions of Hydrated Electrons, Hydrogen Atoms and Hydroxyl Radicals (.OH/.O–) in Aqueous Solution***.
463. Anglada, J.M., M. Martins-Costa, J.S. Francisco, and M.F. Ruiz-Lopez, (2015). ***Interconnection of reactive oxygen species chemistry across the interfaces of atmospheric, environmental, and biological processes***. Acc Chem Res.
464. Gramer, M.J. and T. Ogorzalek, (2007). ***A semi-empirical mathematical model useful for describing the relationship between carbon dioxide, pH, lactate and base in a bicarbonate-buffered cell-culture process***. Biotechnology and Applied Biochemistry, **47**(4): p. 197-204.
465. Hagrot, E., (2011), ***Development of a culture system for modeling of pH effects in CHO cells***, in *Industrial Biotechnology*.
466. Zhang, S., A. Handa-Corrigan, and R.E. Spier, (1992). ***Foaming and media surfactant effects on the cultivation of animal cells in stirred and sparged bioreactors***. Journal of Biotechnology, **25**(3): p. 289-306.
467. Tharmalingam, T., H. Ghebeh, T. Wuerz, and M. Butler, (2008). ***Pluronic Enhances the Robustness and Reduces the Cell Attachment of Mammalian Cells***. Molecular Biotechnology, **39**(2): p. 167-177.
468. Gigout, A., M.D. Buschmann, and M. Jolicoeur, (2008). ***The fate of Pluronic F-68 in chondrocytes and CHO cells***. Biotechnology and Bioengineering, **100**(5): p. 975-987.
469. Peng, H., K.M. Hall, B. Clayton, K. Wiltberger, W. Hu, et al., (2014). ***Development of small scale cell culture models for screening poloxamer 188 lot-to-lot variation***. Biotechnol Prog, **30**(6): p. 1411-8.
470. Hyoung Park, J., M. Sin Lim, J. Rang Woo, J. Won Kim, and G. Min Lee, (2016). ***The molecular weight and concentration of dextran sulfate affect cell growth and antibody production in***

CHO cell cultures. Biotechnol Prog., **32**(5): p. 1113-1122. doi: 10.1002/btpr.2287. Epub 2016 May 12.

471. Delvigne, F.L., J.P., (2008). ***Foam formation and control in bioreactors***. Encyclopedia of Industrial Biotechnology.
472. Yoon, S.K. and Y.-H. Ahn, (2007). ***Application of sodium propionate to the suspension culture of Chinese hamster ovary cells for enhanced production of follicle-stimulating hormone***. Biotechnology and Bioprocess Engineering, **12**(5): p. 497.
473. Li, J., C.L. Wong, N. Vijayasankaran, T. Hudson, and A. Amanullah, (2012). ***Feeding lactate for CHO cell culture processes: impact on culture metabolism and performance***. Biotechnol Bioeng, **109**(5): p. 1173-86.
474. Nilausen, K., (1968). ***Growth-promoting effect of lysolecithin on Chinese hamster cells in vitro***. Nature, **217**(5125): p. 268-269.
475. Sharma, C., B. Drew, K. Head, R. Pusuluri, and M.V. Caple, (2011). ***Analytical techniques for characterization of raw materials in cell culture media***. BMC Proceedings, **5**(Suppl 8): p. P5-P5.
476. Mulukutla Bhanu, C., J. Kale, T. Kalomeris, M. Jacobs, and W. Hiller Gregory, (2017). ***Identification and control of novel growth inhibitors in fed-batch cultures of Chinese hamster ovary cells***. Biotechnology and Bioengineering, **114**(8): p. 1779-1790.
477. Kuschelewski, J., A. Schnellbaecher, S. Pering, M. Wehsling, and A. Zimmer, (2017). ***Antioxidant effect of thiazolidine molecules in cell culture media improves stability and performance***. Biotechnol Prog, **33**(3): p. 759-770.
478. Salazar, A., J. Bleifuß, A. Simon, S. Schüßler, M. Keusgen, et al., (2016). ***Compaction of chemically defined cell culture media increases its dissolution rate through an increase of solvent accessible surface area***. Powder Technology, **301**: p. 110-117.
479. Hogg, R., (2009), ***Mixing and Segregation in Powders: Evaluation, Mechanisms and Processes***. Vol. 27.
480. Trunfio, N., H. Lee, J. Starkey, C. Agarabi, J. Liu, et al., (2017). ***Characterization of mammalian cell culture raw materials by combining spectroscopy and chemometrics***. Biotechnology Progress, **33**(4): p. 1127-1138.
481. McGillicuddy, N., P. Floris, S. Albrecht, and J. Bones, (2018). ***Examining the sources of variability in cell culture media used for biopharmaceutical production***. Biotechnology Letters, **40**(1): p. 5-21.
482. Krishtalik, L.I., (2003). ***pH-dependent redox potential: how to use it correctly in the activation energy analysis***. Biochimica et Biophysica Acta (BBA) - Bioenergetics, **1604**(1): p. 13-21.
483. Burns, J.M., W.J. Cooper, J.L. Ferry, D.W. King, B.P. DiMento, et al., (2012). ***Methods for reactive oxygen species (ROS) detection in aqueous environments***. Aquatic Sciences, **74**(4): p. 683-734.
484. Junker, B., M. Lester, T. Brix, D. Wong, and J. Nuechterlein, (2006). ***A next generation, pilot-scale continuous sterilization system for fermentation media***. Bioprocess and biosystems engineering, **28**(6): p. 351-378.
485. Floris, P., S. Curtin, C. Kaisermayer, A. Lindeberg, and J. Bones, (2018). ***Development of a versatile high-temperature short-time (HTST) pasteurization device for small-scale processing of cell culture medium formulations***. Applied Microbiology and Biotechnology, **102**(13): p. 5495-5504.
486. Monteil, D.T., C.A. Bürki, L. Baldi, D.L. Hacker, M. de Jesus, et al., (2013). ***The optimization of a rapid low-cost alternative of large-scale medium sterilization***. BMC Proceedings, **7**(Suppl 6): p. P45-P45.
487. Yen, S., S. Sokolenko, B. Manocha, A. Patras, F. Daynouri-Pancino, et al., (2014). ***Treating cell culture media with UV irradiation against adventitious agents: Minimal impact on CHO performance***. Biotechnology Progress, **30**(5): p. 1190-1195.
488. Hedberg, Y., G. Herting, and I.O. Wallinder, (2011). ***Risks of using membrane filtration for trace metal analysis and assessing the dissolved metal fraction of aqueous media--a study on zinc, copper and nickel***. Environ Pollut, **159**(5): p. 1144-50.

489. Cao, X., J.A. Loussaert, and Z.Q. Wen, (2016). ***Microspectroscopic investigation of the membrane clogging during the sterile filtration of the growth media for mammalian cell culture.*** Journal of pharmaceutical and biomedical analysis, **119**: p. 10-15.
490. Floris, P., N. McGillicuddy, S. Albrecht, B. Morrissey, C. Kaisermayer, et al., (2017). ***Untargeted LC-MS/MS profiling of cell culture media formulations for evaluation of High Temperature Short Time (HTST) treatment effects.*** Anal Chem, **19**(10).
491. Cao, X., G. Stimpfl, Z.Q. Wen, G. Frank, and G. Hunter, (2013). ***Identification and root cause analysis of cell culture media precipitates in the viral deactivation treatment with high-temperature/short-time method.*** PDA J Pharm Sci Technol, **67**(1): p. 63-73.
492. Nielsen, H.I. and K. Bertheussen, (1991), ***DEGRADING EFFECT OF LIGHT ON CELL CULTURE MEDIA***, in *Production of Biologicals from Animal Cells in Culture*, R.E. Spier, J.B. Griffiths, and B. Meignier, Editors. Butterworth-Heinemann. p. 82-84.
493. Neutsch, L., P. Kroll, M. Brunner, A. Pansy, M. Kovar, et al., (2018). ***Media photo-degradation in pharmaceutical biotechnology - impact of ambient light on media quality, cell physiology, and IgG production in CHO cultures.*** Journal of chemical technology and biotechnology (Oxford, Oxfordshire : 1986), **93**(8): p. 2141-2151.
494. J. S. Zigler, Jr., J.L. Lepe-Zuniga, B. Vistica, and I. Gery, (1985). ***Analysis of the Cytotoxic Effects of Light-Exposed Hepes-Containing Culture Medium.*** In Vitro Cellular & Developmental Biology, **21**(5): p. 282-287.
495. Huvaere, K. and L.H. Skibsted, (2009). ***Light-Induced Oxidation of Tryptophan and Histidine. Reactivity of Aromatic N-Heterocycles toward Triplet-Excited Flavins.*** Journal of the American Chemical Society, **131**(23): p. 8049-8060.
496. Li, Y., W. Zhang, J. Niu, and Y. Chen, (2012). ***Mechanism of Photogenerated Reactive Oxygen Species and Correlation with the Antibacterial Properties of Engineered Metal-Oxide Nanoparticles.*** ACS Nano, **6**(6): p. 5164-5173.
497. Hammond, M., H. Nunn, G. Rogers, H. Lee, A.L. Marghitoiu, et al., (2013). ***Identification of a leachable compound detrimental to cell growth in single-use bioprocess containers.*** PDA journal of pharmaceutical science and technology, **67**(2): p. 123-134.
498. Okonkowski, J., U. Balasubramanian, C. Seamans, S. Fries, J. Zhang, et al., (2007). ***Cholesterol delivery to NS0 cells: Challenges and solutions in disposable linear low-density polyethylene-based bioreactors.*** Journal of Bioscience and Bioengineering, **103**(1): p. 50-59.
499. Steiger, N. and R. Eibl, (2013). ***Interlaboratory Test for Detection of Cytotoxic Leachables arising from Single-Use Bags.*** Chemie Ingenieur Technik, **85**(1-2): p. 26-28.
500. Wood, J., E. Mahajan, and M. Shiratori, (2013). ***Strategy for selecting disposable bags for cell culture media applications based on a root-cause investigation.*** Biotechnology progress, **29**(6): p. 1535-1549.
501. Dorival-García, N., S. Carillo, C. Ta, D. Roberts, K. Comstock, et al., (2018). ***Large-Scale Assessment of Extractables and Leachables in Single-Use Bags for Biomanufacturing.*** Analytical chemistry, **90**(15): p. 9006-9015.
502. Li, B., P.W. Ryan, B.H. Ray, K.J. Leister, N.M. Sirimuthu, et al., (2010). ***Rapid characterization and quality control of complex cell culture media solutions using raman spectroscopy and chemometrics.*** Biotechnol Bioeng, **107**(2): p. 290-301.
503. Alwael, H., D. Connolly, L. Barron, and B. Paull, (2010). ***Development of a rapid and sensitive method for determination of cysteine/cystine ratio in chemically defined media.*** J Chromatogr A., **1217**(24): p. 3863-70. doi: 10.1016/j.chroma.2010.04.036. Epub 2010 Apr 20.
504. Mohabbat, T. and B. Drew, (2008). ***Simultaneous determination of 33 amino acids and dipeptides in spent cell culture media by gas chromatography-flame ionization detection following liquid and solid phase extraction.*** J Chromatogr B Analyt Technol Biomed Life Sci, **862**(1-2): p. 86-92.
505. Troise, A.D., A. Fiore, G. Roviello, S.M. Monti, and V. Fogliano, (2015). ***Simultaneous quantification of amino acids and Amadori products in foods through ion-pairing liquid chromatography–high-resolution mass spectrometry.*** Amino Acids, **47**(1): p. 111-124.

506. Qiu, J., P.K. Chan, and P.V. Bondarenko, (2016). ***Monitoring utilizations of amino acids and vitamins in culture media and Chinese hamster ovary cells by liquid chromatography tandem mass spectrometry***. J Pharm Biomed Anal, **117**: p. 163-72.
507. Biechele, P., C. Busse, D. Solle, T. Scheper, and K. Reardon, (2015). ***Sensor systems for bioprocess monitoring***. Engineering in Life Sciences, **15**(5): p. 469-488.
508. Busse, C., P. Biechele, I. de Vries, K.F. Reardon, D. Solle, et al., (2017). ***Sensors for disposable bioreactors***. Engineering in Life Sciences, **17**(8): p. 940-952.
509. Narang, A.S., V.A. Sheverev, V. Stepaniuk, S. Badawy, T. Stevens, et al., (2014). ***Real-Time Assessment of Granule Densification in High Shear Wet Granulation and Application to Scale-up of a Placebo and a Brivanib Alaninate Formulation***. J Pharm Sci.
510. Kumar, V., M. Taylor, A. Mehrotra, and W. Stagner, (2013). ***Real-Time Particle Size Analysis Using Focused Beam Reflectance Measurement as a Process Analytical Technology Tool for a Continuous Granulation–Drying–Milling Process***. AAPS PharmSciTech, **14**(2): p. 523-530.
511. Heath, A.R., P.D. Fawell, P.A. Bahri, and J.D. Swift, (2002). ***Estimating Average Particle Size by Focused Beam Reflectance Measurement (FBRM)***.
512. Greaves, D., J. Boxall, J. Mulligan, A. Montesi, J. Creek, et al., (2008). ***Measuring the particle size of a known distribution using the focused beam reflectance measurement technique***. Chemical Engineering Science, **63**(22): p. 5410-5419.
513. Fang, Y., C. Selomulya, and X.D. Chen, (2010). ***Characterization of milk protein concentrate solubility using focused beam reflectance measurement***. Dairy Sci. Technol., **90**(2-3): p. 253-270.
514. Druzinec, D., D. Salzig, M. Kraume, and P. Czermak, (2015). ***Micro-bubble aeration in turbulent stirred bioreactors: Coalescence behavior in Pluronic F68 containing cell culture media***. Chemical Engineering Science, **126**(0): p. 160-168.
515. Lu, W., B.D. Bennett, and J.D. Rabinowitz, (2008). ***Analytical strategies for LC-MS-based targeted metabolomics***. Journal of chromatography. B, Analytical technologies in the biomedical and life sciences, **871**(2): p. 236-242.
516. Vailaya, A., (2005). ***Fundamentals of Reversed Phase Chromatography: Thermodynamic and Exothermodynamic Treatment***. Journal of Liquid Chromatography & Related Technologies, **28**(7-8): p. 965-1054.
517. Sentell, K.B. and J.G. Dorsey, (1989). ***Retention mechanisms in reversed-phase liquid chromatography. Stationary-phase bonding density and partitioning***. Analytical Chemistry, **61**(9): p. 930-934.
518. Seto, C., K.P. Bateman, and B. Gunter, (2002). ***Development of generic liquid chromatography-mass spectrometry methods using experimental design***. Journal of the American Society for Mass Spectrometry, **13**(1): p. 2-9.
519. Jandera, P. and P. Janás, (2017). ***Recent advances in stationary phases and understanding of retention in hydrophilic interaction chromatography. A review***. Analytica Chimica Acta, **967**: p. 12-32.
520. Liu, Z. and S. Rochfort, (2014). ***Recent progress in polar metabolite quantification in plants using liquid chromatography–mass spectrometry***. Journal of Integrative Plant Biology, **56**(9): p. 816-825.
521. Studzińska, S., R. Rola, and B. Buszewski, (2017). ***The impact of ion-pairing reagents on the selectivity and sensitivity in the analysis of modified oligonucleotides in serum samples by liquid chromatography coupled with tandem mass spectrometry***. Journal of Pharmaceutical and Biomedical Analysis, **138**: p. 146-152.
522. Gao, S., S. Bhoopathy, Z.P. Zhang, D.S. Wright, R. Jenkins, et al., (2006). ***Evaluation of volatile ion-pair reagents for the liquid chromatography-mass spectrometry analysis of polar compounds and its application to the determination of methadone in human plasma***. Journal of pharmaceutical and biomedical analysis, **40**(3): p. 679-688.
523. Cecchi, T., (2008). ***Ion Pairing Chromatography***. Critical Reviews in Analytical Chemistry, **38**(3): p. 161-213.
524. Dolan, J.W., (2001). ***Retaining Polar Compounds***. LCGC Europe.
525. Dolan, J.W., (2008), ***Ion pairing - blessing or curse?***, in *LCGC Europe*.

526. Sýkora, D., P. Řezanka, K. Záruba, and V. Král, (2019). ***Recent advances in mixed-mode chromatographic stationary phases***. Journal of Separation Science, **42**(1): p. 89-129.
527. Zhang, K. and X. Liu, (2016). ***Mixed-mode chromatography in pharmaceutical and biopharmaceutical applications***. J Pharm Biomed Anal, **128**: p. 73-88.
528. Zhang, L., Q. Dai, X. Qiao, C. Yu, X. Qin, et al., (2016). ***Mixed-mode chromatographic stationary phases: Recent advancements and its applications for high-performance liquid chromatography***. TrAC Trends in Analytical Chemistry, **82**: p. 143-163.
529. Ban, K., Y. Saito, and K. Jinno, (2004). ***Characterization of the Microscopic Surface Structure of the Octadecylsilica Stationary Phase Using a Molecular-Dynamics Simulation***. Analytical Sciences, **20**(10): p. 1403-1408.
530. Banerjee, S. and S. Mazumdar, (2012). ***Electrospray Ionization Mass Spectrometry: A Technique to Access the Information beyond the Molecular Weight of the Analyte***. International Journal of Analytical Chemistry, **2012**: p. 40.
531. Konermann, L., E. Ahadi, A.D. Rodriguez, and S. Vahidi, (2013). ***Unraveling the Mechanism of Electrospray Ionization***. Analytical Chemistry, **85**(1): p. 2-9.
532. Wilm, M., (2011). ***Principles of electrospray ionization***. Molecular & cellular proteomics : MCP, **10**(7): p. M111.009407-M111.009407.
533. Mei, H., (2005), ***Matrix Effects: Causes and Solutions***, in *Using Mass Spectrometry for Drug Metabolism Studies*, W.A. Korfmacher, Editor.
534. Liigand, J., A. Laaniste, and A. Kruve, (2017). ***pH Effects on Electrospray Ionization Efficiency***. Journal of The American Society for Mass Spectrometry, **28**(3): p. 461-469.
535. Griffiths, J., (2008). ***A Brief History of Mass Spectrometry***. Analytical Chemistry, **80**(15): p. 5678-5683.
536. Yost, R.A. and C.G. Enke, (1978). ***Selected ion fragmentation with a tandem quadrupole mass spectrometer***. Journal of the American Chemical Society, **100**(7): p. 2274-2275.
537. Arnaud, C.H., (2018). ***As the triple quadrupole turns 40, mass spec gurus look back on what it's meant to chemistry***. Chemical & Engineering News, **96**(10): p. 15-18.
538. Yang, L., M. Amad, W.M. Winnik, A.E. Schoen, H. Schweingruber, et al., (2002). ***Investigation of an enhanced resolution triple quadrupole mass spectrometer for high-throughput liquid chromatography/tandem mass spectrometry assays***. Rapid communications in mass spectrometry : RCM, **16**(21): p. 2060-2066.
539. Stewart, I.I. and G. Horlick, (1996). ***Developments in the electrospray mass spectrometry of inorganic species***. TrAC Trends in Analytical Chemistry, **15**(2): p. 80-90.
540. Shiea, C., Y.-L. Huang, S.-C. Cheng, Y.-L. Chen, and J. Shiea, (2017). ***Determination of elemental composition of metals using ambient organic mass spectrometry***. Analytica Chimica Acta, **968**: p. 50-57.
541. Tsednee, M., Y.-C. Huang, Y.-R. Chen, and K.-C. Yeh, (2016). ***Identification of metal species by ESI-MS/MS through release of free metals from the corresponding metal-ligand complexes***. Scientific Reports, **6**: p. 26785.
542. Olesik, J.W., (1991). ***Elemental Analysis Using ICP-OES and ICP/MS***. Analytical Chemistry, **63**(1): p. 12A-21A.
543. Giner Martínez-Sierra, J., O. Galilea San Blas, J. Marchante, and J. Garcia Alonso, (2015). ***Sulfur analysis by ICP-MS: A review***. Spectrochimica Acta Part B: Atomic Spectroscopy, **108**: p. 35-52.
544. Smith, E. and G. Dent, (2019), ***Modern Raman Spectroscopy: A Practical Approach***. Wiley.
545. Joy, D.C. and J.B. Pawley, (1992). ***High-resolution scanning electron microscopy***. Ultramicroscopy, **47**(1): p. 80-100.
546. Scimeca, M., S. Bischetti, H.K. Lamsira, R. Bonfiglio, and E. Bonanno, (2018). ***Energy Dispersive X-ray (EDX) microanalysis: A powerful tool in biomedical research and diagnosis***. European journal of histochemistry : EJH, **62**(1): p. 2841-2841.
547. Shindo, D. and T. Oikawa, (2002), ***Energy Dispersive X-ray Spectroscopy***, in *Analytical Electron Microscopy for Materials Science*, D. Shindo and T. Oikawa, Editors. Springer Japan: Tokyo. p. 81-102.

548. Newbury, D.E. and N.W. Ritchie, (2013). ***Is scanning electron microscopy/energy dispersive X-ray spectrometry (SEM/EDS) quantitative?*** Scanning., **35**(3): p. 141-68. doi: 10.1002/sca.21041. Epub 2012 Aug 9.
549. Ambe, F., (2003), ***Tracer technique***, in *Handbook of Nuclear Chemistry*. p. 443-474.
550. Eberle, D.C., (2008). ***Radioactive tracer methods.*** Techniques for Corrosion Monitoring: p. 265-276.
551. Moljk, A., (1954). ***Beta Spectra of C 14 and S 35.*** Physical Review, **96**(2): p. 395-398.
552. Gika, H.G., G.A. Theodoridis, U. Vrhovsek, and F. Mattivi, (2012). ***Quantitative profiling of polar primary metabolites using hydrophilic interaction ultrahigh performance liquid chromatography–tandem mass spectrometry.*** Journal of Chromatography A, **1259**: p. 121-127.
553. Urban, P.L., (2016). ***Quantitative mass spectrometry: an overview.*** Philosophical transactions. Series A, Mathematical, physical, and engineering sciences, **374**(2079): p. 20150382.
554. Bijlsma, S., I. Bobeldijk, E.R. Verheij, R. Ramaker, S. Kochhar, et al., (2006). ***Large-Scale Human Metabolomics Studies: A Strategy for Data (Pre-) Processing and Validation.*** Analytical Chemistry, **78**(2): p. 567-574.
555. Sysi-Aho, M., M. Katajamaa, L. Yetukuri, and M. Oresic, (2007). ***Normalization method for metabolomics data using optimal selection of multiple internal standards.*** BMC Bioinformatics., **8**: p. 93.
556. Kruve, A., R. Rebane, K. Kipper, M.L. Oldekop, H. Evard, et al., (2015). ***Tutorial review on validation of liquid chromatography-mass spectrometry methods: part I.*** Anal Chim Acta, **870**: p. 29-44.
557. Kruve, A., R. Rebane, K. Kipper, M.L. Oldekop, H. Evard, et al., (2015). ***Tutorial review on validation of liquid chromatography-mass spectrometry methods: part II.*** Anal Chim Acta, **870**: p. 8-28.
558. U.S. Department of Health and Human Services, Food and Drug Administration (FDA), Center for Drug Evaluation and Research (CDER), and Center for Veterinary Medicine (CVM), (2013). ***Guidance for Industry - Bioanalytical Method Validation.***
559. Hughes, N.C., E.Y. Wong, J. Fan, and N. Bajaj, (2007). ***Determination of carryover and contamination for mass spectrometry-based chromatographic assays.*** Aaps j, **9**(3): p. E353-60.
560. Taverniers, I., M. De Loose, and E. Van Bockstaele, (2004). ***Trends in quality in the analytical laboratory. II. Analytical method validation and quality assurance.*** TrAC Trends in Analytical Chemistry, **23**(8): p. 535-552.
561. Matuszewski, B.K., M.L. Constanzer, and C.M. Chavez-Eng, (2003). ***Strategies for the Assessment of Matrix Effect in Quantitative Bioanalytical Methods Based on HPLC–MS/MS.*** Analytical Chemistry, **75**(13): p. 3019-3030.
562. Remko, M., D. Fitz, and B.M. Rode, (2010). ***Effect of metal ions (Li+, Na+, K+, Mg2+, Ca2+, Ni2+, Cu2+ and Zn2+) and water coordination on the structure and properties of L-histidine and zwitterionic L-histidine.*** Amino Acids, **39**(5): p. 1309-19.
563. Rotilio, G. and L. Calabrese, (1971). ***EPR study of Cu(II) complexes of tridentate amino acids.*** Archives of Biochemistry and Biophysics, **143**(1): p. 218-225.
564. Ishida, N., A. Okubo, H. Kawai, S. Yamazaki, and S. Toda, (1980). ***Interaction of Amino Acids with Transition Metal Ions in Solution (I) Solution Structure of l-Lysine with Co(II) and Cu(II) Ions as Studied by Nuclear Magnetic Resonance Spectroscopy.*** Agricultural and Biological Chemistry, **44**(2): p. 263-270.
565. Trelstad, R.L., K.R. Lawley, and L.B. Holmes, (1981). ***Nonenzymatic hydroxylations of proline and lysine by reduced oxygen derivatives.*** Nature., **289**(5795): p. 310-2.
566. Kaiser, S.C.E., Regine; Eibl, Dieter, (2011). ***Engineering characteristics of a single-use stirred bioreactor at bench-scale: The Mobius CellReady 3L bioreactor as a case study.*** Eng. Life Sci., **11**(4): p. 359-368.
567. WestVirginia_DepartmentOfEnvironmentalProtection, DEP S.o. ***DO saturation / oxygen saturation monogram.*** 2019; Available from:

https://dep.wv.gov/WWE/getinvolved/sos/Pages/DOSat.aspx / https://www.rtsd.org/cms/lib/PA01000218/Centricity/Domain/418/Dissolved%20Oxygen.pdf
568. TetraPakInternational, (2015), ***Mixing technology An introduction***.
569. Emerson Process Management (2008), ***Fundamentals of ORP measurement***, L. Division, Editor.
570. Berner, R.A., (1981). ***New geochemical classification of sedimentary environments***. J. Sediment. Petrol., **51**(2): p. 359-65.
571. Sessa, F., (2009). ***FMC Environmental Solutions - Oxidation Reduction Potentials (ORP)***.
572. Allan, P., L.J. Bellamy, A. Nordon, D. Littlejohn, J. Andrews, et al., (2013). ***In situ monitoring of powder blending by non-invasive Raman spectrometry with wide area illumination***. Journal of Pharmaceutical and Biomedical Analysis, **76**: p. 28-35.
573. Riolo, D., A. Piazza, C. Cottini, M. Serafini, E. Lutero, et al., (2018). ***Raman spectroscopy as a PAT for pharmaceutical blending: Advantages and disadvantages***. Journal of Pharmaceutical and Biomedical Analysis, **149**: p. 329-334.
574. Scheibelhofer, O., N. Balak, P.R. Wahl, D.M. Koller, B.J. Glasser, et al., (2013). ***Monitoring Blending of Pharmaceutical Powders with Multipoint NIR Spectroscopy***. AAPS PharmSciTech, **14**(1): p. 234-244.
575. Carter, D.E., (1995). ***Oxidation-reduction reactions of metal ions***. Environmental Health Perspectives, **103**(Suppl 1): p. 17-19.
576. European directorate for the quality of medicines and healthcare, (2015). ***Reverse osmosis in Ph. Eur. monograph water for injections (0169)***.
577. Cheng, K.L. and D.-M. Zhu, (2005). ***On Calibration of pH Meters***. Sensors (Basel, Switzerland), **5**(4): p. 209-219.
578. Cheng, K.L., (2001). ***Counterion Triple Layer in Solid/Solution Interface: Stirring and Temperature Effects on pH Measurements***. Journal of Colloid and Interface Science, **239**(2): p. 385-390.
579. Cheng, K.L., (2002). ***Recent development of non-faradaic potentiometry***. Microchemical Journal, **72**(3): p. 269-276.
580. Bours, J.A., (2008). ***Study of Carbon Dioxide Hydrolysis and Diffusion in Four Different Aqueous Environments***.
581. Wiebe, R. and V.L. Gaddy, (1939). ***The Solubility in Water of Carbon Dioxide at 50, 75 and 100°, at Pressures to 700 Atmospheres***. Journal of the American Chemical Society, **61**(2): p. 315-318.
582. Chaplin, M. ***Water redox processes***. 26.02.2018; Available from: http://www1.lsbu.ac.uk/water/water_redox.html.
583. Tedoradze, G.A., (1959). ***Oxidation Kinetics of Chloride Ions on Platinum***. Zh. Fiz. Khim, **33**: p. 129.
584. Patil, R.S., V.A. Juvekar, and V.M. Naik, (2011). ***Oxidation of Chloride Ion on Platinum Electrode: Dynamics of Electrode Passivation and its Effect on Oxidation Kinetics***. Industrial & Engineering Chemistry Research, **50**(23): p. 12946-12959.
585. Thomassen, M., B. Børresen, G. Hagen, and R. Tunold, (2005). ***Chlorine reduction on platinum and ruthenium: the effect of oxide coverage***. Electrochimica Acta, **50**(5): p. 1157-1167.
586. Green, D.E., (1933). ***The reduction potentials of cysteine, glutathione and glycylcysteine***. Biochemical Journal, **27**(3): p. 678-689.
587. Bard, A.J. and L.R. Faulkner, (2000), ***Electrochemical Methods: Fundamentals and Applications, Second Edition***. New York: John Wiley & Sons.
588. Sawyer, D.T., A. Sobkowiak, and J.L.J. Roberts, (1995), ***Electrochemistry for Chemists, 2nd ed.*** New York: John Wiley & Sons.
589. Lo, M., V. Ling, Y.Z. Wang, and P.W. Gout, (2008). ***The xc− cystine/glutamate antiporter: a mediator of pancreatic cancer growth with a role in drug resistance***. British Journal Of Cancer, **99**: p. 464.
590. Kiontke, A., A. Oliveira-Birkmeier, A. Opitz, and C. Birkemeyer, (2016). ***Electrospray Ionization Efficiency Is Dependent on Different Molecular Descriptors with Respect to Solvent pH and Instrumental Configuration***. PLOS ONE, **11**(12): p. e0167502.

591. Kaplan, H., M.A. Hefford, A.M. Chan, and G. Oda, (1984). ***Chemical reactivity of the functional groups of insulin. Concentration-dependence studies***. Biochemical Journal, **217**(1): p. 135-143.
592. Kubota, E., Y. Mochizuki, and M. Yokoi, (1988), ***Conductivity of iron(II) sulfate in aqueous solution at various temperatures***. Vol. 61. 3723-3724.
593. Wells, R.C., (1909). ***THE ELECTRICAL CONDUCTIVITY OF FERRIC SULPHATE SOLUTIONS.1***. Journal of the American Chemical Society, **31**(9): p. 1027-1035.
594. Miller, R.L., W.L. Bradford, and N.E. Peters, (1988), ***Specific conductance; theoretical considerations and application to analytical quality control***, in *Water Supply Paper*.
595. Dry, M.J. and A.W. Bryson, (1988). ***Prediction of redox potential in concentrated iron sulphate solutions***. Hydrometallurgy, **21**(1): p. 59-72.
596. Ribeiro, A.C.F., M.A. Esteso, V.M.M. Lobo, A.J.M. Valente, S.M.N. Simões, et al., (2007). ***Interactions of copper (II) chloride with sucrose, glucose, and fructose in aqueous solutions***. Journal of Molecular Structure, **826**(2): p. 113-119.
597. Sawyer, D.T. and J.L. Roberts, (1988). ***Hydroxide ion: an effective one-electron reducing agent?*** Accounts of Chemical Research, **21**(12): p. 469-476.
598. Pirie, N.W. and K.G. Pinhey, (1929). ***THE TITRATION CURVE OF GLUTATHIONE***. Journal of Biological Chemistry, **84**(1): p. 321-333.
599. Vila-Viçosa, D., V.H. Teixeira, H.A.F. Santos, and M. Machuqueiro, (2013). ***Conformational Study of GSH and GSSG Using Constant-pH Molecular Dynamics Simulations***. The Journal of Physical Chemistry B, **117**(25): p. 7507-7517.
600. Mirzahosseini, A. and B. Noszál, (2016). ***Species-Specific Standard Redox Potential of Thiol-Disulfide Systems: A Key Parameter to Develop Agents against Oxidative Stress***. Scientific Reports, **6**: p. 37596.
601. Finley, J.W., E.L. Wheeler, and S.C. Witt, (1981). ***Oxidation of glutathione by hydrogen peroxide and other oxidizing agents***. Journal of Agricultural and Food Chemistry, **29**(2): p. 404-407.
602. Hamza, A.H., (2017), ***Vitamin C***.
603. Burkitt, M. and B. Gilbert, (1990). ***- Model studies of the iron-catalysed Haber-Weiss cycle and the ascorbate-driven Fenton reaction***. Free Radic Res Commun, **10**(4-5): p. 265-80.
604. Parsons, Harriet T., T. Yasmin, and Stephen C. Fry, (2011). ***Alternative pathways of dehydroascorbic acid degradation in vitro and in plant cell cultures: novel insights into vitamin C catabolism***. Biochemical Journal, **440**(3): p. 375.
605. Pasek, M.A., J.M. Sampson, and Z. Atlas, (2014). ***Redox chemistry in the phosphorus biogeochemical cycle***. Proc Natl Acad Sci U S A., **111**(43): p. 15468-73. doi: 10.1073/pnas.1408134111. Epub 2014 Oct 13.
606. Han, C., J. Geng, H. Ren, S. Gao, X. Xie, et al., (2013). ***Phosphite in Sedimentary Interstitial Water of Lake Taihu, a Large Eutrophic Shallow Lake in China***. Environmental Science & Technology, **47**(11): p. 5679-5685.
607. Al-Sogair, F., H.M. Marafie, N.M. Shuaib, H.B. Youngo, and M.S. El-Ezaby, (2002). ***Interaction of Phosphate with Iron(III) in Acidic Medium, Equilibrium and Kinetic Studies***. Journal of Coordination Chemistry, **55**(9): p. 1097-1109.
608. Wilhelmy, R.B., R.C. Patel, and E. Matijevic, (1985). ***Thermodynamics and kinetics of aqueous ferric phosphate complex formation***. Inorganic Chemistry, **24**(20): p. 3290-3297.
609. Lente, G., M.E.A. Magalhães, and I. Fábián, (2000). ***Kinetics and Mechanism of Complex Formation Reactions in the Iron(III)–Phosphate Ion System at Large Iron(III) Excess. Formation of a Tetranuclear Complex***. Inorganic Chemistry, **39**(9): p. 1950-1954.
610. King, J. and N. Davidson, (1958). ***Kinetics of the Ferrous Iron-Oxygen Reaction in Acidic Phosphate-Pyrophosphate Solutions***. Journal of the American Chemical Society, **80**(7): p. 1542-1545.
611. Elvehjem, C.A., (1930). ***Factors affecting the catalytic action of copper in the oxidation of cysteine***. Biochemical Journal, **24**(2): p. 415-426.

612. Reinke, L.A., D.R. Moore, J.M. Rau, and P.B. McCay, (1995). ***Inorganic Phosphate Promotes Redox Cycling of Iron in Liver Microsomes: Effects on Free-Radical Reactions***. Archives of Biochemistry and Biophysics, **316**(2): p. 758-764.
613. Cher, M. and N. Davidson, (1955). ***The Kinetics of the Oxygenation of Ferrous Iron in Phosphoric Acid Solution***. Journal of the American Chemical Society, **77**(3): p. 793-798.
614. Nath, K.S., AK, (1993). ***Autoxidation of cysteine generates hydrogen peroxide: cytotoxicity and attenuation by pyruvate***. Am J Physiol, **264**(2 Pt 2).
615. Di Salvo, M.L.B., Nediljko; Contestabile, Roberto, (2012), ***PLP-dependent Enzymes: a Powerful Tool for Metabolic Synthesis of Non-canonical Amino Acids1***, in *Beilstein Bozen Symposium on Moleculare Engineering and Control*. Prien (chiemsee), Germany.
616. di Salvo, M.L., R. Contestabile, and M.K. Safo, (2011). ***Vitamin B(6) salvage enzymes: mechanism, structure and regulation***. Biochim Biophys Acta, **1814**(11): p. 1597-608.
617. Sakurai, T., T. Asakura, and M. Matsuda, (1987). ***Transport and metabolism of pyridoxine and pyridoxal in mice***. J Nutr Sci Vitaminol (Tokyo). **33**(1): p. 11-9.
618. Sakurai, T., T. Asakura, A. Mizuno, and M. Matsuda, (1991). ***Absorption and metabolism of pyridoxamine in mice. I. Pyridoxal as the only form of transport in blood***. J Nutr Sci Vitaminol (Tokyo). **37**(4): p. 341-8.
619. Ciardiello, F., B. Sanfilippo, K. Yanagihara, N. Kim, G. Tortora, et al., (1988). ***Differential Growth Sensitivity to 4-cis-Hydroxy-l-proline of Transformed Rodent Cell Lines***. Cancer Research, **48**(9): p. 2483.
620. Nakamura, T., H. Teramoto, Y. Tomtta, and A. Ichihara, (1984). ***L-Proline is an essential amino acid for hepatocyte growth in culture***. Biochemical and Biophysical Research Communications, **122**(3): p. 884-891.
621. Kachur, A.V., C.J. Koch, and J.E. Biaglow, (1999). ***Mechanism of copper-catalyzed autoxidation of cysteine***. Free Radic Res., **31**(1): p. 23-34.
622. Stricks, W. and I.M. Kolthoff, (1951). ***Polarographic Investigations of Reactions in Aqueous Solutions Containing Copper and Cysteine (Cystine). I. Cuprous Copper and Cysteine in Ammoniacal Medium. The Dissociation Constant of Cuprous Cysteinate***. Journal of the American Chemical Society, **73**(4): p. 1723-1727.
623. Munday, R., (1989). ***- Toxicity of thiols and disulphides: involvement of free-radical species***. Free Radic Biol Med, **7**(6): p. 659-73.
624. Saez, G., P.J. Thornalley, H.A.O. Hill, R. Hems, and J.V. Bannister, (1982). ***The production of free radicals during the autoxidation of cysteine and their effect on isolated rat hepatocytes***. Biochimica et Biophysica Acta (BBA) - General Subjects, **719**(1): p. 24-31.
625. Luo, D.S., SW.; Anderson, B. D., (2005). ***Kinetics and mechanism of the reaction of cysteine and hydrogen peroxide in aqueous solution***. J Pharm Sci, **94**(2): p. 304-16.
626. Königsberger, E., Z. Wang, and L.-C. Königsberger, (2000). ***Solubility of L-Cystine in NaCl and Artificial Urine Solutions***. Monatshefte für Chemie / Chemical Monthly, **131**(1): p. 39-45.
627. Kissi, N., K. Curran, C. Vlachou-Mogire, T. Fearn, and L. McCullough, (2017). ***Developing a non-invasive tool to assess the impact of oxidation on the structural integrity of historic wool in Tudor tapestries***. Heritage Science, **5**(1): p. 49.
628. Mamun, M.A., O. Ahmed, P.K. Bakshi, S. Yamauchi, and M.Q. Ehsan, (2011). ***Synthesis and characterization of some metal complexes of cystine: [Mn(C6H10N2O4S2)]; where MII = Mn(II), Co(II), Ni(II), Cu(II), Zn(II), Cd(II), Hg(II) and Pb(II)***. Russian Journal of Inorganic Chemistry, **56**(12): p. 1972-1980.
629. Kim, G., S.J. Weiss, and R.L. Levine, (2014). ***Methionine oxidation and reduction in proteins***. Biochimica et biophysica acta, **1840**(2): p. 901-905.
630. Zyzak, D.V., R.A. Sanders, M. Stojanovic, D.H. Tallmadge, B.L. Eberhart, et al., (2003). ***Acrylamide Formation Mechanism in Heated Foods***. Journal of Agricultural and Food Chemistry, **51**(16): p. 4782-4787.
631. McElearney, K., A. Ali, A. Gilbert, R. Kshirsagar, and L. Zang, (2016). ***Tryptophan oxidation catabolite, N-formylkynurenine, in photo degraded cell culture medium results in reduced cell culture performance***. Biotechnol Prog, **32**(1): p. 74-82.

632. Fox, S.W., (1938). ***THE PREPARATION OF CITRULLINE BY HYDROLYSIS OF ARGININE.*** Journal of Biological Chemistry, **123**(3): p. 687-690.
633. Jiang, C. and J.-Y. Chang, (2005). ***Unfolding and breakdown of insulin in the presence of endogenous thiols.*** FEBS Letters, **579**(18): p. 3927-3931.
634. Giles, N.M., A.B. Watts, G.I. Giles, F.H. Fry, J.A. Littlechild, et al., (2003). ***Metal and Redox Modulation of Cysteine Protein Function.*** Chemistry & Biology, **10**(8): p. 677-693.
635. Yu, N.-T., B.H. Jo, R.C.C. Chang, and J.D. Huber, (1974). ***Single-crystal raman spectra of native insulin: Structures of insulin fibrils, glucagon fibrils, and intact calf lens.*** Archives of Biochemistry and Biophysics, **160**(2): p. 614-622.
636. Ortiz, C., D. Zhang, Y. Xie, V.J. Davisson, and D. Ben-Amotz, (2004). ***Identification of insulin variants using Raman spectroscopy.*** Analytical Biochemistry, **332**(2): p. 245-252.
637. Ortiz, C., D. Zhang, A.E. Ribbe, Y. Xie, and D. Ben-Amotz, (2007). ***Analysis of insulin amyloid fibrils by Raman spectroscopy.*** Biophysical Chemistry, **128**(2): p. 150-155.
638. Kessler, J., S. Yamamoto, and P. Bour, (2017), ***Establishing the Link between Fibril Formation and Raman Optical Activity Spectra of Insulin***. Vol. 19.
639. Dolui, S., A. Roy, U. Pal, A. Saha, and N. Maiti, (2018), ***Structural Insight of Amyloidogenic Intermediates of Human Insulin***. Vol. 3. 2452-2462.
640. Stoner-Ma, D., J.M. Skinner, D.K. Schneider, M. Cowan, R.M. Sweet, et al., (2011). ***Single-crystal Raman spectroscopy and X-ray crystallography at beamline X26-C of the NSLS.*** Journal of synchrotron radiation, **18**(1): p. 37-40.
641. Adar, F., (2015). ***Multiparticle Analysis by Raman Microscopy.*** Spectroscopy online, **30**(2): p. 14-24.
642. Zhu, G., X. Zhu, Q. Fan, and X. Wan, (2011). ***Raman spectra of amino acids and their aqueous solutions.*** Spectrochimica Acta Part A: Molecular and Biomolecular Spectroscopy, **78**(3): p. 1187-1195.
643. Meyers, D. ***www.artistcreation.com***. 2013; Available from: http://www.artiscreation.com/yellow.html#PY42.
644. Kolluru, G.K., X. Shen, S.C. Bir, and C.G. Kevil, (2013). ***Hydrogen sulfide chemical biology: pathophysiological roles and detection.*** Nitric oxide : biology and chemistry, **35**: p. 5-20.
645. Hughes, M.N., M.N. Centelles, and K.P. Moore, (2009). ***Making and working with hydrogen sulfide: The chemistry and generation of hydrogen sulfide in vitro and its measurement in vivo: a review.*** Free Radic Biol Med, **47**(10): p. 1346-53.
646. Shibuya, N., S. Koike, M. Tanaka, M. Ishigami-Yuasa, Y. Kimura, et al., (2013). ***A novel pathway for the production of hydrogen sulfide from D-cysteine in mammalian cells.*** Nature Communications, **4**: p. 1366.
647. Zhao, Y., T.D. Biggs, and M. Xian, (2014). ***Hydrogen sulfide (H2S) releasing agents: chemistry and biological applications.*** Chemical communications (Cambridge, England), **50**(80): p. 11788-11805.
648. Zheng, Y., X. Ji, K. Ji, and B. Wang, (2015). ***Hydrogen sulfide prodrugs—a review.*** Acta Pharmaceutica Sinica B, **5**(5): p. 367-377.
649. Sastre, C., V. Baillif-Couniou, P. Kintz, V. Cirimele, C. Bartoli, et al., (2013). ***Fatal Accidental Hydrogen Sulfide Poisoning: A Domestic Case.*** Journal of Forensic Sciences, **58**(s1): p. S280-S284.
650. Kfir, H., S. Rimbrot, and A. Markel, (2015). ***Toxic effects of hydrogen sulfide: experience with three simultaneous patients.*** QJM: An International Journal of Medicine, **108**(12): p. 977-978.
651. Yoshida, A., N. Yoshimura M Fau - Ohara, S. Ohara N Fau - Yoshimura, S. Yoshimura S Fau - Nagashima, T. Nagashima S Fau - Takehara, et al. ***Hydrogen sulfide production from cysteine and homocysteine by periodontal and oral bacteria.*** (1943-3670 (Electronic)).
652. Korshunov, S. and J.A. Imlay, (2018). ***Quantification of Hydrogen Sulfide and Cysteine Excreted by Bacterial Cells.*** Bio-protocol, **8**(10): p. e2847.
653. Shelef, L.A. and W. Tan. ***Automated detection of hydrogen sulfide release from thiosulfate by Salmonella spp.*** (0362-028X (Print)).
654. Barrett, E.L.C., Marta A., (1987). ***Tetrathionate reduction and production of hydrogen sulfide from thiosulfate.*** Microbiol Rev, **51**(2): p. 192-205.

655. E Dominy, J., C. R Simmons, P. Karplus, A. Gehring, and M. Stipanuk, (2006), ***Identification and Characterization of Bacterial Cysteine Dioxygenases: a New Route of Cysteine Degradation for Eubacteria***. Vol. 188. 5561-9.
656. Smythe, C.V. and D. Halliday, (1942). ***An enzymatic conversion of radioactive sulfide sulfur to cysteine sulfur.*** Journal of Biological Chemistry, **144**(1): p. 237-242.
657. Winter, G., A.G. Cordente, and C. Curtin, (2014). ***Formation of Hydrogen Sulfide from Cysteine in Saccharomyces cerevisiae BY4742: Genome Wide Screen Reveals a Central Role of the Vacuole.*** PLOS ONE, **9**(12): p. e113869.
658. Kreitman, G.Y., J.C. Danilewicz, D.W. Jeffery, and R.J. Elias, (2016). ***Reaction Mechanisms of Metals with Hydrogen Sulfide and Thiols in Model Wine. Part 1: Copper-Catalyzed Oxidation.*** J Agric Food Chem, **64**(20): p. 4095-104.
659. Sekiya, J., A. Schmidt, L.G. Wilson, and P. Filner, (1982). ***Emission of Hydrogen Sulfide by Leaf Tissue in Response to l-Cysteine.*** Plant physiology, **70**(2): p. 430-436.
660. Routh, J.I., (1939). ***The Decomposition of cysteine in aqueous solution.***
661. Kobayasi, N. and M. Fujimaki, (1965). ***On the Formation of Mercaptoacetaldehyde, Hydrogen Sulfide and Acetaldehyde on Boiling Cysteine with Carbonyl Compounds.*** Agricultural and Biological Chemistry, **29**(7): p. 698-699.
662. Uk Ahn, D., E. Joo Lee, X. Feng, W. Zhang, J.H. Lee, et al., (2016). ***Mechanisms of volatile production from sulfur-containing amino acids by irradiation.*** Radiation Physics and Chemistry, **119**: p. 80-84.
663. Ghassemzadeh, L., T.J. Peckham, T. Weissbach, X. Luo, and S. Holdcroft, (2013). ***Selective Formation of Hydrogen and Hydroxyl Radicals by Electron Beam Irradiation and Their Reactivity with Perfluorosulfonated Acid Ionomer.*** Journal of the American Chemical Society, **135**(42): p. 15923-15932.
664. Ershov, B.G., E. Janata, M.S. Alam, and A.V. Gordeev, (2008). ***A pulse radiolysis study of the reactions of the hydrated electron and hydroxyl radical with the oxalate ion in neutral aqueous solution.*** High Energy Chemistry, **42**(1): p. 1-6.
665. Armstrong, D.A. and V.G. Wilkening, (1964). ***Effects of pH in the g-radiolysis of aqueous solution of cysteine and methyl mercaptan.*** Canadian Journal of Chemistry, **42**: p. 2631-2635.
666. Littman, F.E., E.M. Carr, and A.P. Brady, (1957). ***The action of atomic hydrogen on aqueous solutions. I. Effect on silver, cysteine, and glutathione solutions.*** Radiation research, **7**(2): p. 107-119.
667. Chen, K.Y. and J.C. Morris, (1972). ***Kinetics of oxidation of aqueous sulfide by oxygen.*** Environmental Science & Technology, **6**(6): p. 529-537.
668. Boulegue, J., (1978). ***Solubility of Elemental Sulfur in Water at 298 K.*** Phosphorus and Sulfur and the Related Elements, **5**(1): p. 127-128.
669. Simonaitis, R. and J. Heicklen, (1973). ***Reactions of hydroperoxyl radical (HO2) with carbon monoxide and nitric oxide and of oxygen(1D) with water.*** The Journal of Physical Chemistry, **77**(9): p. 1096-1102.
670. St. Laurent, J.B., F. de Buzzaccarini, K. De Clerck, H. Demeyere, R. Labeque, et al., (2007), ***B.1.I - Laundry Cleaning of Textiles***, in *Handbook for Cleaning/Decontamination of Surfaces*, I. Johansson and P. Somasundaran, Editors. Elsevier Science B.V.: Amsterdam. p. 57-102.
671. Beverskog, B. and I. Puigdomenech, (1996). ***Revised pourbaix diagrams for iron at 25–300 °C.*** Corrosion Science, **38**(12): p. 2121-2135.
672. Tanimoto, T., (1958), ***An Elementary Mathematical theory of Classification and Prediction***. Internal IBM Technical Report.
673. Olson, C.F., (1995). ***Parallel algorithms for hierarchical clustering.*** Parallel Comput., **21**(8): p. 1313-1325.

8. Appendix

Table 14: Forecast of best selling drugs in 2024.

	Product	Generic name	Company	Pharmacological class	World wide product sales [$m]			Production process	Production host	Cultivation medium
					2017	2024	CAGR			
1	Humira	adalimumab	AbbVie+ Eisai	Anti-tumour necrosis factor alpha (TNFa) mAb	18922	15233	-0.03	biotechnology	CHO	no human or animal derived ingredients, contains recombinant insulin
2	Keytruda	pembrolizumab	Merck & Co + Otsuka Holdings	Anti-programmed cell death-1 (PD-1) mAb	3823	12686	0.19	biotechnology	CHO	serum free culture medium without animal derived material added during fermentation
3	Revlimid	lenalidomide	Celgene + BeiGene	Immunomodulator	8191	11931	0.06	chemcial synthesis	-	-
4	Opdivo	nivolumab	Bristol-Myers Squibb + Ono Pharmaceutical	Anti-programmed cell death-1 (PD-1) mAb	5725	11247	0.1	biotechnology	CHO	no material of animal or human origin
5	Eliquis	apixaban	Bristol-Myers Squibb	Factor Xa inhibitor	4872	10535	0.12	chemcial synthesis	-	-
6	Imbruvica	ibrutinib	AbbVie + Johnson & Johnson	Bruton's tyrosine kinase (BTK) inhibitor	3196	9557	0.17	chemcial synthesis	-	-
7	Ibrance	palbociclib	Pfizer	Cyclin-dependent kinase (CDK) 4 & 6 inhibitor	3126	8284	0.15	chemcial synthesis	-	-
8	Dupixent	dupilumab	Sanofi	Anti-IL-4 & IL-13 mAb	247	8058	0.64	biotechnology	CHO	process does not contain raw material of animal origin other than CHO cells
9	Eylea	aflibercept	Regeneron Pharmaceuticals+ Bayer + Santen Pharmaceutical	Vascular endothelial growth factor receptor (VEGFr) kinase inhibitor	6282	6827	0.01	biotechnology	CHO	no material of biological origin other than medium for master cell bank contains foetal bovine serum
10	Stelara	ustekinumab	Johnson & Johnson	Anti-IL-12 & IL-23 mAb	4011	6466	0.07	biotechnology	Sp2/0	CDM
11	Biktarvy	bictegravir sodium; emtricitabine; tenofovir alafenamide fumarate	Gilead Sciences	Nucleoside reverse transcriptase inhibitor (NRTI) & HIV integrase inhibitor	-	6103	n/a	chemcial synthesis	-	-
12	Darzalex	daratumumab	Johnson & Johnson	Anti-CD38 mAb	1242	6033	0.25	biotechnology	CHO	no information found
13	Tecentriq	atezolizumab	Roche	Anti-programmed cell death ligand-1 (PD-L1) mAb	495	6006	0.43	biotechnology	CHO	applicants CHO platform
14	Prolia/ Xgeva	denosumab	Amgen + Daiichi Sankyo	Anti-receptor activator of nuclear factor-kappaB ligand (RANKL) mAb	3891	5995	0.06	biotechnology	CHO	no information found
15	Perjeta	pertuzumab	Roche	Anti-human epidermal growth factor (HER2/ErbB-2) mAb	2231	5935	0.15	biotechnology	CHO	applicants CHO platform
16	Xarelto	rivaroxaban	Johnson & Johnson + Bayer	Factor Xa inhibitor	5640	5915	0.01	chemcial synthesis	-	-
17	Ocrevus	ocrelizumab	Roche	Anti-CD20 mAb	883	5875	0.31	biotechnology	CHO	no animal or human origin excipients in manufacturing process and control of manganese
18	Prevnar13	pneumococcal vaccine	Pfizer + Daewoong Pharmaceutical	Pneumococcal vaccine	5693	5756	0	biotechnology	Streptococcus pneumoniae (wt)	soy media complemented with dextrose and magnesium sulfate
19	Cosentyx	secukinumab	Novartis	Anti-IL-17 mAb	2071	5500	0.15	biotechnology	CHO	cell culture media used for cell culture are serum-free, with low protein content and do not contain animal- or human-derived raw materials
20	Soliris	eculizumab	Alexion Pharmaceuticals	Anti-complement factor C5 mAb	3144	5208	0.07	biotechnology	murine myeloma cell line (NS0)	bovine serum albumin (BSA) was included in media, cholesterol obtained from sheep wool grease included in cell culture media

Table 15: Media recipes of commercially available CDM with accessible information about composition.

	Dulbecco´s Modified Eagle´s Medium (DMEM)	**Hybri-Care Medium ATCC ® 46-X**	**enhanced RDF (eRDF)**	**Nutrient Mixture F-12 Ham (Ham´s F12)**	**Iscove's Modified Dulbecco's Media (IMDM)**
	[g/L]	[g/L]	[g/L]	[g/L]	[g/L]
Inorganic Salts					
Calcium Chloride	0.2	0.1914	0.08213	0.0333	0.1653
Cupric Sulfate • $5H_2O$			0.00000075	0.0000025	
Ferrous Sulfate • $7H_2O$			0.00022	0.000834	
Ferric Nitrate • $9H_2O$	0.0001	0.000087			
Magnesium Sulfate (anhydrous)	0.09767	0.09347	0.05237		0.9767
Magnesium Chloride				0.0576	
Potassium Chloride	0.4	0.3828	0.3728	0.224	0.33
Potassium Nitrate					0.000076
Sodium Bicarbonate	3.7			1.176	
Sodium Chloride	6.4	6.1596	6.136	7.599	4.505
Sodium Phosphate Monobasic (anhydrous)	0.109		0.4841		0.109
Sodium Phosphate Monobasic H2O		0.12093			
Sodium Phosphate Dibasic (anhydrous)				0.14204	
Sodium glucuronate H2O		0.0001566			
sodium acetate 3H2O		0.00435			
Sodium Selenite					0.000017
Zinc Sulfate • $7H_2O$			0.00023	0.000863	
Amino Acids					
L-Alanyl-L-Glutamine	0.869				
L-Alanine		0.01048	0.0067	0.009	0.025
L-Arginine • HCl	0.084	0.07579	0.58145	0.211	0.084
L-Asparagine • H_2O		0.01229	0.0946	0.01501	0.0284
L-Aspartic Acid		0.01243	0.04	0.0133	0.03
L-Cystine • 2HCl	0.0626	0.05563	0.1054	0.035	0.09124
L-Glutamic Acid		0.01351	0.0397	0.0147	0.075
L-Glutamine		0.77393	0.9986	0.146	0.584
Glycine	0.03	0.0338	0.0428	0.00751	0.03
L-Histidine • HCl • H_2O	0.042	0.03886	0.07547	0.02096	0.042

	Dulbecco´s Modified Eagle´s Medium (DMEM)	**Hybri-Care Medium ATCC ® 46-X**	**enhanced RDF (eRDF)**	**Nutrient Mixture F-12 Ham (Ham´s F12)**	**Iscove's Modified Dulbecco's Media (IMDM)**
	[g/L]	[g/L]	[g/L]	[g/L]	[g/L]
L-Isoleucine	0.105	0.09292	0.1574	0.00394	0.105
L-Leucine	0.105	0.09313	0.1653	0.0131	0.105
L-Lysine • HCl	0.146	0.13036	0.1973	0.0365	0.146
L-Methionine	0.03	0.02649	0.0492	0.00448	0.03
L-Phenylalanine	0.066	0.05886	0.0743	0.00496	0.066
L-Proline		0.01054	0.0553	0.0345	0.04
L-Hydroxyproline		0.000356	0.0315		
L-Serine	0.042	0.04661	0.0851	0.0105	0.042
L-Threonine	0.095	0.0843	0.1108	0.0119	0.095
L-Tryptophan	0.016	0.01544	0.0184	0.00204	0.016
L-Tyrosine • 2Na •2H_2O	0.10379	0.09236	0.087	0.00778	0.10379
L-Valine	0.094	0.08396	0.109	0.0117	0.094
Vitamins					
Retinol		0.0000218			
vitamin D-2 (ergocalciferol?)		0.0000218			
menadione		0.0000218			
Para Amino Benzoic Acid		0.0000109	3.72		
ascorbic acid		0.00435			
D-Biotin		0.00000218	0.0001	0.0000073	0.000013
Choline Chloride	0.004	0.0035888		0.01396	0.004
Choline bitartrate			0.0557		
Folic Acid	0.004	0.0034822	0.0088	0.00132	0.004
myo-Inositol	0.072	0.00627488	0.1405	0.018	0.0072
nicotinic acid		0.00000548			
Niacinamide	0.004	0.00348548	0.0015	0.000037	0.004
D-Pantothenic Acid (hemicalcium)	0.004	0.0034822	0.00124	0.00048	0.004
Pyridoxal • HCl		0.00348548	0.0005		0.004
Pyridoxine • HCl	0.004	0.00000548	0.001	0.000062	
Riboflavin	0.0004	0.0003502	0.0002	0.000038	0.0004
Thiamine • HCl	0.004	0.00000218	0.0016	0.00034	0.004
Vitamin B_{12}		0.00087	0.00034	0.00136	0.000013
	Dulbecco´s Modified Eagle´s	**Hybri-Care Medium**	**enhanced RDF (eRDF)**	**Nutrient Mixture F-12**	**Iscove's Modified**

	Medium (DMEM)	**ATCC ® 46-X**		**Ham (Ham´s F12)**	**Dulbecco's Media (IMDM)**
	[g/L]	[g/L]	[g/L]	[g/L]	[g/L]
Other					
alpha tocopherol phosphate		0.00000218			
Insulin Zinc Bovine		0.00696			
D-Glucose	4.5	0.957	3.423	1.802	4.5
D-Glucuronolactone		0.0001566			
5-Methylcytosine		0.0000087			
Oxalacetic acid		0.11484			
HEPES		2.07321	3.57		5.958
Hypoxanthine Na			0.001	0.00408	
linoleic acid			0.00002	0.000084	
Phenol Red • Na	0.0159	0.01479	0.005	0.0013	0.016
Putrescine 2HCl			0.00004	0.000161	
Pyruvic Acid • Na		0.05742	0.11	0.11	0.11
Thioctic Acid				0.00021	
Thymidine		0.00087	0.0057	0.00073	
NAD DPN		0.000609			
FAD Disodium Dihydrate		0.000087			
NADP TPN		0.000087			
Uridine-5-Triphosphate		0.000087			
2-Deoxycytidine HCl		0.00087			
2-Deoxyguanosine		0.00087			
2-Deoxyadenosine		0.00087			
Glutathione Reduced		0.00087	0.00049		
Taurine		0.000364			
Cocarboxylase		0.000087			
Tween 80 TM		0.0010875			
Coenzyme A		0.0002175			
Lipoic Acid			0.24		
Streptomycin			171.95		
Benzylpenicillin Potassium			100,000U		

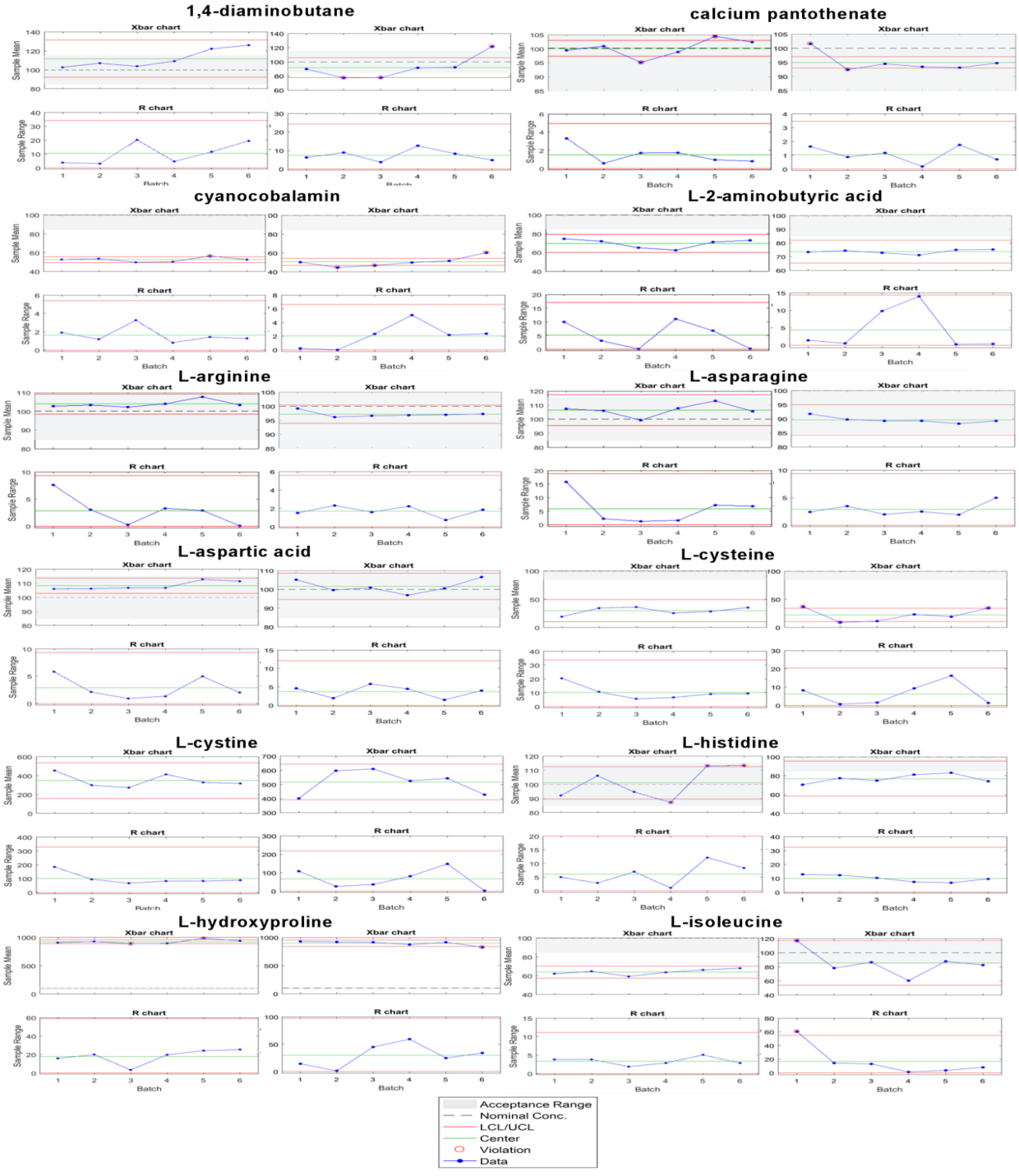

Figure 63: Control charts for compounds 1,4-diaminobutane, calcium pantothenate, cyanocobalamin, L-2-aminobutyric acid, L-arginine, L-asparagine, L-aspartic acid, L-cysteine, L-cystine, L-histidine, L-hydroxyproline and L-isoleucine. The Xbar-R charts on the left of each compound shows QC samples run with batches for measuring model medium 1 preparation and the right Xbar-R chart shows the QC samples run in batches where samples from the storage stability study of model medium 2 were measured. The Xbar chart calculates if the measurement mean is in control and the R charts show if the measurement variation is in control. The dashed line symbolizes the nominal concentration expected in model medium 2 QC sample and the grey area symbolizes the ±15% acceptance range. The lower control limit (LCL) and upper control limit (UCL) are automatically calculated in Matlab and show if the measured values are within the process control ranges. The green line symbolizes the center line. Violation of the control limits are shown by red circles around the blue data.

Figure 64: Control charts for compounds L-isoleucine and L-leucine, L-lysine, L-methionine, L-ornithine, L-phenylalanine, L-proline, L-serine, L-threonine, L-tryptophan, L-valine, myo-inositol and nicotinamide. The Xbar-R charts on the left of each compound shows QC samples run with batches for measuring model medium 1 preparation and the right Xbar-R chart shows the QC samples run in batches where samples from the storage stability study of model medium 2 were measured. The Xbar chart calculates if the measurement mean is in control and the R charts show if the measurement variation is in control. The dashed line symbolizes the nominal concentration expected in model medium 2 QC sample and the grey area symbolizes the ±15% acceptance range. The lower control limit (LCL) and upper control limit (UCL) are automatically calculated in Matlab and show if the measured values are within the process control ranges. The green line symbolizes the center line. Violation of the control limits are shown by red circles around the blue data.

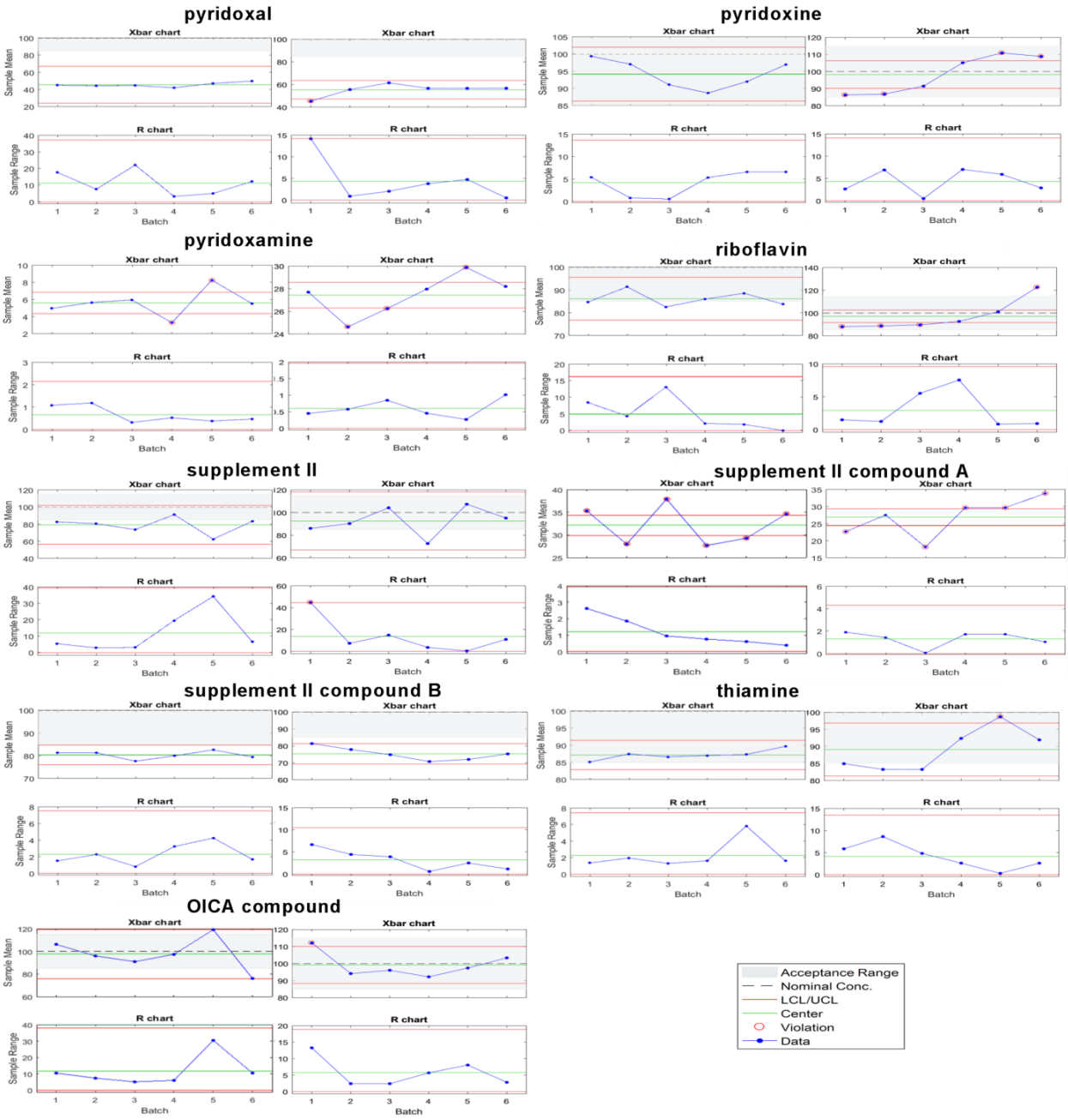

Figure 65: Control charts for compounds pyridoxal, pyridoxine, pyridoxamine, riboflavin, supplement II, supplement II compound A, supplement II compound B, thiamine and OICA compound. The Xbar-R charts on the left of each compound shows QC samples run with batches for measuring model medium 1 preparation and the right Xbar-R chart shows the QC samples run in batches where samples from the storage stability study of model medium 2 were measured. The Xbar chart calculates if the measurement mean is in control and the R charts show if the measurement variation is in control. The dashed line symbolizes the nominal concentration expected in model medium 2 QC sample and the grey area symbolizes the ±15% acceptance range. The lower control limit (LCL) and upper control limit (UCL) are automatically calculated in Matlab and show if the measured values are within the process control ranges. The green line symbolizes the center line. Violation of the control limits are shown by red circles around the blue data.

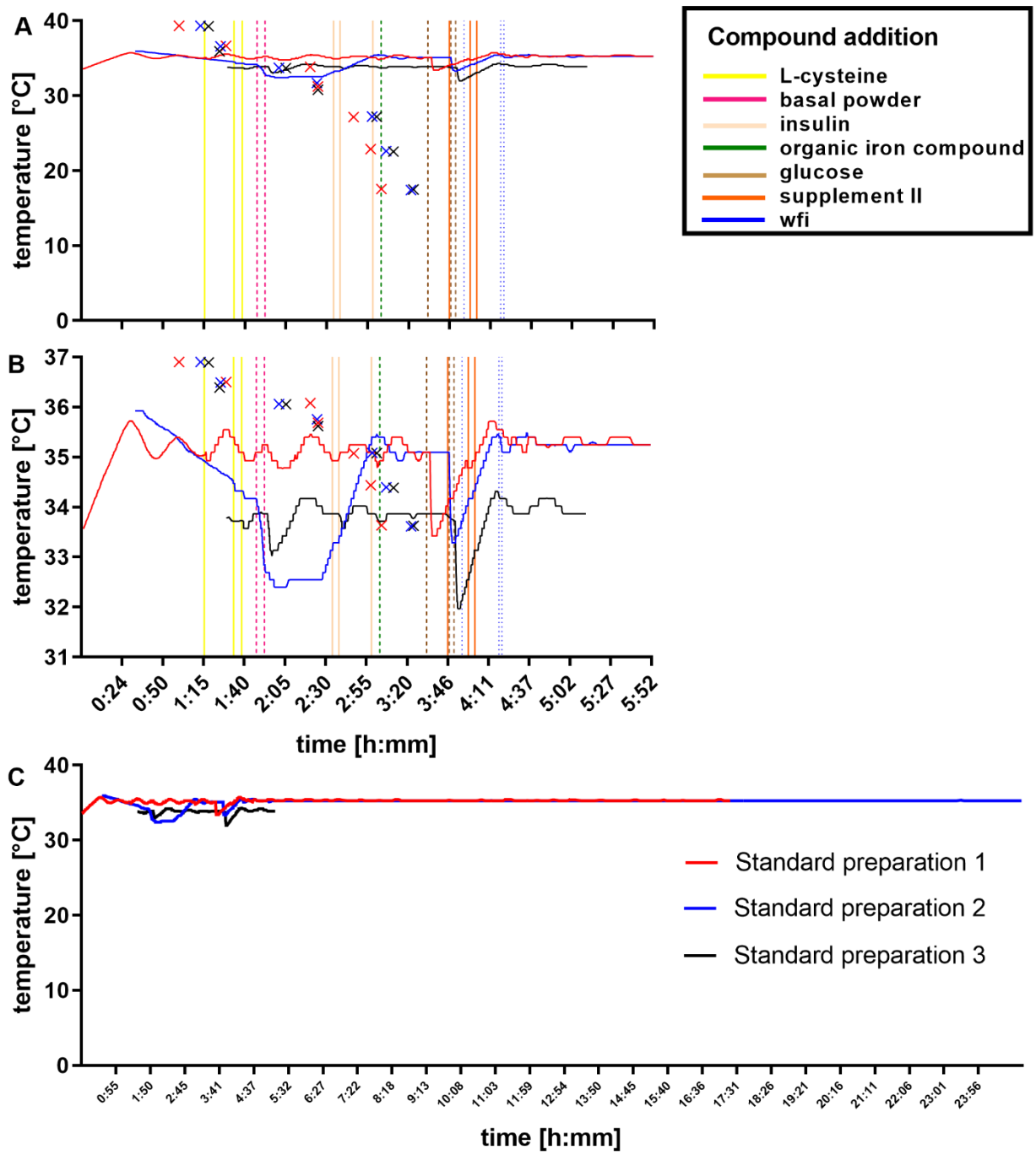

Figure 66: On line temperature profile of univariate sensors during medium preparation. Principally the dissolution of each solid into water is endothermic. It means that breaking molecules apart from the solid state takes energy that the system takes from the environment (solution in tank gets cold). Glucose shows biggest effect because of high quantity and it binds a lot of water molecules decreasing the entropy of water. Because a decrease of entropy is an unfavored reaction some energy is needed to dissolve glucose. A) shows that the temperature remains stable within the range (±2°C) of target preparation temperature at 35°C. B) shows the zoom of the same plot. It can be seen that for standard preparation 2 the basal powder addition significantly decreased temperature. Therefore it can be concluded that it was taken directly out of the coldroom. Standard preparation number 3 generally was one °C below the target. This may come from a wrong setpoint at 34°C or from a mistake in the installation of temperature control system. However this one °C difference is not dramatic at all. With the exception of glucose addition the other compounds show pretty much no significant effect on temperature. Sinus shape observed at this high resolution is from the automatic temperature control. C) long term observation shows that during preparation the most changes in temperature can happen due to powder addition. Over 24 h the temperature remain constant.

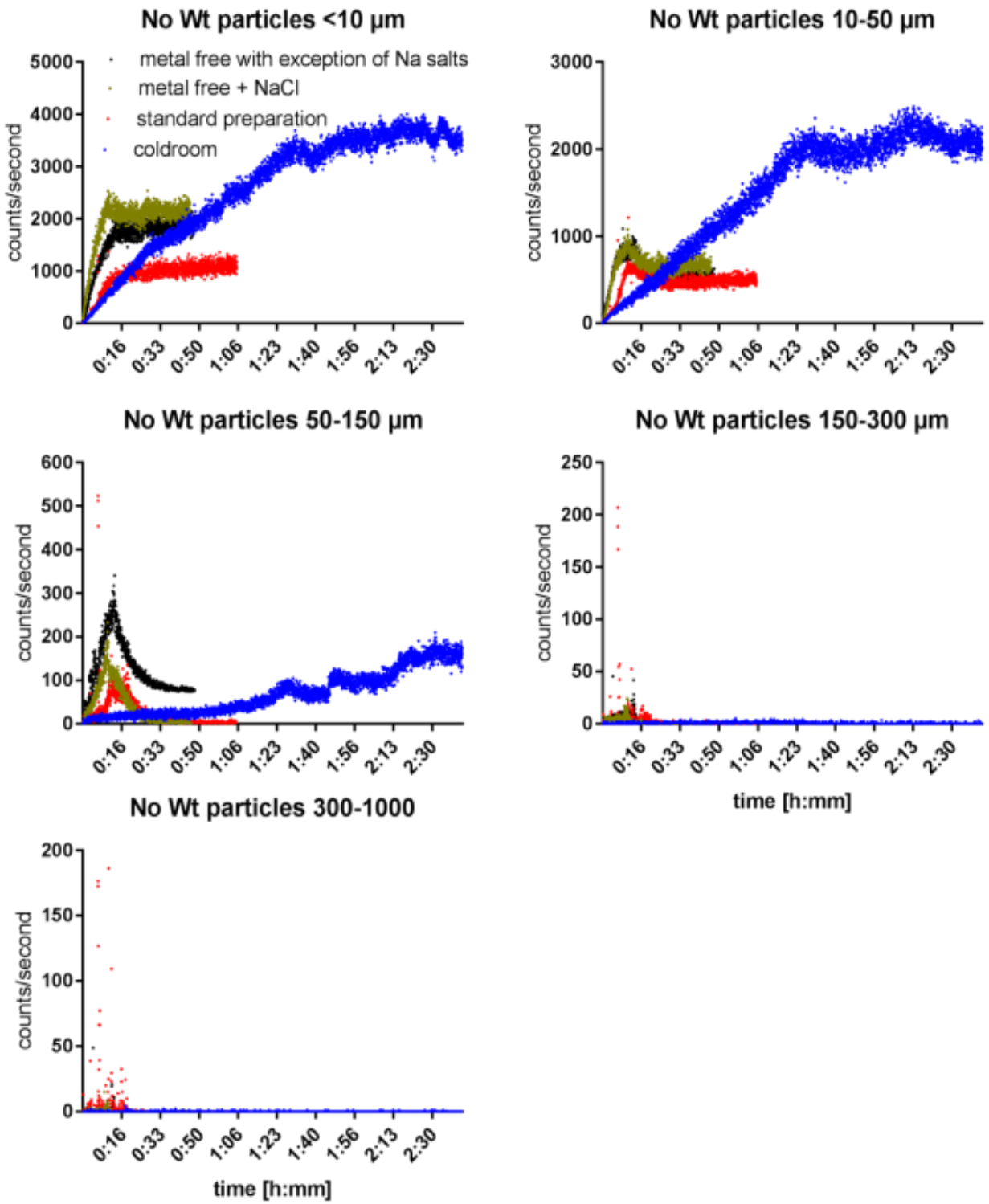

Figure 67: The particle counts per second plotted versus time in model medium 1. Each individual plot shows the particle distribution of individual particle populations categorized by size (smaller than 10 µm, 10 to 50 µm particle size, 50 to 150 µm particle size, 150 to 300 µm particle size and 300 to 1000 µm particle size). No Wt means that the data was not weighed to account for the particle mass contribution.

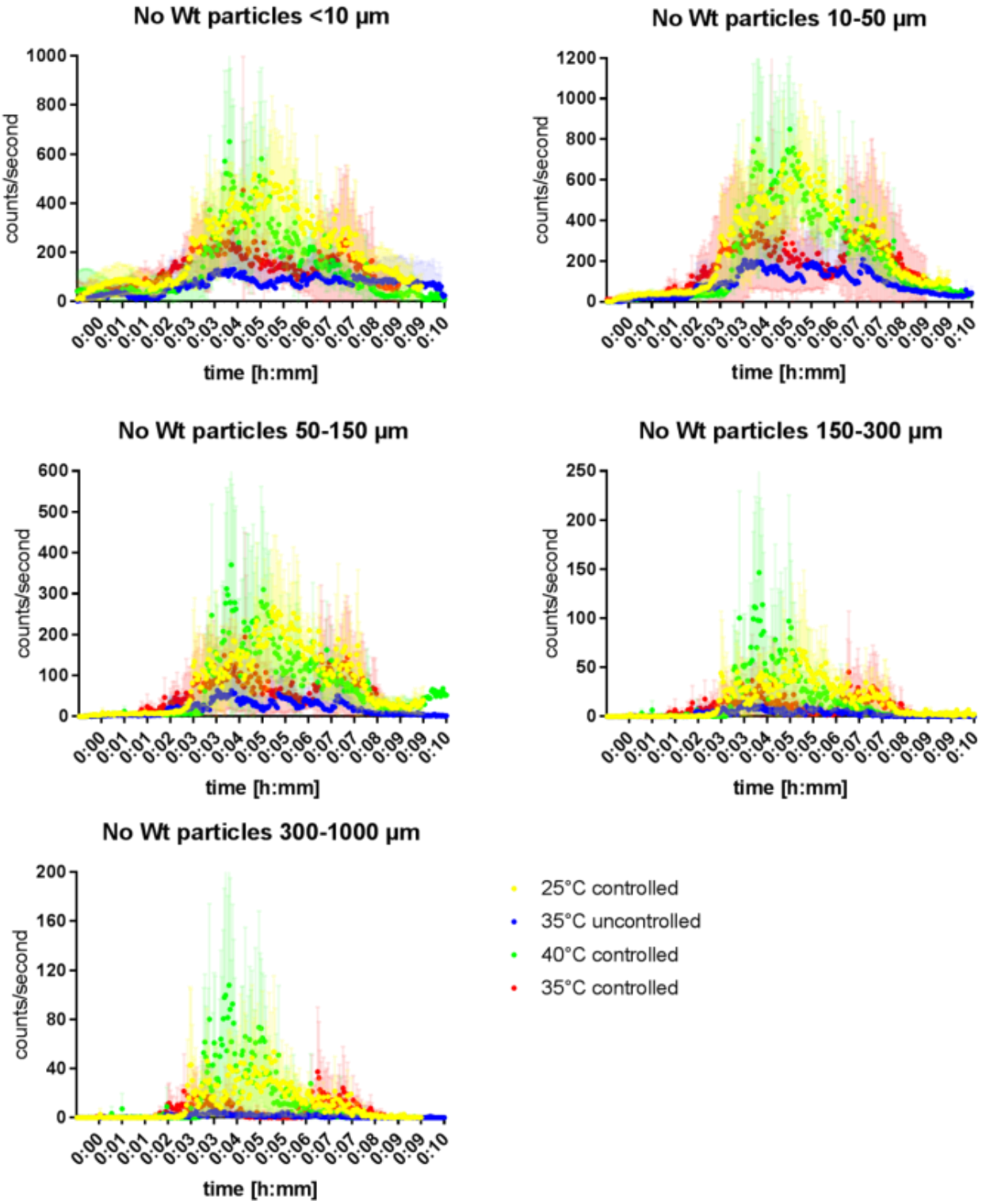

Figure 68: The particle counts per second plotted versus time in model medium 2. Each individual plot shows the particle distribution of individual particle populations categorized by size (smaller than 10 µm, 10 to 50 µm particle size, 50 to 150 µm particle size, 150 to 300 µm particle size and 300 to 1000 µm particle size). The mean of three preparations with standard deviations at the preparation temperature as indicated in legend is schown. No Wt means that the data was not weighed to account for the particle mass contribution.

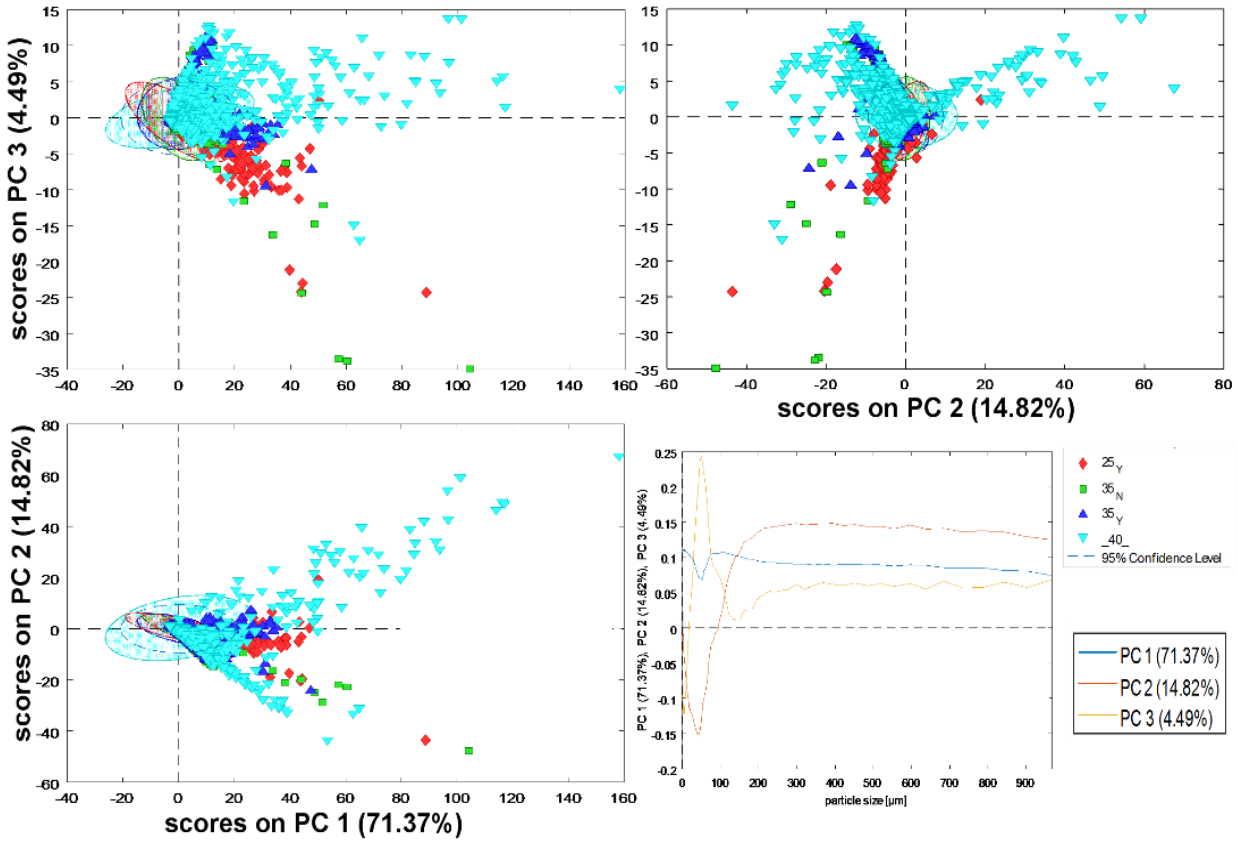

Figure 69: PCA model with data from the FBRM probe 1 only

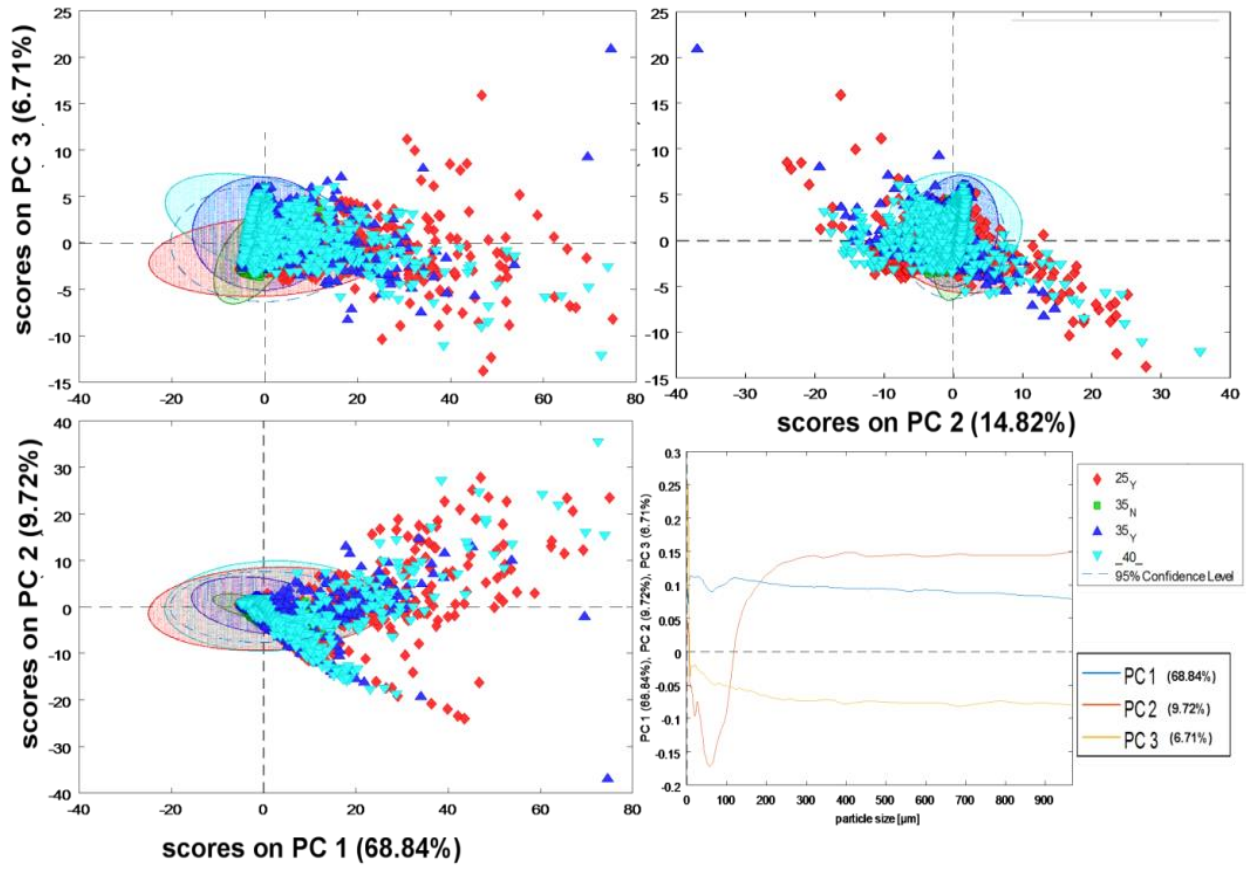

Figure 70: PCA model with data from the FBRM probe 2 only

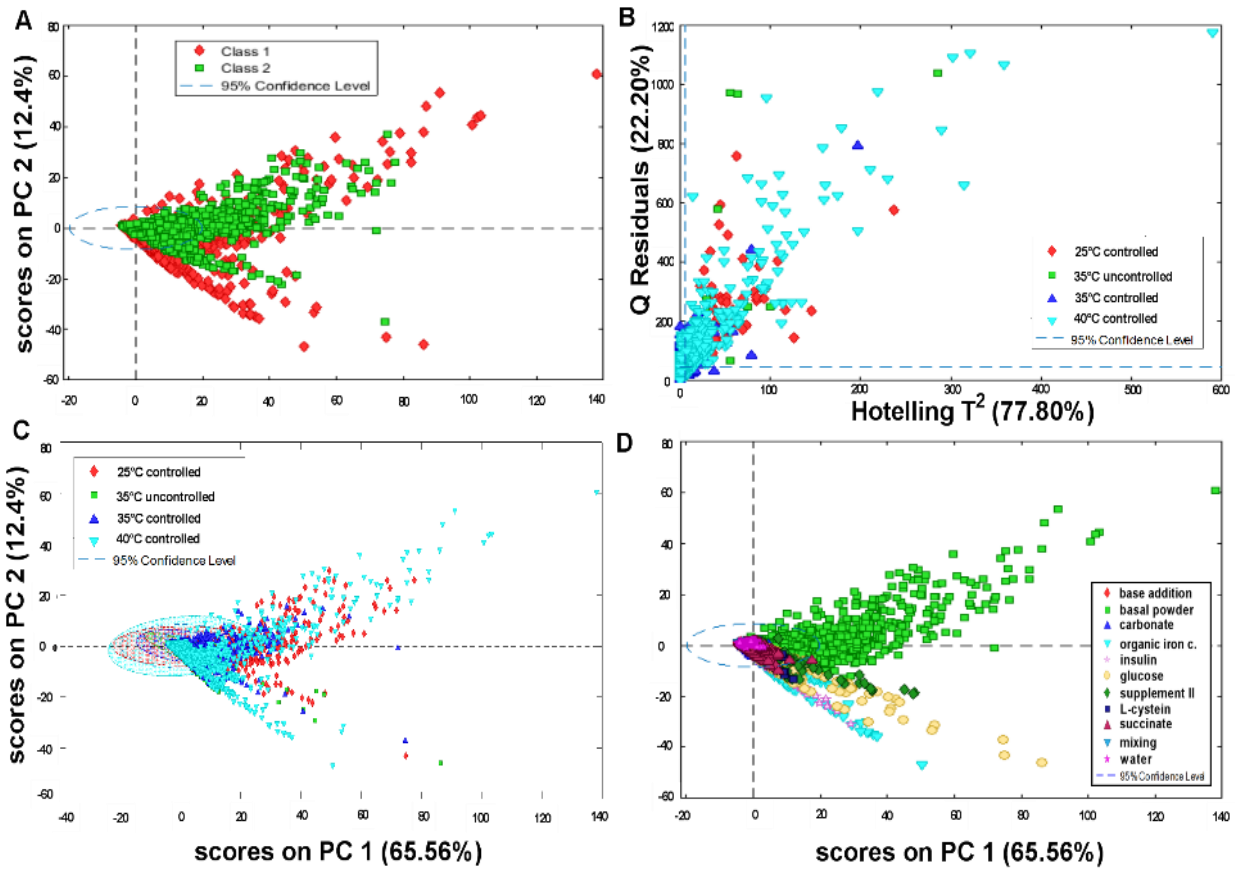

Figure 71: PCA model of FBRM data set using the data of both probes used with two PC´s. A) shows the scores plot colored by the two different probes used. B) shows the hoteling plotted versus the Q residuals. The Q residuals are a means showing the magnitude of variation remaining in the sample after it was projected by the PCA. The hotelling values are a measure for the variation that remains within each sample within the model and in the same time measures how far the sample is apart from the center. C) and D) show the same data as A) colored by preparation condition and by recipe position.

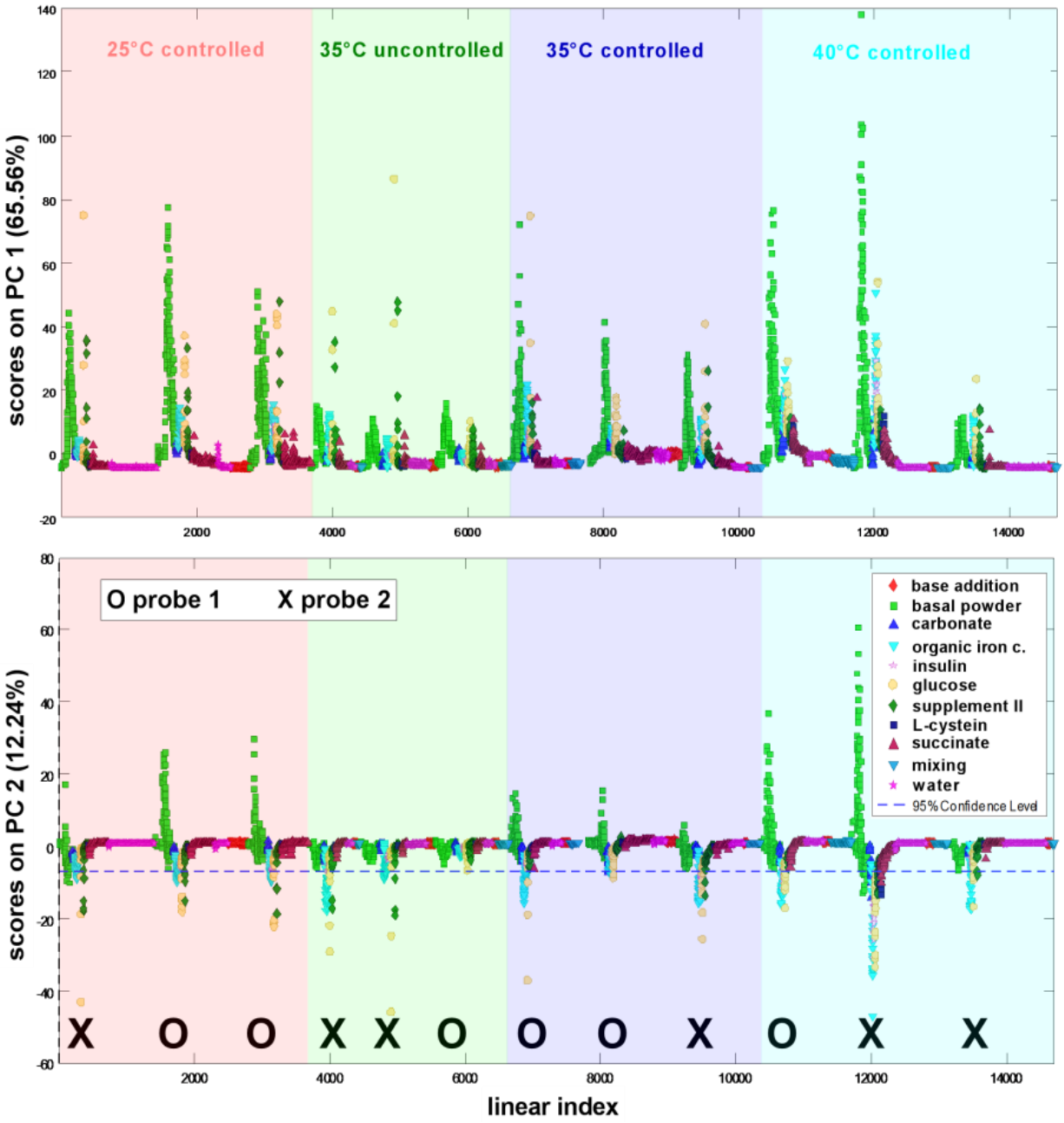

Figure 72: Scores on PC1 and 2 plotted versus linear index (arbitrary scale aligns individual preparations after another).Each preparation starts with the addition of basal powder symbolized by the green rectangles.

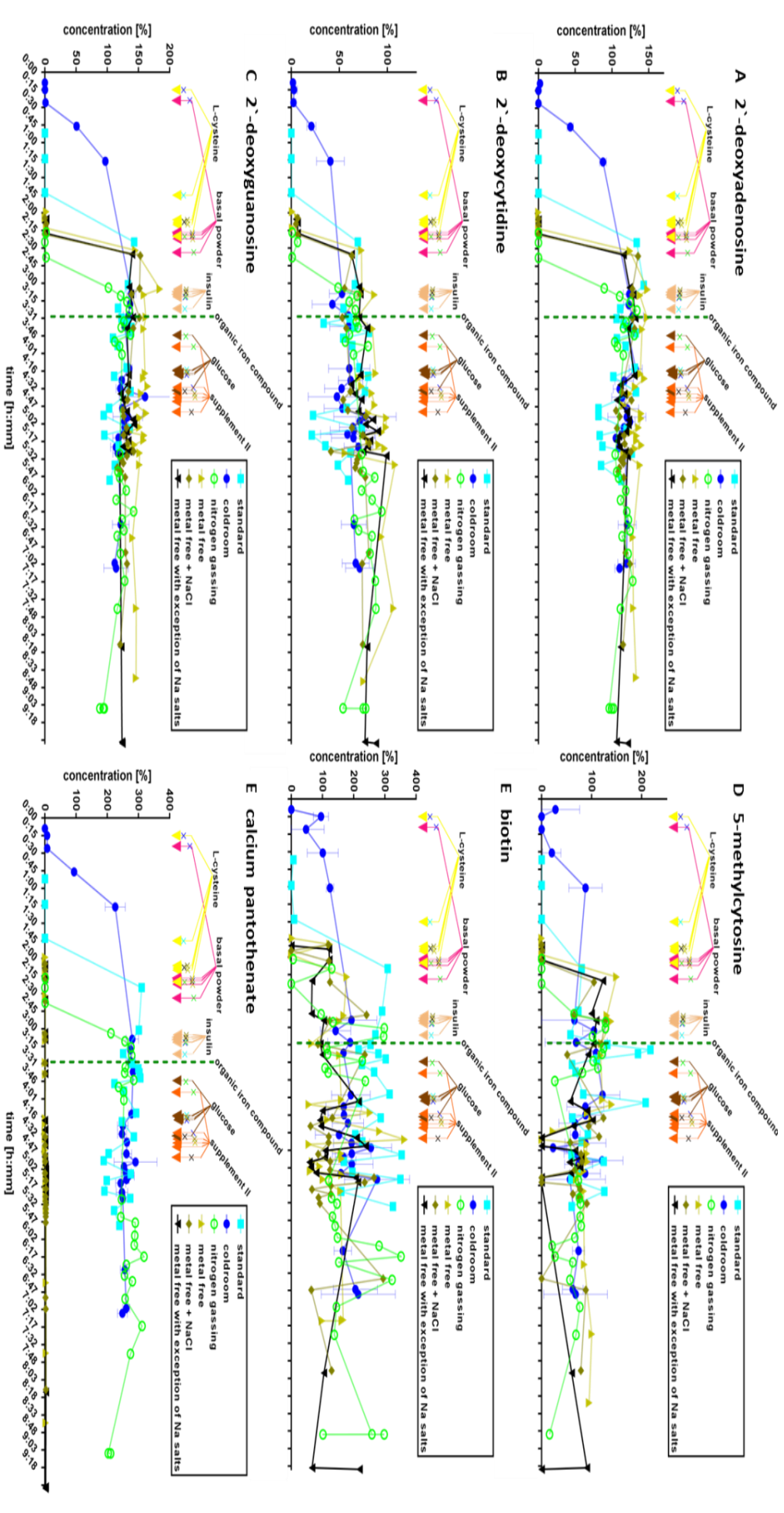

Figure 73: Model Medium 1 compound concentrations over time during medium preparation. A) 2´deoxyadenosine shows the expected concentration over the entire preparation time. B) 2`deoxycytidine shows big variance in coldroom replicates. Measured concentration ranges from 50% to 100% of expectation. Variability comes from low concentration with low SNR. No trend observable in data. C) 2`deoxyguanosine remains at constant concentration over preparation time with a slight overestimation of approximately 25% which is acceptable. D) 5-methylcytosine was used in medium at extremely low concentration. This explains the high variability. No trend observable over preparation time. E) The expected biotin concentration is the same as LoQ. Therefore a high variability and low accuracy can be expected. E) Calcium pantothenate was removed from metal free basal powders. The range for calcium pantothenate in QC samples was 5%. The overestimation by more than 100% in model medium 1 remains unclear. No change over preparation time observable.

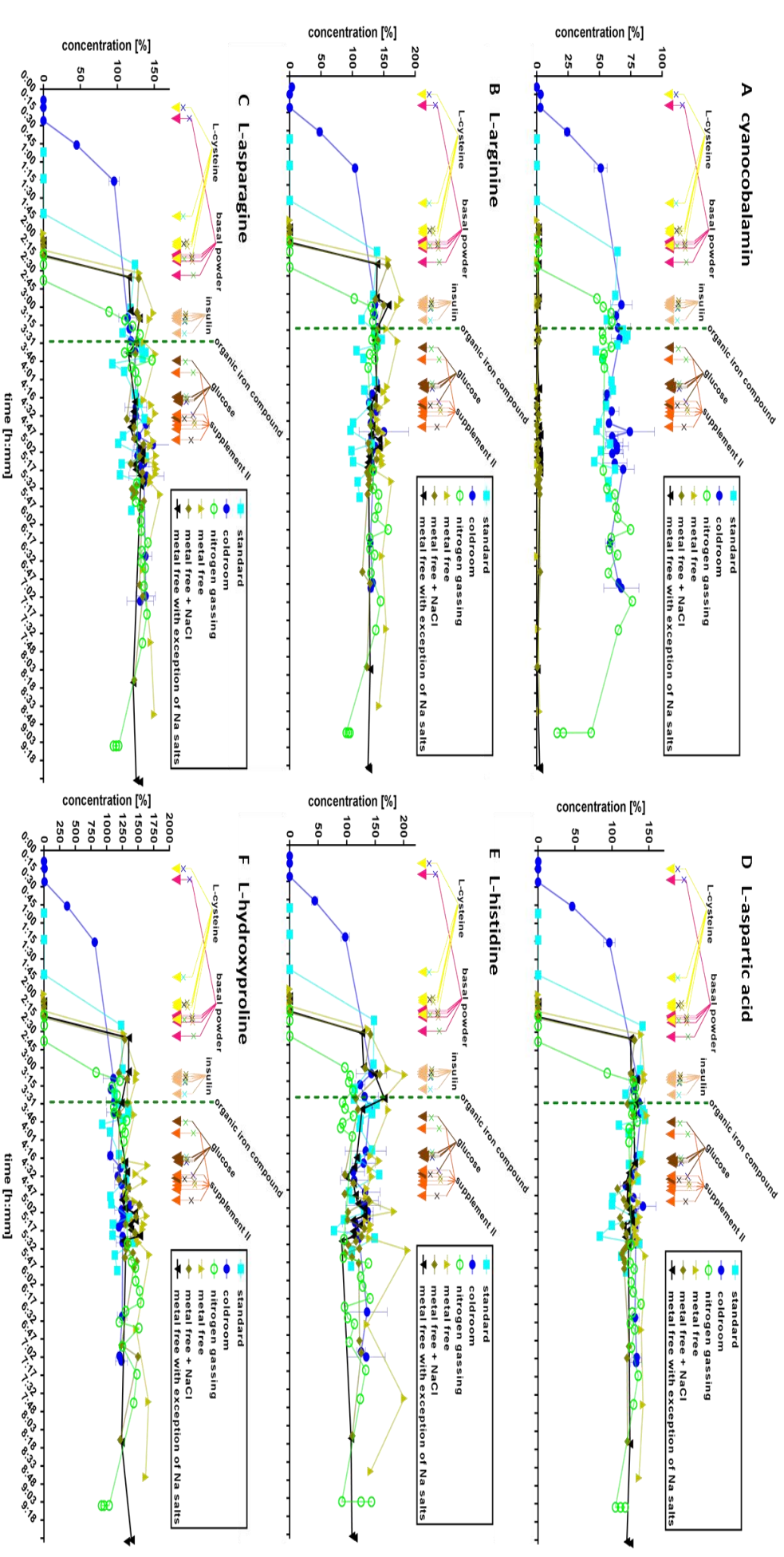

Figure 74: Model Medium 1 compound concentrations over time during medium preparation. A) Cyanocobalamin shows a range of 5.5% in QC samples. Variability in this plot is within this range. Therefore the concentration is to be considered over observation time. Cyanocobalamin was not included in metal free basal powders. B) Expected L-arginine concentration is on average overestimated by 25%. The range in QC samples is 10%. Differences in plot is within expected variability from QC samples. C) Expected L-asparagine concentration is on average overestimated by 25%. The range in QC samples is 20%. Differences in plot is within expected variability from QC samples. D) Expected L-aspartic acid concentration is on average overestimated by 25%. The range in QC samples is 10%. Differences in plot is within expected variability from QC samples. E) Expected L-histidine concentration is on average overestimated by 25%. The range in QC sample is 60%. Therefore the concentration can be considered constant over preparation time. This finding suggests that L-hydroxyproline is present as contaminant descending from L-proline in basal powder.

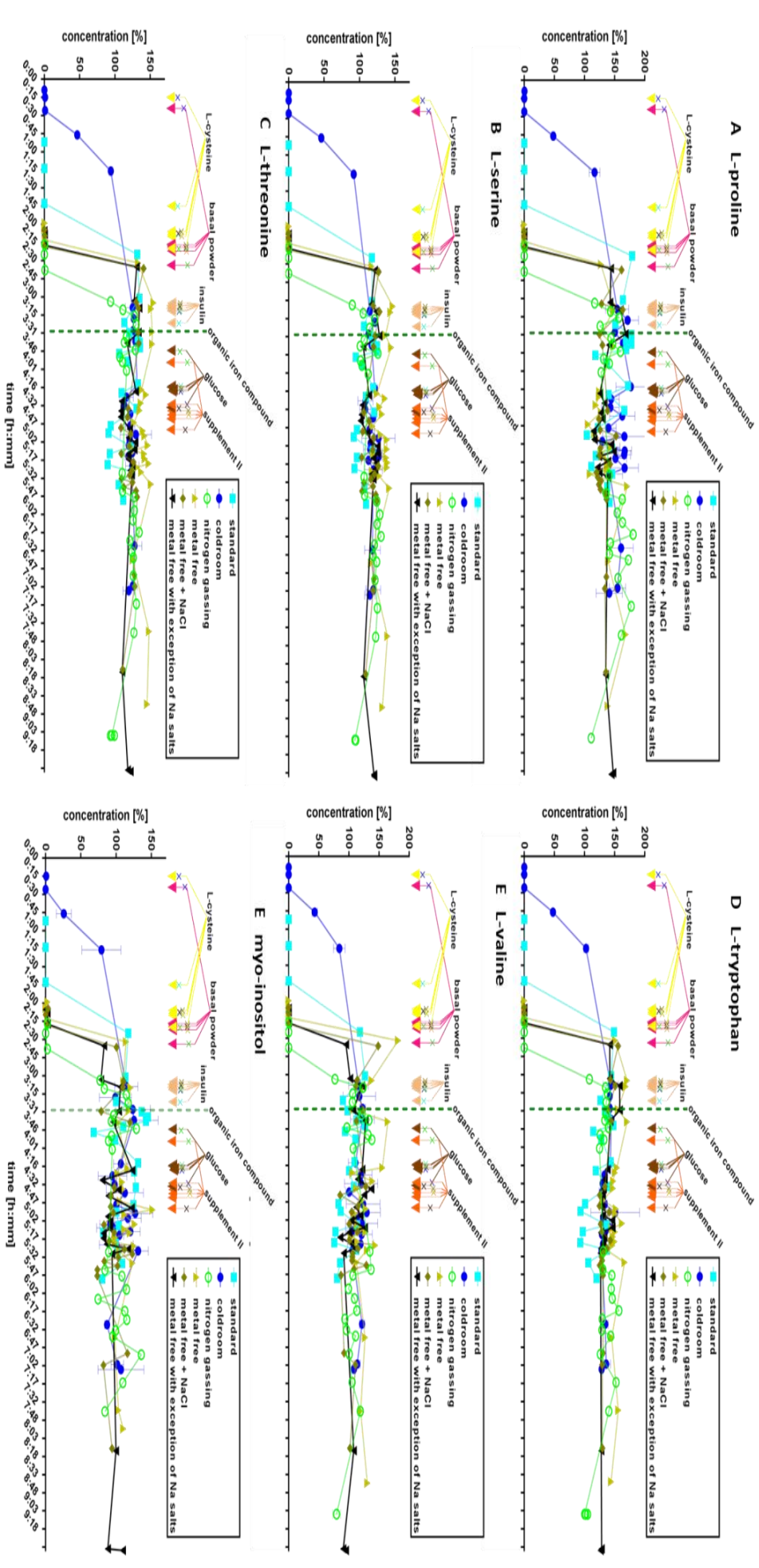

Figure 75: Model Medium 1 compound concentrations over time during medium preparation. A) Expected L-proline concentration is on average overestimated by 50%. The range in QC samples is 20%. Differences in plot is within expected variability from QC samples. B) Expected L-serine concentration is on average overestimated by 25%. The range in QC samples is 10%. Differences in plot is within expected variability from QC samples and no present trend shows that compound is stable over medium preparation. C) Expected L-threonine concentration is on average overestimated by 25%. The range in QC samples is 7%. Differences in plot is within expected variability from QC samples and no present trend shows that compound is stable over medium preparation. D) Expected L-tryptophan concentration is on average overestimated by 25%. The range in QC samples is 6%. Differences in plot is within expected variability from QC samples and no present trend shows that compound is stable over medium preparation. E) Expected L-valine concentration is on average overestimated by 25%. The range in QC samples is 30%. Differences in plot is within expected variability from QC samples and no present trend shows that compound is stable over medium preparation. E) Expected myo-inositol concentration is on average 100%. The range in QC samples is 20%. Differences in plot is within expected variability from QC samples

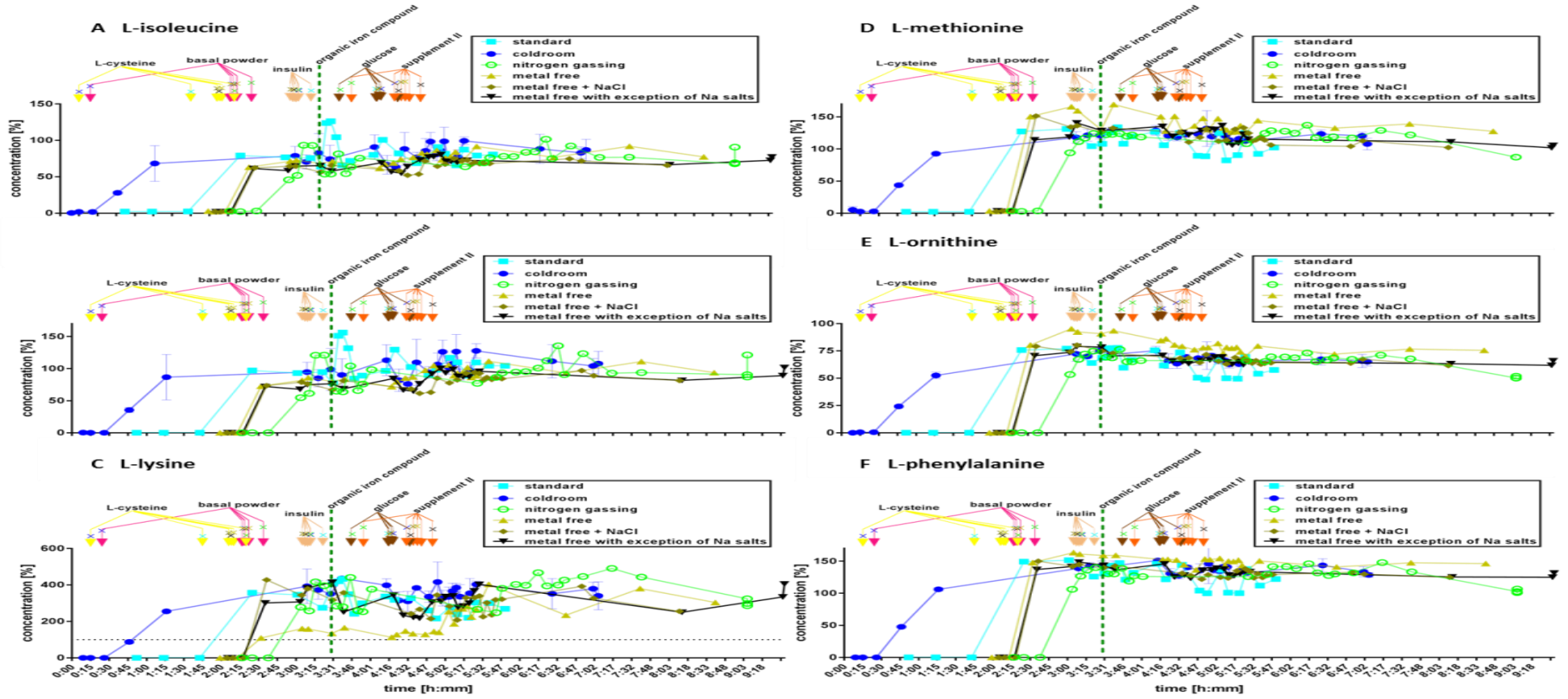

Figure 76: Model Medium 1 compound concentrations over time during medium preparation. A) Expected L-isoleucine concentration is on average underestimated by 25%. The range in QC samples is 10%. Difference in data is within expected variability from QC samples and no present trend shows that compound is stable over medium preparation. B) Expected L-isoleucine and L-leucine concentration is on average 100%. The range in QC samples is 12%. Difference in data is within expected variability from QC samples and no present trend shows that compound is stable over medium preparation. C) Expected L-isoleucine concentration is on average overestimated by 300%. The range in QC samples is 40%. Difference in data over preparation time is within expected variability from QC samples and no present trend shows that compound is stable over medium preparation. The dashed line shows the expected concentration. The metal free preparation almost exactly matches this concentration. Only with the addition of NaOH the level gets similar to other preparation conditions. This suggests that Na^+ forms adducts with L-lysine enhancing the response in the MS detector by a magnitude. . D) Expected L-methionine concentration is on average overestimated by 25%. The range in QC samples is 8%. Difference in data is within expected variability from QC samples and no present trend shows that compound is stable over medium preparation. . E) Expected L-ornithine concentration is on average underestimated by 25%. The range in QC samples is 6%. Difference in data is within expected variability from QC samples and no present trend shows that compound is stable over medium preparation. One exception is the metal free basal powder that consistently shows higher concentrations until pH is adjusted. . F) Expected L-phenylalanine concentration is on average overestimated by 25%. The range in QC samples is 10%. Difference in data is within expected variability from QC samples and no present trend shows that compound is stable over medium preparation

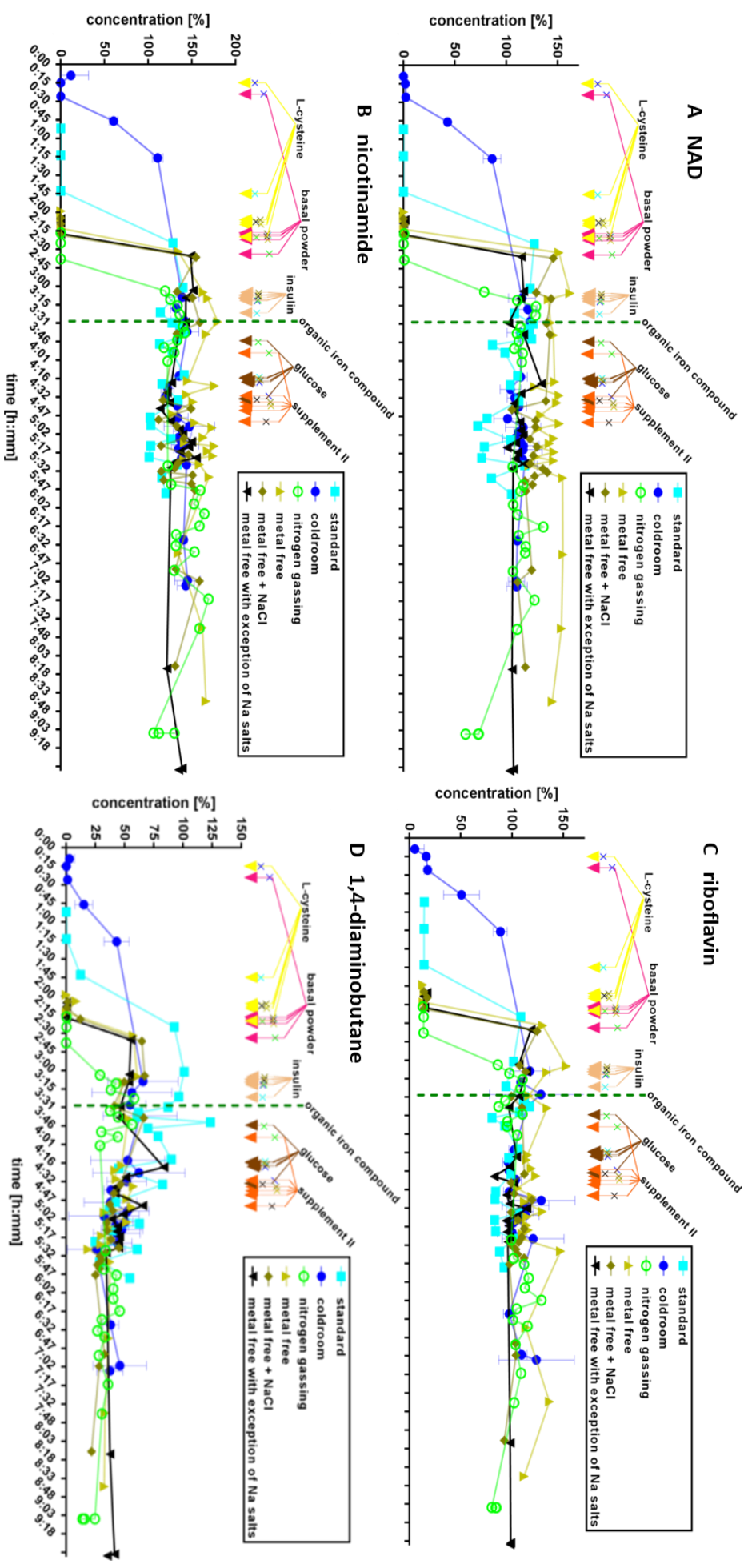

Figure 77: Model Medium 1 compound concentrations over time during medium preparation. A) NAD shows no trends over the preparation time. NAD was not a part of the QC sample. The expected concentration has been met with a scattering of approximately 25%. B) Expected nicotinamide concentration is on average overestimated by 50%. The range in QC samples is 10%. Difference in data is within expected variability from QC samples and no present trend shows that compound is stable over medium preparation. C) Riboflavin has been measured at expected concentration. The range in QC samples is 15%. Difference in data is within expected variability from QC samples and no present trend shows that compound is stable over medium preparation. D) 1,4 diaminobutane (Putrescine) concentration is on average underestimated by approximately 50%. The range in QC sample is 35%. Therefore the apparent concentration decrease after glucose addition cannot be considered significant. However, a glycation reaction with one or two of the molecules primary amines cannot be excluded.

SAFC®

Bioservices Program

Table 1.0 Standard/Trace Elements

	ICP-OES Data: Quality Lab		ICP-MS Data: R&D Lab	
Sample Identification:	87912CP lot 15H306	87913CP lot 15H305	87912CP lot 15H306	87913CP lot 15H305
Units:	ppm	ppm	ppm	ppm
Ba	<0.001	<0.001	NA	NA
Bi	<0.087	<0.087	NA	NA
Ca	<0.151	<0.151	NA	NA
Cd	<0.005	<0.005	<0.001	<0.001
Co	<0.057	<0.057	0.000	0.000
Cr	<0.009	<0.009	0.001	0.001
Cu	<0.337	<0.337	0.000	0.000
Fe	<0.240	<0.240	0.006	0.005
K	0.820	1.023	NA	NA
Li	<0.047	<0.047	NA	NA
Mg	<0.105	<0.105	NA	NA
Mn	<0.007	<0.007	<0.001	0.001
Mo	<0.037	<0.037	0.000	0.000
Na	184.901	192.176	NA	NA
Ni	<0.039	<0.039	<0.001	<0.001
P	<0.346	119.176	NA	NA
Pb	<0.081	<0.081	0.000	0.000
S	54.921	53.375	NA	NA
Sr	<0.001	<0.001	<0.001	<0.001
Zn	0.007	0.009	0.007	0.011
Al	NA	NA	<0.010	<0.010
V	NA	NA	0.000	0.000
As	NA	NA	<0.001	<0.001
Se	NA	NA	<0.073	<0.073
Sn	NA	NA	0.000	0.000
Sb	NA	NA	0.000	0.000
Hg	NA	NA	0.000	0.001

NA – No data available
When the result has a <, it signifies the result is below the limit of quantification

Figure 78: ICP-MS and ICP-OES measurements of metal free and sodium salts containing basal powder.

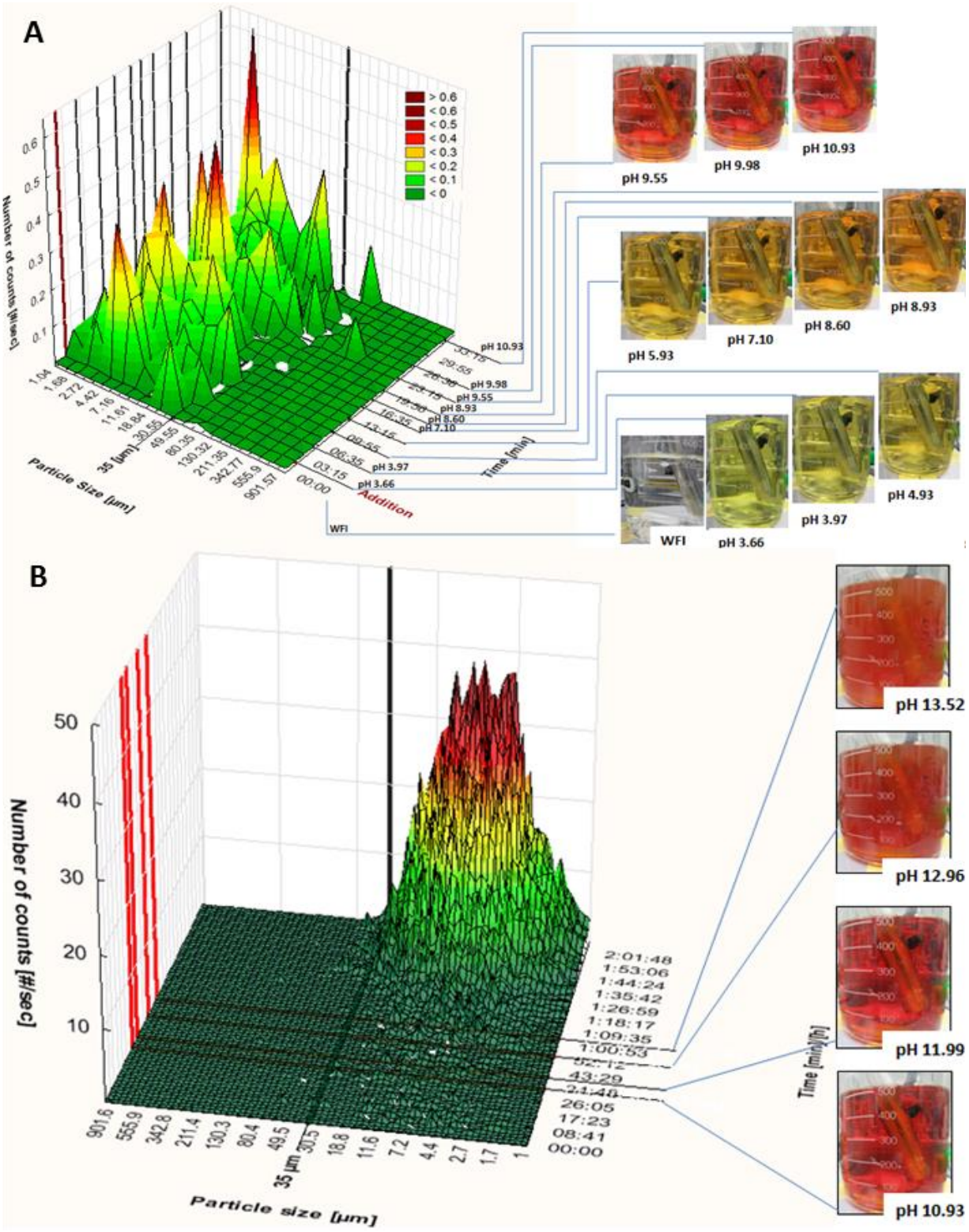

Figure 79: OICA dissolved in water and behavior with titration to basic. A) OICA added to water at a typical concentration used for model medium 1 preparation gave an acidic pH (3.66). The addition of base (NaOH) made turn the color of the solution from bright yellowish green over orange to red at the respective pH units. The particle size distribution remained unchanged in a pH range from 3.66 to 11. B) With reaching a pH of 12 the dissolved OICA started to precipitate what can be seen from the FBRM reading and the pictures on the right hand side. Particle count increased but the size distribution remained constant (1 µm ≥ particle size ≤ 35 µm).

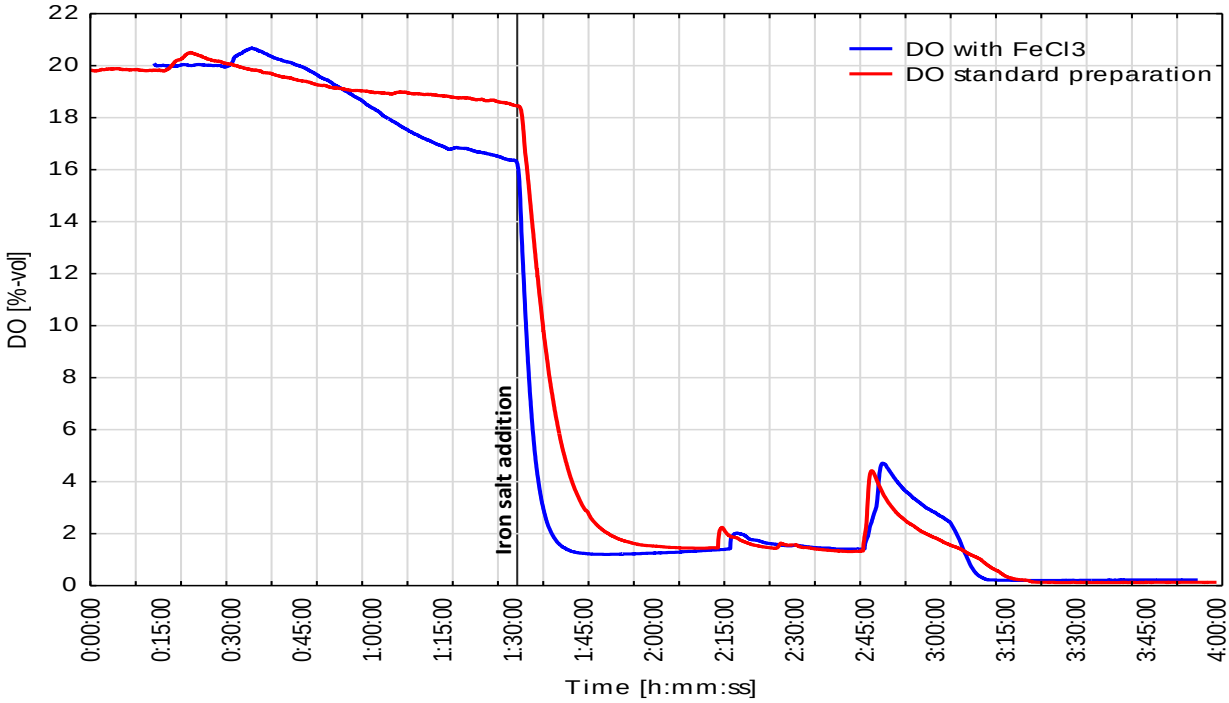

Figure 80: Accountability of iron for the oxygen drop during CDM hydration. OICA is a heterogeneous salt. The exchangeability of OICA with other iron salts is a clear indicator that the oxygen consumption reaction mechanism is caused by iron.

9. Acknowledgements

This thesis would not have been possible without a number of people, to whom I wish to express my gratitude.

First of all, my deepest appreciation goes to Dr. Amandine Calvet for her endless support, countless discussions and her impressive scientific knowledge she shared with me. Not only your assistance in scientific questions but also all the mental support made the day you joined the medium characterization topic one of the most important for me and this thesis. There are so many things I want to thank you for so this page wouldn´t be enough. Therefore I want to say a simple but meaningful Merci Beaucoup!!!

Many thanks go to Professor Thomas Noll. It was a pleasure having you as a supervisor and even though I didn´t have the chance to go to Bielefeld often I always enjoyed your support over long distances. Thanks a lot for the openness to my topic and the valuable advices. Furthermore I want to acknowledge Professor Uwe Bücheler for his support in evaluating the thesis. Thank you very much for finding the time despite all the responsibilities you have to fulfill within BI.

Thanks a lot to Professor Kristian Müller and to Dr. Joe Max Risse for being part of the examining board.

Dr. Benedikt Greulich, thank you very much for starting the characterization of cell culture media topic with me, thanks for the supervision and the support in the management of the special needs of a Ph.D. student within BI. Special thanks for the multitude of runs for training and for racing we completed over the years.

Thanks to Andreas Unsöld, Dr. Jochen Schaub, Dr. Ingo Gorr and Dr. Jan Bechmann for their leadership. Furthermore, many thanks to Markus Rimmele for introducing me into the art of media preparation and the many great sports events we visited together. Also, I want to thank Marina Lang, Ivonne Bettinger and Basti Haas for their support with thesis related topics but also for many important talks outside of work. Thank you! Additionally I want to acknowledge the medium development team and the process development department. Moreover I want to mention Ingrid Krattenmacher, Juliane Schmid and of course the entire IPC team! Thanks a lot for the support in the lab with instruments and for the pragmatic solutions we found with regards to lab organization.

Thank you so much for supporting me in the MS method development Dr. Bartlomiej Krawczyk! It was always a pleasure to work with you and I highly appreciate the time you took on top of your everyday business. Not only thanks for our discussions about molecules flying in the MS but also for the many great conversations about flying in real live and other interesting things…

Thank you very much indeed Ralf Kiesling, Stefan Assfalg, Clemens Miller, Christian Fackler and the entire Isotope group. It was a pleasure to have your support for highly interesting experiments. Additionally to that it was always a great joy working with your great group due to the friendly and welcoming atmosphere. The same was true for the support of Jürgen Jäger, Anita Feyertag and Susanne Kallbach. Thank you very much!

Very important for me was the technical support of Alex Schwarz, Thomy Merk, Kurt, Schorsch Siebenrock and Jörg Schäfer. Thank you very much for helping out “Jugend forscht”!

Furthermore I want to thank my PID office colleagues Dr. Thomas Wucherpfennig, Dr. Raphael Voges, Dr. Fabian Stiefel and Johannes Wutz for the good discussions and scientific vibe during worktime.

Many thanks go also to the numerous students who joined our team over the time. I want to especially thank Mathilda Chatain, Tamara Heermann and Marco Kunzelmann. It was great having you in the team and feeling your passion and support on the topic. Furthermore, I want to thank you for being such

pleasant and sympathetic persons what made it easy and a great experience to lead you through the sometimes a little special BI world.

Thanks a lot to Dr. Michael Zorn for being a great colleague and friend but also for critical proof reading. Sorry, I didn´t find the time to write a 6 pager…

Many thanks to Dr. Samuel Mang, Dr. Nico Pairet and Dr. Cornelia Tilp for the many nights we spent in Café Berlin philosophizing about very important topics. Thanks for being friends.

Und am wichtigsten über die gesamte Zeit der Promotion waren meine Familie und Freunde! Vielen Dank für eure Rückendeckung und grenzenlose Unterstützung in einer sehr intensiven Zeit!

10. Statutory declaration

I declare that I have authored this thesis independently, that I have not used other than the declared references / resources, and that I have explicitly marked all the material which has been quoted either literally or by content from the used sources. This doctoral thesis has not been submitted to any other institution. This is my first attempt for dissertation.

Florian Krattenmacher

Biberach an der Riß, November 17th 2019

Hiermit versichere ich, dass ich die vorliegende Dissertation eigenständig und ohne unerlaubte Hilfe angefertigt habe. Die Dissertation wurde in der vorgelegten oder in ähnlicher Form noch bei keiner anderen Institution eingereicht. Ich habe bisher keine erfolglosen Promotionsversuche unternommen.

Florian Krattenmacher

Biberach an der Riß, 17.11.2019